Investigation into the silencing of heterochromatin in mammalian cells

Thesis submitted by

Theona Natisvili

for the degree of Doctor of Philosophy

Imperial College London

Faculty of Medicine

MRC Clinical Sciences Centre

Gene Control Mechanisms and Disease

London, January 2016

Declaration of originality

Hereby I confirm that this thesis is a result of my own work and findings or ideas by others are appropriately referenced throughout the text. Collaborations are mentioned at the end of each chapter.

Copyright Declaration

The copyright of this thesis rests with the author and is made available under a Creative Commons Attribution Non-Commercial No Derivatives licence. Researchers are free to copy, distribute or transmit the thesis on the condition that they attribute it, that they do not use it for commercial purposes and that they do not alter, transform or build upon it. For any reuse or redistribution, researchers must make clear to others the licence terms of this work.

Abstract

Much of the mammalian genome is composed of repetitive elements, consisting of tandem and interspersed repeats. Heterochromatinisation of pericentromeric tandem satellite repeats plays an important role in centromere formation and maintenance of genome stability. Additionally, several human diseases are caused by microsatellite repeat expansion. Among different classes of interspersed repeats, retro-elements LINEs and SINEs are considered to contribute to genome evolution; however they also pose a potential threat to genome stability. Hence it appears essential that repetitive elements are transcriptionally silenced, which occurs via heterochromatinisation. To further understand heterochromatin formation, this thesis investigated: (i) the frataxin (*FXN)* gene which contains a GAA-repeat expansion causing *FXN* silencing which in turn leads to the neurodegenerative disease Friedreich's ataxia (FRDA); (ii) the effect of proteasome inhibition on the transcription of heterochromatinised DNA repeats. Here, the silenced *FXN* gene was shown to be upregulated by treatment of FRDA patients with the HDAC inhibitor, nicotinamide. This upregulation was accompanied by reduction of the heterochromatin histone modification H3K9me3. Moreover, the proteasome was found at the heterochromatinised *FXN* gene in cells derived from patients, consistent with the hypothesis that, in FRDA, proteasomal degradation of a stalled RNAPII might contribute to *FXN* silencing. Although proteasome inhibition did not upregulate *FXN* transcription, it caused transcriptional activation of pericentromeric satellite repeats which appeared to be independent of cell-cycle perturbations and was accompanied by delocalisation of HP1α from chromocentres without detectable changes in the levels of histone modifications. Proteasome inhibition also increased the number of chromocentres per cell consistent with destabilisation of chromocentres. This effect of proteasome inhibition in upregulation of pericentromeric repeats was shown to be at least partly dependent on activation of heat shock transcription factor and binding of this factor to a consensus sequence within the pericentromeric satellite repeat region.

Publications

- Libri V, Yandim C, Athanasopoulos S, Loyse N, **Natisvili T**, Law PP, Chan PK, Mohammad T, Mauri M, Tam KT, Leiper J, Piper S, Ramesh A, Parkinson MH, Huson L, Giunti P, Festenstein R (2014). Epigenetic and neurological effects and safety of high-dose nicotinamide in patients with Friedreich's ataxia: an exploratory, open-label, dose-escalation study. **Lancet** 384, 504-513
- Yandim C, **Natisvili T,** and Festenstein R (2013). Gene regulation and epigenetics in Friedreich's ataxia. **Journal of Neurochemistry** 126 Suppl 1, 21-42

Acknowledgments

Firstly I would like to thank my supervisor Prof Richard Festenstein for giving me the opportunity to do this PhD in his lab, for guiding me and supporting me all the way through.

I would like to thank Raquel Silva and Giulia Emanuelli for all the help with the experiments and great support and fun in the lab. A special thanks to Cihangir Yandim for great discussions, for sharing the ideas with me, supporting me and providing invaluable help with figure preparation presented in this thesis. The projects presented here would not have reached this stage without their contribution and help.

Moreover, I would like to thank Sathiji Nageshwaran and Helen Figueira for all the help and support especially during stressful days at the end of this Ph.D.

I would like also to thank Dr M. Pook for treating the mice, Prof A. Nakai for providing knockout cells, Dr P. Sabbattini and Prof N. Dillon for providing the spike RNA. Finally I would like to thank all the remaining members of GCMD, Lorenzo Orietti, Marta Mauri, Pui Pik Law, Aravind Ramesh and Jackson Chan as well as the examiners for taking time to read the thesis.

Contents

List of figures **13**

List of tables **18**

Abbreviations **19**

CHAPTER 1: General Introduction **23**

1. Chromatin structure 23

2. Heterochromatin 25

2.1 Properties of heterochromatin 25

2.2 Heterochromatin regulation 26

2.2.1 Histone modifications 26

2.2.1.1 Histone acetylation 28

2.2.1.2 Histone methylation 29

2.2.1.2.1 Formation and function of H3K4 methylation 30

2.2.1.2.2 Formation and function of H3K36 methylation 30

2.2.1.2.3 Formation and function of H4K20 methylation 31

2.2.1.2.4 Formation and function of H3K9 methylation 32

2.2.2 Heterochromatin protein 1 33

2.2.3 DNA methylation 36

2.2.4 RNA interference 37

3. Repetitive DNA Element 39

3.1 Transposons 41

3.1.1 DNA transposons 41

3.1.2 Retrotransposons 41

3.1.2.1 Long interspersed nuclear elements (LINEs) 42

3.1.2.2 Short interspersed nuclear elements (SINEs) 43
3.1.3 Regulation of Retrotransposons 45
3.2 Satellite repeats 46
3.3 Regulation of centromeres and pericentromeres 49
3.3.1 Centromeres 49
3.3.2 Pericentromeres 50
3.3.3 Pericentromeric transcription 52
4. Cellular stress and transcription of pericentromeric repeat 54
4.1 Cellular stress 54
4.1.1 Heat shock proteins (HSPs) 54
4.1.2 Heat shock transcription factors (HSFs) 55
4.2 Transcription of pericentromeric satellite repeats upon cellular stress 59
4.2.1 Nuclear Stress Bodies 60
4.2.2 Formation of NSBs 60
5. Friedreich's ataxia 64
5.1 Frataxin protein 65
5.2 Transcriptional regulation of the *FXN* gene 66
5.3 Transcriptional repression of the *FXN* gene by expanded GAA repeats 68
5.4 HDAC inhibitors and FRDA 70
6. The proteasome 73
6.1 Structure of the proteasome 73
6.2 Protein ubiquitination and degradation 75
6.3 Chromatin regulated function of proteasome 77
6.4 Proteasome recruitment to the chromatin 78
6.5 Function of the Proteasome in transcription 80
7. Hypothesis, Objectives and Aims 82

CHAPTER 2: The effect of high dose nicotinamide in patients with Friedreich's ataxia..... 83

2.1 Introduction 83

2.2 Results 83

2.2.1 Phase 1 clinical trial 83

2.2.2 Phase 2 Clinical trial 88

2.3 Discussion 91

2.4 Contributions 93

CHAPTER 3: Binding of the proteasome to the *FXN* gene and the effect of proteasome inhibition on the *FXN* expression. 94

3.1 Introduction 94

3.2 Results 101

3.2.1 Expression of *FXN* is significantly reduced in FRDA disease cell lines 101

3.2.2 Decreased levels of histone acetylation and increased level of H3K9me3 histone modifications on the *FXN* gene in FRDA cell lines 103

3.2.3 Increased binding of the proteasome at the pathologically silenced *FXN* gene...105

3.2.4 Restored global level of RNAPII upon proteasome and transcriptional inhibition in lymphoblastoid cell lines (Healthy and FRDA).....108

3.2.5 The effect of *in vitro* proteasome and/or transcriptional inhibition on the cell viability and the levels of *FXN* expression 110

3.2.6 The effect of *in vivo* proteasome inhibition on the *FXN* and heterochromatin repeat (major, minor) expression.....114

3.3 Discussion.....120

3.3.1 Heterochromatinisation of the *FXN* gene in FRDA.....120

3.3.2 Proteasome binding to the RNAPII stalling site on the *FXN* gene.....122

3.3.3 Downregulation of *FXN* expression and upregulation of heterochromatic repeat expression with proteasome inhibition.....125

3.4 Contributions 129

CHAPTER 4: Effects of proteasome inhibition and the cell cycle on regulation of constitutive heterochromatin 130

4.1 Introduction 130

4.2 Results 133

4.2.1 Proteasome inhibition results in the upregulation of major satellite repeat expression 133

4.2.2 Effect of the proteasome inhibition on transcription of heterochromatic repeats 135

4.2.3 Cell cycle dependent transcription of heterochromatic repeats 136

4.2.4 Cell cycle independent expression of major satellite repeat and SINE B1 upon proteasome inhibition. 142

4.2.5 Transcription dependent increase of major satellite repeat expression upon proteasome inhibition 146

4.2.6 RNA FISH analysis confirms the increase transcription of the major satellite repeat upon proteasome inhibition 152

4.2.7 No change on the main heterochromatic/euchromatic histone modification marks on the major satellite repeat locus upon proteasome inhibition 157

4.2.8 No change of H3K9me3 distribution on the pericentromeric heterochromatin foci (chromocentres) upon proteasome inhibition. 160

4.2.9 Alteration of the HP1α in the cells upon proteasome inhibition 162

4.2.10 Proteasome inhibition leads to an increased number of heterochromatic domains (chromocentres) in NIH3T3 cells 166

4.2.11 Cell cycle regulated changes of the number of chromocentres 169

4.2.12 Analysis of the effects of cell cycle pertubations due to proteasome inhibition on the number of chromocentres per cell. 173

4.3 Discussion 177

4.3.1 Cell cycle mediated regulation of heterochromatic repeats.....177

4.3.2 The effect of proteasome inhibition in regulation of transcription of heterochromatic repeats.....181

4.3.3 Possible role of RNAPI and/or RNAPIII in transcription of major satellite repeats 186

4.4 Contributions.....188

CHAPTER 5: Investigating the molecular mechanism of the major satellite repeat transcriptional upregulation upon proteasome inhibition 189

5.1 Introduction.....189

5.2 Results.....190

5.2.1 Investigation of proteasome binding in heterochromatic repeats. 190

5.2.2 Small overall increase of 20S proteasome binding on various chromatin regions upon proteasome inhibition.....192

5.2.3 The effect of proteasome inhibition on distribution and binding of RNAPII in heterochromatin regions.....194

5.2.4 Proteasome inhibition induces activation of the cell stress response pathway in NIH3T3 cells 200

5.2.5 Heat shock activates the transcription of major satellite repeats in NIH3T3 cells 202

5.2.6 Suppression of the cell stress response abolishes the transcriptional activation of major satellite repeats upon proteasome inhibition 204

5.2.7 HSF1 binds to major satellite repeats upon proteasome inhibition 207

5.2.8 Transduction of NIH3T3 cells enhances the activation of transcription of major satellite repeat upon proteasome inhibition 209

5.2.9 The HSF1 knockout partially reduced the expression of major satellite repeats upon proteasome inhibition in immortalized mouse embryonic fibroblasts (iMEFs) ...214

5.3 Discussion.....218

5.3.1 Does proteasome mediate the degradation of RNAPII at major satellite repeats leading to its transcriptional activation? 218

5.3.2 Proteasome inhibition partly upregulates major satellite repeat transcription by activating the heat shock stress pathway. 221

5.4 Contributions 226

CHAPTER 6: CONCLUSION 227

CHAPTER 7: MATERIALS AND METHODS 231

7.1 Cell lines 231

7.2 Transgenic YG8 mice containing human frataxin transgene (*hFXN*) 232

7.3 Primary cells - Isolation of human peripheral blood mononuclear cells (PBMCs) 233

7.4 Drug preparation and treatments 233

7.5 Genotyping for gender determination in NIH3T3 and iMEFs 234

7.6 Phenol/chloroform DNA extraction 234

7.7 Chromatin immunoprecipitation (ChIP) 234

7.8 Total RNA extraction 237

7.9 Complementary DNA (cDNA) synthesis 238

7.10 Quantitative real time polymerase chain reaction (qPCR) 239

7.11 Analysis of frataxin protein 241

7.12 Western blot 241

7.13 Propidium Iodide (PI) staining for cell cycle analysis 242

7.14 Counterflow centrifugal elutriation 243

7.15 Immunofluorescence 244

7.16 RNA *in situ* hybridization (RNA-FISH) 245

7.17 Chromocentre cluster analysis by Imagestream X 246

7.18 Lentivirus-mediated short hairpin RNA (shRNA) knockdown 246

7.19 Materials and Reagents 248

APPENDIX 250

SUPPLEMENTARY FIGURES 251

SUPPLEMENTARY TABLES 255

REFERENCES 261

List of figures

Figure 1.1: Nucleosome and chromatin structure

Figure 1.2: Mammalian cell nucleus during interphase

Figure 1.3: HP1 isoforms and Heterochromatin formation/spreading

Figure 1.4: Summary of the factors regulating switching between heterochromatin and euchromatin

Figure 1.5: Schematic representation of DNA repetitive elements

Figure 1.6: Overview of characteristics of non-LTR retrotransposons LINE L1 and SINE B1 in the mouse genome

Figure 1.7: Overview of characteristics of classic satellite repeats in the mouse genome

Figure 1.8: A schematic representation of the chromocentre formation in an interphase cell nucleus by three individual chromosomes

Figure 1.9: Members of human and mouse HFS family with schematic representation of the functional domains

Figure 1.10: Representative HSF1 post-translational modifications (PTMs) and HSF1 activation cycle

Figure 1.11: A summary of known stressors that were shown to induce pericentromeric repeat transcription in human cells

Figure 1.12: Transcription of human Satellite III repeats and NSBs formation Figure

Figure 1.13: The human *FXN* gene and its known regulatory elements

Figure 1.14: A hypothetical model for the heterochromatin formation of the *FXN* gene with pathologically expanded GAA repeats.

Figure 1.15: Inhibition of SIRT by nicotinamide

Figure 1.16: Structure of the 26S proteasome

Figure 1.17: Protein ubiquitination and proteasome mediated degradation

Figure 2.1: The effect of single, escalating doses of nicotinamide on frataxin protein concentration in patients with Friedreich's ataxia over 24 h.

Figure 2.2: Plasma nicotinamide, *FXN* mRNA and frataxin protein analysis of single-doses of nicotinamide over 24h in PBMCs

Figure 2.3: The chromatin Immunoprecipitation analysis against heterochromatic (H3K9me3) and euchromatic (H3ac) histone marks on the regions flanking the GAA repeats of the *FXN* locus

Figure 2.4: Plasma nicotinamide, *FXN* mRNA and frataxin protein analysis after daily doses of nicotinamide over 5 days

Figure 2.5: The chromatin Immunoprecipitation analysis against heterochromatic (H3K9me3) and euchromatic (H3ac) histone marks on the regions flanking the GAA repeats of the *FXN* locus

Figure 2.6: Hypothetical mechanism by which nicotinamide might antagonise the pathological *FXN* gene silencing that causes Friedreich's ataxia

Figure 3.1: RNAPII CTD phosphorylation patterns at (A) paused gene and (B) actively transcribed gene.

Figure 3.2: Investigation of RNAPII dynamics at exon 1 of the *FXN* gene.

Figure 3.3: Proteasome inhibition by PS341 restores the S2P-RNAPII levels upon transcriptional inhibition by α-amanitin in FRDA cell lines and has no effect in healthy cell line.

Figure 3.4: Expression of *FXN* is significantly reduced in FRDA cell lines

Figure 3.5: The H3K9me3 and H3ac profile along the *FXN* gene in health and FRDA cell lines.

Figure 3.6: The proteasome binding along the FXN gene in healthy and FRDA_1 cell lines.

Figure 3.7: The total RNAPII level is restored upon concomitant proteasome and transcriptional inhibition in Healthy and FRDA cell lines.

Figure 3.8: The effect of proteasome and transcriptional inhibition on the survival of Healthy, FRDA_1 and FRDA_2 cell lines

Figure 3.9: *In vitro* proteasome inhibition downregulates *FXN* expression in Healthy and FRDA cell lines.

Figure 3.10: The effect of *in vivo* proteasome inhibition of the *FXN* trangene expression in cerebellum and heart tissue of YG8 transgenic mice.

Figure 3.11: The effect of *in vivo* proteasome inhibition on the expression of the heterochromatic repeats in the cerebellum and heart tissues.

Figure 4.1: Structural changes of chromatin during difference phases (G1, S, G2, M) of the cell cycle.

Figure 4.2: Proteasome inhibition leads to only minor morphological changes during the time course of treatment

Figure 4.3: Proteasome inhibition results in increased transcript level of major satellite repeat.

Figure 4.4: The schematic view of the principal of cell synchronisation by centrifugal elutriation

Figure 4.5: Cell fractions, enriched at specific phases of the cell cycle were obtained by centrifugal elutriation

Figure 4.6: Cell cycle regulated expression of the major and minor satellite repeats

Figure 4.7: The effect of proteasome inhibion on the cell cycle of NIH3T3 cells.

Figure 4.8: The time course effect of the proteasome inhibition in the expression of major satellite, minor satellite, LINE L1 and SINE B1 repeats.

Figure 4.9: The time course effect of the proteasome and/or RNAPII inhibition in the expression of *c-MYC*, major satellite, minor satellite, LINE L1 and SINE B1 repeats.

Figure 4.10: The time course effect of the RNAPII inhibition in the expression of c-MYC and major satellite repeat expression.

Figure 4.11: The time course effect of the proteasome and/or all RNA polymerases (RNAPI, II and III) inhibition in the expression of major satellite, minor satellite, LINE L1 and SINE B1 repeats.

Figure 4.12: RNA–FISH analysis of major satellite repeat transcription upon proteasome inhibition.

Figure 4.13: RNA-FISH analysis of major satellite transcription sites in cells upon proteasome inhibition.

Figure 4.14: Representative 3D images obtained from the RNA-FISH using Velocity software for NIH3T3 cells treated with DMSO and MG132 for 4h with probe against major satellite repeat transcript.

Figure 4.15: The proteasome treatment does not affect the global chromatin histone modification marks on the repetitive elements

Figure 4.16: Proteasome inhibition does not affect H3K9me3.

Figure 4.17: HP1α distibution change upon 4h of proteasome inhibition

Figure 4.18: HP1α distibution change upon 8h of proteasome inhibition

Figure 4.19: Total HP1α protein levels remain similar upon proteasome inhibition

Figure 4.20: The distribution of the number of chromocentres per cell is increased by proteasome inhibition.

Figure 4.21: Comparison of distribution of the number of chromocentres per cell upon proteasome inhibition

Figure 4.22: Cell fractions, enriched at specific phase of the cell cycle were obtained by centrifugal elutriation

Figure 4.23: Chromocentre distribution is affected by cell cycle. Not elutriated and fractions with different cell cycle profile were stained with DRAQ5 and imaged using ImageSteeamX.

Figure 4.24: Comparison of distributions of the number of chromocentres per cell.

Figure 4.25: Summary of cell cycle effects on the transcription of pericentromeric and centromeric repeats and number of chromocentre distribution per cell

Figure 5.1: Proteasome distribution within the cell.

Figure 5.2: Proteasome subunit β6 is recruited to heterochromatic regions, active gene (GAPDH) and inactive gene (MOG) in NIH3T3 cells measured by ChIP-qPCR.

Figure 5.3: Proteasome inhibition induces slight overall increase of proteasome binding on heterochromatin regions, active gene (GAPDH) and inactive gene (MOG).

Figure 5.4: S2P-RNAPII and S5P-RNAPII binding on the heterochromatic repeats were unaffected by proteasome inhibition.

Figure 5.5: Immunofluorescence analysis for S5P-RNAPII upon proteasome inhibition.

Figure 5.6: Immunofluorescence analysis for S2P-RNAPII upon proteasome inhibition.

Figure 5.7: Activation of the cell stress response pathway upon treatment of cells with proteasome inhibitor MG132.

Figure 5.8: Effect of the heat shock on the expression of *HSF1, HSP70, HSP90* and heterochromatic repeats including major, minor, LINE L1 and SINE B1.

Figure 5.9: The effect of HSF1 and proteasome inhibition on the expression of *HSF1, HSP70* and heterochromatic repeats.

Figure 5.10: Transcription factor HSF1 binds to major satellite repeats upon proteasome inhibition

Figure 5.11: HSF1 knockdown in NIH3T3 cells.

Figure 5.12: The effect of the HSF1 knockdown in the expression of major satellite repeats followed by treatment of NIH3T3 cells with proteasome inhibitor.

Figure 5.13: The basal heterochromatic repeats expression levels in HSF1 wild type (+/+) and HSF1 null (-/-) iMEFs

Figure 5.14: The effect of the proteasome inhibition on the expression of HSP70 and major satellite repeats in wild type and HSF1 knockout cells.

Figure 6.1: Model of pericentromeric major satellite repeat activation with proteasome inhibition

Figure 7.1: Experiment workflow for elutriation

Figure S.1: Figure S1: Sex determination in NIH3T3 cells and HSF1+/+ and HSF1-/- iMEFs.

Figure S2: Gating strategy for the ImageStreamX analysis.

Figure S3: Alignment of a portion of pericentromeric major satellite and centromeric minor satellite consensus sequence with the canonical binding sequence of the HSF1 transcription factor.

Figure S4: Representative images of the HEK293T transfection with shRNA and packaging plasmids.

Figure S5: Representative images of NIH3T3 cells after lentiviral infection.

* 'S' stands for supplementary

List of tables

Table 1: Common histone modifications and there effect on the gene transcription

Table 2: Cell viability of Healthy, FRDA_1 and FRDA_2 cell lines upon treatment with proteasome inhibitor MG132, transcriptional inhibitors ActDα/amanitin and concomitant treatment of MG132 with ActD or α-amanitin for 8h.

Table 3: Euclidian distances between cell cycle profile upon proteasome inhibition and different fractions of elutriated and not elutriated material obtained from PI staining

Table 4: Analysis of FRDA YG8 transgenic mouse line

Table S1: A summary from chromatin features of the *FXN* gene.

Table S2: List of primers for Chapter 2 and 3

Table S3: List of primers for Chapter 4 and 5

Table S4: List of Antibodies

* 'S' stands for supplementary

Abbreviations

A	Adenine
Ac	Acetylated
ActD	Actinomycin D
ADP	Adenosine diphosphate
ALDOA	Aldolase A
ALRsat	α satellite repeat
ASH1L	ASH1-like protein
ATP	Adenosine triphosphate
ATPase	Adenosine triphosphate catalyse
AUBK	Aurora B kinase
Bp	base pair
BML-210	N_1-[2-aminophenyl]-N_8-phenyloctanediamide
C	Cytosine
CD	Chromodomain
cDNA	complementary deoxyribonucleic acid
ChIP	Chromatin Immunoprecipitation
CP	Core particle
CPC	Chromosomal passenger complex
CSD	Chromoshadow domain
Ct	Cycle threshold
CTD	Carboxyl terminal domain
CTDF	CCCCTC-binding factor
DNA	Deoxyribonucleic acid
DAPI	4,6-diamidino-2-phenylindole
DBD	DNA binding domain
DEPC	Diethyl Pyrocarbonate
DMSO	Dimethyl sulfoxide
DNMT	DNA methyltransferase
DPE	Downstream promoter-like
DRB	5,6-Dichloro-1-β-D-ribofuranosylbenzimidazole
DRG	Dorsal root ganglia
DUB	Deubiquitinating
E1	Ubiquitin activating enzyme
E2	Ubiquitin conjugating enzyme
E3	Ubiquitin ligase
EBV	Epstein-Barr Virus
EDTA	Ethylenediaminetetraacetic acid
e.g	for example
EN	endonuclease
ES cells	Embryonic stem cells
ESR1	Estrogen receptor α
et al.,	Et alli
Ex1	Exon 1
FACS	Fluorescent activated cell sorting
Fe	Iron
FISH	Fluorescence in situ hybridization
FRDA	Freidreich's Ataxia
FXN	Frataxin

GAPDH	Glyceraldehyde 3-phosphate dehydrogenase
GFP	Green Florescence Protein
H	Histone
HAT	Histone acetyltransferase
HDAC	Histone deacetylase
HDACi	Histone deacetylase inhibitor
HKDM	Histone lysine demethylase
HKMT	Histone lysine methyltransferase
HP1	Heterochromatin protein 1
HPRT	Hypoxanthine phosphoribosyltransferase
HR	Heptad repeat
HP-C	Heptad repeat C domain
HSE	Heat shock sequence element
HSF	Heat Shock transcription Factor
HSP	Heat Shock Protein
IF	Immunofluorescence
iMEF	Immortalised Mouse Embryonic Fibroblast
IP	Immunoprecipitation
iPSC	Induced pluripotent stem cell
K	Lysine
Kb	Kilobase
kDa	kilo Dalton
Kg	kilo gram
L1	Long Interspersed Nuclear Elements 1
LINEs	Long Interspersed Nuclear Elements
lncRNA	Long noncoding RNA
LTR	Long terminal repeat
M	Molar
M phase	Mitotic phase
MBD	Methyl-CpG-binding domain
me2	Di-methylation
me3	Tri-methylation
mg	Mini gram
MG132	(Z-Leu-Leu-Leu-al) peptide aldehyde proteasome inhibitor
Min	minute
mM	mini molar
MM	Multiple myeloma
Ml	mini litre
MLL	mixed lineage leukemia
MOG	myelin oligodendrocyte glycoprotein
mRNA	Messenger RNA
N terminal	Amino terminal
NAD+	Nicotinamide adenine dinucleotide
nm	Nanometre
NSB	Nuclear Stress Body
OAADPr	O-acetyl ribose
ORF	Open reading frame
PBS	Phosphate buffered saline
PBMC	Peripheral blood mononuclear cell
PCR	Polymerase Chain Reaction
PDZK3	PDZ domain containing protein

PFA	Paraformaldehyde
PG	Perichromatin granule
pH	pH value
PI	Propidium Iodide
piRNA	Piwi-interacting RNA
PMSF	Phenylmethanesulfonylfluoride
PRC1	Polycomb repressor complex 1
PRC2	Polycomb repressor complex 2
PTM	Post-translational modification
q	Long arm of chromosome
qRT-PCR	Quantitative real time polymerase chain reaction
R	Arginine
rDNA	Ribosomal DNA
RIP	RNA immunoprecipitation
RNA	Ribonucleic acid
RNAP	Ribonucleic acid polymerase
RNAPII	Ribonucleic acid polymerase II
RNAse	Ribonuclease
RNAi	Ribonucleic acid interference
RPN	Regulartory particle non- adenosine triphosphate catalyse
RPs	Regulatory particles
RPT	Regulatory Particle Triple-A protein
rRNA	ribosomal RNA
RT	Reverse transcriptase/room temperature
S	Svedberg unit
S phase	Synthesis phase
S2P	phosphorylated at serine 2
S5P	phosphorylated at serine 5
SAHA	suberoylanilide hydroxamic acid
SAM	S-adenosyl-L-methionine
SDS	sodiumdodecylsulfate
Sec	Second
Seq	Sequencing
Ser	Serine
SET1	SET-domain containing 1
SET2	SET-domain containing 2
SETD7	SET-domain containing 7
SINEs	Short Interspersed Nuclear Elements
SIRT1	Sirtuin 1
siRNA	Small interfering RNA
shRNA	small hairpin ribonucleic acid
SMYD3	SET and MYND domain containing 3
SUV39H	suppressor of variegation 3-9 homolog
SUV420H	suppressor of variegation 4-20 homolog
SRF	Serum response factor
SRY	male sex determining region of Y
T	Thymine
TATA	TATA box (DNA)
TCR	Transcription Coupled Repair
TFIID	Transcription factor II D
TFAP2	Transcription factor AP2

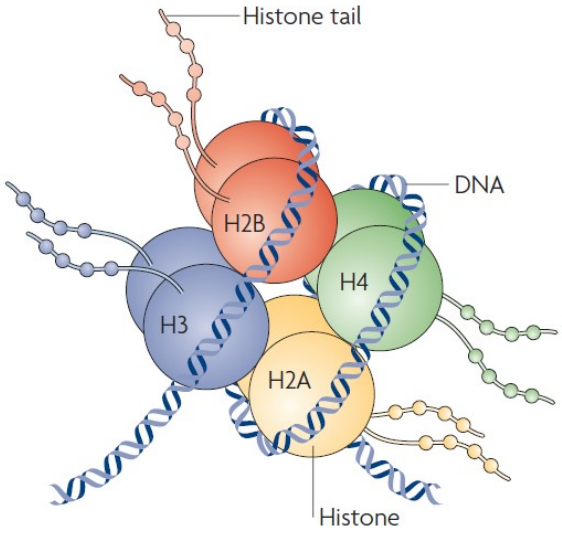
tRNA	Transfer Ribonucleic acid
TSA	Trichostatin
TSD	Target site duplication
TSS	Transcription Start Site
UPS	Ubiquitin proteasome system
UTR	Untranslated region
Vol	volume
Wt	weight
Zn	Zinc
µl	microliter
^{o}C	Degree Celsius
%	percentage
3’	3 primer end
5’	5 primer end

CHAPTER 1: General Introduction

1. Chromatin structure

In the nuclei of eukaryotic cells DNA is complexed with proteins to form nucleosomes which are the basic subunits of chromatin. Eukaryotic nucleosome is formed by 146 base pairs of DNA wrapped around octamers of the four core histone proteins H2A, H2B, H3 and H4. Each histone consists of a globular domain and a flexible N-terminal tail, which protrudes from the surface of a nucleosome (Figure 1.1A) (Kornberg, 1974; Luger, Mader, Richmond, Sargent, & Richmond, 1997). Adjacent nucleosomes are joined by a varying length of linker DNA which interacts with histone H1 triggering chromatin compaction (Woodcock, Skoultchi, & Fan, 2006). Until recently it was believed that chromatin compaction occurs through a hierarchical packaging model where nucleosomes form a 10nm thick "beads-on-a-string" conformation, which coil into a 30nm higher ordered fibre, which further compacts into 100-200nm fibres (Finch & Klug, 1976; F. Song *et al*., 2014; Tremethick, 2007; Widom, 1992; Woodcock & Dimitrov, 2001). However, recent study (Ricci, Manzo, Garcia-Parajo, Lakadamyali, & Cosma, 2015) using super resolution nanoscopy combined with computer simulation, argues against this ordered fibre structure, suggesting that nucleosomes are arranged into distinct domains called nucleosome clutches alongside the chromatin fibre. Each nucleosome clutch, which consists of heterogeneous number of nucleosomes, is separated by a nucleosome depleted region. The larger and denser clutches, contain more nucleosomes and are enriched with histone H1, forming the closed chromatin structure - heterochromatin. On the contrary, smaller and less dense clutches are associated with RNA polymerase II (RNAPII) and forms a more open chromatin structure - euchromatin (Ricci *et al.*, 2015) (Figure 1.1B).

A



B

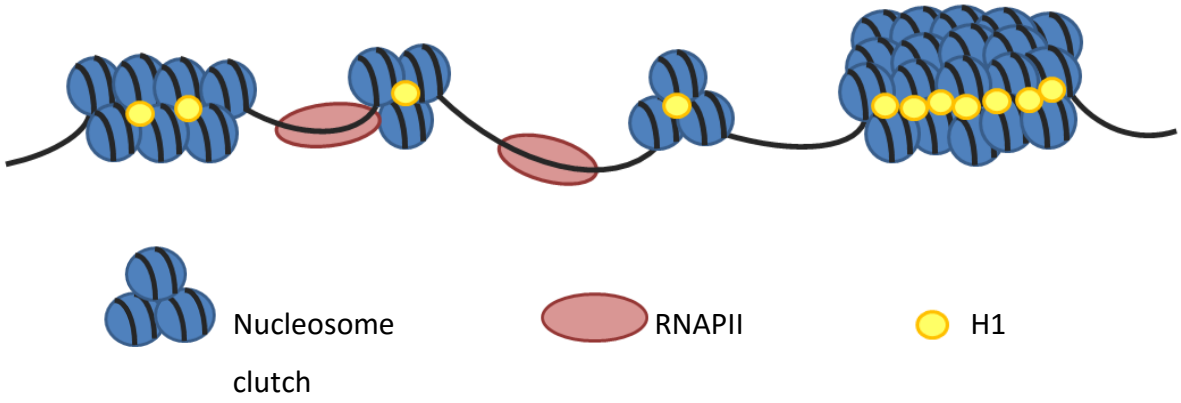


Figure 1.1: Nucleosome and chromatin structure. (A) Nucleosome: The nucleosome is formed by the wrapping of 146bp DNA around octamers of the four core histone proteins H2A, H2B, H3 and H4. Each histone consists of a globular domain and N-terminal tails which protrude from the surface of the nucleosome (B) Chromatin structure: Chromatin is formed by nucleosome clutches. Each nucleosome clutch, which consists of a varying number of nucleosomes, is separated by nucleosome depleted regions. RNAPII is preferentially associated with smaller clutches and nucleosome depleted regions representing euchromatin regions whereas H1 is enriched in larger clutches representing heterochromatin regions. A is adapted from (Tsankova, Renthal, Kumar, & Nestler, 2007). B is based on the (Ricci *et al*., 2015)

2. Heterochromatin

Originally the eukaryotic genome was first seen to be divided into two major compartments, by examining different DNA staining in an interphase cell nucleus under the microscope. Lightly stained areas of nucleus are known as euchromatin and darkly, densely stained areas comprise the heterochromatin (Heitz, 1928) (Figure 1.2).

2.1 Properties of heterochromatin

There are significant differences both structurally and functionally between heterochromatin and euchromatin. Euchromatin is rich in transcriptionally active genes whereas highly compact heterochromatin is associated with transcriptional repression. A major role of the heterochromatin structure is to prevent the accessibility of dedicated machineries involved in transcription or other DNA based processes to the underlying DNA sequences. Other characteristics of heterochromatin include a reduced recombination rate, replication in late S-phase of the cell cycle and cluster formation primarily close to the nuclear periphery (Dillon & Festenstein, 2002).

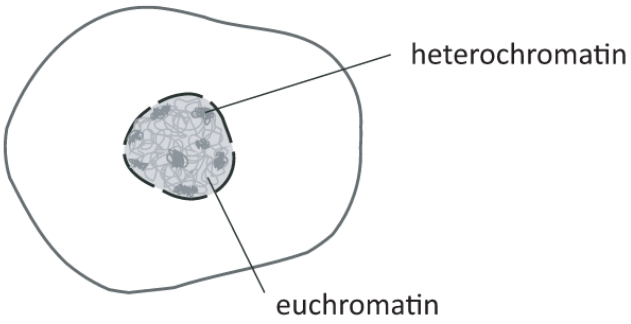


Figure 1.2: Mammalian cell nucleus (presented as grey) during interphase. Image of cells after DNA staining shows different compartment of the chromatin. The dark regions represent closed, transcriptionally silenced chromatin area (heterochromatin) whereas light region consist from transcriptional active, open chromatin area (euchromain) Adapted from (Yandim, Natisvili, & Festenstein, 2013).

Heterochromatin is further divided into facultative and constitutive heterochromatin (Natarajan & Schmid, 1971). Facultative heterochromatin is established through silencing of genes upon developmental cues therefore may form at various regions of the chromosomes. On the other hand, in most organisms, constitutive heterochromatin is considered as a more static structure, established at various repetitive DNA elements, therefore forming at the same genomic regions in all the cell types (Dillon, 2004).

2.2 Heterochromatin regulation

In multicellular organisms, heterochromatin is epigenetically regulated by various mechanisms including i) post-translational histone modifications ii) DNA cytosine methylation and iii) RNA interference.

2.2.1 Histone modifications

The histone consists of a globular domain and a flexible N-terminal tail, which protrudes from the surface of the nucleosome (Luger *et al*., 1997). Each histone can be a subject to post-translational modifications including acetylation, methylation, phosphorylation, ubiquitylation, sumoylation, ADP ribosylation, deiminitaion, proline isomerization (Bannister & Kouzarides, 2011) and recently discovered crotonylation (Sabari *et al*., 2015). These modifications occur typically at the flexible N-terminal tail of core histones and are catalysed by numerous nuclear enzymes that act mainly on the lysine (K), arginine (R) or serine (S) residues. Nonetheless, some modifications have also been recently reported to occur on the globular histone domain (Bannister & Kouzarides, 2011). The diversity of histone modifications and their possible combinations contribute to the formation of the so called "histone code" which is thought to be established and regulated by the activity of "writers" and "erasers" which install and remove the modifications respectively. The main functions of these modifications are (i) changing the overall structure of chromatin by directly

affecting the hydrophobic or electrostatic state of histones or (ii) providing binding sites for chromatin "readers" which in turn can recruit additional chromatin modifiers and remodelling enzymes (Jenuwein & Allis, 2001). Importantly, the majority of the histone modifications appear to be reversible biochemical alterations, ensuring that chromatin regulation is a dynamic process that can respond to different cellular conditions (Kouzarides, 2007). The common histone modifications and their effects on the transcription are shown in Table 1.

This thesis will cover only acetylation and methylation of the N-terminal histone tails, which represent the most studied modifications.

Histone modification	Modified residue	Transcriptional Activity
Acetylation	H3 (K9, K14, K18, K56) H4 (K5, K8, K12, K16) H2A H2B (K5, K15, K16)	Activation
Methylation	H3 (K4, K36, K79)	Activation
	H3 (K9, K27) H4 (K20)	Repression
Phosphorylation	H3 (S10)	Activation
Ubiquitination	H2A (K119) H2B (K120)	Activation Repression
Sumoylation	H4 (K5, K8, K12, K16) H2A (K125) H2B (K5, K15, K16)	Repression
Crotonylation	H3 (K18)	Activation

Table 1: Common histone modifications and there effect on the gene transcription. Adapted from (Allis, 2007) and based on (Sabari *et al*., 2015)

2.2.1.1 Histone acetylation

Histone acetylation was the first histone modification discovered present at various lysine residues of the N-terminal histone tails (Phillips, 1963). This histone modification is catalyzed by counteracting the action of two classes of enzymes with relative low substrate specificity: histone deacetylases (HDACs) and histone acetyltransferases (HATs) which remove and install acetyl groups from histones respectively. Addition of acetyl groups to the histone N-terminal tails neutralises the positive charge of lysine residues, thereby weakening the attraction between DNA and the positively charged histones. This has the effect of opening up the chromatin structure which allows easier access of the transcriptional machinery to the underlying DNA sequences (Bannister & Kouzarides, 2011; Gorisch, Wachsmuth, Toth, Lichter, & Rippe, 2005; Tse, Sera, Wolffe, & Hansen, 1998; Zentner & Henikoff, 2013). Hence acetylation is primarily associated with the transcriptionally active state of chromatin with euchromatic regions being hyperacetylated in contrast with heterochromatin regions that are hypoacetylated (Halleck & Gurley, 1981; Hebbes, Thorne, & Cranerobinson, 1988; Jeppesen & Turner, 1993; Shahbazian & Grunstein, 2007; Suka, Suka, Carmen, Wu, & Grunstein, 2001; Vaquero *et al*., 2004). Inhibition of the acetylation process or the components of the histone acetylation pathway is shown by multiple studies to cause heterochromatin disruption in mammalian cell lines (Robbins *et al*., 2005; Taddei, Maison, Roche, & Almouzni, 2001; L. P. Wu *et al.*, 2008).

Additionally, histone acetylation has also been shown to form a platform for recruitment of several bromodomain-containing proteins which can directly or indirectly regulate the transcription (Josling *et al.,* 2012, Kanno *et al.,* 2004, Dey *et al.,* 2003). For example BRD4 was shown to function as transcriptional regulator by recruiting positive transcription elongation factor complex (PTEFb) to the target sites (Jang *et al.,* 2005, Yang *et al.,* 2005) as well as interacting with elongating RNAPII (Kanno *et al.,* 2014) resulting in the release of the RNAPII from the promoter proximal pausing. However, it is noteworthy that a study has also revealed the link between histone acetylation and transcriptional repression, which was shown to be mediated through BRD4 bromodomain proteins (Wu & Chiang, 2007).

2.2.1.2 Histone methylation

Methylation of histone tails (at lysine and arginine residues) is a more complex phenomenon, compared to acetylation, since it is associated with both the active and the repressed chromatin state – depending on the type of methylation and the position of the methylated histone residue (Kouzarides, 2007). The outcome of the histone methylation is primarily creation of binding sites recognised by the chromatin 'readers' and alteration of hydrophobicity which in turn induces conformation changes of the histones (D. Y. Lee, Teyssier, Strahl, & Stallcup, 2005).

The knowledge regarding the arginine methylation, which can exist only as mono and dimethylation (Bedford & Richard, 2005) is limited and will not be discussed further in this thesis.

The lysine methylation can exist as mono, di and trimethylation. This covalent histone modification which involves the transfer of a methyl group (R-CH3) from S-adenosyl-L-methionine (SAM) to the N – terminal histone tails, is carried out by evolutionarily conserved histone lysine methyltrasferases (HKMTs). On the other hand, removal of the methyl group from histones is catalysed by histone lysine demethylases (HKDMs) (J. C. Black, Van Rechem, & Whetstine, 2012; Y. Shi & Whetstine, 2007; Shilatifard, 2006).

Unlike enzymes involved in regulation of histone acetylation, HKMTs and HKDMs are highly specific to distinct histone residues. Among the many histone methylation sites identified to date, histone H3 trimethylation of residue K4 and K36 are primarily found in euchromatic regions (Hon, Hawkins, & Ren, 2009), whereas histone H3 methylation of residue K9 and histone H4 methylation of K20 are predominantly associated with constitutive heterochromatic regions (Kourmouli *et al.*, 2004; Martens *et al.*, 2005; Saksouk, Simboeck, & Dejardin, 2015; Schotta *et al.*, 2004). More details regarding these modifications will be discussed in the following section. In contrast, the facultative heterochromatin regions are mostly linked with trimethylation on residue K27 on histone 3 (H3K27me3), which is established through EZH2 HKMT, known as part of Polycomb repressor complex 2 (PRC2). The H3K27m3 forms a platform for recruitment of PRC1 complex in order to form a compact chromatin structure therefore transcriptional silence facultative heterochromatin (Heard, 2005; Plath *et al.*, 2003; Simon & Kingston, 2013).

2.2.1.2.1 Formation and function of H3K4 methylation

Among many histone modifications that are generally associated with transcriptional activation is histone 3 lysine 4 (H3K4) methylation (Santos-Rosa *et al.*, 2002; Strahl, Ohba, Cook, & Allis, 1999). This mark exists as mono, di and tri-methylation and is catalysed by a single SET domain containing 1 (SET1) HKMTs in yeast and by a number homologues of the SET1-family in mammals including SET1A, SET1B, mixed lineage leukemia (MLL -1, -2, -3, -4) family of enzymes, SET and MYND domain containing 3 (SMYD3), SET domain-containing protein 7 (SETD7), small or homeotic discs 1 ASH1-like protein (ASH1L) (Briggs *et al.*, 2001; Brinkmeier *et al.*, 2015; Dou *et al*., 2006; Gu & Lee, 2013; Hamamoto *et al.*, 2004; J. H. Lee, Tate, You, & Skalnik, 2007; Roguev *et al.*, 2001; Soares, Radman-Livaja, Lin, Rando, & Buratowski, 2014; South, Harmeyer, Serratore, & Briggs, 2013; Yokoyama *et al.*, 2004).

Each methylation level has a distinct distribution and function. More specifically, H3K4me3 is particularly enriched at active or poised promoters (close to the TSS) of genes and is established co-transcriptionally thought that HKMTs interact with the serine 5-phosphorylated C-terminal domain of RNAPII (initiating RNAPII) (Ardehali *et al*., 2011; Krogan *et al.*, 2003; J. H. Lee & Skalnik, 2008; Ng, Robert, Young, & Struhl, 2003).

Following deposition, H3K4me3 mediates the recruitment of various factor that promote transcription, such as HATs, chromatin remodellers and the transcription factor II D (TFIID) (Clouaire, Webb, & Bird, 2014; Lauberth *et al.*, 2013; Vermeulen *et al.*, 2007; Wysocka *et al*., 2006). On the other hand H3K4me2 is found downstream of the promoter, throughout the gene body and is associated with HDACs which in turn deacetylates histones (T. Kim & Buratowski, 2009; T. Kim, Xu, Clauder-Munster, Steinmetz, & Buratowski, 2012; C. L. Liu *et al.,* 2005; Pokholok *et al.*, 2005). Finally, H3K4me1 is mainly present at active, closed or poised enhancers with as yet unknown function (Shlyueva, Stampfel, & Stark, 2014).

2.2.1.2.2 Formation and function of H3K36 methylation

One of the histone modifications that regulates chromatin structure during transcription is histone H3 lysine 36 methylation (H3K36me). In yeast, all three methylation states, mono, di and tri are established by a single SET domain containing 2 (SET2) HKMT (Strahl *et al.*, 2002).

However, the higher eukaryotes contain several HKMTs that show preference for different methylation levels. For example nuclear receptor SET domain-containing 1, 2, 3 (NSD1, -2, -3) catalyses mono and dimethylation of H3K36 generating H3K36me1 and H3K36me2 respectively, whereas SET2 has a specific trimethylase activity where it adds a methyl group to H3K36me2 thereby creating H3K36me3, which positively correlates with transcription rates (Wagner & Carpenter, 2012). Each methylation state of H3K36 has a different distribution within the cells, with an overall progressive shift from mono, to di and to tri methylation from the promoter to the 3' end of active genes (Bannister *et al.*, 2005; Bell *et al.*, 2007).

The SET2 mediated methylation of H3K36me3 is regulated by the Serine 2-phosphorylated C-terminal domain of RNAPII (elongating RNAPII), which directly interacts and recruits the SET2 HKMT to its target sites (Krogan *et al.*, 2003; B. Li, Howe, Anderson, Yates, & Workman, 2003; J. Li, Moazed, & Gygi, 2002; T. Xiao *et al.,* 2003). Subsequently, the H3K36me3 serves as a binding site for HDAC complex recruitment which in turn deacetylates histones and re-establishes the compact chromatin structure in the wake of transcribing RNAPII (Carrozza *et al.,* 2005; Joshi & Struhl, 2005; B. Li *et al.,* 2003). Furthermore, H3K36me3 also suppresses histone exchange as well as inhibiting the interaction of H3 with histone chaperones throughout the coding regions (Keogh *et al.*, 2005; Venkatesh *et al.,* 2012).

Notably, the function of H3K36 methylation is not restricted to transcriptional activation as it has also been associated with various other processes, including DNA repair and alternative splicing (Fnu *et al.*, 2011; Jha & Strahl, 2014; Kolasinska-Zwierz *et al.*, 2009; Luco *et al.,* 2010).

2.2.1.2.3 Formation and function of H4K20 methylation

Methylation of histone H4 lysine 20 is an evolutionarily conserved histone modification mark existing in mono, di and trimethylation states. Each state has a different biological function and is established by activity of distinct HKMTs (Jorgensen, Schotta, & Sorensen, 2013). Monomethylation of H4K20 is catalysed by SET8/PR-Set7 and is predominantly associated with DNA replication (Abbas *et al.*, 2010; Fang *et al*., 2002; Jorgensen *et al.,* 2007; Nishioka *et al.,* 2002; Tardat *et al.,* 2010; S. M. Wu *et al.*, 2010). On the other hand,

dimethylation of H4K20 is mediated by SUV420H1 (suppressor of variegation 4-20 homologue – isoform 1) and serves as a binding site for DNA damage recognition proteins and thereby facilitates DNA damage repair (Botuyan *et al.*, 2006; Sanders *et al.,* 2004; Schotta *et al.*, 2008). Lastly, trimethylation of H4K20 is catalysed by the activity of SUV420H2 (suppressor of variegation 4-20 homologue – isoform 2) enzymes and is considered as another "hallmark" of constitutive heterochromatin (Benetti *et al.,* 2007; Schotta *et al.,* 2004; Schotta *et al.*, 2008). A mechanism of SUV420H2 targeting to heterochromatin regions is believed to occur through synergistic interactions with multiple heterochromatin proteins (M. Hahn *et al.,* 2013; Schotta *et al.,* 2004).

The function of SUV420H2 in heterochromatin regions is not clear however evidence suggests that SUV420H2 induces chromatin compaction through interaction with heterochromatin proteins as well as cohesin recruitment to heterochromatin, a molecule important in chromatid cohesion and chromosome segregation (M. Hahn *et al.,* 2013).

2.2.1.2.4 Formation and function of H3K9 methylation

The initial step of mammalian heterochromatin formation is proposed to occur through monomethylation of free histone H3 at the lysine 9 residue which is thought to take place before incorporation into chromatin within the cytoplasm. This reaction is catalysed by Prdm3 and Prdm16 HMTs, whose concomitant depletion was shown to disrupt heterochromatin structure (Pinheiro *et al.*, 2012). The monomethylated H3K9 (H3K9me1) is then translocated from the cytoplasm to the nucleus and incorporated at heterochromatin sites where it is further di and trimethylated by H3K9-specific lysine methyl-transferases, SUV39H1/2 (suppressor of variegation 3-9 homologue; two isoforms -1 and -2) (Pinheiro *et al*., 2012; Rea *et al.*, 2000).

The activity of SUV39H is an important factor for the regulation of constitutive heterochromatin as loss of SUV39H was reported to impair mammalian heterochromatin (A. H. Peters *et al.*, 2003; A. H. F. M. Peters *et al.,* 2001).

Importantly, H3K9me3 is regarded as the "hallmark" of constitutive heterochromatin in the majority of eukaryotes and serves as a docking site for binding of heterochromatin protein (HP1) (Bannister *et al.,* 2001; Guenatri, Bailly, Maison, & Almouzni, 2004; Lachner, O'Carroll, Rea, Mechtler, & Jenuwein, 2001; Mosch, Franz, Soeroes, Singh, & Fischle, 2011).

2.2.2 Heterochromatin protein 1

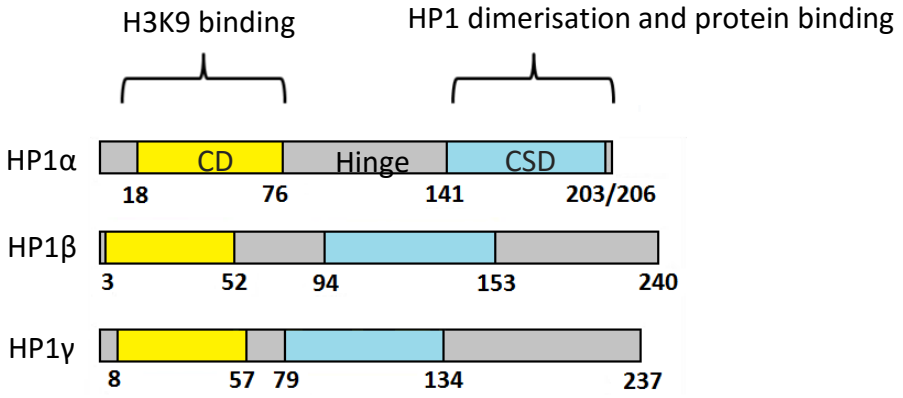
Heterochromatin protein 1 (HP1) is a highly conserved non-histone chromosomal protein, present in all eukaryotic organism, ranging from fission yeast to mammals, with the exception of budding yeast *Saccharomyces cerevisiae* (P. B. Singh *et al.,* 1991). In mammals it consists of three isoforms named HP1α, HP1β and HP1γ. Structurally, all isoforms contain an N-terminal chromodomain (CD), a hinge domain and a C-terminal chromoshadow domain (CSD) (Figure 1.3A) (Canzio, Larson, & Narlikar, 2014; Hiragami & Festenstein, 2005). The CD functions as the chromatin-binding domain as it specifically recognises H3K9 methylation, with the highest binding efficiency for H3K9me3 over H3K9me2 or H3K9me1 (Bannister *et al.,* 2001; Fischle *et al.,* 2003; Lachner *et al.,* 2001). On the other hand the CSD is responsible for HP1 dimerization and interaction with numerous proteins containing PXVXL (where P = Proline, V = Valine, L = Leucine and x is any amino acid) penta-peptide motif (Brasher *et al.,* 2000; Cowieson, Partridge, Allshire, & McLaughlin, 2000; Thiru *et al.,* 2004), HDACs (C. L. Zhang, McKinsey, & Olson, 2002), DNA methyltransferases (DNMTs) (Bachman, Rountree, & Baylin, 2001; Fuks, Hurd, Deplus, & Kouzarides, 2003; Lehnertz *et al.,* 2003) and SUV39H (Aagaard *et al.,* 1999; Bannister *et al.*, 2001; Hiragami & Festenstein, 2005; Yamamoto & Sonoda, 2003). Notably, previous reports concluded that the interaction of HP1 with SUV39H creates a positive feedback loop for formation and maintenance of heterochromatin as well as stimulating its spreading into adjacent regions (Figure 1.3B) (S. I. Grewal & Jia, 2007; Muller-Ott *et al.,* 2014; Schotta *et al.,* 2002). However, a recent study clearly showed that SUV39H1-HP1 binding is dispensable for H3K9me3 (Muramatsu *et al.,* 2013). Lastly, a variable length hinge region that connects the CD with CSD is less evolutionary conserved and was reported to binds to histone H1, DNA and RNA in order to enhance HP1 binding affinity for nucleosomes containing H3K9me3 (Badugu, Yoo, Singh, &

Kellum, 2005; Meehan, Kao, & Pennings, 2003; Muchardt *et al.*, 2002; Nielsen *et al.,* 2001; Smothers & Henikoff, 2001; T. Zhao, Heyduk, Allis, & Eissenberg, 2000).

The interaction of HP1 with chromatin is not a static but rather a dynamic interaction affected by various cellular processes including differentiation and cell cycle (Cammas, Herzog, Lerouge, Chambon, & Losson, 2004; Cheutin *et al.*, 2003; Festenstein *et al.*, 2003; Minc, Allory, Worman, Courvalin, & Buendia, 1999). For example, although H3K9me3 is present throughout the cell cycle, HP1α was reported to get evicted from heterochromatin during the mitosis (Fischle *et al.*, 2005).

Despite the structural similarities, different HP1 isoforms have distinct localization patterns within cells, with HP1α and HP1β predominantly associated with heterochromatin regions (Wreggett *et al.*, 1994), whereas HP1γ was found to be located both in euchromatic and heterochromatin regions (Fanti, Berloco, Piacentini, & Pimpinelli, 2003; Minc *et al.*, 1999; Minc, Courvalin, & Buendia, 2000). Furthermore, different HP1 isoforms also have distinct cellular functions, as different phenotypes were detected in mice deficient for each HP1 isoform (Abe *et al.*, 2011; Aucott *et al.,* 2008; Brown *et al.,* 2010; Hiragami & Festenstein, 2005; Minc *et al.,* 1999; Nielsen *et al.*, 2001). It is also noteworthy that functions of HP1 are not restricted to gene repression and heterochromatin formation, as growing evidence also indicates its role in transcriptional activation (Johansson, Stenberg, Pettersson, & Larsson, 2007; Kwon *et al.,* 2010; Mateescu, Bourachot, Rachez, Ogryzko, & Muchardt, 2008; Piacentini, Fanti, Berloco, Perrini, & Pimpinelli, 2003; Saint-Andre, Batsche, Rachez, & Muchardt, 2011; Vakoc, Mandat, Olenschock, & Blobel, 2005).

A



B

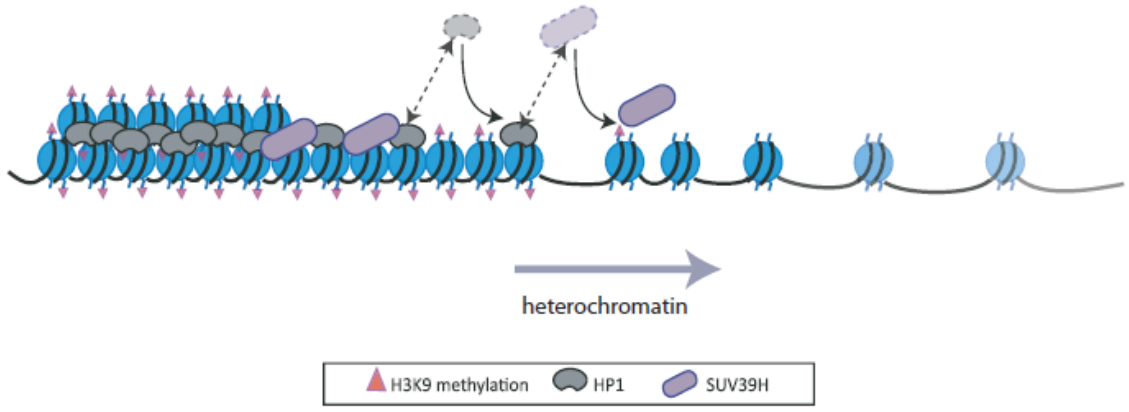


Figure 1.3: HP1 isoforms and Heterochromatin formation/spreading. (A) HP1 isoforms: Mammals contain three HP1 isoforms which contain N-terminal H3K9 binding chromodomain (CD), a linker hinge domain and a C-terminal chromoshadow domain (CSD) that is involved in HP1 dimerisation and protein binding. (B) Heterochromatin formation and spreading by combinatory activity of HP1 and SUV39H. SUV39H catalyse H3K9 methylation, which is recognised by HP1 protein. Once HP1 binds, it can cause spreading of H3K9me3 to adjacent nucleosomes via its direct association with SUV39H. In addition, HP1 via its chromoshadow domain is able to self-associate and lead to the spread of heterochromatin. Although this was a good model for heterochromatin formation, recent data argue against its veracity (Muramatsu *et al.,* 2013). B Adapted from (Yandim *et al.*, 2013).

2.2.3 DNA methylation

DNA methylation is a highly conserved epigenetic modification of DNA, present in most eukaryotic organisms that impacts upon many cellular process including heterochromatin, gene expression and genome stability (Feng *et al.*, 2010; Law & Jacobsen, 2010). In mammals it is mainly established within the CpG dinucleotide context where cytosine is covalently methylated on the fifth position (5-methylcytosine, 5mC) by activity of three distinct DNA methyltransferases, DNMT1, DNMT3a and DNMT3b (X. Cheng & Blumenthal, 2008; Holliday & Pugh, 1975; Riggs, 1975). DNMT1 is the so called maintenance DNMT regulating faithful maintenance of methylation patterns upon DNA replication (Hermann, Goyal, & Jeltsch, 2004), whereas DNMT3a and DNMT3b are *de novo* DNMTs that catalyse new DNA methylation patterns predominantly during early development and gametogenesis (Okano, Bell, Haber, & Li, 1999) .

Despite, the stable maintenance of DNA methylation patterns in somatic cells, passive or active DNA demethylation (genome-wide loss of 5mC) takes place during specific stages of development (H. Wu & Zhang, 2014).

Importantly, 60-80% of human CpGs are methylated in somatic cells, many of which occur in heterochromatin regions (Z. D. Smith & Meissner, 2013). Consistently, many chromatin repressive factors (SUV39H1/2 and HP1) were reported to associate with DNMTs (DNMT3a/3b) (Cedar & Bergman, 2009; Lehnertz *et al.*, 2003) . On the contrary, the CpG islands which are found in approximately 70% of annotated promoters, including all housekeeping and developmentally regulated genes are constantly hypomethylated (Deaton & Bird, 2011; Z. D. Smith & Meissner, 2013). Moreover DNA methylation may affect gene transcription by physically blocking the access of proteins that bind to unmethylated CpGs or attract methyl-CpG-binding domain proteins (MBDs), which in turn form docking sites for number of chromatin remodelling factor such as HDACs (Dhasarathy & Wade, 2008; P. L. Jones *et al.*, 1998b; R. P. Sharma, Gavin, & Grayson, 2010).

Notably altered DNA methylation patterns have been associated with many diseases including cancer and neurodegenerative diseases (De Zhu, 2005; K. D. Hansen *et al.*, 2011; Lopez-Serra & Esteller, 2012; H. Y. Lu, Liu, Deng, & Qing, 2013; Nishida, Kudo, Nagasaka, Ikai, & Goel, 2012; S. Sharma, Kelly, & Jones, 2010; H. Wood, 2013).

2.2.4 RNA interference

RNA interference (RNAi) is a post-transcriptional gene silencing mechanism mediated through small RNA sequences (Castel & Martienssen, 2013). One class of these sequences include small interfering RNAs (siRNAs) which were shown to be required for constitutive heterochromatin formation in the fission yeast, *S. Pombe* (S. I. Grewal & Elgin, 2007; Reinhart & Bartel, 2002; Wassenegger, 2005). During this pathway dsRNA that generate from antisense transcription of heterochromatin regions is cleaved into siRNA by endoribonuclease activity of Dicer enzyme. These siRNAs are subsequently incorporated into a multi-protein complex, (RITS- RNA-induced transcriptional gene silencing) and target the heterochromatic regions where they recruit Clr4 (SUV39H homologue) which in turn catalyses H3K9me3 therefore inducing chromatin compaction and repression (Djupedal & Ekwall, 2009; Noma *et al.*, 2004; Verdel *et al.,* 2004; T. A. Volpe *et al.,* 2002; Yu, Jih, Iglesias, & Moazed, 2014). Notably, this mechanism is mainly studied in yeast. Despite the conservation of mechanisms involved in heterochromatin formation, evidence is sparse that RNAi components play role in heterochromatin formation in mammals.

The summary of the main epigenetic factors that regulate transcriptionally repressed heterochromatin versus transcriptionally active euchromatin is shown in Figure 1.4. Importantly, local concentration of these factors and the presence of the binding sites at a given locus can greatly influence the final transcriptional state (Dillon & Festenstein, 2002; Yandim *et al.*, 2013)

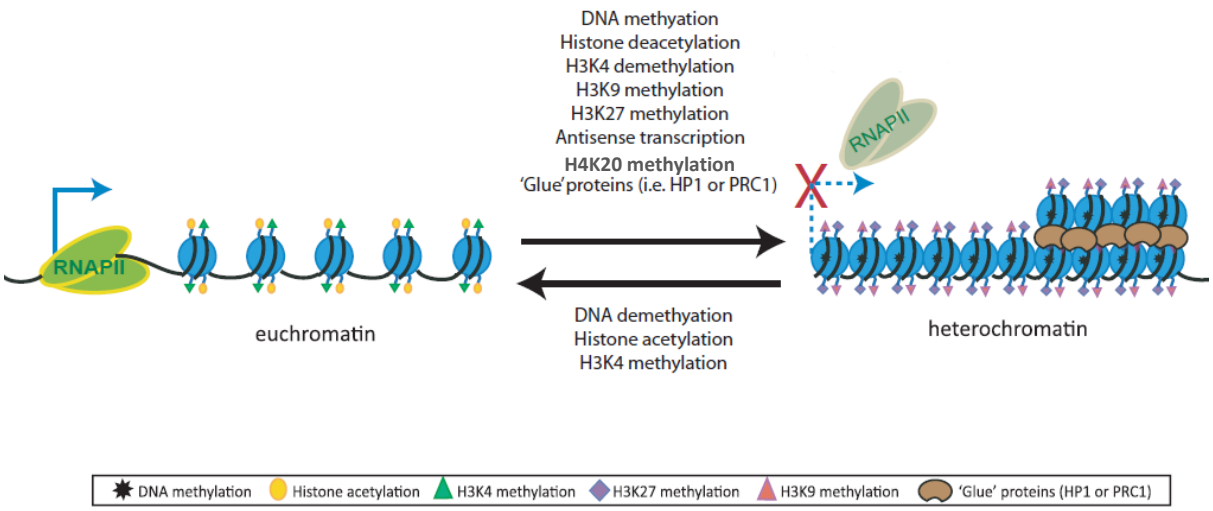


Figure 1.4: Summary of the factors regulating switching between heterochromatin and euchromatin. Euchromatin is associated with DNA histone acetylation, H3K4m and lack of DNA methylation. Heterochromatin is linked with DNA methylation, histone deacetylation, H3K4 demethylation, H4K20m, H3K9m, H3K27m and "glue" proteins including HP1 and PRC1. Adapted from (Yandim *et al.*, 2013).

3. Repetitive DNA Element

The majority of the mammalian genome is known to consist of repetitive DNA elements and non-coding sequences including intragenic and regulatory sequences (E. S. Lander *et al.*, 2001; Waterston *et al.*, 2002). More specifically, only 4% of the mouse genome comprises coding sequences, whereas 44% is repetitive and 52% noncoding DNA. Similar composition occurs in the human genome with 55% repetitive sequences. Heterochromatinisation of these elements is important for maintenance of both chromosome structure and genome integrity (Peng & Karpen, 2009; A. H. F. M. Peters *et al.,* 2001; J. M. Peters, Tedeschi, & Schmitz, 2008; Pidoux & Allshire, 2005).

Repetitive DNA elements are classified into two major categories; interspersed repetitive elements, which are singular repetitive elements that are distributed throughout the genome and tandem repetitive elements which are present in a head to tail orientation without sequences between repeating units (Martens *et al.,* 2005; Padeken *et al.,* 2015). Each of the categories is further divided into several subfamilies. Interspersed repetitive elements are mainly comprised of transfer DNA (tDNA), gene paralogues and all transposons. On the other hand tandem repetitive elements consist of ribosomal DNA repeats (rDNAs), gene tandems and satellite DNA repeats which are in turn divided into mini/micro-satellites and classic satellites. Classic satellite DNA repeats can be further subdivided based on their chromosomal distribution into telomeric, pericentromeric and centromeric satellites (Richard *et al.,* 2008). A schematic representation of different class of repetitive DNA elements is shown in Figure 1.5.

This thesis is mainly focused on transposons and satellite repeats. Hence their basic structure, function and regulation will be discussed in the following sections.

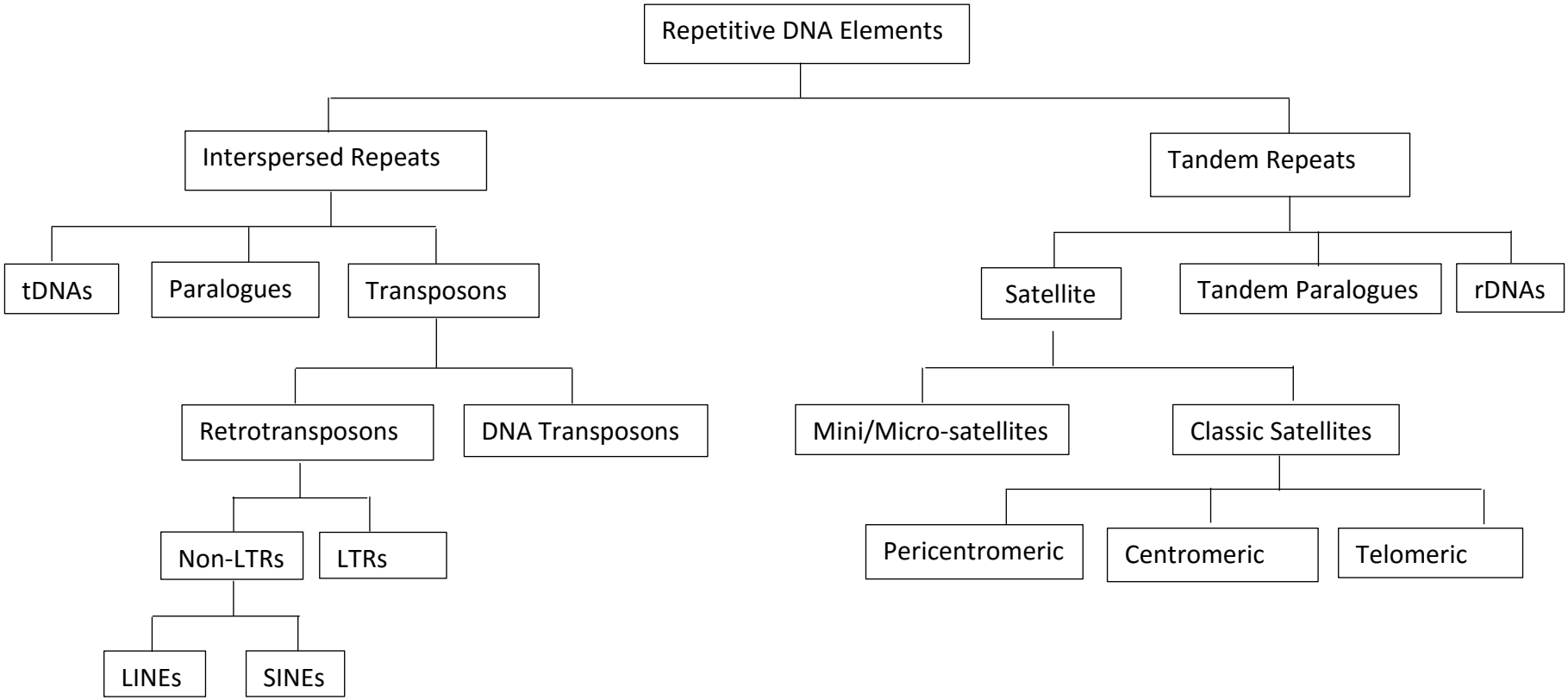


Figure 1.5: Schematic representation of DNA repetitive elements. Based on the reviews (Padeken, Zeller, & Gasser, 2015; Richard, Kerrest, & Dujon, 2008)

3.1 Transposons

Transposons are widespread mobile genomic sequences that have the ability to move to different parts of the genome through transposition. Based on their mechanism of transposition, transposons are broadly classified in two main groups, DNA transposons and retrotransposons. DNA transposons use a “cut and paste” mechanism to insert themselves into new genomic locations whereas retrotransposons use “copy and paste” mechanisms via RNA as an intermediate (Y. J. Kim, Lee, & Han, 2012; Smit, 1996; Wicker *et al.*, 2007; Zamudio & Bourc'his, 2010).

3.1.1 DNA transposons

Structurally, DNA transposons consist of a gene encoding transposase that is flanked on both sides by Inverted Terminal Repeats (ITRs). The transposase, acting as an endonuclease, recognises and binds these ITRs to catalyse the excision of the transposon from the existing locus, which is subsequently integrated into a new genomic location. The cleavage of the two DNA stands forms Target Site Duplications (TSDs) sites, which comprises a distinctive mark per DNA transposon (Levin & Moran, 2011; Munoz-Lopez & Garcia-Perez, 2010). Based on the homology of the transposases, sequence of ITR and/or TSD, DNA transposons are divided into 10 different families. Among them, Tc1 represents the most common family (Feschotte & Pritham, 2007).

3.1.2 Retrotransposons

Retrotransposons are the second major class of transposons that are able to duplicate themselves in the host genome through an RNA intermediate which is first reverse transcribed into a complementary DNA (cDNA) followed by integration into a new random genomic location. These elements are divided in two categories, retrotransposons with long terminal repeats (LTR retrotransposons) and without LTR (non-LTR retrotransposons) (Goodier & Kazazian, 2008; Levin & Moran, 2011; Padeken *et al.*, 2015). The LTR class of retrotransposons have structural and functional similarities with retroviruses (Grandbastien, 2015) and will not be discussed further in this thesis. Non-LTR retrotransposons are ancient

genetic elements that are further subdivided into long interspersed nuclear elements (LINEs) and short interspersed nuclear elements (SINEs) (Han, 2010).

3.1.2.1 Long interspersed nuclear elements (LINEs)

LINEs are the autonomous class of non-LTR retrotransposons found preferentially in AT rich regions in eukaryotic genomes (E. S. Lander *et al.*, 2001). Their size varies between 6-8 kb and they are transcribed (or are evolutionary remnants of what were previously transcribed) to RNA predominantly by RNAPII. LINEs can be further divided into several subcategories such as L1, L2 or L3. Among them LINE-L1 is the most abundant and the only active LINE element within the mammalian genome (Richard *et al.*, 2008). It constitutes 17% of the human genome out of which 99.8% appears to be inactive due to internal rearrangement, mutations and 5' end truncation (Knight, 2009; Konkel & Batzer, 2010; E. S. Lander *et al.*, 2001).

Structurally LINE-L1 elements contain the following regions: i) 5'UTR region which serves as an RNAPII promoter and transcription factor binding site, (ii) two 'open reading frames' (ORFs), *ORF1* and *ORF2*; *ORF1* encodes a chaperone protein that binds to RNA whereas *ORF2* encodes protein with endonuclease (EN) and reverse transcriptase activity (RT), both essential for cDNA synthesis and insertion respectively and iii) a 3'UTR polyadenylation site (Babushok & Kazazian, 2007; Erwin, Marchetto, & Gage, 2014) (Figure 1.6A).

The transposition of the active LINE-L1 occurs in 3 steps: i) the endonuclease nicks the target double-stranded DNA, (ii) poly(T) sequence anneals with LINE-L1 mRNA poly (A) tail at the nick site and cDNA is synthesized by reverse transcriptase and (iii) LINE-L1 mRNA gets degraded followed by second start synthesis and ligation, which results in the insertion of a full or a partial new LINE copy into a new genomic location (Deininger & Batzer, 2002; Jurka, 1997; Levin & Moran, 2011; Padeken *et al.*, 2015).

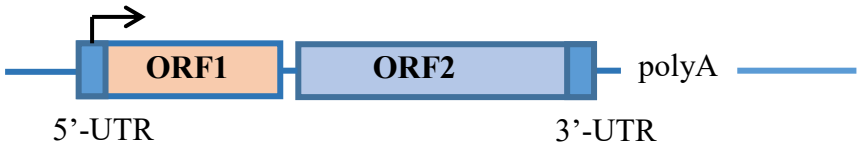
3.1.2.2 Short interspersed nuclear elements (SINEs)

SINEs are a non-autonomous class of retrotransposons found preferentially in GC rich regions in eukaryotic genomes (E. S. Lander *et al.*, 2001). These elements are short (100-400bp) pseudogenes containing RNAPIII promoters and are dependent on the molecular machinery encoded by LINE elements for their transposition in the host genome as these elements do not encode any proteins (Dewannieux, Esnault, & Heidmann, 2003; Ivics & Izsvak, 2010).

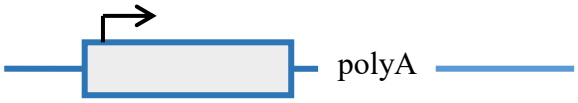
SINEs are among the most abundant repetitive elements in the mammalian genome, represented mainly by Alu and MIR in primates and B1 (a homologue to Alu), B2, and ID in rodents (Zamudio & Bourc'his, 2010). Both Alu and B1 elements consist of two and one monomers respectively (Figure 1.6B) and are products of a 7SL RNA gene duplication which occurred 80 million years ago, whereas the remainder is derived primarily from tRNA genes (Daniels & Deininger, 1985; Kramerov & Vassetzky, 2005; Tsirigos & Rigoutsos, 2009).

A summary of the structure, the length and the copy number of LINEL1 and SINEB1 elements in the mouse genome is shown in Figure 1.6.

A



B



C

	Full-length repeat unit	Copy number
LINE L1	~6 kb	>500 000
SINE B1	300 bp	>500 000

Figure 1.6: Overview of characteristics of non-LTR retrotransposons LINE L1 and SINE B1 in the mouse genome. (A) Structural organisation of LINE L1 element. LINE L1 consists of a 5'UTR which serves as an RNAPII promoter, two ORFs that encode chaperone proteins that bind to RNA, an endonuclease (EN) and a reverse transcriptase (RT) and a polyA tail. (B) Structural organisation of SINE B1 element. SINE B1 is a short pseudogene with encoding no proteins, it contains an RNAPIII promoter and polyA tail. (C) Table illustrating the repeat unit length and the copy number of LINE L1 and SINE B1 elements. C was adapted and modified from (Martens *et al.*, 2005).

3.1.3 Regulation of Retrotransposons

Although the majority of retrotransposons are inactive and unable to transpose due to mutations or truncations, some of them are still active and affect the mammalian genome in many different ways including altering gene expression and splicing, generating insertion mutations, creating and repairing DNA double-strand breaks, generating genomic rearrangements (such as deletions, duplications and inversions) (Cordaux & Batzer, 2009). All these effects may contribute to genomic evolution; however they can also pose a potential threat to genomic stability. Therefore it is not surprising that retrotransposition has been associated with many diseases, such as cancer, β-thalassemia, Duchenne muscular dystrophy, cystic fibrosis (Belancio, Hedges, & Deininger, 2008; Callinan & Batzer, 2006; J. M. Chen, Stenson, Cooper, & Ferec, 2005; Deininger & Batzer, 1999; Gualtieri *et al.*, 2013; Lanikova *et al.*, 2013; Musova *et al.,* 2006; Schneider, Duffield, Symer, & Burns, 2009; K. Yoshida, Nakamura, Yazaki, Ikeda, & Takeda, 1998).

In order to protect the genome from these deleterious effects, cells have acquired several epigenetic mechanisms to prevent mobilization of retrotransposons. Interestingly, these mechanisms differ in cycling and postmitotic cells. In somatic cells, DNA methylation is the primary driving factor for the silencing, with generally these elements being hypemethylated whereas histone modifications play only a minor role (Bierhoff, Postepska-Igielska, & Grummt, 2014; Hutnick, Huang, Loo, Ma, & Fan, 2010; O'Donnell & Burns, 2010; Rollins *et al.,* 2006; Teneng, Montoya-Durango, Quertermous, Lacy, & Ramos, 2011; Turelli *et al.,* 2014; Walsh, Chaillet, & Bestor, 1998).

However in postmitotic cells, in addition to DNA methylation, long noncoding RNAs (lncRNAs) were shown to trigger upregulation of H4K20me3 via recruitment of SUV420H to the locus (Bierhoff, Dammert, *et al.*, 2014). Some evidence also suggests RNA dependent silencing of retrotransposons (Faulkner *et al.,* 2009). For example in human cells bidirectional transcripts from LINE L1 elements were revealed to generate siRNAs that suppress retrotransposition by an RNAi mechanism (N. Yang & Kazazian, 2006). Additionally in the germline and in human induced pluripotent stem cells (iPSCs) Piwi-interacting RNA (piRNA) that derives from retrotransposon transcripts were shown to associate with PIWI proteins and mediate de novo DNA methylation and subsequent silencing of

retrotransposons (Aravin *et al.,* 2008; De Fazio *et al.,* 2011; Kuramochi-Miyagawa *et al.,* 2008; Marchetto *et al.,* 2013).

Importantly, the expression of retrotransposons seems to be dynamic and stage specific according to a recent study, where LTR (IAP) and non-LTR (LINE L1) retrotransposons were shown to reactivate in both parental genomes after fertilization through gain of the active H3K4me3 mark and are repressed during early mouse embryogenesis (Fadloun *et al.,* 2013).

3.2 Satellite repeats

Satellite repeats are characterized by large tandem repeats present as array blocks in the genome with lengths reaching several millions of nucleotides. These elements are categorised into three groups based on the length of the repeat unit. The first group consists of the classic satellites, which is further divided into telomeric, centromeric and pericentromeric repeats. The second and third category of satellite repeats consists of minisatellites and microsatellites respectively (Richard *et al.*, 2008). The length of minisatellites repeat units is 10-60bp (Jeffreys, 1997; Jeffreys, Wilson, & Thein, 1985) whereas microsatellites are shorter with a repeat unit between 1-6bp long (Abdul-Muneer, 2014; Ellegren, 2000).

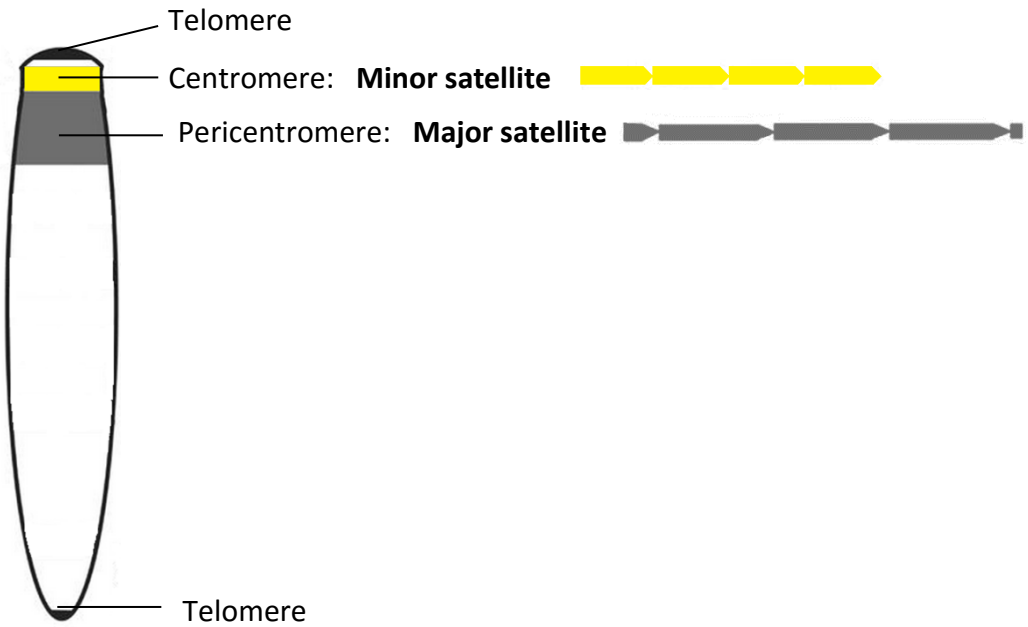
Telomeric repeats are comprised of a highly conserved hexameric 5'-TTAGGG-3' repeat sequence whose array constitutes the ends of eukaryotic chromosomes, the telomeres (Meyne, Ratliff, & Moyzis, 1989; Moyzis *et al.,* 1988; Wicky *et al.,* 1996). This specific DNA motif is recognised by conserved DNA binding machineries that are recruited to telomeres and regulate their structure and function (Y. Huang, Liang, Liu, Huang, & Songyang, 2014; Palm & de Lange, 2008; Schoeftner & Blasco, 2009).

Centromeric repeats are present at the centromere, whereas pericentromeric repeats form the regions flanking the centromeres called pericentromeres (Eymery, Callanan, & Vourc'h, 2009). In contrast to the telomeric repeat, the DNA sequences of centromeric and

pericentromeric repeats are not conserved and differ significantly between species or even between chromosomes of the same species (Allshire & Karpen, 2008; Heslop-Harrison, Brandes, & Schwarzacher, 2003; Saksouk *et al.,* 2015). For example the human centromere is comprised of arrays of 171 bp α-satellite repeats, whereas pericentromeres contain array of chromosome specific pericentromeric repeats including satellites I, II and III, β-satellite and γ-satellite (J. H. Kim *et al.,* 2009; M. K. Rudd, Wray, & Willard, 2006; Vissel, Nagy, & Choo, 1992). On the other hand in mice the centromeric and pericentromeric repeats consist of minor satellite repeats and A/T-rich major satellite repeats respectively (Guenatri *et al.,* 2004; Komissarov, Gavrilova, Demin, Ishov, & Podgornaya, 2011; Martens *et al.,* 2005). A summary of the location, structure, the length and the copy number of major and minor satellites in the mouse genome is shown in the Figure 1.7.

Although telomeres have an important role in protecting chromosomal integrity (Murnane, 2012; O'Sullivan & Karlseder, 2010), this thesis is mainly focused on centromeres and pericentromeres.

A



B

	Full-length repeat unit	Copy number
Major satellite repeat	234 bp	>200 000
Minor satellite repeat	123 bp	>50 000

Figure 1.7: Overview of characteristics of classic satellite repeats in the mouse genome. (A) Schematic representation of the location and the general organisation of major and minor satellite repeats in a mitotic mouse chromosome. (B) Table illustrating the repeat unit length and the copy number of major and minor satellite repeats. Adapted and modified from (Martens *et al.*, 2005).

3.3 Regulation of centromeres and pericentromeres

Centromeres and pericentromeres have distinct chromatin structures, both of which are important for kinetochore assembly and proper chromosomal segregation during cell division (Ekwall, 2007; Fukagawa & Earnshaw, 2014; Rosic, Kohler, & Erhardt, 2014; Vos, Famulski, & Chan, 2006; Westhorpe & Straight, 2013).

3.3.1 Centromeres

Centromeres contain the centromere-specific histone H3 variant CENP-A which consists of a structural as well as functional foundation for the kinetochore formation (B. E. Black & Bassett, 2008; Guse, Carroll, Moree, Fuller, & Straight, 2011; Hori, Shang, Takeuchi, & Fukagawa, 2013; Perpelescu & Fukagawa, 2011; Warburton *et al.*, 1997). This histone variant is periodically interrupted by nucleosomes containing H3K4me2 that is normally associated with open chromatin structures (Bergmann *et al.,* 2011; Stimpson & Sullivan, 2011; Sullivan & Karpen, 2004). Furthermore H4K20me1 has been recently identified to be an important factor for functional centromere formation (Hori *et al.,* 2014). Additionally these domains generally lack heterochromatin histone modifications, lack histone acetylation and contain DNA methylation, giving the centromere an unusual chromatin structure that differs from both euchromatin and heterochromatin (Choy, Acuna, Au, & Basrai, 2011; Gopalakrishnan, Sullivan, Trazzi, Della Valle, & Robertson, 2009; Jeppesen, Mitchell, Turner, & Perry, 1992; Luo & Preuss, 2003; Okano *et al.*, 1999; Sullivan & Karpen, 2004).

Importantly, centromeres that consist of arrays of centromeric satellite repeats have been reported to be transcriptionally active in multiple organisms, including plants, vertebrates and invertebrates. The regulation of the transcription is not clear; however these non-coding transcripts are believed to play an important role in centromere formation and function (Bouzinba-Segard, Guais, & Francastel, 2006; F. L. Chan & Wong, 2012; Choi *et al.*, 2011; Gent & Dawe, 2012; H. R. Lee, Neumann, Macas, & Jiang, 2006; Y. X. Li & Kirby, 2003; Ohkuni & Kitagawa, 2011; Pezer & Ugarkovic, 2008; Sadeghi, Siggens, Svensson, & Ekwall, 2014; Scott, 2013; Topp, Zhong, & Dawe, 2004; L. H. Wong *et al.*, 2007; Yan *et al.*, 2006). For

example transcripts from minor satellite repeats and α-satellite repeats in mouse and human respectively were revealed to facilitate the recruitment of centromeric proteins such as CENP-C, INCENP, Survivin and aurora B kinase (AUBK) to centromeres (F. L. Chan *et al.*, 2012; Y. Q. Du, Topp, & Dawe, 2010; Ferri, Bouzinba-Segard, Velasco, Hube, & Francastel, 2009; L. H. Wong *et al.*, 2007).

Moreover, some studies also suggest that the balance of the centromeric transcription is equally important factor for centromere activity. Loss of centromeric transcript was accompanied by defective incorporation of CENP-A in centromeres during mitotic exit leading to a gradual centromere inactivation (Bergmann *et al.,* 2011; F. L. Chan *et al.,* 2012). Similarly, overexpression of these transcripts caused displacement of CENP-A as well as failure of further recruitment of these molecules to centromere resulting to centromere inactivation (Bergmann *et al.,* 2012).

3.3.2 Pericentromeres

Pericentromeres are regions of the chromosomes that display constitutive heterochromatin structure. It is though vital for these regions to be maintained in a highly condensed chromatin state in order to provide a structural support for the centromere and to ensure genome stability in eukaryotic cells (Allshire, Nimmo, Ekwall, Javerzat, & Cranston, 1995; Kellum & Alberts, 1995; A. H. Peters *et al.*, 2001; Vos *et al.,* 2006).

As mentioned in the previous section, pericentromeric regions are comprised of arrays of pericentromeric satellite repeats without conservation of their DNA sequence among different species. However, the common features between different pericentromeric regions are (i) the repetitive nature of these elements that might be an important factor for heterochromatin formation by an unknown mechanism (Garrick, Fiering, Martin, & Whitelaw, 1998; Henikoff, 1998) and (ii) the combination of specific repressive epigenetic modifications, including DNA methylation, histone hypoacetylation, H3K9me3, H3K64me3, H4K20me3 and associated HP1α/β proteins that cause pericentromeric heterochromatinisation (Bannister *et al.,* 2001; S. I. S. Grewal & Moazed, 2003; Lange *et al.,*

2013; Lehnertz *et al.*, 2003; Probst & Almouzni, 2011; Saksouk *et al.,* 2015; Schotta *et al.,* 2004) .

Recent studies have confirmed the transcription of pericentromeric satellite repeats, albeit the heterochromatinisation of the locus (Enukashvily & Ponomartsev, 2013; Eymery, Horard, *et al.,* 2009; Hall, Mitchell, & O'Neill, 2012; Rosic *et al.,* 2014). Compared to the total number of genomic pericentromeric repeats, only a small subset (2% to > 10%) is believed to be transcribed, suggesting that transcription occurs as a rare event (Saksouk *et al.,* 2015). Furthermore, this transcription was shown to be mediated by RNAPII (Djupedal *et al.,* 2005; Kato *et al.,* 2005; J. Lu & Gilbert, 2007) and derived from both strands generating sense (in mice: T-rich; in humans: GGAAT) or antisense (in mice: A-rich; in humans: ATTCC) non-coding transcripts (Bulut-Karslioglu *et al.,* 2012; Jolly *et al.*, 2004b; Rudert, Bronner, Garnier, & Dolle, 1995).

Generally the transcription in cells is regulated by transcription factors that bind to the promoter regions of the target elements (Jolma *et al.,* 2013; T. I. Lee & Young, 2013; Voss & Hager, 2014). Although the pericentromeric satellite repeats do not contain promoter elements, several transcription factors have been shown to bind to these repeats. In mice, the transcription factors Pax3 and Pax6 were discovered to repress the transcription from both strands by directly binding to the pericentromeric major satellite repeats (Bulut-Karslioglu *et al.,* 2012). The same study showed that simultaneous depletion of both transcription factors resulted in dramatic upregulation of major satellite repeats transcription accompanied by loss of repressive H3K9me3 and H4K20me3 marks from pericentromeric heterochromatin and impaired chromosome segregation (Bulut-Karslioglu *et al.,* 2012). Furthermore, transcription factors HSF1 and TONEBP were shown to bind to human pericentromeric Satellite III repeats on chromosome 9 and subsequently upregulate the transcription upon heat and osmotic cellular stress respectively (Jolly *et al.*, 2002; Jolly, Morimoto, Robert-Nicoud, & Vourc'h, 1997; Valgardsdottir *et al.,* 2005; Valgardsdottir *et al.*, 2008). Additional transcription factors, including Snail1, (Millanes-Romero *et al.,* 2013), SALL1 (Yamashita, Sato, Asashima, Wang, & Nishinakamura, 2007), KAP1 (also known as TIF1β or TRIM28) (Bartova, Pachernik, Kozubik, & Kozubek, 2007; Matsui *et al.,* 2010) and

GFi1B were also detected to bind to mouse pericentromeric heterochromatin (Vassen, Fiolka, & Moroy, 2006).

3.3.3 Pericentromeric transcription

In mammalian systems low levels of pericentromeric satellite repeats transcription has been detected under various physiological conditions, including cell cycle, senescence, development and differentiation.

A study in 2007 revealed that transcription of pericentromeric satellite repeat in mouse mammary gland cell line is regulated by the cell cycle (J. Lu & Gilbert, 2007). The author's identified two distinct populations of major satellite repeat transcripts. The first population consisted of large (> 1 kb), heterogeneous transcripts synthesized during the late G1 and early S phase of the cell cycle. This population was suggested to be involved in preparing heterochromatin for reassembly at the replication fork. On the other hand the second population was observed exclusively during mitosis consisting of transcripts smaller than 200 nucleotides. This second population was suggested to function in heterochromatin formation by recruiting the HP1 back to pericentromeric heterochromatin followed mitosis (J. Lu & Gilbert, 2007). This was concluded based on the facts that HP1 is (i) evicted from the pericentromeric heterochromatin during mitosis (Fischle *et al.*, 2005; R. Wu, Singh, & Gilbert, 2006) and (ii) tethered to heterochromatin by an RNA molecule (Maison *et al.,* 2002).

Other studies have also indicated a link between replicative senescence and transcriptional activation of pericentromeric satellite repeat which was accompanied by chromosome decondensation and reduced level of DNA methylation (Enukashvily, Donev, Waisertreiger, & Podgornaya, 2007; Gaubatz & Cutler, 1990).

Furthermore, the transcription of the pericentromeric repeats was shown to be developmentally regulated in the mouse genome. For example in mouse embryos accumulation of pericentromeric transcripts were detected in the central nervous system whereas in adult mice the expression was restricted to liver and testis (Rudert *et al.*, 1995). Moreover, in two cells stage embryos, a burst of pericentromeric repeats transcription was

found to be strand and parental specific leading to chromocentre formation (Probst *et al.,* 2010) which is a nuclear structure formed from the clustering of pericentromeric heterochromatin from multiple chromosomes (Guenatri *et al.,* 2004) (Figure 1.8). Additionally, during the epithelial-to-mesenchymal transition step of embryonic development, major satellite repeat transcription was shown to be downregulated with transient release of HP1α from pericentromeric heterochromatin. The observed repression was attributed to binding of the Snail1 transcription factor to pericentromeric heterochromatin which in turn recruits the H3K4me3 specific deaminase LOXL2 corepressor, in order to oxidize H3 and repress major satellite transcription (Millanes-Romero *et al.,* 2013).

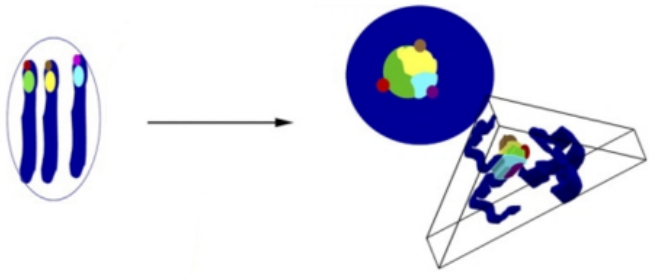


Figure 1.8: A schematic representation of the chromocentre formation in an interphase cell nucleus by three individual chromosomes. Each chromosome contains pericentromeric satellite (large dots) and centromeric satellite (small dots) regions. Pericentromeric satellites from different chromosome associate in clusters forming chromocentre, whereas centromeric satellites surround the chromocentre as separated domains. Adapted from (Guenatri *et al.*, 2004).

Finally aberrant overexpression of pericentromeric satellite repeat has been detected in numerous pathological conditions, including cellular stress (Jolly *et al.,* 2004a; Rizzi *et al.,* 2004; Valgardsdottir *et al.,* 2008), cancer (Eymery, Horard, *et al.,* 2009; Narayan *et al.,* 1998; Qu, Dubeau, Narayan, Yu, & Ehrlich, 1999; Ting *et al.,* 2011) and several genetic disorders (Hassan, Norwood, Gimelli, Gartler, & Hansen, 2001; Miniou *et al.,* 1994; Shumaker *et al.,* 2006).

4. Cellular stress and transcription of pericentromeric repeats

4.1 Cellular stress

Cellular functions are required to be maintained in a fine balance for normal function and survival. This equilibrium is closely regulated with many factors that detect slight variation and induce homeostatic compensation (e.g temperature). However cells often become stressed when the ability to compensate is surpassed. Depending on the nature and the intensity of the stressor, that can be either environmental or a pathological factor, cells respond by various mechanisms to protect from stress induced damage. A main mechanism includes activation of heat shock transcription factors (HSFs) which in turn mediates drastic transcriptional upregulation of heat shock gene expression leading in synthesis of heat shock proteins (HSPs) (Morimoto, 1993; Welch, 1992). Notably, there are also several other mechanisms activated for specific stressors such as activation of p53 upon exposure to UV (Bruins *et al.*, 2004; Kapoor & Lozano, 1998; Latonen, Taya, & Laiho, 2001). However, this thesis will focus only on the response mediated by the heat shock pathway.

4.1.1 Heat shock proteins (HSPs)

Heat shock proteins are a highly conserved family of proteins that function as molecular chaperones to maintain intracellular protein homeostasis by facilitating accurate folding of misfolded proteins and preventing protein aggregation. Additionally these proteins function as cellular lifeguards by blocking several steps of the apoptotic pathway (Schmitt, Gehrmann, Brunet, Multhoff, & Garrido, 2007). HSPs are divided into five groups based on their molecular weight: HSP100, HSP90, HSP70, HSP60 and the small HSPs (Liang & MacRae, 1997; Waters, Lee, & Vierling, 1996). Each group contains highly conserved regulatory heat shock sequence elements (HSEs) on their proximal promoter regions which serve as binding sites for HSFs (Amin, Ananthan, & Voellmy, 1988; Amin, Fernandez, Ananthan, Lis, & Voellmy, 1994; Pelham, 1982; Perisic, Xiao, & Lis, 1989; H. Xiao & Lis, 1988).

4.1.2 Heat shock transcription factors (HSFs)

Heat shock transcription factors are a family of transcription factors best known on regulating the expression of genes involved in the stress response. In mammals the HSF family consists of HSF1, HSF2, HSF3 and HSF4 (Fujimoto & Nakai, 2010; Pirkkala, Nykanen, & Sistonen, 2001) as well as more recently identified HSFY/HSFY2 and HSFX (Figure 1.9) (Bhowmick, Takahata, Watanabe, & Satta, 2006; Kichine *et al.*, 2012; Kinoshita *et al.,* 2006; Shinka *et al.,* 2004; Tessari *et al.,* 2004).

Structurally, the HSF monomer contains a helix-loop-helix DNA binding domain (DBD) oligomerization domain (HR-A and HR-B) and a C-terminal heptad repeat C domain (HR-C) (Figure 1.9) (Akerfelt, Morimoto, & Sistonen, 2010; Littlefield & Nelson, 1999). The DBD is the most conserved domain within the HSF family and recognises HSEs throughout the genome (Harrison, Bohm, & Nelson, 1994; S. J. Kim, Tsukiyama, Lewis, & Wu, 1994; Littlefield & Nelson, 1999; Vuister *et al.*, 1994). The oligomerization domain consists of an array of hydrophobic heptad repeats A and B and mediates HSF homo or heterotrimerization upon its activation (Peteranderl & Nelson, 1992; Rabindran, Haroun, Clos, Wisniewski, & Wu, 1993; Sorger & Nelson, 1989). Lastly, the HR-C domain suppresses spontaneous HSF trimerization in the absence of stimuli (Y. Chen, Barlev, Westergaard, & Jakobsen, 1993; Rabindran *et al.,* 1993). Notably, while the DRB domain is found in all members of the HSF family, the HR-C domain is completely absent from HSF4 (Nakai *et al.,* 1997), a factor which is involved in differentiation and has no effect on the stress response (Fujimoto *et al.,* 2004; Min, Zhang, Moskophidis, & Mivechi, 2004; X. H. Shi *et al.,* 2009). Furthermore, HSFY/HSFY2 and HSFX with yet unknown cellular function lack both HR-C and oligomerization domains (Shinka *et al.,* 2004).

Among different members of the HSF family, HSF1 is believed to be the main stress response regulator by helping to preserve cellular integrity during stress conditions (McMillan, Xiao, Shao, Graves, & Benjamin, 1998; Vihervaara & Sistonen, 2014). HSF1 is a ubiquitously expressed phosphoprotein predominantly present in the nucleus (Jolly *et al.,* 1997; Khaleque *et al.,* 2008; Mercier, Winegarden, & Westwood, 1999; Vujanac, Fenaroli, & Zimarino, 2005). The activity of this protein is regulated by various factors and post-

translational modifications including phosphorylation, acetylation and sumoylation (Figure 1.10A) (Y. M. Xu, Huang, Chiu, & Lau, 2012)

A

B

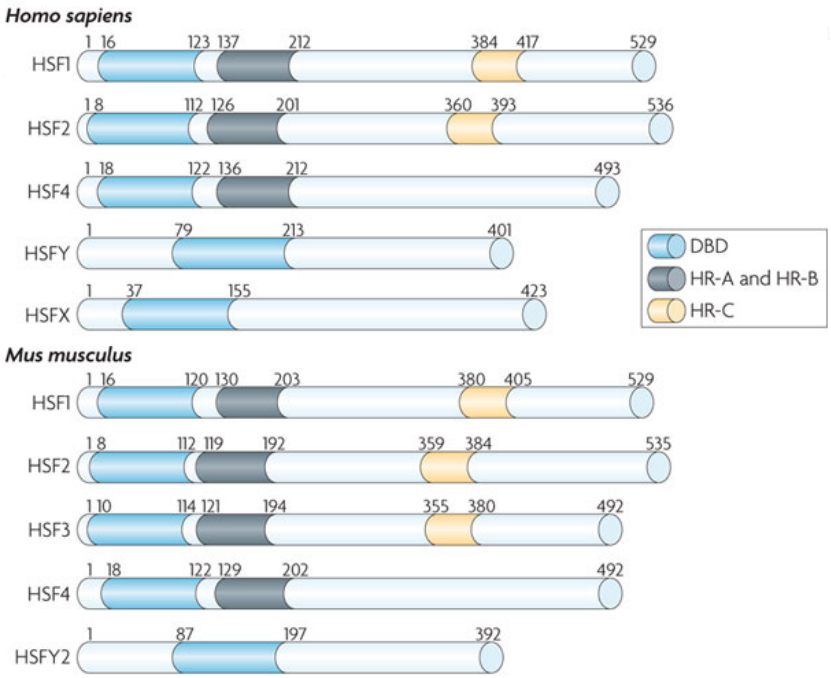


Figure 1.9: Members of human and mouse HFS family with schematic representation of the functional domains. (A) HSF family in human is comprised of HSF1, HSF2, HSF4 and recently identified HSFY and HSFX. (B) HSF family in mouse consists of HSF1, HSF2, HSF3, HSF4 and HSFY2. The functional domains of HSF1-4 members of the mammalian HSF family (exception of human HSF4) are a highly conserved DNA binding domain (DBD), oligomerization heptad repeat A and B (HR-A and HR-B) domain and C-terminal heptad repeat C domain (HR-C). Adapted from (Akerfelt *et al.*, 2010).

In the absence of cellular stress the HSF1 monomer, known to be constitutively phosphorylated on Ser303 and Ser307 residues (Chu, Zhong, Soncin, Stevenson, & Calderwood, 1998; Kline & Morimoto, 1997; Knauf, Newton, Kyriakis, & Kingston, 1996) forms an inactive complex by weakly interacting with heat shock proteins including HSP90 (Ali, Bharadwaj, O'Carroll, & Ovsenek, 1998; Zou, Guo, Guettouche, Smith, & Voellmy, 1998).

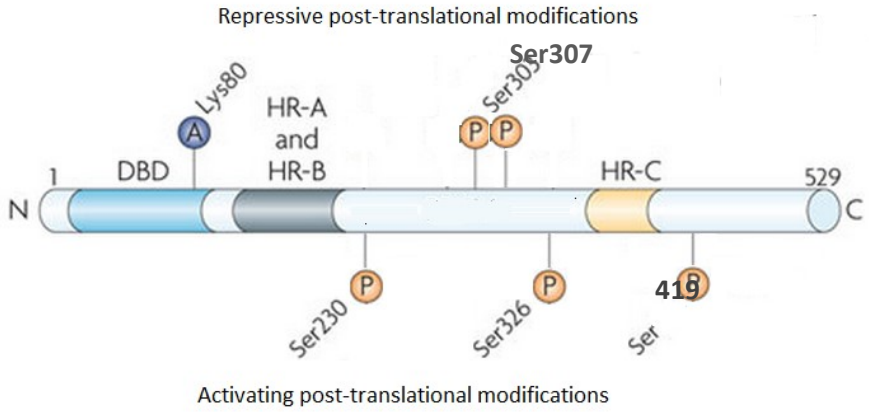
In response to stress HSF1 becomes activated by (i) dissociating from the repressed complex, (ii) forming a trimer and (iii) acquiring multiple PTMs including phosporylation on multiple serine residues (up to 12) such as Ser230, Ser326 and Ser419 (Akerfelt *et al.*, 2010; Guettouche, Boellmann, Lane, & Voellmy, 2005; Holmberg *et al.,* 2001). The activated trimer binds to the HSE of the stress-responsive gene, recruits coactivators and induces their transcription (Fujimoto *et al.,* 2012; Petesch & Lis, 2012; S. T. Smith *et al.,* 2004; Takii *et al.,* 2015b; D. M. Xu, Zalmas, & La Thangue, 2008; Zobeck, Buckley, Zipfel, & Lis, 2010) (Figure 1.10B).

However, this transcription is a transient process and upon synthesis of the target proteins the HSF1 is deactivated and released from DNA. The deactivation occurs through a negative feedback loop, where newly synthesized HSP70 and HSP40 bind and inhibit the activity of HSF1 (Abravaya, Myers, Murphy, & Morimoto, 1992; Baler, Welch, & Voellmy, 1992; Y. H. Shi, Mosser, & Morimoto, 1998; Sugito *et al.*, 1995; Vjestica, Zhang, Liu, & Oliferenko, 2013). On the other hand the release of HSF1 from the DNA is triggered by acetylation of the Lys80 residue in the DBD domain (Figure 1.10B) (Westerheide, Anckar, Stevens, Sistonen, & Morimoto, 2009).

Despite the well–established role of HSF1 in regulation of heat shock response, growing evidence also suggests that HSF2 can greatly influence the expression of heat shock target genes in an HSF1 dependent manner (Bjork & Sistonen, 2010; Ostling, Bjork, Roos-Mattjus, Mezger, & Sistonen, 2007; Sandqvist *et al.*, 2009).

Finally it is noteworthy that in addition to cell stress, the functions of HSFs are implicated during immune response (Inouye *et al.,* 2004; I. S. Singh, He, Hester, Fenton, & Hasday, 2004; V. Singh & Aballay, 2006; M. Song, Pinsky, & Kellum, 2008; Y. Xie, Chen, Stevenson, Auron, & Calderwood, 2002) and development (eg. brain development, oogenesis, spermatogenesis) (Akerfelt *et al.,* 2008; Y. H. Chang *et al.,* 2006; Fujimoto *et al.,* 2004; Kallio *et al.,* 2002; Min, Han, Lee, Kim, & Park, 2000; Rallu *et al.,* 1997; Takaki *et al.,* 2006; G. H. Wang *et al.,* 2004; G. H. Wang, Zhang, Moskophidis, & Mivechi, 2003).

A



B

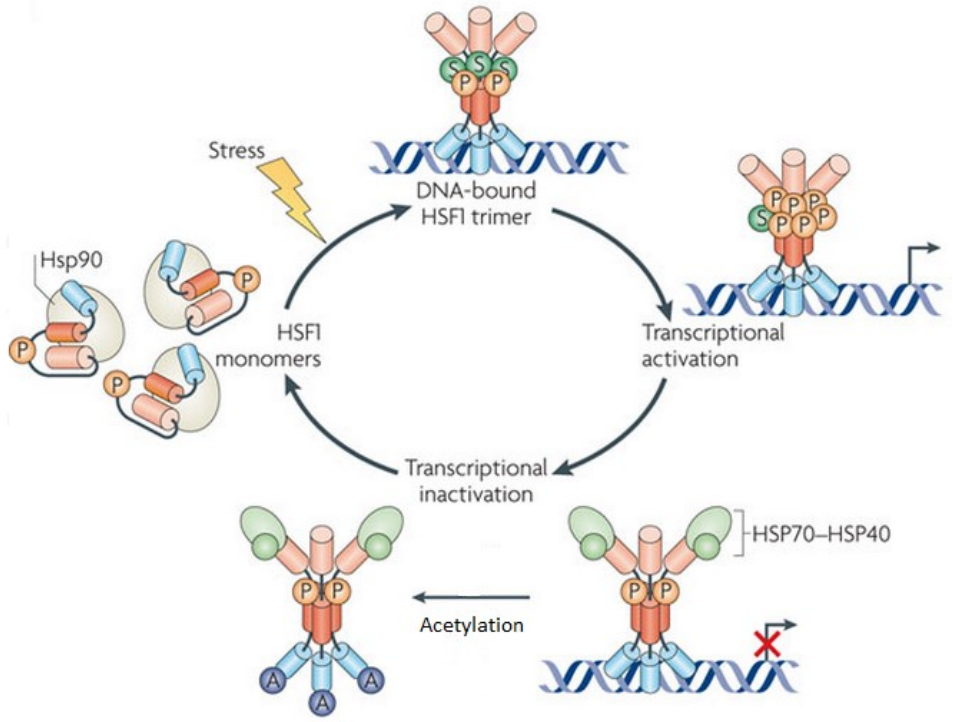


Figure 1.10: Representative HSF1 post-translational modifications (PTMs) and HSF1 activation cycle. (A) HSF1 is subject to multiple PTMs including phosphorylation (P), acetylation (A) and sumoylation (S). There modifications act as repressors or activators depending on the residue and the type of modification. Repressed HSF1 monomer is constitutively phosphorylated on Ser303 and Ser307 residues. In response to cellular stress, HSF1 becomes hypephosporylated. Among these sites phosphorylation of residues Ser230, Ser326 and Ser419 are the most studied. Acetylation of Lys80 releases the HSF1 complex from the DNA. (B) In the absence of cellular stress the HSF1 monomer forms an inactive complex by interacting with HSP90. Upon stress HSF1 dissociates from the complex, trimerizes, acquires multiple PTMs and binds to target regions inducing their transcriptional activation. The transcriptional activation is terminated by negative feedback loop from HSPs and HSF1 acetylation which releases the trimer from the DNA. Adapted and modified from (Akerfelt *et al.*, 2010).

4.2 Transcription of pericentromeric satellite repeats upon cellular stress

Numerous cellular stress conditions, including heat shock, hyperosmosis, exposure to ultraviolet light as well as to various hazardous chemicals and heavy metals were shown to cause transcriptional activation of pericentromeric satellite repeats (Eymery, Callanan, *et al.*, 2009; Eymery, Horard, *et al.,* 2009; Jolly *et al.,* 1997; Rizzi *et al.,* 2004; Sengupta, Parihar, & Ganesh, 2009; Valgardsdottir *et al.,* 2008). The level and the orientation of transcripts were dependent of the nature of the stressor, with the majority of examined stressor inducing transcription exclusively in the sense orientation. However, during the heat shock, which has been studied in more details, transcription has been reported to occur from both strands, with the sense orientation representing the main proportion of the transcripts (Valgardsdottir *et al.,* 2008). A summary of the effect of all the examined stresses to date is shown in Figure 1.11.

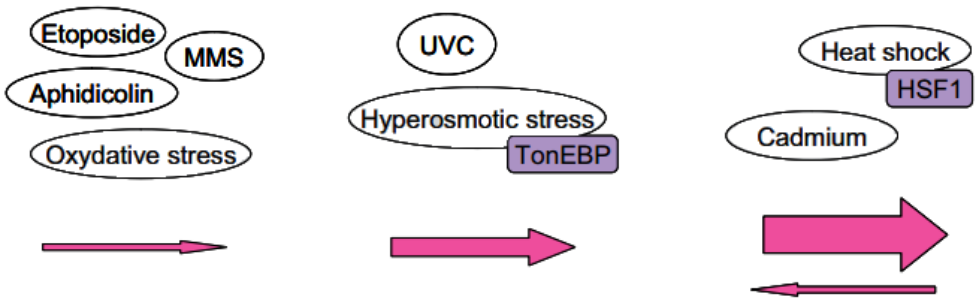


Figure 1.11: A summary of known stressors that were shown to induce pericentromeric repeat transcription in human cells. Different stresses have been found to induce either a low (small pink arrow), medium (moderate pink arrow) or high (large pink arrow) derepression of pericentromeric satellite repeats. So far, only transcription factors HSF1 and TonEBP were shown to mediate the expression of pericentromeric repeats under heat shock and hyperosmotic stress respectively. The sense transcript orientation is indicated as a right pointing arrow, whereas the antisense is shown as a left pointing arrow. UVC=ultraviolet light C, MMS=methyl methanesulphonate. Adapted and modified from (Eymery, Callanan, *et al.*, 2009).

Specifically for humans, the transcription of pericentromeric satellite repeats upon cell stress has been predominantly associated with formation of nuclear stress bodies (Biamonti, 2004; Jolly *et al.*, 2002).

4.2.1 Nuclear Stress Bodies

The exposure of human cells to several different stresses (e.g heat shock, proteasome inhibitors and heavy metals) results in the formation of distinct nuclear structures termed nuclear stress bodies (NSBs) (Biamonti & Vourc'h, 2010; Cotto, Fox, & Morimoto, 1997; Mahl, Lutz, Puvion, & Fuchs, 1989). These are large structures ranging from 0.3–3 μm in diameter and are assembled on several human heterochromatic regions (chromosomes 9, 12, 15) (Denegri *et al.*, 2002). Each NSB consists of a cluster of multiple ribonucleoproteins complexes called Perichromatin Granules (PGs) whose function remains still unknown (Charlier, Lamaye, Thelen, & Thiry, 2009; Chiodi *et al.,* 2000; Mahl *et al.,* 1989). However some possible roles that have been proposed to date include: (i) control of transcription and splicing, (ii) establishment of the heterochromatin structure upon stress and (iii) activation of genes adjacent to the NSBs (Biamonti & Vourc'h, 2010). Additionally, while NSBs can form in any human cell type, so far no such structures have been detected in rodent cells (Denegri *et al.,* 2002).

4.2.2 Formation of NSBs

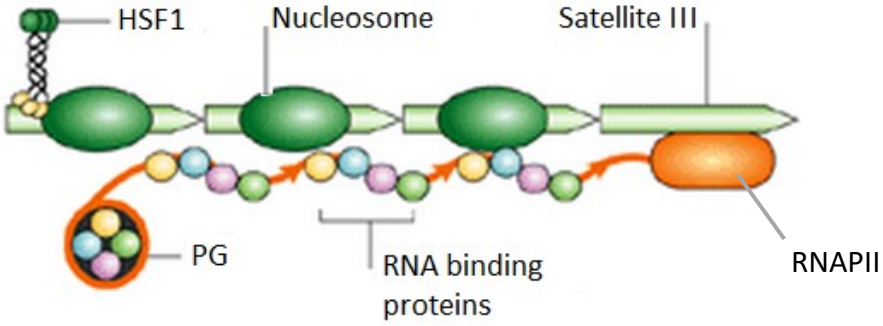
The formation of NSBs has been mostly studied by exposure of cells to heat shock. Upon heat shock of human cells, HSF1 becomes activated and directly binds primarily to the pericentromeric heterochromatin q11-q12 region of human chromosome 9, which consist of an array of Satellite III repeats (Jolly *et al.,* 2002; Jolly *et al.,* 2004a; K. W. Jones, Prosser, Corneo, & Ginelli, 1973; Rizzi *et al.,* 2004). Interestingly, in humans, the binding of HSF1 to Satellite III repeats occurs despite the absence of canonical HSE elements within its consensus sequence. Subsequently, the binding of HSF1 triggers a series of events leading to the assembly of PGs that form the NSBs. These events include: (i) Chromatin remodelling by directly recruiting HATs which induce histone acetylation thereby creating a more open chromatin structure (ii) recruitment of RNAPII, (iii) transcription of Satellite III repeats (Jolly *et al.,* 2004a; Rizzi *et al.*, 2004) and (iv) binding of several RNA-binding proteins such as splicing factors through direct interaction with Satellite III transcript (Figure 1.12) (Chiodi *et al.,* 2004; Denegri *et al.,* 2001; Metz, Soret, Vourc'h, Tazi, & Jolly, 2004). The Satellite III

transcripts are stable non-coding RNAs that remain associated with the transcription sites in the nucleus (Valgardsdottir *et al.*, 2005; Valgardsdottir *et al.,* 2008).

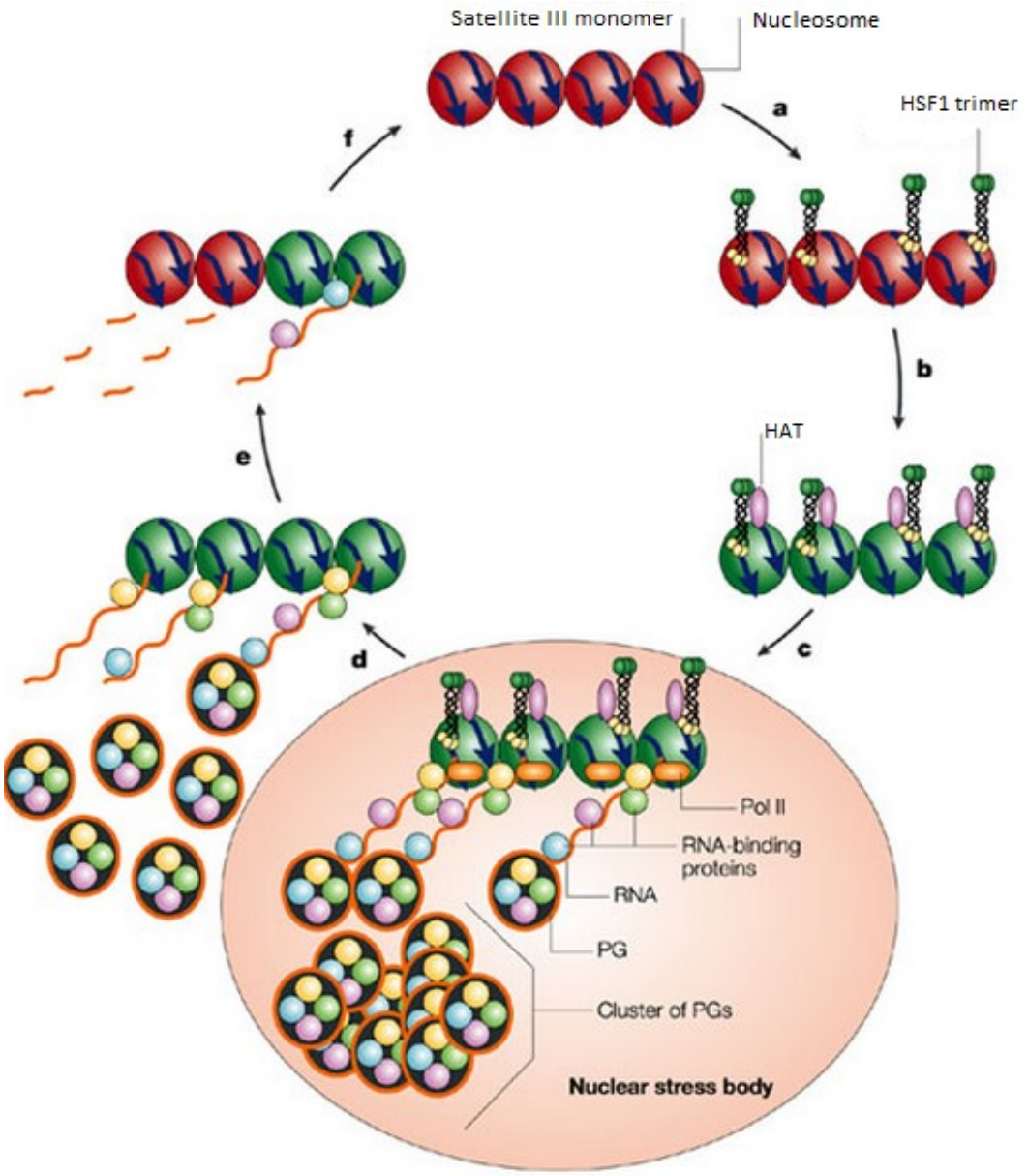
There is a discrepancy regarding the size of these transcripts, with some studies indicating size larger than 10 Kb (Jolly *et al.,* 2004a) whereas others suggest a heterogeneous length varying between 5 and 2 Kb (Rizzi *et al.,* 2004). The transcription of these repeats is dependent on the activated HSF1 trimer, since deactivation and release of HSF1 results in dissociation of HAT and RNAPII leading to transcriptional inactivation. This is followed by disassembly of PGs and diffusion of RNA-binding proteins within the nucleus. Finally, satellite III transcripts get degraded and the locus re-establishes the high compact heterochromatin structure (Figure 1.12B) (Jolly *et al.,* 2004a; Rizzi *et al.,* 2004).

It is noteworthy that HSF2 has also been shown to bind to Satellite III repeats in an HSF1 – dependent manner (Alastalo *et al.,* 2003; Sandqvist *et al.,* 2009).

A



B



See next page for figure legend

Figure 1.12: Transcription of human Satellite III repeats and NSBs formation. (A) Transcription of Satellite III repeats. The HSF1 trimer binds to the Satellite III repeats leading to transcriptional activation and generation of Satellite III transcripts. These transcripts remain at the transcription site, recruit RNA-binding proteins and assemble into PGs complex. (B) Formation and dissociation of NSBs. In the absence of the stress, satellite III (blue arrow) is heterochromatinised (red nucleosome). a. In the presence of stress, the HSF1 trimer binds to Satellite III repeats sequence and b recruits HAT inducing histone acetylation (green nucleosome). c. This is followed by RNAPII recruitment, transcription of Satellite III repeats and assembly of PGs by direct binding of RNA-binding proteins to the Satellite III transcript. Multiple PGs then cluster and form NSBs. d. The HSF1 trimer dissociate along with RNAPII and HAT resulting in transcriptional termination. This is followed by destruction of PGs and release of the RNA-bound proteins in the nucleus. e. Satellite III RNA gets degraded and a high order chromatin structure starts forming on the locus. f. Finally the region re-establishes its original structure. Adapted from (Biamonti, 2004).

5. Friedreich's ataxia

Importantly, a significant number of neurological disorders such as Huntington disease and Friedreich's ataxia are caused by expansion of a specific class of microsatellite repeats (a category of repetitive DNA elements see figure 1.5) called trinucleotide repeats (Brouwer, Willemsen, & Oostra, 2009; Budworth & McMurray, 2013; Everett & Wood, 2004; McMurray, 2010). Such repeats, in common with pericentromeric satellite repeats have been reported to repress transcription, in a similar manner (Saveliev *et al.,* 2003) (see below). This thesis is partly focused on Friedreich's ataxia therefore the pathology and cause of the disease will be discussed in this section.

Friedreich's ataxia (FRDA) is the most common autosomal recessive neurodegenerative disorder occurring mainly in Caucasians with a frequency between 1:30 000 and 1:50 000 (Koeppen, 2011, 2013; Vankan, 2013). Clinically, the disease is characterised by dysarthria, progressive limb and gait ataxia, lower limb areflexia, loss of vibratory and position sense, atrophy and weakness of the distal extremities, scoliosis, diabetes mellitus and hypertrophic cardiomyopathy, which is the frequent cause of fatality. Neurologically, dorsal root ganglia (DRG), spinocerebellar tracts, cerebellum and medulla are predominantly affected tissues from the disease (Durr *et al.*, 1996; Koeppen, 2013; Parkinson, Boesch, Nachbauer, Mariotti, & Giunti, 2013; A. H. Wood & Dubrey, 2013). At present there is no effective disease modifying therapy.

The vast majority of FRDA cases (96%) are caused by pathological GAA repeat expansion in the first intron of the *FXN* gene on both alleles (Campuzano *et al.*, 1996). Notably the age at onset and severity of the disease are proportional to the expansion of the GAA repeats; with patient onset during childhood usually have the longest expansion (Durr *et al.,* 1996; Filla *et al.,* 1996; Montermini, Andermann, *et al.,* 1997; Montermini, Richter, *et al.,* 1997; Nachbauer *et al.,* 2014). The result of GAA repeat expansion is transcriptional repression of the *FXN* gene, leading to a partial deficiency in the mitochondrial protein frataxin (Campuzano *et al.,* 1997; Campuzano *et al.,* 1996; Koutnikova *et al.,* 1997). The level of frataxin mRNA correlates well with the severity of the FRDA disease, with patients having ~13-30% of frataxin mRNA relative to healthy individuals whereas heterozygous asymptomatic carriers generally expressing ~40% of frataxin mRNA relative to healthy

controls (Pianese *et al.,* 2004). Additionally, it is worth mentioning that in 4% of cases, FRDA was reported to result from GAA-repeat expansion on one *FXN* allele and missense and nonsense mutation within the other allele of the *FXN* gene (Anheim *et al.,* 2012; Bartolo, Mendell, & Prior, 1998; Bidichandani, Ashizawa, & Patel, 1997; Cossee *et al.,* 1999; Sacca *et al.,* 2013; Zuhlke *et al.*, 2004).

5.1 Frataxin protein

Human frataxin is a highly conserved and ubiquitously expressed protein (Adinolfi, Trifuoggi, Politou, Martin, & Pastore, 2002; Gibson, Koonin, Musco, Pastore, & Bork, 1996). Initially, it is translated as a 210aa precursor in the cytoplasm followed by translocation into the mitochondria, where it undergoes functional maturation mediated by peptidase cleavage (Condo *et al.,* 2007; Koutnikova *et al.,* 1997; Koutnikova, Campuzano, & Koenig, 1998; Schmucker, Argentini, Carelle-Calmels, Martelli, & Puccio, 2008).

The mature protein (14kD) is associated with the inner mitochondrial membrane and its main functions are reported to be (i) iron-sulfur (Fe-S) cluster biogenesis (Stehling, Elsasser, Bruckel, Muhlenhoff, & Lill, 2004), (ii) iron chaperoning (Bulteau *et al.,* 2004), (iii) iron storage (Cavadini, O'Neill, Benada, & Isaya, 2002), (iv) heme biosynthesis (Yoon & Cowan, 2004) and (v) control of iron mediated oxidative tissue damage (Jiralerspong, Ge, Hudson, & Pandolfo, 2001; Park, Gakh, Mooney, & Isaya, 2002; A. Wong *et al.,* 1999). Therefore, deficiency of frataxin severely disrupts mitochondrial function through iron accumulation (Babcock *et al.,* 1997; Bradley *et al.,* 2000; Foury & Cazzalini, 1997; Gonzalez-Cabo & Palau, 2013) and increases the sensitivity to oxidative stress through deregulation of intracellular antioxidant defences (Chantrel-Groussard *et al.,* 2001; Gomes & Santos, 2013; Jiralerspong *et al.,* 2001; Schulz *et al.,* 2000; Shan *et al.*, 2013). Furthermore, frataxin has also been implicated in regulation of apoptosis (Loria & Diaz-Nido, 2015; Mincheva-Tasheva, Obis, Tamarit, & Ros, 2014; Palomo, Cerrato, Gargini, & Diaz-Nido, 2011; Santos, Ohshima, & Pandolfo, 2001). For example depletion of frataxin was shown to cause (i) apoptosis of primary rat DRG neurons associated with an increase in intracellular Ca^{2+} levels and alteration of Ca^{2+} mediated signalling pathway (Mincheva-Tasheva *et al.,* 2014) and (ii)

upregulation of several pro-apoptotic factors including p53 and BAX as well as activation of the caspase-3 pathway, leading to cell death in differentiated neuron like cells (Palomo *et al.,* 2011).

5.2 Transcriptional regulation of the *FXN* gene

As illustrated in Figure 1.13A, the human *FXN* gene is located on the positive strand on chromosome 9 (9q21.11) and consists of 4 introns and 5 exons. The gene contains 3 putative CpG islands with the first of them residing in exon 1 and part of intron 1 (Yandim *et al.*, 2013). Importantly, polymorphic (GAA)n repeats are located within the first intron of the *FXN* gene, in the centre of an Alu element (Campuzano *et al.,* 1996; Clark *et al.,* 2004; Montermini, Andermann, *et al.*, 1997) followed by a mononucleotide tract of adenines (poly A) (Monticelli *et al.*, 2004). In unaffected individuals expansions of the GAA repeats may exist up to 30 triplets, whereas in disease causing mutations the expansion ranges from 70 to more than 1700 repeats (Vankan, 2013). Furthermore, few repetitive elements including L2 (LINE) are also present along the *FXN* gene, with as yet unknown function (Greene, Entezam, Kumari, & Usdin, 2005) .

The *FXN* gene is known to contain two main TSSs; TSS1 and TSS2 which are found 221 bp and 62 bp upstream of the ATG translation start site respectively (Campuzano *et al.*, 1996; Kumari, Biacsi, & Usdin, 2011). Interestingly, the promoter regions were reported to contain instead of a TATA box, Inr/downstream promoter-like (Inr/DPE) elements starting 24bp downstream of TSS1, whose deletion was shown to significantly impair *FXN* expression (Figure 1.13B) (Greene *et al.*, 2005).

So far, only limited data is available regarding the regulation and identity of the transcription factors that orchestrate *FXN* transcription, which is considered to be expressed in all cells at low levels, with relatively higher levels reported in DRG, cerebellum and tissues with high metabolic rate including heart and liver (Campuzano *et al.,* 1996; Koutnikova *et al.*, 1997). Nevertheless, a few of the factors that were shown to be recruited to the regions flanking the TSS and ATG include CCCCTC-binding factor (CTCF) (Al-Mahdawi, Sandi, Mouro Pinto, & Pook, 2013; De Biase, Chutake, Rindler, & Bidichandani, 2009) as well as Serum Responsive Factor (SRF) and Transcription Factor AP2 (TFAP2) (K. Y. Li *et al.,* 2010), factors

important for neural and neural crest development respectively (Figure 1.13B) (Alberti *et al.,* 2005; Eckert, Buhl, Weber, Jager, & Schorle, 2005; Knoll *et al.,* 2006; P. P. Y. Lu & Ramanan, 2011; Ramanan *et al.,* 2005).

Finally, physiological regulation of *FXN* expression is believed to be dependent on the intracellular iron concentration, as iron depletion results in downregulation of *FXN* expression in both healthy and FRDA cells (K. Y. Li, Besse, Ha, Kovtunovych, & Rouault, 2008).

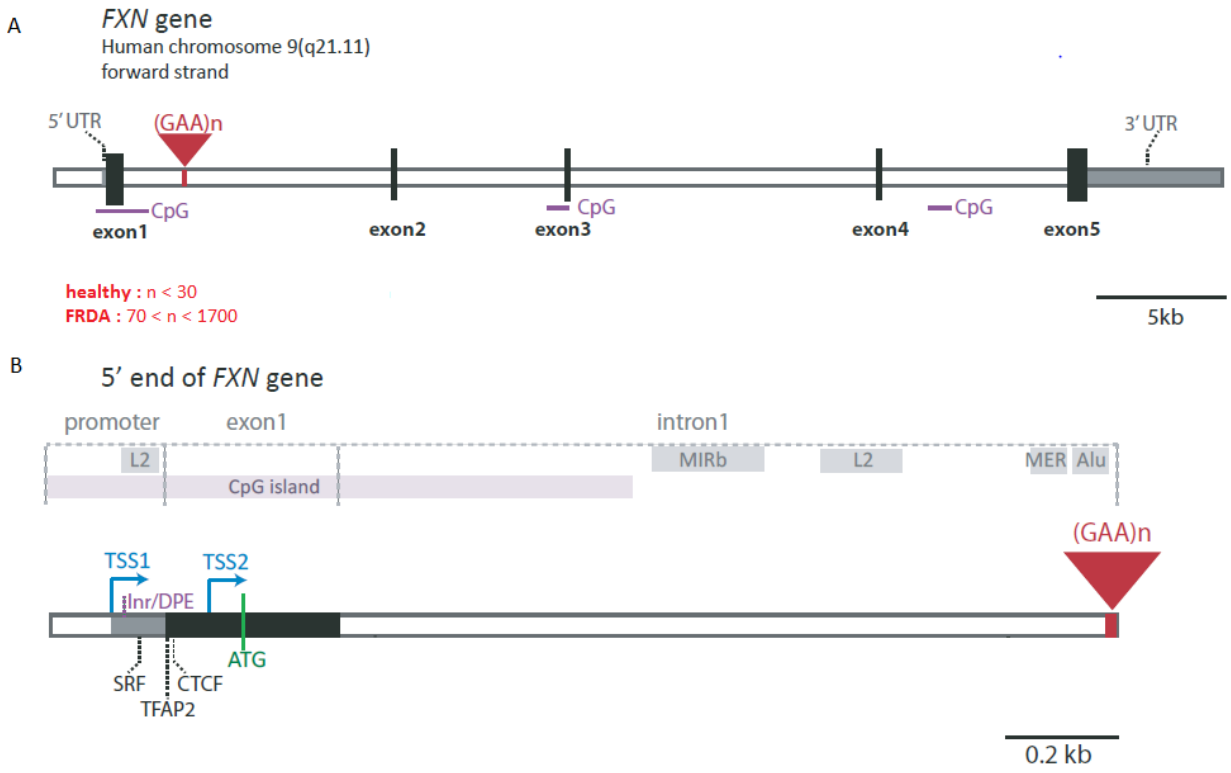


Figure 1.13: The human *FXN* gene and its known regulatory elements. (A) The human *FXN* gene is located on chromosome 9 and consists of five exons and contains three putative CpG islands. The first intron of the gene harbours a number of (GAA)n repeats whose expansion leads to FRDA disease. (B) Regulatory elements at the 5'end of the *FXN* gene. *FXN* is known to be transcribed from two transcription sites, TSS1 and TSS2. The regions between TSS1 and ATG is known to contain Inr/DPE elements and to bind SRF, TFAP2 and CTCF factors. There are also a number of repetitive elements found along the *FXN* gene. Adapted and modified from (Yandim *et al.*, 2013)

5.3 Transcriptional repression of the FXN gene by expanded GAA repeats

The silencing-triggers and the exact molecular mechanism by which GAA repeat expansion induces *FXN* gene repression is not clear; however two models have been proposed which may act in concert or individually (Figure 1.14) (Schulz & Pandolfo, 2013).

The first model suggests that the expanded GAA repeat causes an unusual non-B DNA conformation, the so called "sticky DNA" structure (Sakamoto *et al.,* 1999; Vetcher *et al.,* 2002), as well as RNA:DNA hybrids, the so called R-loops (Grabczyk, Mancuso, & Sammarco, 2007; Groh, Lufino, Wade-Martins, & Gromak, 2014; Reddy *et al.,* 2011). These unusual conformations form physical blockage, therefore stalling the RNAPII and preventing the transcriptional elongation process (Figure 1.14A) (Groh *et al.,* 2014; McIvor, Polak, & Napierala, 2010; Sakamoto, Ohshima, Montermini, Pandolfo, & Wells, 2001).

The second model suggests that GAA repeat expansions induces heterochromatin formation, thereby epigenetically silencing the *FXN* gene (Figure 1.14B, 1.14C). This hypothesis was derived from a study where expression of a heterochromatin-sensitive human cell surface reporter gene (hCD2) was shown to be repressed in the presence of pathologically expanded GAA repeats in a manner reminiscent of position-effect variegated gene silencing (PEV) mechanism in transgenic mice (Saveliev, Everett, Sharpe, Webster, & Festenstein, 2003). The same study also correlated the repression of the reporter gene with a decrease in promoter accessibility as well as enhanced silencing through overexpression of heterochromatin protein 1 (HP1) (see section 2.2.2), a well-known PEV modifier (Saveliev *et al.*, 2003). Consistently, heterochromatin associated histone modifications H3K9me3, H3K9me2, H4K20me3 and H3K27me3 were shown to be increased upstream of the expanded GAA on the *FXN* locus whereas the histone acetylation levels including H3K9ac, H3K14ac, H4K5ac, H4K8ac, H4K12ac and H4K16ac were revealed to be decreased at both the promoter and gene body of the *FXN* gene in variety of FRDA model systems such as lymphoblastoid cell lines, fibroblast cell lines, primary human and mouse tissues (P. K. Chan *et al.,* 2013; Chutake, Costello, Lam, & Bidichandani, 2014; Y. Li *et al.,* 2015; Yandim *et al.*, 2013). Lastly, various studies have also reported hypermethylation and hypomethylation of CpG islands upstream and downstream of pathologically expanded GAA repeats respectively (Al-Mahdawi *et al.,* 2013; Yandim *et al.,* 2013), which further supports the

heterochromatinisation of the FXN gene in FRDA. However the factors that initiate the heterochromatin formation on the locus are still unknown.

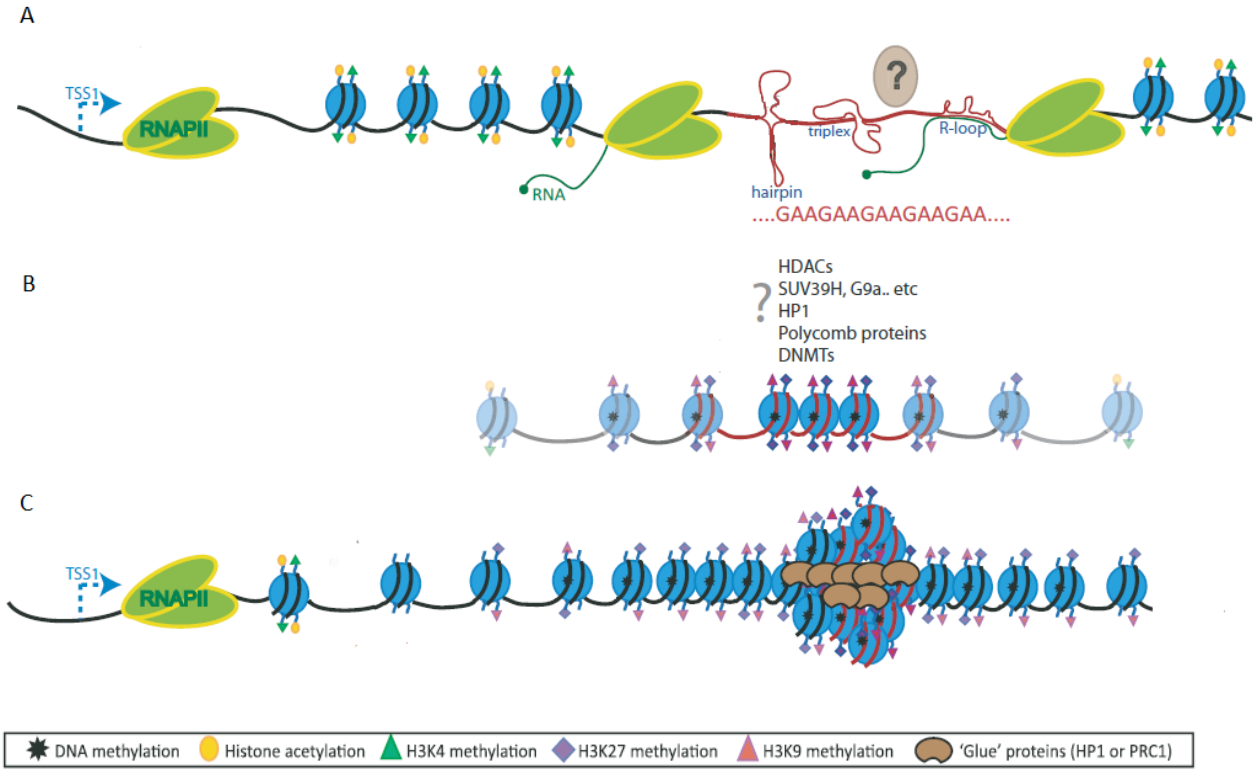


Figure 1.14: A hypothetical model for the heterochromatin formation of the *FXN* gene with pathologically expanded GAA repeats. (A) The expansion of GAA repeats (shown in red) triggers non-B DNA conformations (e.g triple, hairpin) and RNA:DNA hybrids (R-loop) formation. These structures form physical blockage and potentially stall on–going transcription. (B) Recruitment of heterochromatin factors to the *FXN* locus. Although there is no evidence yet, the repetitive nature of the region and the unusual conformations may recruit chromatin modifying factors including SUV39H, HP1 and DNMTs. (C) The region proximal to the GAA repeats contain classic heterochromatin marks including DNA methylation, histone deacetylation, H3K9me3 and H3K27me3. Adapted and modified from (Yandim *et al.*, 2013)

5.4 HDAC inhibitors and FRDA

Since FRDA is a disease associated with heterochromatinisation of the *FXN* gene, targeting of factors that prevent heterochromatin formation could potential prove to be a good approach to find candidates for FRDA therapeutics. One group of these factors are HDACs whose inhibition would shift the equilibrium towards acetylation and hence a more open chromatin state.

As mentioned in a previous section (see section 2.2.1.1) HDACs catalyse the removal of acetyl groups from ε-N-acetyl-lysine amino acid of histones which increases the attraction between DNA and positively charged histones (Haberland, Montgomery, & Olson, 2009; X. J. Yang & Seto, 2007). This in turn would permit other histone modifications associated with a higher order chromatin structure, including methylation, to be established on the locus (Alper *et al.*, 2013; Buscaino *et al.,* 2013; Nakayama, Rice, Strahl, Allis, & Grewal, 2001; Yamada, Fischle, Sugiyama, Allis, & Grewal, 2005). Furthermore histone deacetylation is required for the repression, mediated by DNA methylation and methyl-CpG-binding protein MeCP2 (P. L. Jones *et al.,* 1998a; Nan *et al.,* 1998). Therefore HDACs are generally considered as transcriptional repressors. Based on sequence similarity and function, HDACs are classified into four major groups, HDAC class I, II, and IV that require Zn^{2+} for deacetylase activity and class III (also known as Sirtuin or silent information regulator, SIRT1–7) that require nicotinamide adenine dinucleotide (NAD^{+}) as a cofactor (Glozak & Seto, 2007).

To date, various molecules have been developed to inhibit HDAC activity. The classical HDAC inhibitors, including Trichostatin (TSA) and suberoylanilide hydroxamic acid (SAHA also known as vorinostat) target solely class I, II and IV HDACs through binding to the zinc-containing catalytic domain of HDAC (Codd, Braich, Liu, Soe, & Pakchung, 2009; Richon *et al.*, 1996; M. Yoshida, Kijima, Akita, & Beppu, 1990). On the other hand class III HDAC inhibitors including nicotinamide and sirtinol function as NAD+ analogues or specific sirtuin structural inhibitors (Alcain & Villalba, 2009; Cen, 2010).

In recent years, numerous HDAC inhibitors have been developed as potential candidates for treatment of numerous neurodegenerative diseases, including Friedreich's ataxia (Chuang, Leng, Marinova, Kim, & Chiu, 2009; Didonna & Opal, 2015; Dietz & Casaccia, 2010;

Falkenberg & Johnstone, 2014; Marek *et al.*, 2013; S. Sharma & Taliyan, 2015; Simoes-Pires *et al.,* 2013; Soragni *et al.,* 2011; K. Xu, Dai, Huang, & Jiang, 2011).

Previous studies using classical HDAC inhibitors targeting mainly class I and II HDACs including TSA, SAHA (Herman *et al.,* 2006), sodium valproate (Gottlicher *et al.,* 2001) and suberoyl bishydroxamic acid (Rai *et al.,* 2008) did not shown any significant effect on the *FXN* expression in FRDA patient cells lines neither in transgenic mouse models. However *N*1-[2-aminophenyl]-*N*8-phenyloctanediamide (BML-210), a class I HDAC inhibitor was first shown to significantly upregulate *FXN* mRNA expression in FRDA primary lymphocytes and cell lines by increasing histone acetylation marks (H3K14, H4K5 and H4K12) (Herman *et al.,* 2006). Furthermore, synthesis of BML-210 derivatives revealed a number of pimelic diphenylamide molecules that specifically inhibit class I HDACs and increase *FXN* expression in various FRDA models. Some of these molecules (compound 106, 109, 136) were shown to significantly upregulate *FXN* mRNA and protein levels in the heart and the nerve tissue of KIKI (GAA_{230}) and YG8 FRDA mouse models accompanied by an increase of the acetylation (H3K14, H4K5, H4K8 and H4K16) levels and no change of H3K9me3 levels (Rai *et al.,* 2010; Rai *et al.,* 2008; Sandi *et al.*, 2011). Importantly, the reversal of silencing of the *FXN* gene is not restricted to class I HDAC inhibitors, as the class III HDAC inhibitor nicotinamide was also shown to restore the *FXN* expression in several FRDA models, including FRDA primary cells, cell lines and mouse models associated with reversal of the condensed chromatin structure formed by GAA repeats expansion (P. K. Chan *et al.,* 2013).

Nicotinamide is the amide of nicotinic acid (also known as Vitamin B3) and a non-competitive end product inhibitor of SIRT1 HDAC (Avalos, Bever, & Wolberger, 2005; Bitterman, Anderson, Cohen, Latorre-Esteves, & Sinclair, 2002).

SIRT1 is a member of the class III HDACs that localises in the nucleus (Byles *et al.,* 2010; Michishita, Park, Burneskis, Barrett, & Horikawa, 2005; Vaquero *et al.,* 2004) and is implicated in heterochromatin formation. The mechanism of chromatin compaction by SIRT1 includes deacetylation of the targets H4K16 and H3K9 histones (Imai, Armstrong, Kaeberlein, & Guarente, 2000; Vaquero *et al.,* 2004) followed by recruitment and deacetylation of linker histone H1, loss of transcriptionally active chromatin mark H3K79me2 (Vaquero *et al.,* 2004) and recruitment of SUV39H1 which in turn methylates H3K9 generating repressed chromatin H3K9me3 mark (Vaquero *et al.,* 2007).

Notably SIRT1 can also target other substrates beside histones such as the cell cycle regulator P53 (Atkins *et al.*, 2014; Gonfloni *et al.,* 2014; Vaziri *et al.,* 2001), DNA replication regulator TopBP1 (R. H. Wang *et al.,* 2014) and various transcription factors (e.g NFκB, FOXOs, RORγt,) (Brunet *et al.,* 2004; H. N. Kim *et al.,* 2015; Lim *et al.,* 2015; Yeung *et al.,* 2004).

Biochemically, the deacetylaton process of SIRT1 consists of the transfer of an acetyl group from acetyl-lysine substrate to the ADP-ribose of NAD^+ molecule causing the hydrolysis with subsequent release of O-acetyl ribose (OAADPr) and nicotinamide (Denu & Gottesfeld, 2012; Sauve *et al.,* 2001; Sauve, Wolberger, Schramm, & Boeke, 2006). However, an excess of free nicotinamide blocks the release of nicotinamide and therefore prevents hydrolysis of NAD^+ (Figure 1.15) (Avalos *et al*., 2005; Bitterman *et al.,* 2002).

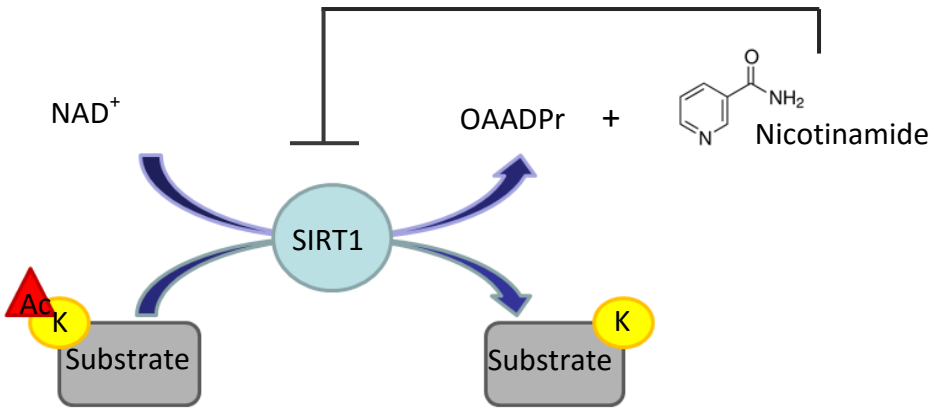


Figure 1.15: Inhibition of SIRT by nicotinamide. SIRT1 transfers the Acetyl group from the acetyl-lysine substrate to NAD^+ leading to the release of OAADPr and nicotinamide as well as deacetylation of the substrate. The free nicotinamide blocks the SIRT1 activity. K represents the Lysine residue and Ac the acetyl group.

6. The proteasome

Protein turnover is a vital cellular function predominantly controlled by the ubiquitin proteasome system (UPS). At its centre is the highly conserved (found in all three biological super-kingdoms) protease complex, the proteasome, which recognises, unfolds and degrades the poly-ubiquitin tagged (some exceptional cases is ubiquitin-independent) aged, misfolded or damaged proteins. Therefore it is an essential component of the cell that regulates protein quality maintenance both in cytoplasm and nucleus (Wojcik & DeMartino, 2003). Moreover proteasome function is further linked with other cellular processes including DNA damage repair, transcription, signal transduction, cell division, cell differentiation, apoptosis and adaptation to environmental signals through (i) regulation of proteolytic processing and maturation of various polypeptides and (ii) degradation of many key cell regulators (Jariel-Encontre, Bossis, & Piechaczyk, 2008; Stadtmueller & Hill, 2011). Importantly, impairment of the proteasome function has been associated with cellular aging (Carrard, Bulteau, Petropoulos, & Friguet, 2002) and various pathological conditions such as cancer and neurodegenerative diseases (Adams, 2003a; Adams *et al.*, 1999b; Catalgol & Grune, 2012; Dantuma & Bott, 2014; Q. Huang & Figueiredo-Pereira, 2010; Pajonk & McBride, 2001; Rajkumar, Richardson, Hideshima, & Anderson, 2005).

6.1 Structure of the proteasome

The most common eukaryotic proteasome is found as a 26S holoenzyme complex with a molecular mass of 2.5 MDa. It is comprised of the catalytic 20S core particle (CP) capped at one or both ends by the regulatory 19S particle (RP) (Figure 1.16) (T. Jung & Grune, 2013; Lasker *et al.,* 2012; Nickell *et al.,* 2009).

The 20S particle is a barrel-like structure of four stacked rings, with two outer heptameric α subunits (α1-7) and two inner heptameric β subunits (β1-7) structured in a α7- β7- β7- α7 manner (Groll *et al.,* 1997; Heinemeyer, Trondle, Albrecht, & Wolf, 1994; Unno *et al.,* 2002). The proteolytic activity of the CP is restricted to β1 (caspase-like), β2 (trypsin-like) and β5 (chymotrypsin-like) subunits which face the inner chamber of the cylinder and function synergistically to cleave the substrate proteins into small peptides (Groll *et al.,* 1999; Heinemeyer, Fischer, Krimmer, Stachon, & Wolf, 1997; Kunjappu & Hochstrasser, 2014). In

contrast, α subunits functions as a “gate”, preventing the access of incorrect substrate to the catalytic chamber (Groll *et al.*, 2000).

Importantly the 20S CP is an intrinsically enzymatically repressed complex that requires a 19S regulatory particle (also known as PA700) in order for the substrate to enter the catalytic chamber (Stadtmueller & Hill, 2011). Therefore proteolysis is a highly regulated process dependent on the 19S particle which main function is recognition of the polyubiquitinated substrate, deubiquitination, protein unfolding and translocation into the 20S particle (C. W. Liu & Jacobson, 2013). It is further divided into the base and the lid (G. C. Lander *et al.,* 2012).

The 19S base contains six ATPases (Rpt1-6) forming a hetero-hexamer ring and four regulatory proteins (non – ATPase, Rpn 1, 2, 10, 13) (G. C. Lander *et al.,* 2012; Tomko, Funakoshi, Schneider, Wang, & Hochstrasser, 2010). The ATPases serve to unfold the substrate, and then facilitate opening of the “gate” to allow entry of the substrate into the channel of the CP (Bar-Nun & Glickman, 2012; Beckwith, Estrin, Worden, & Martin, 2013; Rabl *et al.,* 2008; Sledz *et al.,* 2013). On the other hand, Rpn1/Rpn2 are scaffolding proteins providing a docking site for substrate recruitment (Elsasser *et al.*, 2002; Rosenzweig, Bronner, Zhang, Fushman, & Glickman, 2012) whereas Rpn10/Rpn13 act as the ubiquitin receptors (Hamazaki, Hirayama, & Murata, 2015; Husnjak *et al.,* 2008).

The 19S lid contains 9 non-enzymatic regulatory proteins (Rpn3, Rpn5-9, Rpn11-12 and Rpn15) and is directly involved in substrate recognition and protein deubiquitination (Glickman *et al.*, 1998; G. C. Lander *et al.,* 2012; Pathare *et al.,* 2014; Verma *et al.,* 2002).

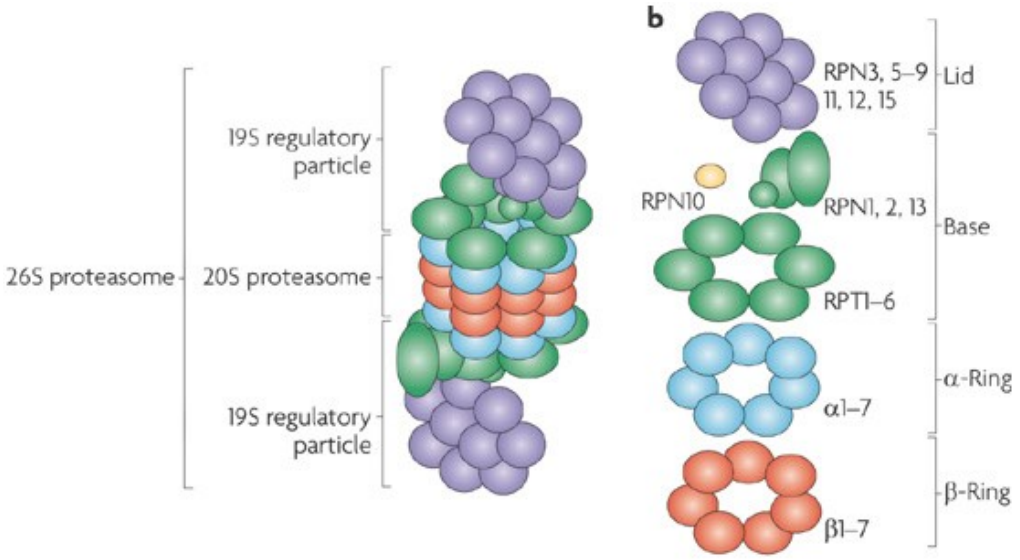


Figure 1.16: Structure of the 26S proteasome. The 26S proteasome consists of a 20S core particle and two 19S regulatory particles. The 20S consists of two heptameric α rings (α1-7) and two heptameric β rings (β1-7). The 19S particle is further divided into the base and the lid. The base consists of an ATPase (RPT1-6) ring and non-ATPase regulatory proteins (RPN1, 2, 13, 10) whereas the lid contains 9 regulatory proteins (RPN 3, 5-9, 11, 12, and 15). Adapted from (Murata, Yashiroda, & Tanaka, 2009).

6.2 Protein ubiquitination and degradation

A poly-ubiquitin chain, linked to target proteins is considered to be the main recognition signal for the proteasome–dependent degradation pathway (Pickart, 1997). Notably, some studies have also reported ubiquitin-independent proteasome degradation (Asher, Lotem, Sachs, Kahana, & Shaul, 2002; Asher, Tsvetkov, Kahana, & Shaul, 2005; Bercovich, Rosenberghasson, Ciechanover, & Kahana, 1989; Erales & Coffino, 2014; Kong *et al.*, 2006; Shringarpure, Grune, Mehlhase, & Davies, 2003). The mechanism behind ubiquitin-independent proteasome degradation remains poorly understood. Generally it is believed that this pathway could be a remnant of the pre-ubiquitin wold, as the proteasome has a longer evolutionary history compared to ubiquitin or could provide an alternative regulatory level of protein degradation (Erales & Coffino, 2014).

Ubiquitin is a highly conserved 76 amino acid peptide that can be covalently attached through formation of a bond between the terminal glycine of the ubiquitin and the lysine-48 residue in the target protein. This attachment takes place in 3 steps: firstly, the ubiquitin is activated in an ATP-dependent manner by the ubiquitin-activating enzyme (E1), creating a high energy thioester intermediate (E1- S~ubiquitin). Secondly, the activated ubiquitin is transferred from E1 to one of the many (over 40) ubiquitin-conjugating enzymes (E2), generating a second high-energy thioester intermediate (E2-S~ubiquitin). Finally, the ubiquitin is transferred directly or indirectly from the E2-S~ubiquitin to the target protein that it is specifically bound to by ubiquitin-ligase (E3) (Figure 1.17) (Berndsen & Wolberger, 2014; Pickart & Eddins, 2004). In humans, over 600 E3 ligases have been identified to date (W. Li *et al.*, 2008). The mechanism of target protein recognition by the E3 ligases is poorly understood but it is believed that some protein conformation changes might play a role.

Importantly, monoubiquitination by itself can modulate protein function, without triggering them for degradation (Gupta-Rossi *et al.*, 2004; Haglund *et al.*, 2003; Kodadek, 2010; Sigismund, Polo, & Di Fiore, 2004; Terrell, Shih, Dunn, & Hicke, 1998). Only further attachment of ubiquitin via intermolecular ubiquitin glycine-lysine bonds can act as a marker for proteasomal recognition and degradation (Sadowski & Sarcevic, 2010).

Finally, it is worth mentioning that ubiquitination is a dynamic process and deubiquitination can also occur, mediated by various deubiquitinating enzymes (DUB) (Amerik & Hochstrasser, 2004; Ventii & Wilkinson, 2008).

One substrate for ubiquitination and further degradation is a permanently or temporarily stalled/arrested RNAPII (Gillette, Gonzalez, Delahodde, Johnston, & Kodadek, 2004a; Malik, Bagla, Chaurasia, Duan, & Bhaumik, 2008; Wilson, Harreman, & Svejstrup, 2013).

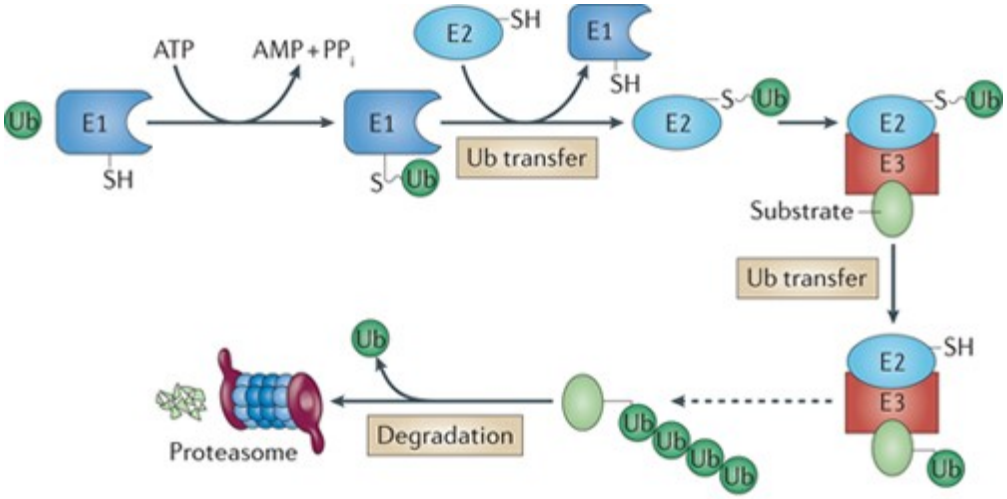


Figure 1.17: Protein ubiquitination and proteasome mediated degradation. Initially the ubiquitin is activated in an ATP-dependent manner by E1 creating high-energy thioester intermediate (E1- S~ubiquitin). The ubiquitin is then transferred from E1 to E2 generating a second high-energy trioester intermediate (E2-S~ubiquitin). Finally the ubiquitin is transferred to substrate mediated by substrate bound E3. Polyubiquitinated substrates get degraded by the proteasome. Adapted from (Maupin-Furlow, 2012).

6.3 Chromatin regulated function of proteasome

Although the function of the proteasome was believed to be restricted to the cytoplasm, numerous studies revealed a proteolytic and non-proteolytic role of the proteasome in the nucleus of eukaryotic cells (Adori *et al.*, 2006; Enenkel, 2014; Mengual, Arizti, Rodrigo, GimenezAmaya, & Castano, 1996; Reits, Benham, Plougastel, Neefjes, & Trowsdale, 1997). Growing evidence now suggests that proteasome is associated with chromatin (Geng, Wenzel, & Tansey, 2012; McCann & Tansey, 2014; A. Palmer *et al.,* 1996), with some studies reporting identical or overlapping binding patterns for both proteasome particles (19S and 20S) (Auld, Brown, Casolari, Komili, & Silver, 2006; Geng & Tansey, 2012; Krogan *et al.,* 2004b; Sikder, Johnston, & Kodadek, 2006; Szutorisz, Georgiou, Tora, & Dillon, 2006) whilst others have specifically focused on 19S RP (Ferry *et al.,* 2009; Kitagawa, Ishii, Takeda, & Matsumoto, 2014b; Malik, Shukla, Sen, & Bhaumik, 2009; Satoh *et al.,* 2009; Schwarz, Sohn, Kaiser, Jensen, & Mansky, 2010; Uprety, Lahudkar, Malik, & Bhaumik, 2012). Notably, there

are also some reports claiming that 19S and 20S particles associate with the chromatin in an independent and different manner (Gillette *et al.,* 2004a; F. Gonzalez, Delahodde, Kodadek, & Johnston, 2002). Therefore the discrepancy of the findings makes it difficult to discriminate if the proteasome holoenzyme or its individual components are recruited on the chromatin.

6.4 Proteasome recruitment to the chromatin

Overall, interaction studies between proteasome subunits and chromatin by chromatin immunoprecipitation (ChIP) suggest a broad association of the proteasome with chromatin. Specifically, in yeast, proteasome particles, both 19S and 20S, were shown to be rapidly recruited to the RNAPII transcribed *GAL10* gene upon its activation. Once activated, the proteasome was found to be associated with the entire transcribed portion of the *GAL10* gene and rapidly dissociated from chromatin upon transcriptional termination, mirroring the RNAPII kinetics (Geng & Tansey, 2012; Sikder *et al.*, 2006). On the contrary, previous studies have reported that only 19S associates with the RNAPII transcribed *GAL1* promoter upon its induction, while 20S is recruited later mainly accumulating at the 3'end of the gene (Gillette, Gonzalez, Delahodde, Johnston, & Kodadek, 2004b; F. Gonzalez *et al.,* 2002). Furthermore, the proteasome was also found to be recruited to regions transcribed by RNAPIII including noncoding RNA and tRNA genes in a transcriptionally–dependent manner (Geng & Tansey, 2012). The association of the proteasome with transcriptionally active genomic regions is further strengthened by genome wide studies, where one or more proteasome subunits were revealed to be bound with the majority of transcriptionally active regions in the yeast genome (Auld *et al.,* 2006; Sikder *et al.,* 2006). Interestingly, the recruitment of the proteasome is not restricted to transcription sites, as budding yeast subtelomeres/telomeres (Geng & Tansey, 2012) and fission yeast centromeres (Kitagawa, Ishii, Takeda, & Matsumoto, 2014a) were also found to be associated with both proteasome particles and 19S RP respectively. Moreover, a study in mouse embryonic stem (ES) cells reported binding of the 19S and 20S proteasome at the cryptic (intergenic) gene promoters

(Szutorisz *et al.*, 2006). Likewise the 19S RP was shown to be recruited to the promoter-proximal and coding regions on the reporter gene in HeLa cells, whereas 20S was found to be associated weakly with the promoter-proximal regions and absent from coding regions (Lassot *et al.,* 2007). Finally, the proteasome is also identified by a number of independent studies to get recruited to double-stranded DNA break sites where it degrades the stalled RNAPII (T. T. Huang & D'Andrea, 2006; Krogan *et al.,* 2004a; K. B. Lee, Wang, Lippard, & Sharp, 2002; Malik *et al.,* 2008). The presence of the proteasome on different compartments of chromatin suggests that its function is not restricted to regulating a specific process but rather a variety of chromatin functions.

So far, three different models have been proposed to explain the mechanism of the recruitment of the proteasome holoenzyme or its individual components to chromatin (McCann & Tansey, 2014). The first model suggests that the proteasome is directly interacting with chromatin bound factors such as the Gal4 activator (C. Chang *et al.,* 2001; F. Gonzalez *et al.*, 2002) and nucleosomal histones (Chaves, Baskerville, Yu, & Reed, 2010; Qian *et al.,* 2013). In the second model proteasome recruitment to chromatin is occurring through interaction with intermediate (adaptor) proteins such as Cks1 and Cdk1 bound to histone tails (Morris *et al.,* 2003). Lastly, the third model, which can also explain the wide association of the proteasome with different chromatin regions, suggests that proteasome is simply recruited to chromatin through recognition of ubiquitinated proteins. This model comes in agreement with a recent study where 20S proteasome and ubiquitin were shown by ChIP-seq analysis to have similar pattern of genomic distribution, with significant rearrangement occurring upon proteasome inhibition (Catic *et al.,* 2013). Furthermore, the same study revealed an increase in ubiquitin conjugated substrates bound to highly expressed genes with proteasome inhibition, indicating that the proteasome might be recruited to chromatin in order to degrade the ubiquitinated proteins.

6.5 Function of the Proteasome in transcription

Increasing evidence suggests that one of the chromatin related functions of the proteasome is regulation of transcription (Geng *et al.*, 2012). Since the proteasome is known to affect a large number of cellular pathways, it is often difficult to discriminate the direct from its indirect effect on transcription. Still, a number of genome-wide studies have identified the effect of the proteasome in transcriptional regulation, as chemical or genetic proteasome inhibition was shown to significantly disturb the expression patterns of a large proportion of the genome in yeast, mouse and human cells (Dembla-Rajpal, Seipelt, Wang, & Rymond, 2004; Fleming *et al.,* 2002; Z. Y. Tang, Wu, Gao, & Shen, 2008; Zimmermann *et al.*, 2000).

Transcription is a highly regulated process that can be categorised in 3 main phases: initiation, elongation and termination. Each phase is regulated by multiple factors that directly or indirectly associate with RNA polymerase and facilitate RNA synthesis. Importantly, the proteasome holoenzyme or its individual components are implicated in all 3 phases.

Firstly, the proteasome regulates the levels and binding of activators as well as recruitment of co-activators at 5' regulatory regions, therefore controlling transcriptional initiation (Durairaj & Kaiser, 2014). For example, in yeast, the ATPase activity of 19S RP was shown to affect the stability and binding of the Gal4 transcriptional activator to promoters (Ferdous *et al.*, 2007; F. Gonzalez *et al.*, 2002; Nalley, Johnston, & Kodadek, 2006). Furthermore, the same particle was shown to act as a chaperone to recruit the co-activator complex SAGA to DNA bound activators including Gal4 (D. Y. Lee, Ezhkova, *et al.,* 2005; Malik *et al.*, 2009)

Secondly, the proteasome is thought to promote transcription elongation. For instance, 19S was shown to physically interact with the yeast transcription elongation factor CDC68 (Ferdous, Gonzalez, Sun, Kodadek, & Johnston, 2001). The same study also revealed elongation defects caused by mutations in 19S particle both in vivo and in vitro. Another study found recruitment of the 19S RP to the yeast transcription elongation complex PAF1, that was shown to be mediated though adaptor protein Cks1. This interaction was demonstrated to be essential for efficient transcriptional elongation by providing energy for nucleosome eviction (Pan, Sun, Wohlschlegel, & Reed, 2013). This was further strengthened by a previous finding where a 19S mutant was seen to display high nucleosome density

along the *GAL1* locus upon transcriptional induction, indicating impairment in the process of nucleosome eviction (Chaves *et al.*, 2010).

Finally, the proteasome is thought to enable release of the RNAPII form the 3'end of the coding sequences leading to termination of transcription (Gillette *et al.,* 2004a).

So far, the majority of studies were performed in yeast and they indicate a role of the proteasome in regulation of transcriptional activation (Auld *et al.,* 2006; Fatyol & Grummt, 2008; Ferdous *et al.,* 2001; F. Gonzalez *et al.,* 2002; Kang, Pirskanen, Janne, & Palvimo, 2002; D. Y. Lee, Ezhkova, *et al.*, 2005; Sulahian, Johnston, & Kodadek, 2006). However few studies, mostly in mammalian cells, suggest that the proteasome regulates not only transcriptional activation but also repression. A recent study in human cells revealed that inhibition of the 20S proteasome results in increased levels of RNAPII and the active chromatin mark H3K4me3 at the glucocorticoid responsive gene promoter, where proteasome binding was identified (Kinyamu & Archer, 2007). Another study on mouse embryonic stem (ES) cells proposed that the proteasome blocks nonspecific transcription initiation by preventing preinitiation complex formation at cryptic gene promoters (Szutorisz *et al.,* 2006). The same study showed that the 19S and 20S particles are assembled into a functional 26S proteasome at cryptic promoter sites and degrade RNAPII or a member of the pre-initiation complex that drives the transcription at these ectopic sites, thereby suppressing permissive transcription. This is an agreement with the effect of proteasome inhibition, which resulted in a significant increase in the transcription of intergenic and intragenic regions (Szutorisz *et al.,* 2006). Moreover, a study performed in the liver of rats revealed that proteasome inhibition led to global hypomethylation (especially at H3K9 and H3K27 residues) and hyperacetylation (Oliva, Dedes, Li, French, & Bardag-Gorce, 2009). Finally another example comes from the HIV promoter, where the 26S proteasome was reported to repress its transcription during the latent viral stage (Lassot *et al.,* 2007).

7. Hypotheses, Objectives and Aims

Preliminary observations indicated that the proteasome was associated with heterochromatin both in pericentromeric and the pathological GAA triplet-repeat expansion. Therefore, the main hypothesis examined in this PhD thesis was that heterochromatin-mediated transcriptional repression might be dependent on proteasomal function. Additionally, this thesis also addressed the hypothesis that it might be possible to inhibit pathologically heterochromatinisation of the *FXN* gene in the incurable neurodegenerative disease as a potential radical therapy.

The general objectives of this Ph.D were thus to investigate the transcriptional silencing of several DNA repetitive elements in mammalian cells and the factors that regulate their repression. The factors examined included an HDAC inhibitor (nicotinamide), the proteasome, cell cycle and HSF1. The DNA regions studied were: (i) the pathologically heterochromatinised *FXN* gene, (ii) pericentromeric repeats, (iii) centromeric repeats and (iv) LINE L1 and SINE B1 retrotransposons.

The main aims of this Ph.D were therefore:

- To assess the effect of HDAC inhibitor nicotinamide on the chromatin structure and expression of the *FXN* gene in FRDA patients (clinical trial) (chapter 2).
- To investigate the heterochromatinisation of the *FXN* gene and the effect of proteasome inhibition on the expression of the *FXN* gene (chapter 3).
- To determine the effect of proteasome inhibition on transcription of heterochromatic repeats (chapter 4).
- To understand the role of the proteasome in maintenance of constitutive heterochromatin (chapter 4 and chapter 5).

CHAPTER 2: The effect of high dose nicotinamide in patients with Friedreich's ataxia

2.1 Introduction

It has previously been shown from our lab that treatment with the HDAC inhibitor nicotinamide can significantly upregulate *FXN* expression in primary human cells, cell lines and disease-affected tissues derived from a mouse model for Friedreich's ataxia by apparent remodelling of the pathologically heterochromatinised *FXN* locus (P. K. Chan *et al.*, 2013). More specifically, this *FXN* upregulation was accompanied by (i) a reduction in H3K9me3 and H3K27me3 and (ii) an increase in H3 and H4 acetylation marks on the FXN locus. These findings lead to a clinical study to assess whether nicotinamide could be safely used to reactivate the epigenetically silenced *FXN* gene in FRDA patients. The study was conducted in three phases. Phase 1 was a single-dose, dose escalating phase undertaken over five visits. In phase 2 patients were administered escalating daily doses for five days and in phase 3 they were given their maximum tolerated dose daily for 8 weeks. It should be noted that this study was a collaborative effort and has been published in the Lancet my main contribution was the analysis of chromatin by ChIP.

2.2 Results

2.2.1 Phase 1 clinical trial

The first phase of the clinical trial was performed to investigate the minimum dose at which nicotinamide could be safely used to upregulate *FXN* expression in ten FRDA patients. This was achieved by orally given escalating doses of 0, 2, 4, 6, 7 and 8 g of nicotinamide at five different visits, with at least one week washout period between each visit. The treatment of all doses was well tolerated with the main side effect of nausea. Blood samples were collected before treatment and at 2, 4, 8 and 24h after dosing to analyse the pharmacokinetics and pharmacodynamics of nicotinamide, by measuring the plasma level of

nicotinamide as well as *FXN* mRNA and frataxin protein in peripheral blood mononuclear cells (PBMCs). In addition, the blood samples were collected at 8h at the last visit where 8 g of nicotinamide were given to patients, to analyse any possible changes in the chromatin structure of the *FXN* gene.

Analysis of the effect of single, escalating doses of nicotinamide on frataxin protein concentration in patients with Friedreich's ataxia over 24h revealed a statistically significant increase at 8h after administration of single dose of 2-8 g nicotinamide, with highest level at 7 and 8 g. Moreover, no change of the frataxin protein level was observed at 2h after being given a single dose of 2-8 g of nicotinamide, with non-significant increase at 4h. Noticeably frataxin protein concentration was returned to baseline by 24h (Figure 2.1).

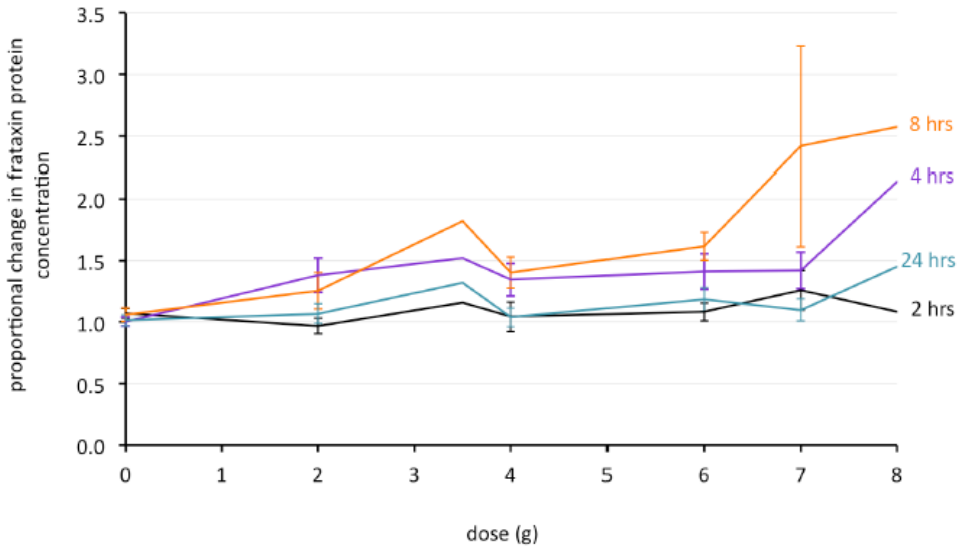


Figure 2.1: The effect of single, escalating doses of nicotinamide on frataxin protein concentration in patients with Friedreich's ataxia over 24 h. Data are mean values for the proportional change in concentration of frataxin protein in peripheral blood mononuclear cells (simple ratio relative to baseline). Error bars show SEs. For 0 g, n=10; 2 g, n=10; 3·5 g, n=1; 4 g, n=10; 6 g, n=9; 7 g, n=4; 8 g, n=1. The proportional change from baseline to 8 h showed a significant increase with increasing dose (p=0·0004). Adapted from (Libri *et al.*, 2014).

Further analysis of plasma nictonamide, *FXN* mRNA and frataxin protein in peripheral blood mononuclear cells showed that treatment with a single dose of 4g (Figure 2.2B) and 6g (Figure 2.2C) of oral nicotinamide, results in an initial dose-dependent upregulation of plasma nicotinamide which peaked at 2h after treatment, followed by *FXN* mRNA expression peaking at 4h and then frataxin protein concentration that peaked at 8h (Figure 2.2B, 2.2C). No change of the *FXN* mRNA and frataxin protein was observed in the control group (Figure 2.2A). This finding agrees with the hypothesis that nicotinamide acts at the transcriptional level.

The plasma nicotinamide levels after reaching their peak at 2h of treatment decreased gradually, in line with previously reported studies of the nicotinamide half-life (Horsman, Hoyer, Honess, Dennis, & Overgaard, 1993; Stratford & Dennis, 1994; Stratford *et al.*, 1996). Noticeably the reduction of the *FXN* mRNA levels was faster than the frataxin protein concentration, consistent with the fact that the half-life of the mRNA is shorter than the half-life of the frataxin protein (Rufini *et al.,* 2011).

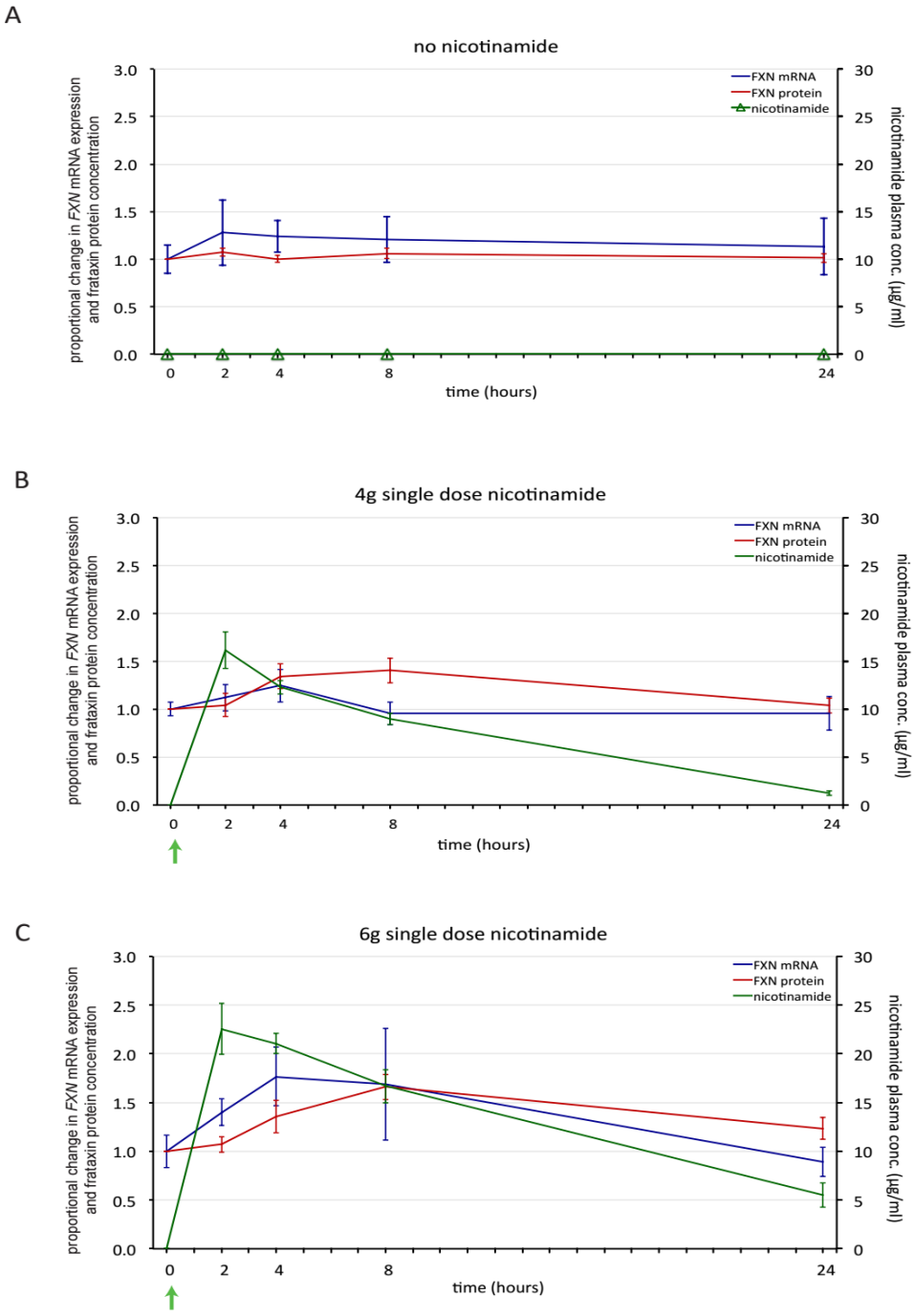


Figure 2.2: Plasma nicotinamide, *FXN* mRNA and frataxin protein analysis of single-doses of nicotinamide over 24h in PBMCs for (A) no nicotinamide n=10, (B) a single 4 g dose, n=10 and (C) a single 6 g dose n=9. Each measurement is shown as a simple ratio relative to each individual's baseline; the mean for all subjects of this proportional change is shown. Green arrow indicates the dose timing. Error bars show SEs. Adapted from (Libri *et al.*, 2014).

Moreover chromatin immunoprecipitation was performed to investigate the mechanism of *FXN* mRNA expression upregulation. Heterochromatic H3K9me3 and euchromatic H3Ac histone modification marks were examined on the regions flanking the GAA repeats in the first intron of the *FXN* gene. The results showed a reduction of the H3K9me3 in patients treated with nicotinamide after the dose compared to pre-dose although this was not statistically significant. No statistically significant change of the H3ac mark was observed on the regions examined (Figure 2.3B).

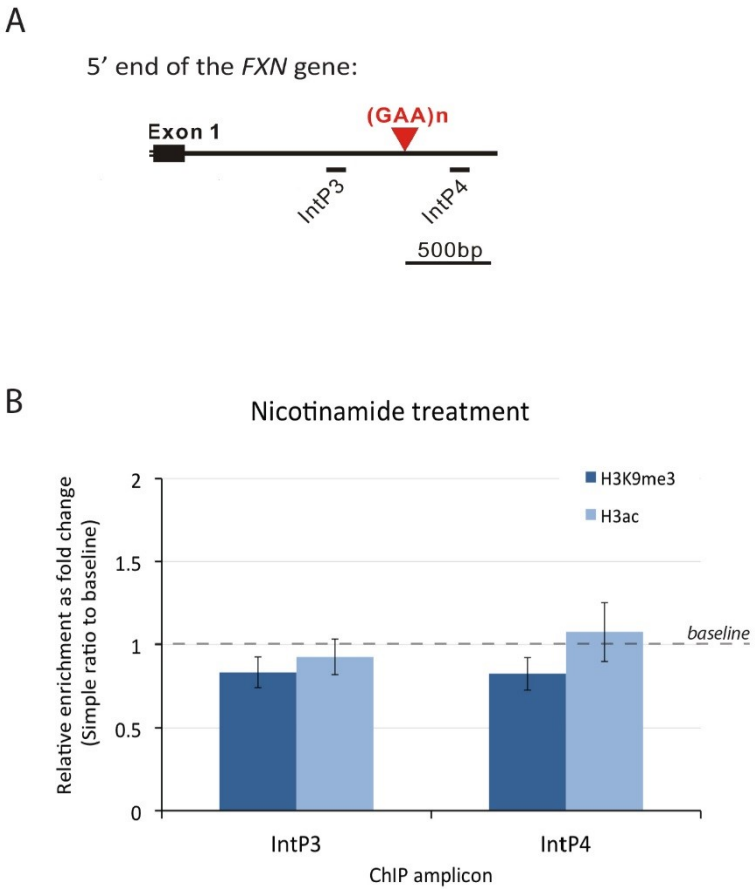


Figure 2.3: Chromatin immunoprecipitation analysis of heterochromatic (H3K9me3) and euchromatic (H3ac) histone marks on the regions flanking the GAA repeats of the *FXN* locus. Patients were given a single dose of 8g nicotinamide followed 8 hours later by ChIP–qPCR using H3K9me3 and H3ac antibodies in PBMCs. (A) The location of the primers used to analyse the regions flanking the GAA repeats in intron 1 of the *FXN* gene. (B) Changes in the levels of H3K9me3 and H3ac between pre-dose (baseline) and 8 hours post-dose. Data were normalised against H3 followed by background subtraction (no antibody) and are shown as enrichment relative to baseline. As an internal control the data were also normalised to average of housekeeping genes for H3ac and α-satellite repeats for H3K9me3 (see material and methods). Error bars show SEs, n=8.

2.2.2 Phase 2 Clinical trial

The second phase of the clinical trial was performed to investigate the pharmacokinetics and pharmacodynamics of nicotinamide in relation to upregulation of *FXN* mRNA expression after dosing with nicotinamide for 5 consecutive days. In total 8 FRDA patients were administrated 3.5 g of nicotinamide on the first day, 4 g on the second day, 5 g on the third day and 6 g on fourth and fifth day. Two FRDA patients were used as a control group to identify any changes in *FXN* expression that was not due to treatment with nicotinamide. Blood samples were collected before dosing and 2, 4 and 8 h after dosing to check, as in Phase 1, the plasma nicotinamide levels, *FXN* mRNA expression and frataxin protein concentration levels. Additionally on the fifth day of treatment blood samples were taken 8h post-dose to analyse the chromatin structure on the *FXN* gene.

The results from the plasma and peripheral blood mononuclear cells showed an initial increase in nicotinamide levels that peaked at 2h irrespective of dose upon, followed by an increase in *FXN* mRNA expression and then the frataxin protein concentration (Figure 2.4B), while there was no change in the control group (Figure 2.4A). A similar pattern was observed in phase 1 of this study (Figure 2.2). However in Phase 2, after decay of nicotinamide, *FXN* mRNA expression fell to the initial levels, whereas frataxin protein concentration was maintained constantly at higher levels than the pre-dose (Figure 2.4).

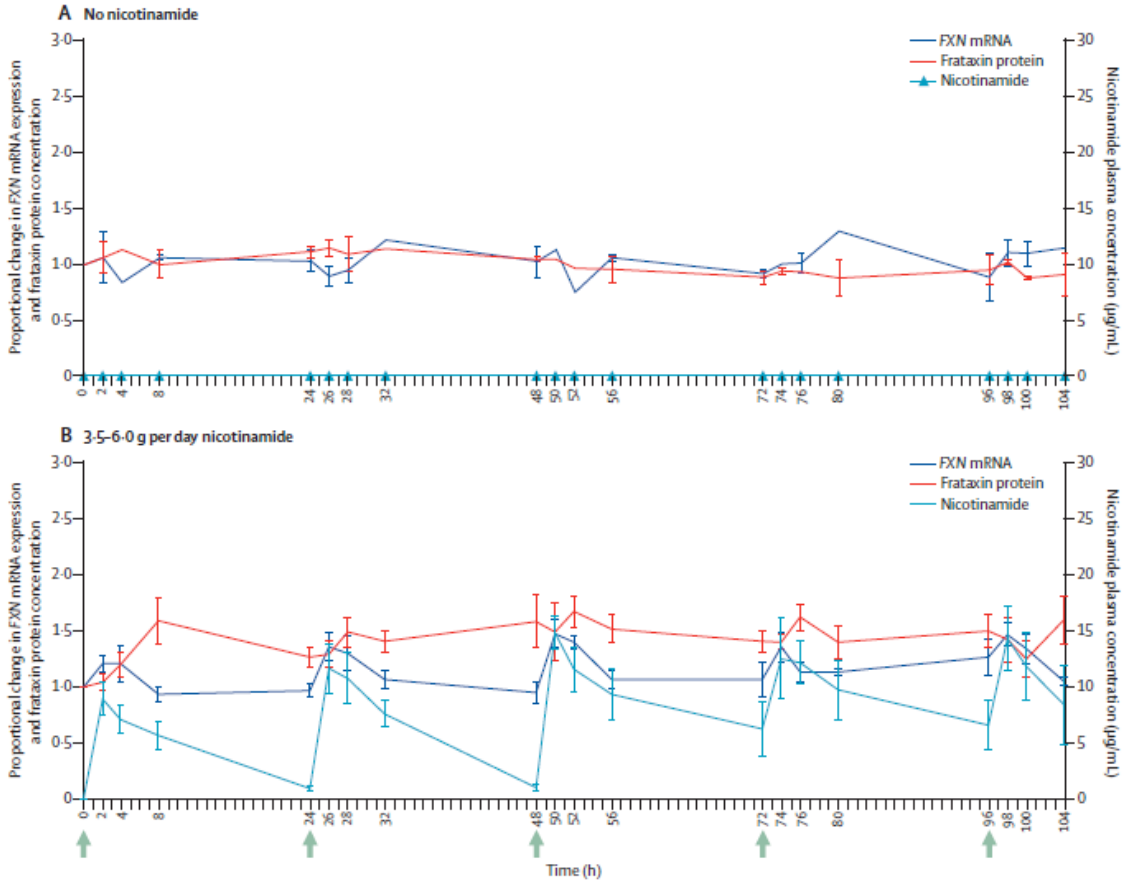


Figure 2.4: Plasma nicotinamide, *FXN* mRNA and frataxin protein analysis after daily doses of nicotinamide over 5 days. Data are mean values for nicotinamide plasma concentration and proportional changes in *FXN* mRNA expression and frataxin protein concentration in PBMCs (simple ration relative to baseline) for (A) no nicotinamide n=2 and (B) escalating doses of 3.5 – 6 g per day over 5 days. Error bars SEs, n=8. Green arrows indicate the time of dosing. Adapted from (Libri *et al.*, 2014).

Moreover chromatin immunoprecipitation was performed using antibodies against H3K9me3 and H3ac marks and DNA was amplified by qPCR using primers flanking the GAA repeats in intron 1 of *FXN* gene, as previously described in Phase 1. The H3K9me3 showed highly statistically significant down regulation, whereas the H3ac showed an increase, although this was not statistically significant, at both examined regions in treated patients before and after dose (Figure 2.5B).

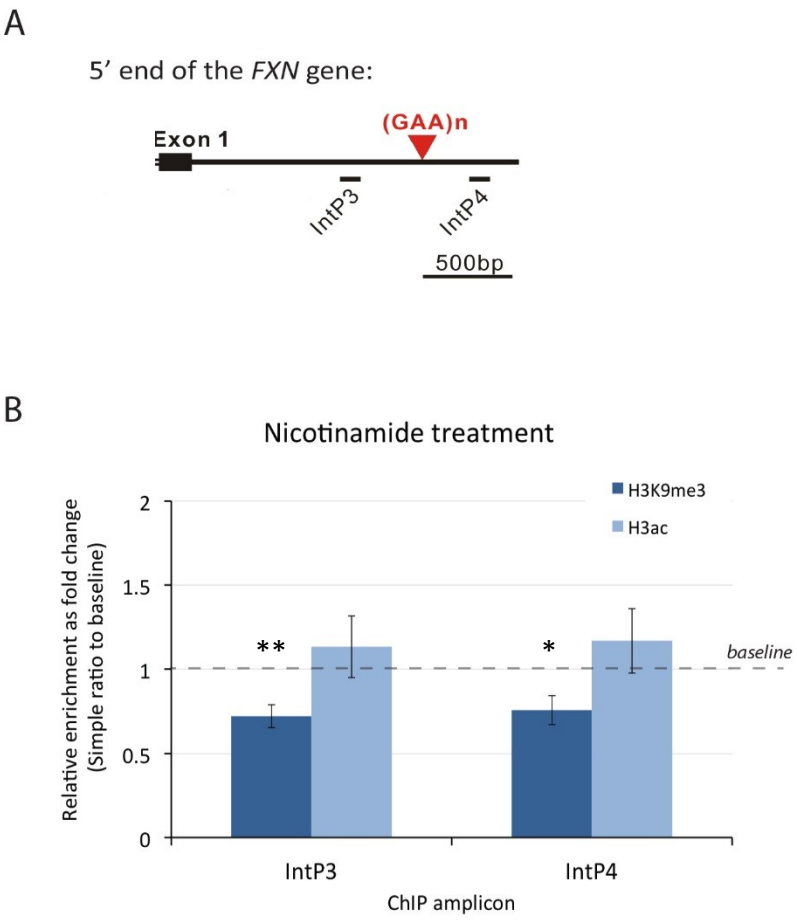


Figure 2.5: Chromatin immunoprecipitation analysis of heterochromatic (H3K9me3) and euchromatic (H3ac) histone marks on the regions flanking the GAA repeats of the *FXN* locus. Patients were given a daily dose of nicotinamide over 5 consecutive days followed by ChIP-qPCR using H3K9me3 and H3ac antibodies in PBMCs. (A) The location of the primers used to analyse the regions flanking the GAA repeats in intron 1 of the *FXN* gene. (B) Changes in the levels of H3K9me3 and H3ac between pre-dose (baseline) and post-dose of nicotinamide. Data were normalised against H3 followed by background subtraction (no antibody) and are shown as enrichment relative to baseline. As an internal control the data were also normalised to average of housekeeping genes for H3ac and α-satellite repeats for H3K9me3 (see material and methods). Error bars show SEs, n=8. Students t test: $^{**}p < 0.01$, $^{*}p < 0.05$. Adapted from (Libri *et al.*, 2014).

2.3 Discussion

The results shown in this chapter demonstrate that nicotinamide can restore *FXN* transcription at the pathologically silenced *FXN* gene in patients with FRDA. More specifically both phases of this study revealed that nicotinamide is effective in upregulating the *FXN* mRNA transcription thereby increasing the frataxin protein concentration in PBMCs, this correlated with a significant reduction in the heterochromatic modification H3K9me3 and a non-significant increase in the H3ac marks on the regions flanking the GAA repeats in intron 1 of the *FXN* gene. This is perhaps not surprising since nicotinamide was previously shown not only to inhibit class III HDACs but also to inhibit SUV39H methyltransferase activity (Vaquero *et al.*, 2007). A hypothetical mechanism through which nicotinamide may antagonise the pathological *FXN* gene silencing is shown in the Figure 2.6.

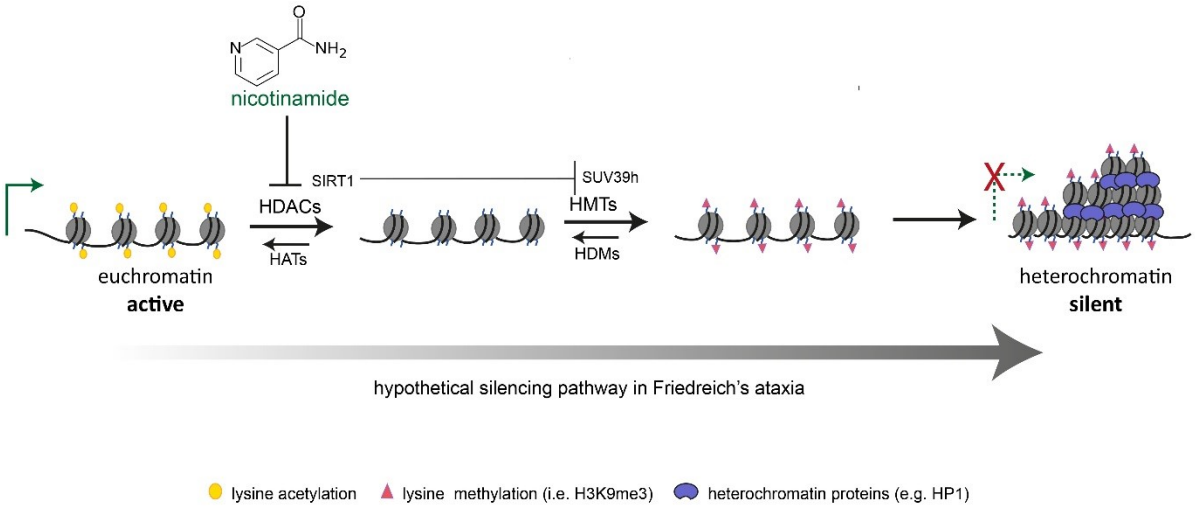


Figure 2.6: Hypothetical mechanism by which nicotinamide might antagonise the pathological *FXN* gene silencing that causes Friedreich's ataxia. Adapted from (Libri *et al.*, 2014)

As mentioned in the general introduction (section 5.4), many studies have previously shown the effect of HDAC inhibition on the upregulation of *FXN* mRNA expression in patient lympoblastoid cell lines and PBMCs. In recent years, some HDAC inhibitors have been tested as potential drugs for cancer treatment in various clinical trials (Bolden, Peart, & Johnstone, 2006; Gui, Ngo, Xu, Richon, & Marks, 2004; Mottamal, Zheng, Huang, & Wang, 2015;

Walkinshaw & Yang, 2008). The study shown in this chapter is the first known clinical trial of the potential use of an HDAC inhibitior nicotinamide as a treatment for Friedreich's ataxia. Another HDAC inhibitor (RG2833) was recently shown to reverse the *FXN* gene silencing in FRDA neurons derived from patient iPSCs to a similar degree as nicotinamide (Soragni *et al.*, 2014). The RG2833 compound was demonstrated to upregulate the *FXN* mRNA expression and frataxin protein concentration, with concomitant change of the epigenetic state of the *FXN* gene in these neuronal cells. Furthermore, the investigators identified a significant increase in H3K9 acetylation, accompanied by increased *FXN* mRNA in blood from patients treated with RG2833 (Soragni *et al.*, 2014). However, the major drawback is that this compound does not pass across the blood-brain barrier easily and converts from active to potential inactive toxic metabolic products (benzamidazole and products of amidolysis), which have a long elimination period *in vivo* (Soragni *et al.,* 2014). On the other hand nicotinamide has good bioavailability, good safety profile, is rapidly absorbed after oral administration and rapidly penetrates all tissues, including easily passing through the blood-brain barrier (Hoane, Kaplan, & Ellis, 2006; Knip *et al.,* 2000; Spector & Kelley, 1979; Stratford & Dennis, 1994).

Beside the ability to upregulate the expression of the *FXN* gene in FRDA, nicotinamide is also known to play a role in reducing effects of the oxidative stress, a major factor contributing to the pathology of FRDA (Crowley, Payne, Bernstein, Bernstein, & Roe, 2000; F. Li, Chong, & Maiese, 2006). Therefore this ability further strengthens the use of nicotinamide as a potential therapeutic agent.

In summary the results in this chapter suggest that:

- Treatment of FRDA patients with nicotinamide upregulates the *FXN* expression in PBMCs which is accompanied by reduction of H3K9me3 levels. This suggests that HDAC inhibition can overcome pathological silencing in humans providing a potential therapeutic avenue for this currently incurable disease.

2.4 Contributions

FXN RNA and protein analysis was performed by Dr C.Yandim. The plasma nicotinamide levels were analysed by Dr Sophie Piper. Theona Natisvili performed the majority of ChIP experiments, with some help from Ms. Pui Pik Law.

CHAPTER 3: Binding of the proteasome to the *FXN* gene and the effect of proteasome inhibition on the *FXN* expression.

3.1 Introduction:

Recently, the Gene Control Mechanisms and Disease Group at the CSC carried out a study to investigate a possible mechanism for transcriptional repression of the *FXN* gene with expanded GAA repeats. Specifically, during the study, the distribution of RNAPII with different phosphorylation residues (Serine5 or Serine2) on its carboxy-terminal domain (CTD) was analysed via chromatin immunoprecipitation along the *FXN* locus using (i) healthy and FRDA patient lymphoblastoid cell lines (Healthy, FRDA_1 and FRDA_2) and (ii) primary cells. Serine5 phosphorylated RNAPII (S5P-RNAPII) has been shown by ChIP to be enriched at the promoter regions of active genes and so-called 'paused genes' where RNAPII has stalled near the promoter whereas Serine2 phosphorylated RNAPII (S2P-RNAPII) is associated with transcriptional elongation (Brookes & Pombo, 2009) (Figure 3.1). The results revealed an unusual binding distribution along the *FXN* gene, in both patient and healthy cells (manuscript under revision, PhD thesis Yandim 2012). The enrichment for S5P-RNAPII was found by ChIP to peak at exon 1 and rapidly decreased while moving downstream into the intron 1 to a similar extent in cells from both healthy and FRDA patients. Surprisingly, the S2P-RNAPII which typically increases steadily though the coding regions of active genes, had a similar distribution to S5P-RNAPII with a prominent peak found at exon 1 and with overall a relatively higher signal in FRDA cell lines compared to the healthy cell line. The unusual stalling of S2P-RNAPII was further supported by RNA Immunoprecipitation (RIP) using an anti-S2P-RNAPII antibody in the healthy cell line where 6-fold enrichment was detected for RNA transcripts from exon 1 relative with a region ~600bp downstream within the first intron (PhD thesis (Yandim, 2012). These results suggest that RNAPII is stalled at exon 1 in both healthy and FRDA derived cells and is consistent with a previous study (E. Kim, Napierala, & Dent, 2011) where more primary transcript was detected upstream rather than downstream of the identified RNAPII stalling site. These results are also consistent with several additional reports showing defects in the transcription elongation process at the *FXN* gene (E. Kim *et al.,* 2011; Y. Li *et al.*, 2015; Punga & Buhler, 2010). However it is noteworthy

that some studies have also attributed the reduction of the *FXN* transcription due to defects in the transcription initiation (Chutake *et al.,* 2014; Chutake *et al.,* 2015) or even both transcriptional initiation and elongation process (Kumari *et al.,* 2011).

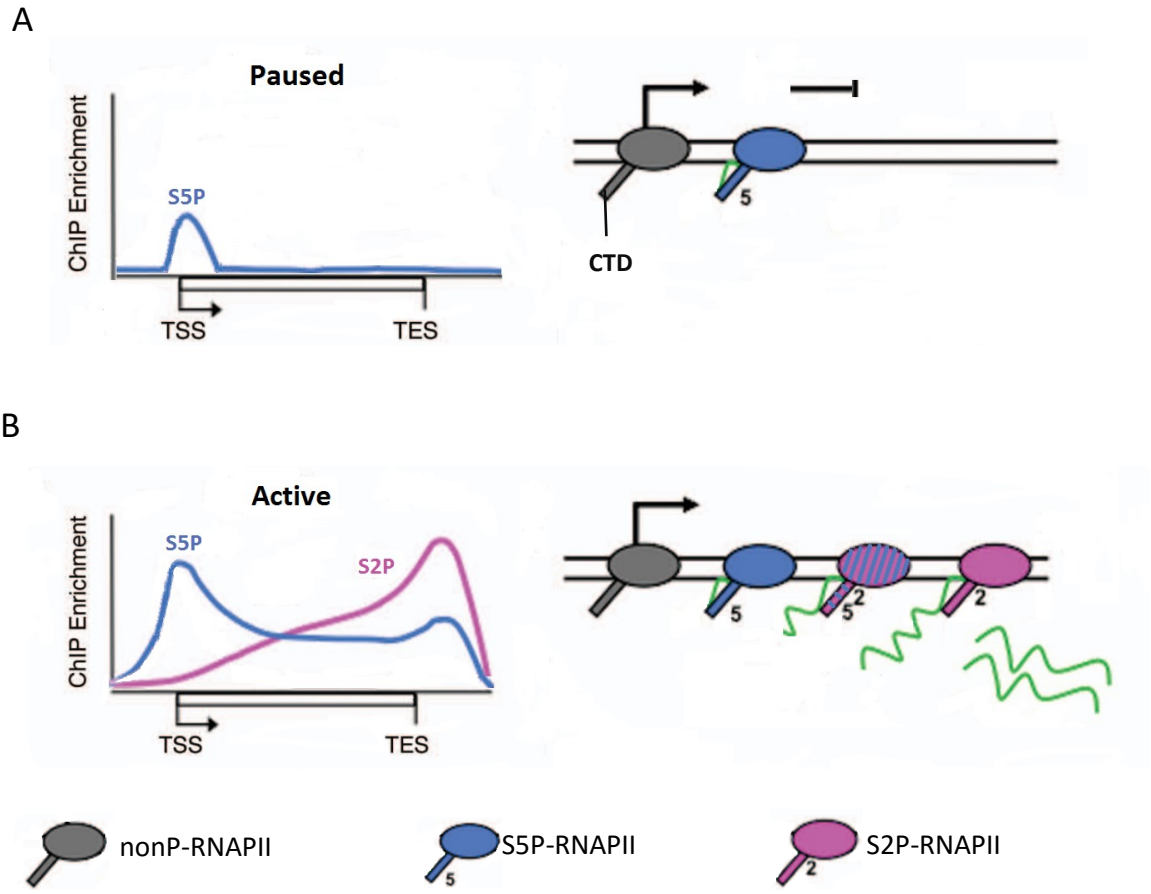
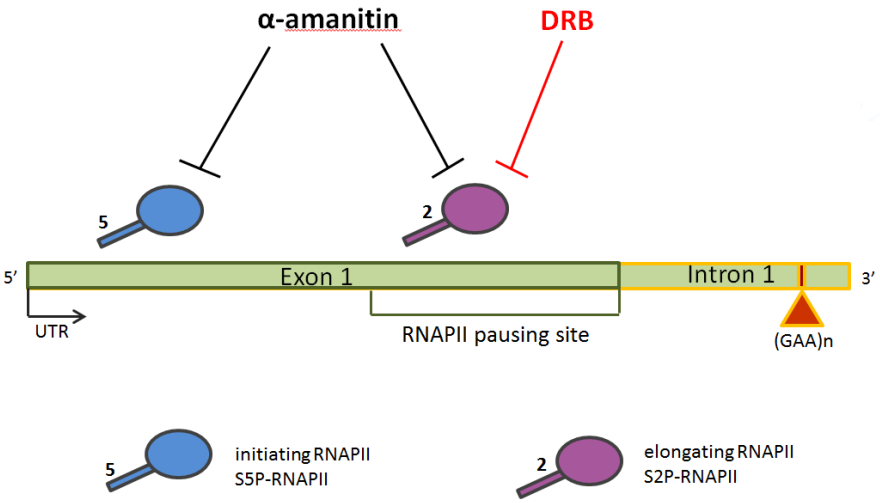


Figure 3.1: RNAPII CTD phosphorylation patterns at (A) paused gene and (B) actively transcribed gene. Hypophosphorylated (nonP-RNAPII) is recruited to the promoter region and becomes phosphorylated at Ser5 CTD residue. S5P-RNAPII progresses toward the pausing site (promoter proximal region) where phosphorylation of Ser2 CTD residue permits the transcriptional elongation to take place. TSS, transcription start site; TES, transcription end site. Based on (Brookes & Pombo, 2009, 2012; Phatnani & Greenleaf, 2006).

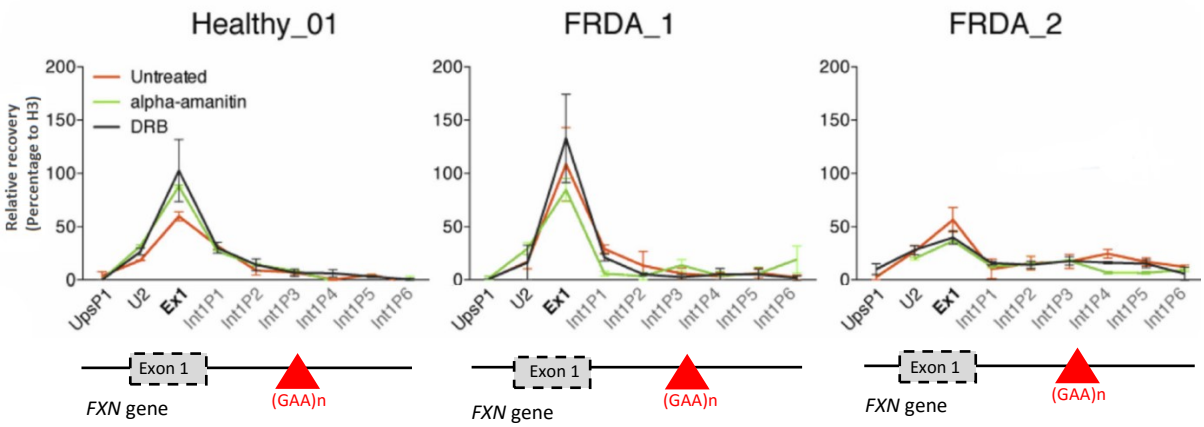
Furthermore, in order to investigate the dynamics of RNAPII at exon 1 in more detail α-amanitin and 6-dichloro-1β-ribofuranosylbenzimidazol (DRB) were used to inhibit the RNAPII and assess by ChIP the effect of the inhibition on the distribution of S2P and S5P-RNAPII across the *FXN* gene. α-amanitin completely freezes RNAPII by blocking the translocation step of the transcript polymerization reaction (Brueckner & Cramer, 2008; Bushnell, Cramer, & Kornberg, 2002; Chafin, Guo, & Price, 1995; X. Q. Gong, Nedialkov, & Burton, 2004) whereas DRB prevents elongation by inhibiting CDK9 which is required for S2 phosphorylation of the RNAPII CTD (Bensaude, 2011; Chodosh, Fire, Samuels, & Sharp, 1989; Dubois, Nguyen, Bellier, & Bensaude, 1994; S. Q. Xie, Martin, Guillot, Bentley, & Pombo, 2006). Thus, the DRB will prevent RNAPII which initiated from proceeding to elongation leaving only the already S2P-RNAPII to continue elongating (Figure 3.2A).

A

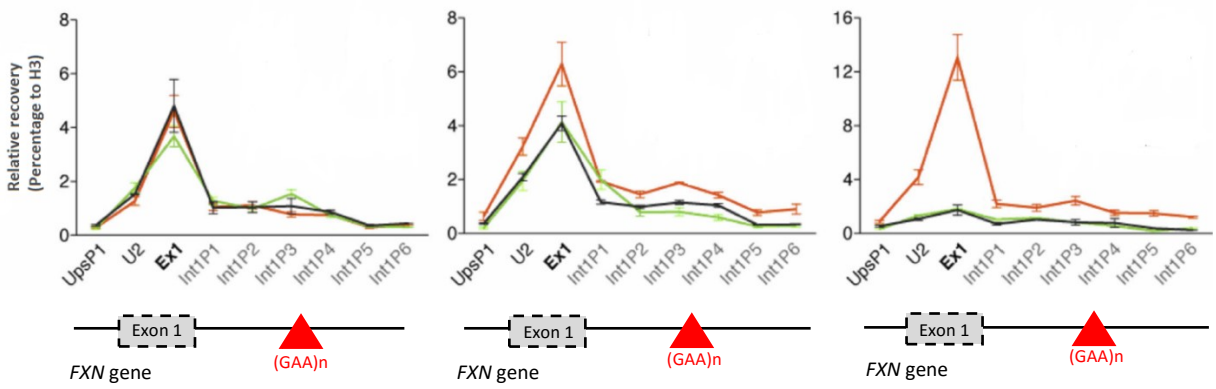


B

S5P-RNAPII



S2P-RNAPII



See next page for figure legend

Figure 3.2: Investigation of RNAPII dynamics at exon 1 of the *FXN* gene. (A) Principle behind examining the dynamics of RNAPII on the *FXN* gene. RNAPII was inhibited with α-amanitin which inhibits both initiating and elongating forms of RNAPII or DRB which inhibits only the elongating form of RNAPII. The distribution of RNAPII (S5P- and S2P-RNAPII) after its inhibition was assessed using ChIP, as shown in (B). (B) S2P-RNAPII remained stalled at exon 1 of the *FXN* gene in healthy cells but it was reduced following transcriptional inhibition in FRDA cell lines. S5P-RNAPII remained unaffected. X axis shows regions of the *FXN* gene identified by PCR and below is shown a schematic of the *FXN* gene indicating the site of GAA repeat expansion. B adapted and modified with permission from (PhD thesis (Yandim, 2012)).

In the healthy cell line, both inhibitors induced a small increase of the S5P-RNAPII and only a minor decrease of S2P-RNAPII enrichment at exon 1 (Figure 3.2B). These results are consistent with stalling of RNAPII at exon 1 of the *FXN* gene as the inhibition by DRB did not result in a decrease in the peak for RNAPII seen at exon 1. Furthermore, the resistance of a S2P-RNAPII peak to both inhibitors indicates that in the healthy cell line the elongating RNAPII is surprisingly protected against proteasome mediated degradation as persistently stalled S2P-RNAPII (e.g during DNA damage) is normally degraded by the ubiquitin-proteasome system (Daulny & Tansey, 2009; K. B. Lee *et al.*, 2002; Somesh *et al.,* 2005; Somesh *et al.,* 2007; L. Y. Yang, Jiang, & Rangel, 2003). Thus, in the healthy *FXN* gene the RNAPII is not only stalled but is also unusually refractory to S2P-dependent degradation by the proteasome. In contrast to the healthy cell lines, treatment of patient cells lines with both transcriptional inhibitors induced a reduction of S2P-RNAPII levels at exon 1, whereas S5P-RNAPII remained unaffected (Figure 3.2B). These results together with the recruitment of the 19S proteasome on the patient *FXN* gene, analysed by ChIP, suggested that the proteasome might degrade the stalled S2P-RNAPII in the patient cell lines thereby preventing the transcription of the gene. Therefore, to investigate this possibility, the proteasome was inhibited at the same time as transcriptional inhibition and the level of S2P-RNAPII on the *FXN* gene was assessed. The inhibition of the proteasome was achieved by using the well-known proteasome inhibitor PS-341 (Pyz-Phe-boroLeu, Bortezomib, Velcade®). PS341 is a dipeptide molecule targeting primarily proteasomal β5 (chymotrypsin-like) site and secondarily the β1 (caspase-like) site (Berkers *et al.*, 2005). It has high cell permeability, prolonged chemical stability and is the first approved proteasome inhibitor

used in patients to treat acute myeloid leukaemia (Chauhan, Hideshima, Mitsiades, Richardson, & Anderson, 2005; Field-Smith, Morgan, & Davies, 2006; Meenaghan *et al.,* 2010b; Richardson, Mitsiades, Hideshima, & Anderson, 2006; Sonneveld *et al.*, 2012).

As illustrated in Figure 3.3, treatment of patient cells with PS341 prevented the α-amanitin induced reduction of S2P-RNAPII in exon 1, supporting the hypothesis of proteasome dependent regulation of RNAPII at the *FXN* gene with pathologically expanded GAA repeats in FRDA. In contrast, simultaneous treatment of healthy cells with PS341 and α-amanitin had no effect on the level of RNAPII on the normal *FXN* gene (Figure 3.3), confirming the refractory nature of S2P-RNAPII to proteasome degradation in healthy individuals. Unpublished data from (Ph.D thesis (Yandim, 2012).

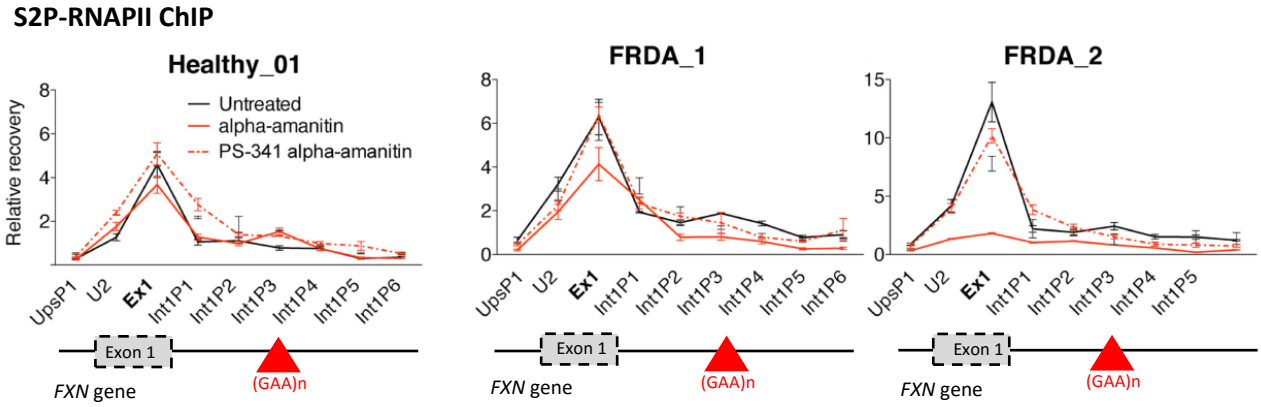


Figure 3.3: Proteasome inhibition by PS341 restores the S2P-RNAPII levels upon transcriptional inhibition by α-amanitin in FRDA (FRDA_1 and FRDA_2) cell lines and has no effect in a healthy cell line (Healthy_01). Graphs represent the binding of S2P-RNAPII measured by ChIP across the *FXN* gene after α-amanitin, PS341 and PS341 plus α-amanitin treatments. X axis shows regions of the *FXN* gene identified by PCR and below is shown a schematic of the *FXN* gene indicating the site of GAA repeat expansion. B adapted and modified with permission from Adapted and modified with permission from (Ph.D thesis (Yandim, 2012).

The main goal of this chapter was to further understand the role of the proteasome in regulation of *FXN* gene expression in FRDA and more specifically:

- To investigate the heterochromatinisation of the *FXN* gene with pathologically expanded GAA repeats by measuring the repressive H3K9me3 and activating H3ac marks across the *FXN* gene in healthy and patient cell lines.
- To assess the possible binding of the 20S CP of the proteasome which is required for proteasomal degradation along the *FXN* gene in healthy and patient cell lines, as previously only the binding of 19S RP was studied (Yandim, 2012).
- To assess the global changes of the RNAPII levels upon proteasome and transcriptional inhibition, as previously the dynamics of RNAPII was studied specifically on the *FXN* gene.
- To re-analyse the effect of the proteasome inhibition on the levels of mRNA and primary *FXN* transcripts in FRDA, both *in vitro* and *in vivo* using RNA spike to obviate the need for endogenous loading controls, as previously results suggested that proteasome inhibition might restore S2P-RNAPII levels at exon 1 in the *FXN* gene by increasing the reservoir of RNAPII available for transcription. (PhD thesis (Yandim, 2012).

3.2 Results

3.2.1 Expression of *FXN* is significantly reduced in FRDA disease cell lines

In order to confirm the *FXN* repression in FRDA, *FXN* primary transcript RNA and mRNA levels were measured by q-RT-PCR in healthy (GM14926) and patient (GM15850, GM15851) EBV-transformed lymphoblastoid cell lines (Figure 3.4). Noticeably, both patient cell lines have similar levels of GAA repeat expansion (GM15850: 650/1030 repeats; GM16234: 580/1030 repeats) but different levels of *FXN* expression. More specifically, the *FXN* mRNA expression was revealed to be 11 % and 28 % in GM15850 (hereinafter called FRDA_1) and GM16234 (hereinafter called FRDA_2) respectively, relative to the GM14926 (hereinafter called Healthy) cell line. Similarly, the expression of primary transcript was reduced to 12 % and 28 % in FRDA_1 and FRDA_2 respectively, compared to the healthy control (Figure 3.4B).

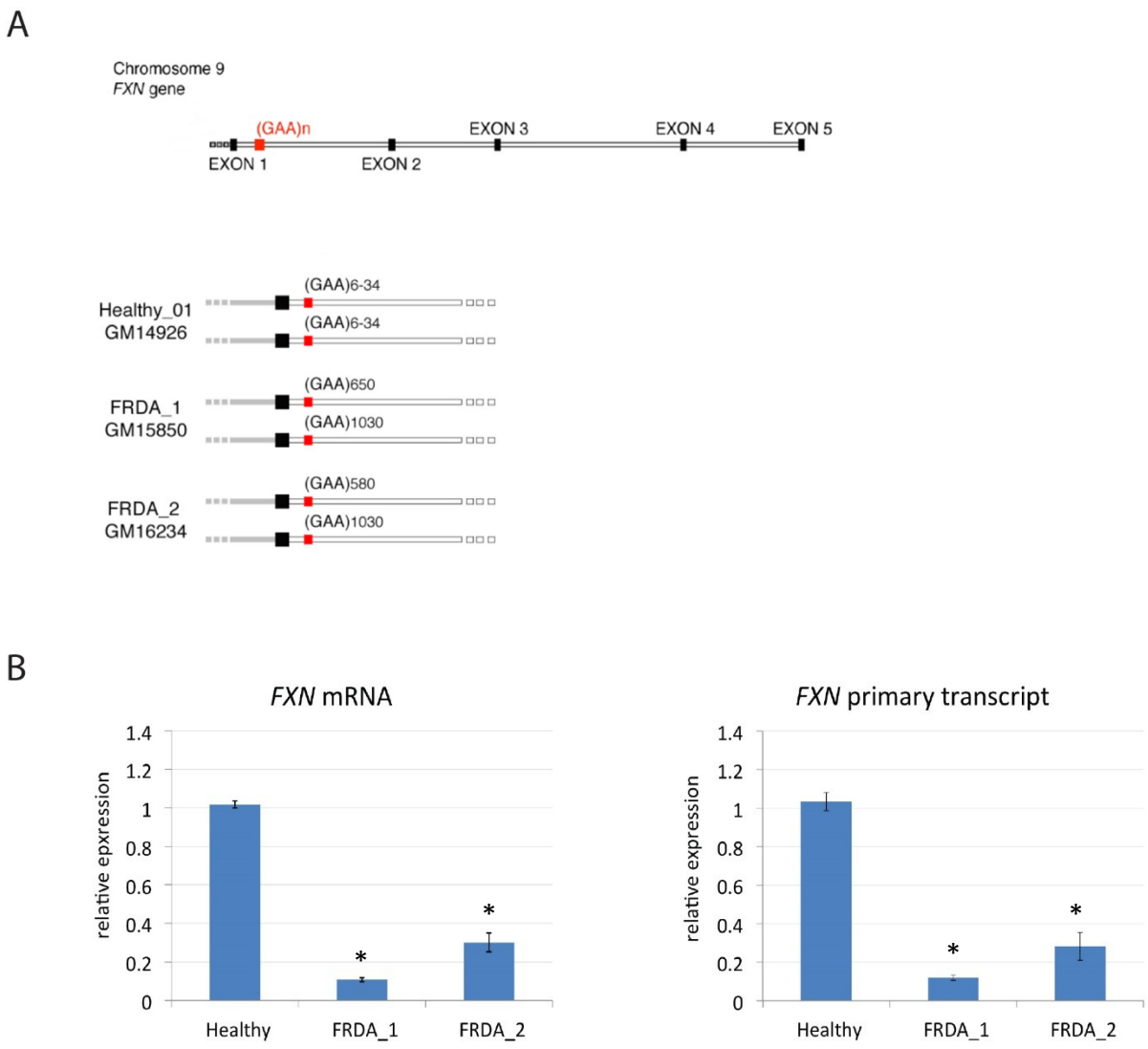


Figure 3.4: Expression of *FXN* is significantly reduced in FRDA cell lines. (A) EBV-transformed human lymphoblastoid cell lines derived from healthy individual and two FRDA patients showing the length of GAA repeat within intron 1 of *FXN* gene. Exons are indicated by black boxes. The red box/arrow shows the GAA repeat. (B) *FXN* primary transcript and mRNA expression levels in the cell lines were detected by q-RT-PCR. The relative expression was normalised against *GAPDH* and are shown as fold change relative to Healthy cell line. Error bar = SEM of at least 3 biological replicates. *p < 0.05 (Student's 't' test)

3.2.2 Decreased levels of histone acetylation and increased level of H3K9me3 histone modifications on the FXN gene in FRDA cell lines

Considering that (i) previous studies have revealed that GAA repeats can stimulate heterochromatin mediated silencing by recruiting heterochromatin-related proteins (such as histone methyltransferases) (Yandim *et al.*, 2013) and (ii) *FXN* is significantly repressed in the patient cell lines, we set out to investigate the chromatin status along the *FXN* gene in patient and healthy controls. For this, chromatin immunoprecipitation was performed with antibodies against the normally repressive histone modification mark H3K9me3 and histone modification mark H3ac which is associated with an open chromatin structure (see general introduction section 2.2.1.2.4 and 2.2.1.1). Immunoprecipitated material was quantified using qPCR with primers covering the *FXN* gene locus from ~4500bp upstream of transcription start site to ~5000bp downstream of GAA repeat in intron 1 (Figure 3.5A). Additionally, primers against beta-globin (β-globin) and alpha-satellite (ALRsat) were used as positive controls for repressed chromatin; a primer against the housekeeping gene Glyceraldehyde-3-phosphate dehydrogenase (GAPDH) was used as positive control for active chromatin (Figure 3.5).

As expected, the levels of H3K9me3 were low throughout the examined *FXN* locus in the healthy cell line where the gene is actively transcribed. On the contrary, higher levels of H3K9me3 were observed in all investigated *FXN* regions in two FRDA cell lines relative to the healthy cell line, while both controls (β-globin and ALRsat) showed similar levels of modification among all three cell lines. Importantly, H3K9me3 was particularly enriched in exon 1 of the *FXN* gene, with a minor enrichment occurring in the regions flanking the GAA repeats (In1P3 and In1P4) (Figure 3.5B).

On the other hand, the overall histone H3 acetylation (H3ac) levels were noted to peak in exon 1 for all three cell lines, with a gradual decrease upon moving towards the GAA repeats in intron 1 of the *FXN* gene. However, overall lower levels of enrichment were demonstrated to be present at these regions in two FRDA cell lines when compared to the healthy cell line. Both controls, GAPDH for positive control and ALRsat for negative control, had similar levels of H3ac enrichment in all the three cell lines (Figure 3.5C).

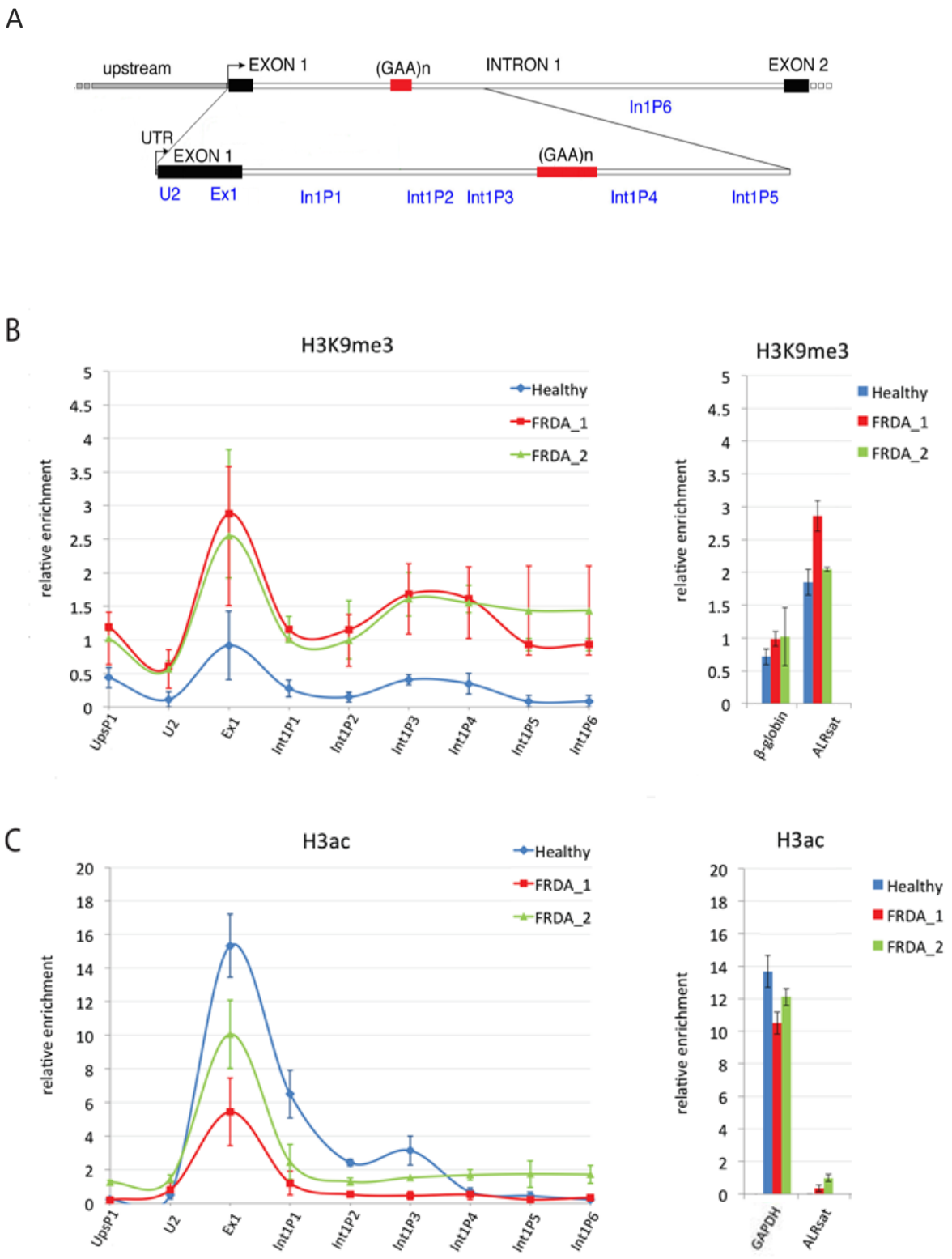


Figure 3.5: The H3K9me3 and H3ac profile along the *FXN* gene in health and FRDA cell lines. (A) Schematic representation of the position and name of primer sets used to study the *FXN* gene locus. (B) H3K9me3 and (C) H3ac was analysed by chromatin immunoprecipitation and qPCR. ChIP signals are shown as relative enrichment to H3 with background subtraction. β-globin, ALRsat and GAPDH were used as controls. Error bar represent SEM, n=2-3

Analysis of FRDA patient cell lines demonstrated (i) higher levels of H3K9me3 throughout the *FXN* gene and (ii) primarily lower levels of H3ac in exon 1 of the *FXN* gene, confirming its pathological heterochromatinisation and transcriptional repression in FRDA. Interestingly, while the H3K9me3 levels were found to be similar in the two patient cell lines, the H3ac levels were higher in FRDA_2 compared with FRDA_1 which is consistent with the expression levels of the *FXN* in these two patient cells lines (see Figure 3.4B).

3.2.3 Increased binding of the proteasome at the pathologically silenced *FXN* gene

As mentioned in the introduction of this chapter, data from the GCMD lab showed marked reduction of the stalled S2P-RNAPII within the first exon of the *FXN* gene upon transcriptional inhibition in FRDA disease cell lines but not in the healthy cell line. One possible explanation for the observed S2P-RNAPII sensitivity at the pathologically silenced *FXN* locus was degradation of the stalled RNAPII complex by the proteasome, as had previously been shown in transcription–coupled DNA repair (K. B. Lee *et al.*, 2002; Somesh *et al.,* 2005; Somesh *et al.,* 2007; L. Y. Yang *et al.,* 2003). To test this hypothesis, ChIP was performed using two different antibodies against catalytic subunits of the proteasome (20S) to investigate whether the proteasome was actively recruited to the *FXN* gene. Immunoprecipitated material was quantified using qPCR with primers covering the *FXN* gene locus from ~4500bp upstream of transcription start site to ~5000bp downstream of GAA repeat in intron 1, as in the previous experiment (Figure 3.6A). Additionally, primers against β-globin, ALRsat and GAPDH regions were used as controls for inactive, repetitive element and active regions of the genome respectively.

The result revealed binding of proteasome throughout the *FXN* locus, with an overall higher enrichment in the FRDA disease cell line compared to healthy cell line (Figure 3.6B, 3.6C). More specifically, the binding of the proteasome peaked in exon 1, and the regions flanking the GAA repeats in all the examined cell lines (Int1P3 and Int1P4). However, a prominent peak was only observed in exon 1 in the FRDA cells. Notably, proteasome ChIP signal was

also detected in all the controls, with similar enrichment levels between healthy and disease cell lines (Figure 3.6B, 3.6C). This is not surprising, as many studies have shown the regulatory role of the proteasome at fully active genes (G. A. Collins & Tansey, 2006; Ferdous *et al.*, 2001; Hegde & Upadhya, 2006; D. Y. Lee, Ezhkova, *et al.,* 2005; Lipford, Smith, Chi, & Deshaies, 2005; Muratani, Kung, Shokat, & Tansey, 2005) and transcriptionally inactive regions of the genome (Szutorisz *et al.,* 2006).

The proteasome complex consists not only of the catalytic particle (20S) but also of the regulatory particle (19S) (Adams, 2003b). The result presented in this thesis builds on our previous finding that the 19S proteasome is also present on the *FXN* locus in FRDA (Yandim, 2012) and adds weight to the hypothesis that the *FXN* associated proteasome may be competent to degrade chromatin associated proteins such as RNAPII.

Interestingly, comparison of the proteasome binding profile with the repressive histone modification H3K9me3 mark throughout the *FXN* locus revealed similar distribution pattern (compare Figure 3.5B and 3.6C), with exon 1 and regions flanking the GAA repeats showing the highest enrichment. Both H3K9me3 and proteasome were enriched at exon 1 in the patient cell lines (Figure 3.5 and 3.6). Importantly, this is the same region where S2P-RNAPII was previously shown to be stalled in all the cell lines but only significantly reduced upon transcriptional inhibition in the FRDA cell line. Furthermore, as mentioned above (see Figure 3.3) treatment of cells with proteasome inhibitor concomitant with transcriptional inhibitor restored the S2P-RNAPII level on the exon 1 in the patient cell lines, whereas no effect was shown in the healthy cell line. However, whether this restoration of S2P-RNAPII level is specific to the *FXN* gene will be investigated in the following section.

The results so far suggest that the proteasome may have an important regulatory role in FRDA pathology, by possibly rendering the stalled RNAPII on the FXN gene with expanded GAA repeat more susceptible to degradation.

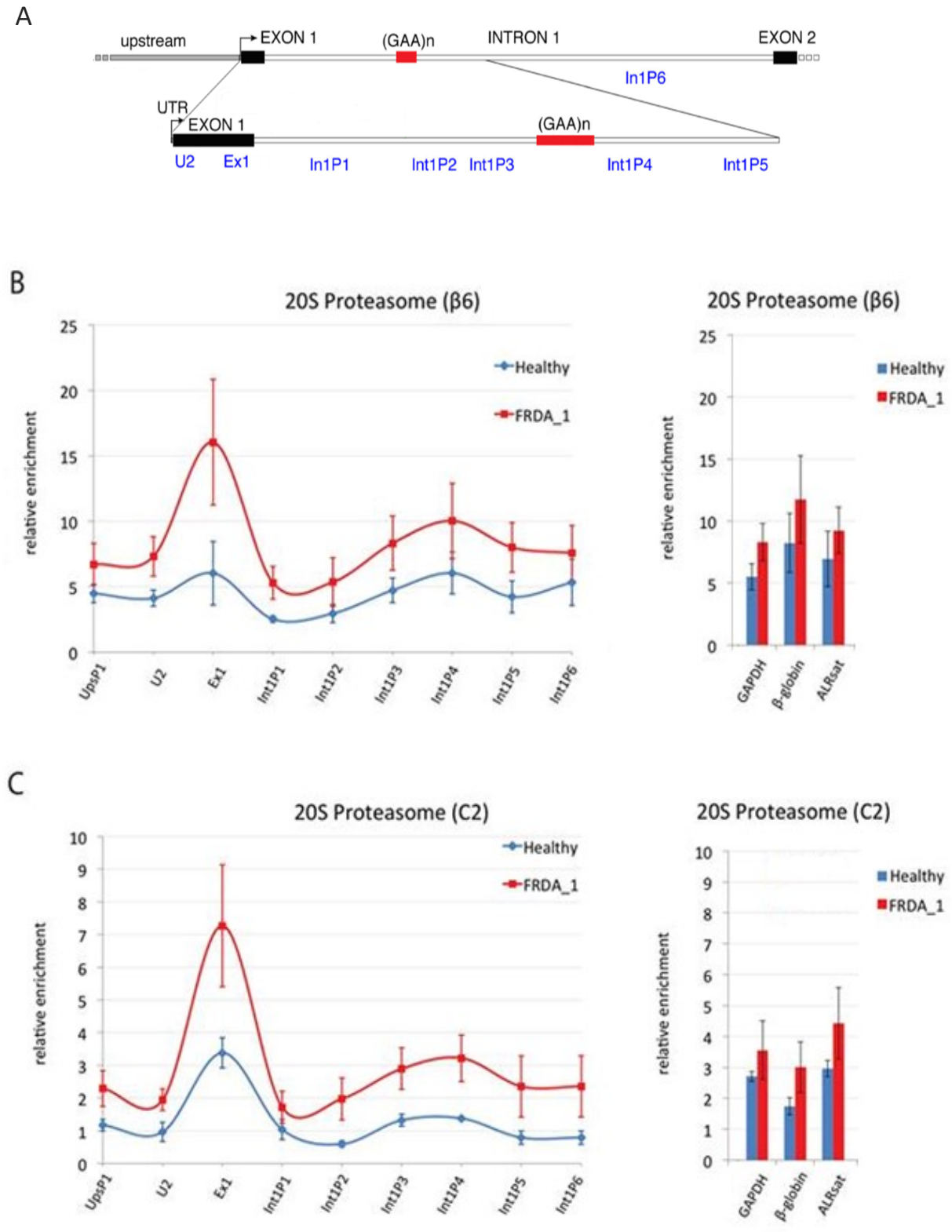


Figure 3.6: The proteasome binding along the FXN gene in healthy and FRDA_1 cell lines. (A) Schematic representation of the position and name of primer sets used to study the *FXN* gene locus. (B, C) The proteasome binding was analysed by ChIP using two different antibodies and immunoprecipitated material was measured by qPCR. ChIP signals are shown as relative enrichment to H3 with background subtraction. β-globin, ALRsat and GAPDH were used as controls. Error bar represent SEM n=3.

3.2.4 Restored total level of RNAPII upon proteasome and transcriptional inhibition in lymphoblastoid cell lines (Healthy and FRDA)

What is the effect of the proteasome and transcriptional inhibition on the global RNAPII level? To answer this question, healthy and patient lymphoblastoid cell lines were treated with proteasome inhibitor MG132, simultaneously with the transcriptional inhibitor α-amanitin. MG132 (Z-Leu-Leu-Leu-al) is a C-terminal peptide aldehyde that blocks the proteolytic activity of all 20S catalytic core subunits (β1, β2 and β5) of the proteasome (Berkers *et al.*, 2005; Tsubuki *et al.,* 1993). It is a widely used proteasome inhibitor as it performs in a highly selective manner and is highly cell permeable (Elliott, Zollner, & Boehncke, 2003; Kisselev & Goldberg, 2001). As mentioned in the introduction of this chapter α-amanitin is a potent and selective RNAPII inhibitor interfering with the translocation step of the transcript polymerization reaction.

Here, initially the cells were treated with MG132 at a final concentration of 10μM and α-amanitin (65 μg/ml) was added in a culture medium an hour later. This was performed in order to give a sufficient time frame for the proteasome inhibition to occur before transcriptional inhibition would take place. After adding the α-amanitin, cells were treated for an additional 8h in the presence of both drugs. Subsequently, cells were collected and lysed using lysis buffer. Total RNAPII and S5P-RNAPII levels were measured by western blot. It is worth mentioning that multiple attempts were made to measure the S2P-RNAPII, but no antibody was found to be efficient for the western blot analysis.

The level of RNAPII was shown to increase upon proteasome inhibition and decrease upon transcriptional inhibition in both healthy and FRDA cell lines. Considering that (i) α-amanitin induces stalling of RNAPII (Brueckner & Cramer, 2008; X. Q. Gong *et al.*, 2004; M. D. Rudd & Luse, 1996) and (ii) stalled RNAPII is sensitive to proteasomal mediated degradation (Karakasili, Burkert-Kautzsch, Kieser, & Strasser, 2014; Nguyen *et al.,* 1996; Svejstrup, 2007) it was therefore expected that concomitant treatment of cells with MG132 and α-amanitin restored the total RNAPII levels in all the examined cell lines (Figure 3.7A). Similar results were also obtained for S5P-RNAPII (Figure 3.7B).

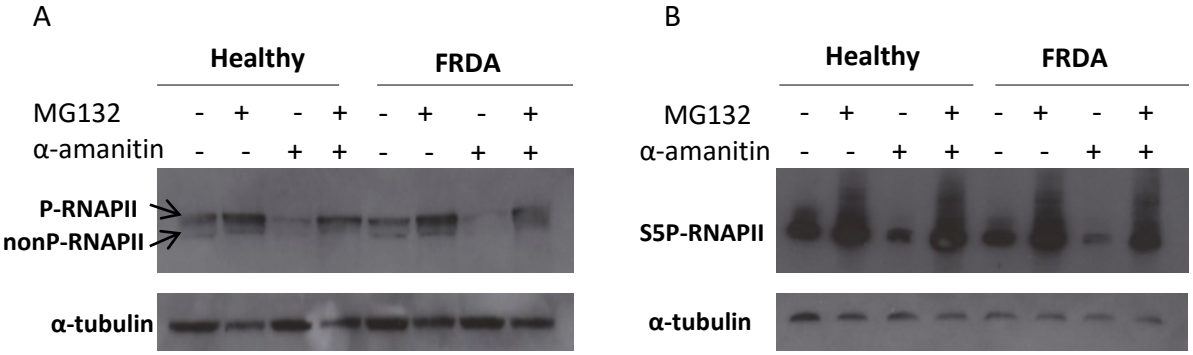


Figure 3.7: The total RNAPII level is restored upon concomitant proteasome and transcriptional inhibition in Healthy and FRDA cell lines. Healthy and FRDA cell lines were treated with MG132 for 1h followed by α – amanitin and MG132 treatment for an additional 8h. Total protein cell lysate was immunoblotted with antibodies against total RNAPII (A) and S5P-RNAPII (B). α-tubulin served as a loading control.

These results are reminiscent of the RNAPII dynamics at the *FXN* gene in patient cell lines, where proteasome inhibition prevented the α-amanitin induced depletion of RNAPII in exon 1. In contrast, no effect was seen in the healthy cell lines (Figure 3.3), indicating an unusual RNAPII dynamics at the normal *FXN* gene where, upon stalling, RNAPII is resistant to proteasomal degradation. Hence, the RNAPII at the *FXN* gene in the healthy cells lines appears protected against proteasome mediated degradation.

3.2.5 The effect of *in vitro* proteasome and/or transcriptional inhibition on the cell viability and the levels of *FXN* expression

The recovery of RNAPII stalling at exon 1 in the *FXN* gene in FRDA raised the possibility that proteasome inhibition could influence the *FXN* expression in FRDA by restoring the reservoir of RNAPII available for transcription. In order to investigate this, healthy and patient lymphoblastoid cell lines were treated with the proteasome inhibitor MG132 alone or simultaneously with transcription inhibitors α-amanitin and Actinomycin D (ActD). As mentioned above, α-amanitin is a specific inhibitor of RNAPII, whereas ActD inhibits all three RNA polymerases by intercalating into DNA (Bensaude, 2011; Trask & Muller, 1988).

Consistently with the previous experimental setup, cells were initially incubated with 10μM MG132 for an hour, before adding α-amanitin (65μg/ml) or ActD (20μg/ml) in the culture medium followed by an additional 8h of treatment in the presence of either MG132, α-amanitin, ActD or both MG132 and α-amanitin/ActD. Cells were sampled to assess viability by measuring the cell number using Guava flow cytometry (Figure 3.8 shows absolute cell numbers); the remaining cells were used for RNA extraction followed by q-RT-PCR in order to determine the expression levels of *FXN* mRNA and *FXN* primary RNA transcripts.

Analysis of cell viability upon proteasome and transcriptional inhibition

As shown in Figure 3.8 and Table 2, incubation of cells with MG132 was found to decreased the cell survival reaching 70%, 82% and 78% in Healthy, FRDA_1 and FRDA_2 cell lines respectively. Moreover, cellular viability decreased to 73%, 81% and 88% upon treatment with ActD in Healthy, FRDA_1 and FRDA_2 cell lines respectively, whereas treatment with 65μg/ml α-amanitin for this period had little or no effect on viability. In addition, the cellular viability was similarly affected upon concomitant treatment with MG132 and ActD/α-amanitin as well as MG132 treatment alone in all the examined cell lines (Figure 3.8, Table 2).

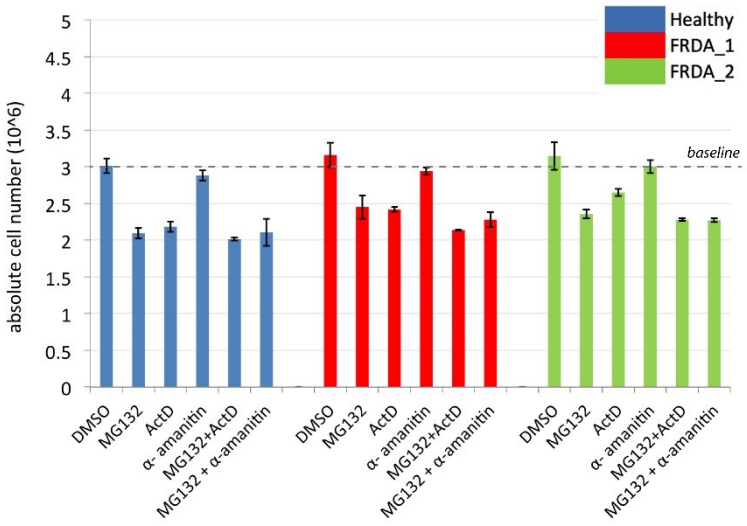


Figure 3.8: The effect of proteasome and transcriptional inhibition on the survival of Healthy, FRDA_1 and FRDA_2 cell lines. 3X10^6 cells were treated with MG132, α-amanitin and ActD for 8h and cells were counted by Guava flow cytometry. Data represent absolute number of cells. Baseline indicated the starting number of cells (dashed line). Error bars = SEM of at least 2 biological replicates.

Treatment	**Healthy (n=2-3) Viability (%)**	**FRDA_1 (n=2-3) Viability (%)**	**FRDA_2 (n=2-3) Viability (%)**
DMSO	100	100	100
MG132	70	82	78
ActD	73	81	88
α-amanitin	96	98	100
MG132+ActD	67	71	76
MG132+α-amanitin	70	76	76

Table 2: Cell viability of Healthy, FRDA_1 and FRDA_2 cell lines upon treatment with proteasome inhibitor MG132, transcriptional inhibitors ActDα/amanitin and concomitant treatment of MG132 with ActD or α-amanitin for 8h. Values represent the average percentage of cell viability of 2-3 biological replicates.

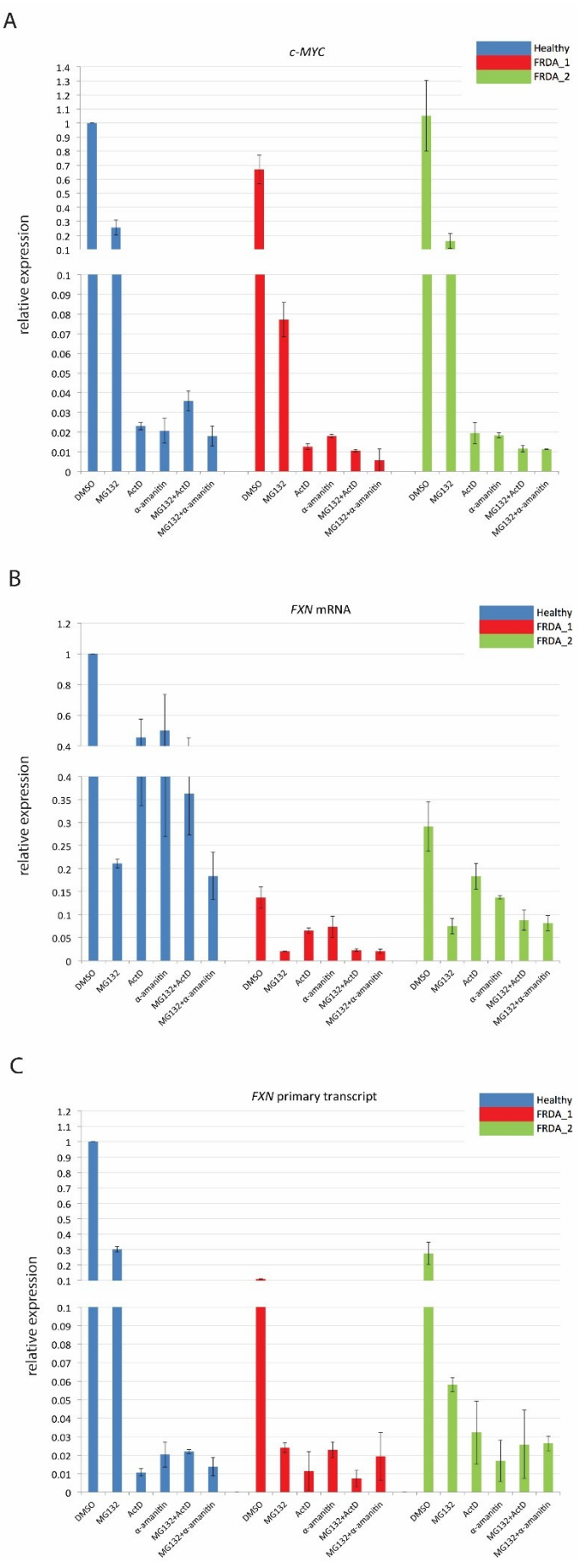
Analysis of FXN expression upon proteasome and transcriptional inhibition

Consistent with effective transcriptional inhibition by both ActD and α-amanitin the short lived *c-MYC* transcript was completely lost after 8h of treatment with both transcription inhibitors. There was a significant reduction of the *c-MYC* mRNA upon MG132 treatment in all the cells lines (Figure 3.9A), consistent with previously published studies although the mechanism is unknown (Bhatt *et al.*, 2013; J. Jung *et al.,* 2012; Suk *et al.,* 2015).

Furthermore, treatment of cells with transcriptional inhibitors for 8h, resulted in 50% reduction of the *FXN* mRNA levels in both Healthy and FRDA cell lines (Figure 3.9B), broadly consistent with the formal measurement of half-life (Punga & Buhler, 2010).

Following the proteasome inhibition, both *FXN* mRNA and primary *FXN* transcripts were significantly downregulated in all the examined EBV cell lines. Similar levels of *FXN* mRNA downregulation were also obtained with concomitant treatment of Healthy and FRDA cell lines with proteasome inhibitor and transcriptional inhibitors (Figure 3.9B, 3.9C). Moreover, simultaneous treatment of cells with MG132 and ActD/α-amanitin resulted in similar levels of primary *FXN* transcript reduction as MG132 treatment alone in FRDA cells lines, indicating the effect of M132 is likely to be transcriptional rather than affecting the stability of the *FXN* RNA (Figure 3.9C).

Contrary to what might expected if the proteasome was degrading stalled RNAPII at the FXN locus (Figure 3.3) as previously hypothesised its inhibition resulted in repression rather than upregulation of the FXN levels. It is possible that the recruitment of the proteasome to the *FXN* locus (Figure 3.6) and the downregulation of *FXN* expression upon proteasome inhibition (Figure 3.9B, 3.9C) indicated an additional *active* role for the proteasome in the regulation of *FXN* gene transcription (see more details in the discussion) in addition to effects it might have in removing stalled RNAPII at the stalling site.



See next page for figure legend

Figure 3.9: *In vitro* proteasome inhibition downregulates *FXN* expression in Healthy and FRDA cell lines. *c-MYC* mRNA (A), *FXN* mRNA (B) and primary *FXN* transcript (C) were analysed by q-RT-PCR after MG132, ActD, α – amanitin, MG132 plus ActD (MG132 + ActD) and MG132 plus α – amanitin (MG132 + α – amanitin) treatments. MG132 was added to the cell culture one hour before adding α – amanitin/ActD. Data are presented as the relative expression normalised against spike and shows fold change relative to DMSO (vehicle) treatment of healthy cell line. Error bars = SEM of 2-3 biological replicates. *c-MYC* expression served as a control for the RNAPII inhibition.

3.2.6 The effect of *in vivo* proteasome inhibition on the *FXN* and heterochromatin repeat (major, minor) expression

Although proteasome inhibition was previously shown to rescue the degradation of stalled RNAPII at the *FXN* gene in patient EBV derived cells it did not result in *FXN* upregulation (see above). In parallel an *in vivo* approach was also adopted to address whether proteasome inhibition could upregulate *FXN* at the transcriptional level. An additional rationale for the use of *in vivo* approach stems from the finding that FXN protein itself is subject to proteasomal degradation (Rufini *et al.*, 2011) suggesting that proteasomal inhibition might be therapeutically useful. Considering that FRDA is a degenerative disease, affecting central and peripheral nerve tissue (e.g cerebellum) as well as heart (Koeppen, 2011; Payne, Pride, & Babbey, 2011), YG8 transgenic mice (see materials and methods) which provide a mouse model for FRDA (Al-Mahdawi *et al.,* 2004) were used to assess the effect of the proteasome inhibition directly in some of the affected tissues. YG8 transgenic mice (C57BL/6J background) contain two copies of the human *FXN* transgene with 190+90 repeats (Al-Mahdawi *et al.,* 2004) and show reduced levels of Frataxin protein (42% cerebellum, 25% heart) compared to wild type animals (Al-Mahdawi *et al.,* 2006). Moreover these mice exhibit increased sensitivity to oxidative stress leading to an FRDA-like phenotype characterised by progressive neuron and cardiac pathology (Al-Mahdawi *et al.*, 2006).

Furthermore, previous studies have shown that the proteasome is widely associated with different compartments of chromatin, such as actively transcribed genes (Geng & Tansey, 2012; Sikder *et al.*, 2006), centromeres (Kitagawa *et al.,* 2014b) telomeres (Geng & Tansey, 2012) as well as intergenic (cryptic) transcription start sites (Szutorisz *et al.,* 2006). In this chapter it was shown that the proteasome is recruited to the *FXN* gene (Figure 3.6), with an increase in binding occurring at the pathologically heterochromatinised *FXN* locus. Therefore, in order to investigate whether the proteasome has a role in regulation of heterochromatic regions, the expression of major and minor satellite repeats consisting of pericentromeric and centromeric regions respectively was also analysed upon *in vivo* proteasome inhibition.

Although there are many examples of administrating the proteasome inhibitor MG132 in animals (Caron *et al.,* 2011; B. Chen *et al.*, 2010; Inoue *et al.*, 2009; Jamart, Raymackers, An, Deldicque, & Francaux, 2011), some studies suggest that MG132 is only partially effective *in vivo*, due to its rapid metabolism (C. M. Lee, Kumar, Riley, & Morgan, 2010). Therefore an alternative, for *in vivo* studies is the proteasome inhibitor PS341 which is already licensed for use in humans.

Here, 3 groups of female and male YG8 transgenic mice were intraperitoneally injected with 0.075mg/kg (low dose - group 1), 0.375 mg/kg (medium dose - group 2) and 0.750mg/kg (high dose - group 3) PS341 once a day for 5 consecutive days, whereas the untreated control group (group 4) was given the same volume of physiological saline (vehicle). Cerebellum and heart tissues were collected from each group followed by RNA extraction and q-RT-PCR using specific primers against (i) human *FXN* transgene, (ii) major satellite repeat and (iii) minor satellite repeat.

As shown in Figure 3.10A, no significant change was identified in the *FXN* transgene expression in cerebellum tissue both in female and male mice upon *in vivo* proteasome inhibition. However the heart tissue revealed a sexual dimorphism, where downregulation of the *FXN* transgene expression was observed in the male mice with low and high dose of PS341, consistent with *in vitro* proteasome inhibition in EBV cell lines (see Figure 3.9). On the other hand, no change was seen in female mice (Figure 3.10B).

Interestingly*, in vivo* treatment of male mice with high dose (0.750mg/kg) of PS341 upregulated the expression of major and minor satellite repeats in both cerebellum and heart tissue, with greater effect occurring in the heart tissue (Figure 3.11A, 3.11C). On the contrary, in the female mice, a small upregulation of the major and minor satellite repeats was seen in cerebellum (Figure 3.11B), while expression of these repeats was either unchanged or downregulated in the heart tissue (Figure 3.11D).

Overall these data suggest that *in vivo* proteasome inhibition results in no change or downregulation of *FXN* expression in cerebellum and heart tissue respectively. This observed downregulation was sex-dependent occurring exclusively in the male mice. Additionally, the upregulation of heterochromatic repeats upon *in vivo* proteasome inhibition in the male mice indicates a role of the proteasome in repression of these repeats.

A possible explanation for the difference observed between cerebellum and heart tissue could be due to the availability of the drug, as PS341 was previously reported to cross the blood-brain barrier poorly (Hemeryck *et al*., 2007).

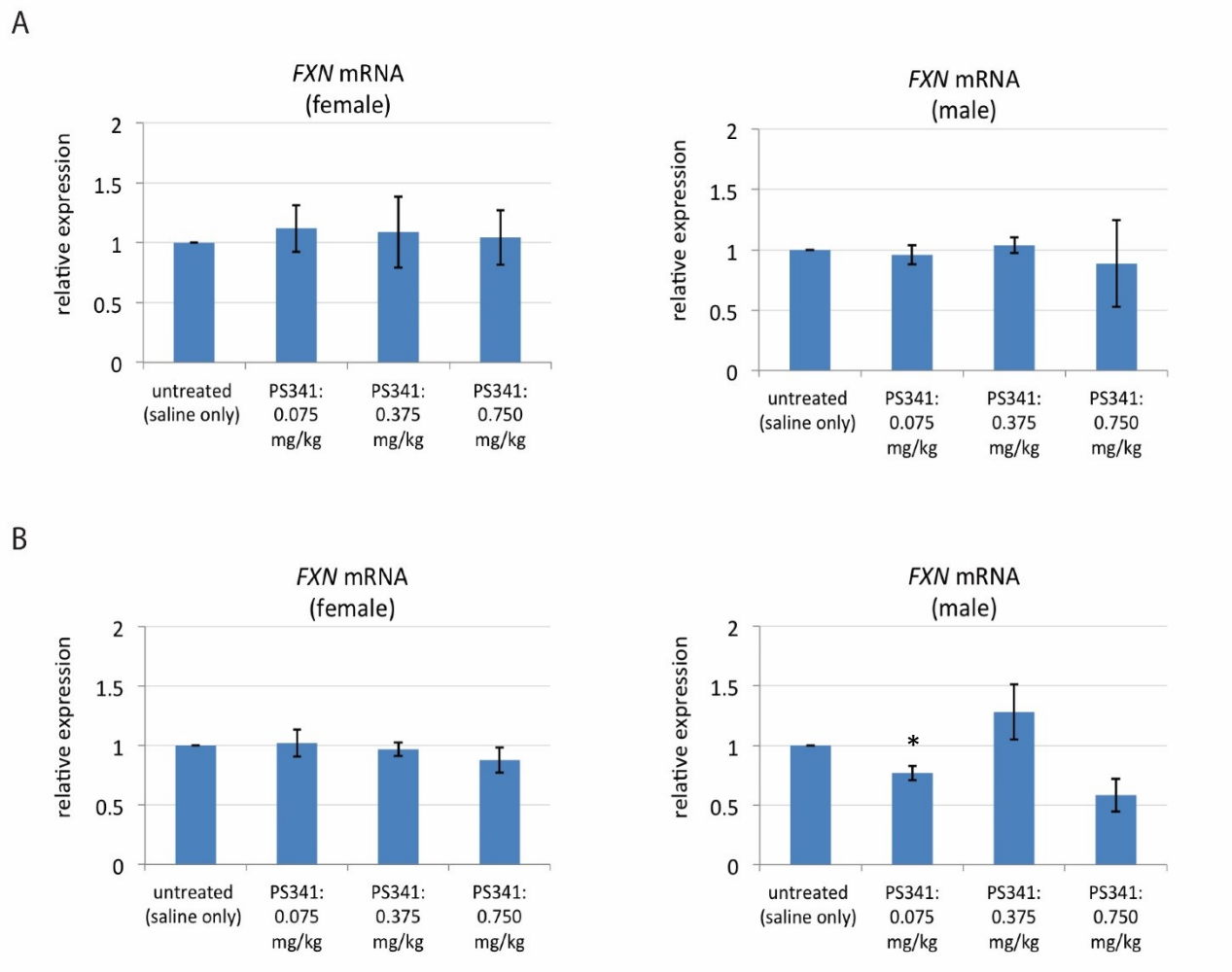
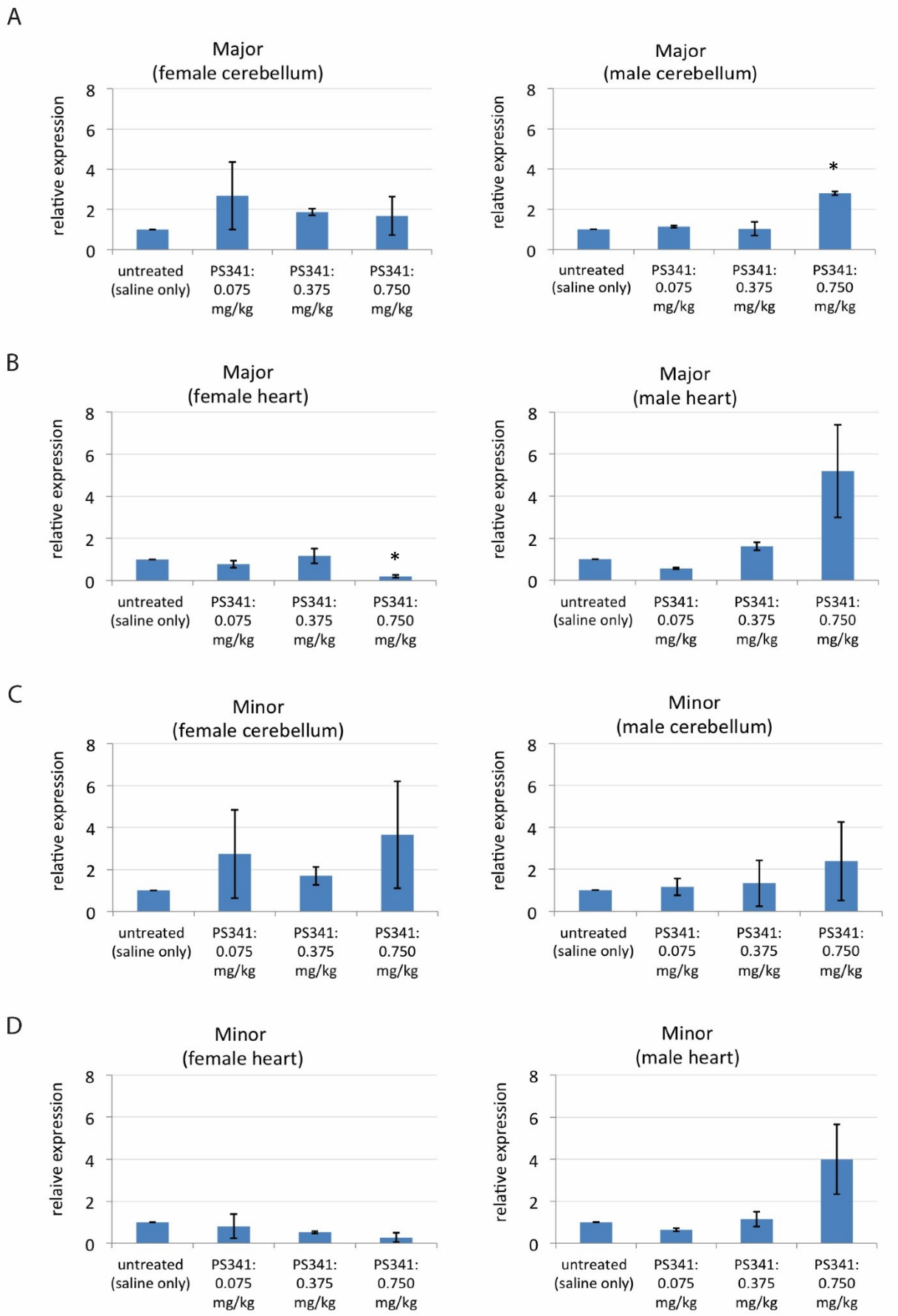


Figure 3.10: The effect of *in vivo* proteasome inhibition of the *FXN* trangene expression in Cerebellum (A) and Heart tissue (B) of YG8 transgenic mice. The mice were injected intraperitoneally with 0.075mg/kg, 0.375 mg/kg and 0.750mg/kg PS341 while untreated controls received only saline for 5 consecutive days. Analyses of mRNA levels were conducted by q-RT-PCR using specific primers against human *FXN* transgene. Data are presented as the relative expression normalised against GAPDH and shows fold change relative to untreated control group. Error bars = SEM of at least 2 biological replicates. *$p < 0.05$ (Student's 't' test).



See next page for figure legend

Figure 3.11: The effect of *in vivo* proteasome inhibition on the expression of the heterochromatic repeats in the cerebellum (A, C) and heart (B, D) tissues. YG8 transgenic mice were injected intraperitoneally with 0.075mg/kg, 0.375 mg/kg and 0.750mg/kg PS341 while untreated controls received only saline for 5 consecutive days. RNA was extracted and major satellite (A, B) and minor satellite (C, D) repeats were analysed by q-RT-PCR. Data are presented as the relative expression normalised against GAPDH and shows fold change relative to untreated control group. Error bars = SEM of at least 2 biological replicates. *$p < 0.05$ (Student's 't' test).

3.3 Discussion

3.3.1 Heterochromatinisation of the *FXN* gene in FRDA

As mentioned in the introduction, two models have been proposed to explain the transcriptional repression of the *FXN* gene with pathologically expanded GAA repeats.

The first model suggests that GAA repeats physically block RNAPII elongation though formation of abnormal non-B DNA structural confirmations (eg. triplex, hairpin) and DNA:RNA hybrids (R-loops) (Yandim *et al*., 2013). So far, the existence of such structures has been mainly studied in nucleosome-free plasmids *in vitro* or in *Escherichia coli* (Grabczyk *et al.,* 2007; Ohshima, Montermini, Wells, & Pandolfo, 1998; Reddy *et al.,* 2011; Sakamoto *et al.,* 1999). Notably the presence of R-loops has only been recently detected *in vivo* over the expanded GAA repeat region on the native *FXN* gene in patient cells (Groh *et al*., 2014). Further studies on the endogenous *FXN* gene are required to determine the presence and the role of these structural conformations in the pathology of FRDA.

The second model proposes that GAA repeats induce heterochromatinisation of the locus that epigenetically silence the *FXN* gene (Yandim *et al.,* 2013). In this chapter, the heterochromatin modification H3K9me3 was shown to be elevated throughout the *FXN* gene with pathologically expanded GAA repeats in FRDA EBV cell lines, relative to the healthy cell lines. This repressive mark was found to be particularly enriched in Ex1 and the regions flanking the GAA repeats. In contrast to the heterochromatin mark, the euchromatic H3ac was shown to be reduced in regions upstream of the abnormally expanded GAA repeats in patient EBV cell lines, compared to the healthy cell line. Interestingly, despite the difference in the mRNA and primary transcript FXN expression between the two examined FRDA cell lines, the level of H3K9me3 was found to be similar. However the difference in the expression between the patient cell lines was well correlated with the H3ac levels. More specifically, patient (FRDA_2) with lowest level of *FXN* expression, exhibited the lowest level of H3ac on the regions upstream of GAA repeats. Taken together, these results suggest high-order chromatin structure formation caused by GAA repeat expansion in FRDA and is consistent with previously published studies investigating post-translational histone modification profiles along the *FXN* locus (Al-Mahdawi *et al*., 2008; De Biase *et al.,* 2009; Greene, Mahishi, Entezam, Kumari, & Usdin, 2007; Herman *et al.,* 2006; E. Kim *et al.,* 2011;

Y. Li *et al.,* 2015; Punga & Buhler, 2010). A summary of these studies investigating the chromatin changes on the *FXN* gene in shown in supplementary table S1.

Additionally, further evidence indicating heterochromatinisation of the *FXN* gene in FRDA include:

(i) Increased DNA methylation of CpG sites upstream of GAA repeats in various models of FRDA (Al-Mahdawi *et al.*, 2013).

(ii) Decreased binding of the chromatin insulator protein CTCF at the 5' UTR region of the *FXN* gene in FRDA fibroblast cell lines and cerebella tissues (Al-Mahdawi *et al.,* 2013; De Biase *et al.,* 2009). CTCF functions to prevent the spreading of heterochromatin (Ong & Corces, 2014), therefore reduced occupancy of this factor on the *FXN* gene would potentially permit the spreading of heterochromatin from the expanded GAA repeats towards the promoter and resultant gene silencing. However it is worth mentioning that the spreading was recently shown to be restricted to the *FXN* locus and did not affect the expression of the adjacent genes (Y. Li *et al.,* 2015).

(iii) Heterochromatin silenced genes have a tendency to localise close to the nuclear periphery, interacting with nuclear lamina proteins (Andrulis, Neiman, Zappulla, & Sternglanz, 1998; Bolzer *et al.,* 2005; Dietzel, Zolghadr, Hepperger, & Belmont, 2004; Guelen *et al.,* 2008; Van de Vosse, Wan, Wozniak, & Aitchison, 2011). Similarly, the *FXN* gene with pathologically expanded GAA repeats was recently found to reposition to the nuclear periphery (Silva, Brown, Buckle, Wade-Martins, & Lufino, 2015).

To date, neither the mechanism behind heterochromatinisation induced by GAA repeat expansion, nor the factors regulating its formation is known. Heterochromatin formation is controlled by multiple chromatin modifiers, such as H3K9 methyltransferases G9a and SUV39H. A chemical inhibition of G9a HKMT reduced the levels of H3K9me2/3, however this reduction was not accompanied by significant upregulation of *FXN* expression (Groh *et al.*, 2014; Punga & Buhler, 2010) In future, it would be interesting to assess the effect of SUV39H as well as EZH2/PRC2 in the regulation of *FXN* silencing. Certainly, identifying the key chromatin modifiers responsible for the *FXN* heterochromatinisation in FRDA and hence it's repression will open a new avenue in developing effective treatments.

3.3.2 Proteasome binding to the RNAPII stalling site on the *FXN* gene

Data from the GCMD lab (see more details in the Introduction of this chapter) revealed that the initiating (S5P) and elongating (S2P) forms of RNAPII are stalled within Ex1 of the *FXN* gene at similar levels in both healthy and patient cell lines (PhD thesis (Yandim, 2012). Consistently, a recent study identified, using chromatin immunoprecipitation, a high accumulation of total RNAPII at Ex1 of the *FXN* gene in both healthy and patient cell lines. However, the overall level of RNAPII was found to be significantly reduced in patient cells relative to the healthy control, which correlated with the difference in the *FXN* expression levels. Furthermore, the same study further measured actively transcribing RNAPII using a nuclear run-on assay and revealed significant transcriptional reduction upstream of GAA repeats, consisted with the RNAPII ChIP results (Groh *et al*., 2014). Similarly, Kim *et al.,* also showed an enrichment of total RNAPII in Ex1 of the FXN gene in healthy cell lines, which was significantly decreased in FRDA cells (E. Kim *et al.,* 2011).

The stalling of RNAPII at the promoter-proximal region is a widespread biological phenomenon occurring in multiple regions of the genome such as *HSP70* (Gilmour & Lis, 1986; H. Tang, Liu, Madabusi, & Gilmour, 2000), *c-MYC* (Eberhardy & Farnham, 2001; Krumm, Meulia, Brunvand, & Groudine, 1992), DHFR and γ-actin (C. Cheng & Sharp, 2003). The proposed functions of promoter-proximal RNAPII stalling include: (i) establishing a permissive chromatin structure by maintaining the nucleosome – free promoter region in order to allow transcription factors and co-activators to easily access the DNA template, (ii) activating several genes simultaneously and rapidly upon a given stimulus e.g during heat shock and (iii) serving as a checkpoint for an efficient capping of the nascent RNA (Adelman & Lis, 2012). Whereas in the promoter-proximal region, the initialling RNAPII is known to be the predominant form, on the *FXN* gene, both initiating and elongating forms of RNAPII were detected. Therefore, this stalling effect was more reminiscent of RNAPII stalling during transcriptional arrest. So far, numerous factors, including topological constrains (Brill & Sternglanz, 1988; Garcia-Rubio & Aguilera, 2012), chromatin structure (Izban & Luse, 1991; Kireeva *et al*., 2005), sequences that are difficult to transcribe (Hawley, Wiest, Holtz, & Wang, 1993; Kerppola & Kane, 1988) and bulky DNA adducts have been suggested to induce permanent or temporary RNAPII stalling/arresting (Wilson *et al.,* 2013). In the case of the *FXN* gene, the stalling could potentially arise from the abnormal DNA conformations and

heterochromatin formation by GAA repeats. Indeed previous *in vitro* and in bacteria studies reported stalling of RNAPII induced by GAA repeats (Grabczyk *et al.*, 2007; Grabczyk & Usdin, 2000).

Importantly, the high affinity of RNAPII binding to its template prevents its dissociation from the stalled sites. Hence, the stalled RNAPII might not only cause transcriptional blocking of the gene, but also interfere with the transcription-coupled repair process. Interestingly, organisms may have evolved to solve this problem by utilizing the proteasome complex to degrade the stalled RNAPII (Wilson *et al.*, 2013). The molecular mechanism of how RNAPII becomes a target for degradation by the proteasome is still not clear. However, an *in vitro* study found that the hyper-phosphorylated form of RNAPII is subject to degradation (Mitsui & Sharp, 1999) and studies in yeast revealed that only the elongating form of RNAPII can become ubiquitinated (Huibregtse, Yang, & Beaudenon, 1997; Somesh *et al.,* 2005). Consistently, the proteasome was shown to degrade the stalled elongating form of RNAPII at Ex1 of the *FXN* gene in the presence of pathologically expanded GAA repeats, as elongating RNAPII levels were restored in the presence of both transcriptional and proteasome inhibitors (see more details in the introduction of this chapter). In contrast, no such effect was seen in the healthy controls, indicating that stalled RNAPII on the *FXN* gene is protected against degradation. In this chapter, the stalling effect of RNAPII induced by transcriptional inhibition and further degradation by the proteasome was investigated at the global level by western blot. Thus, use of the proteasome inhibitor either alone or in combination with the transcriptional inhibitor resulted in an increase in the overall level of RNAPII. This indicated that stalling induced by transcriptional inhibition leads to RNAPII degradation by the proteasome. The main novel finding presented in this chapter is the binding of the 20S proteasome along with the *FXN* gene, which was particularly high in Ex1 of the *FXN* gene in FRDA cells compared to healthy control. This elevated level of 20S proteasome overlaps with the RNAPII stalling site which would be consistent with there being direct degradation of RNAPII by the proteasome in Ex1 of the *FXN* gene only in the presence of pathologically expanded GAA repeats. On the other hand, low levels of 20S proteasome on the *FXN* gene in the healthy cells comes in agreement with the insensitivity of the stalled RNAPII to proteasome-induced degradation. One possible explanation for the difference in the recruitment of the proteasome between healthy and FRDA patient cells

could be due to an unusual conformation of RNAPII in the healthy cells or the absence of either RNAPII ubiquitination or an unknown factor that is recognised by the proteasome. Furthermore, the stalling of RNAPII in the healthy cells could serve as an additional check point for the *FXN* gene transcription, as this gene is required under normal conditions to be transcribed at low levels and overexpression was previously shown to be toxic for the cell (Navarro *et al*., 2011). Interestingly, the pattern of proteasome enrichment was reminiscent of the H3K9me3, suggesting that proteasome recruitment might be an important factor for abnormal chromatin formation caused by the GAA repeat expansion. Also, it is worth mentioning that the binding of the proteasome was validated using two different antibodies and is consistent with 19S binding along the *FXN* gene (PhD thesis (Yandim, 2012), implying that 26S proteasome is recruited to the *FXN* gene. However, more subunits are required to be further analysed, in order to confirm the presence of proteasome holoenzyme rather than its individual particles on the *FXN* locus.

How do the pathologically expanded GAA repeats recruit the proteasome to the *FXN* gene? One possible hypothesis could be through interacting with Mismatch repair proteins such as MSH2/MSH3, factors that were previously shown to bind to both GAA repeats (Bourn, Rindler, Pollard, & Bidichandani, 2009; J. T. Du *et al.,* 2012; Ezzatizadeh *et al.,* 2012; Halabi, Ditch, Wang, & Grabczyk, 2012) and the proteasome (Hernandez-Pigeon, Laurent, Humbert, Salles, & Lautier, 2004). Moreover, proteasome could be recruited to the site in response to the presence of ubiquitinated RNAPII. Even though RNAPII ubiquitination at the *FXN* gene was not analysed, it is possible that degradation occurs through the classical ubiquitin-proteasome pathway. The precise mechanism by which RNAPII becomes a target for ubiquitination and further degradation by the proteasome is still not clear. In yeast, a proposed model for stalled RNAPII degradation consists of three main steps: (i) monoubiquitination of the stalled elongating form of RNAPII by the E3 ubiquitin ligase Rsp5 (NEDD4 is the closest mammalian homologue), (ii) recognition of the monoubiquitinated form of RNAPII and subsequent polyubiquitination catalysed by the Elongin E3 ligase complex (Elongin A/B/C-Cullin mammalian homologue) and (iii) recruitment of the 26S proteasome and degradation of the largest subunit of RNAPII (Rbp1) causing its disassembly (Harreman *et al*., 2009; Wilson *et al.,* 2013). This mechanism of RNAPII degradation is thought to be conserved in mammals, although the factors that catalyze each step have yet

to be all confirmed. To date, even though many E3 ubiquitin ligases have been identified (e.g BRCA1-BARD1, NEDD4), only NEDD4 knock-down was shown to significantly reduce DNA damage induced RNAPII ubiquitination in mammalian cells (Anindya, Aygun, & Svejstrup, 2007). However, the NEDD4 knockdown did not show any significant effect on the expression of the *FXN* gene in both healthy and FRDA patient EBV cell lines (data not shown). Besides NEDD4, the human cells contain 5 other Rsp5 homologues including AIP4, Smurf1, Smurf2, WWP1, and WWP2 (Anindya *et al*., 2007) which could potentially ubiquitinate RNAPII. Further analysis is required to directly determine the mechanisms underlying the recruitment and the degradation of RNAPII by the proteasome at the *FXN* gene in FRDA.

3.3.3 Downregulation of *FXN* expression and upregulation of heterochromatic repeat expression with proteasome inhibition

The proteasome was shown to bind and potentially degrade the stalled RNAPII at Ex1 of the *FXN* gene with pathologically expanded GAA repeats. Given these results it was surprising that *in vitro* and *in vivo* proteasome inhibition did not cause any upregulation of *FXN* expression but rather induced either a marked decrease or no change in the transcript levels. More specifically, *in vitro* treatment with proteasome inhibitor resulted in a clear reduction of the *FXN* gene transcription, in both healthy and FRDA EBV cell lines. On the other hand, *in vivo* proteasome inhibition had virtually no effect on the *FXN* expression in the cerebellum while the effect was downregulation and no change in the heart tissue derived from male and female FRDA-model mice respectively. There are number of explanations that could account for the difference observed between *in vitro* and *in vivo* proteasome inhibition including the concentration of the inhibitor as the dose used for *in vivo* treatment was 5 times less than *in vitro*, duration of the treatment, different systems to mention a few. Additionally the variation in the effect on *FXN* expression between heart and cerebellum tissue could be due to different accessibility of the inhibitor to the target tissues.

So far, the majority of studies correlate the proteasome with activation of gene transcription rather than repression. Therefore the downregulation of both *FXN* and *c-MYC* expression shown here (Figure 3.9) is consistent with the function of the proteasome in facilitating RNAPII mediated gene transcription (Geng *et al*., 2012). As discussed in the Introduction, the proteasome affects each step of the transcriptional process (initiation, elongation, termination). For example at the promoter region, the proteasome is known to be required for activator turnover and recruitment of the co-activators (F. Gonzalez *et al.,* 2002). Also, the proteasome is thought to promote transcriptional elongation through interacting with various elongation factors (e.g FACT) and RNAPII (Ferdous *et al.,* 2001; Gillette *et al.,* 2004a; Sun, Johnston, & Kodadek, 2002). Lastly, the proteasome function is needed for accurate transcriptional termination as inhibiting its activity was shown to increase read through of a transcriptional termination site (Gillette *et al.,* 2004a). Therefore, recruitment of the proteasome to the *FXN* gene might degrade the stalled RNAPII, however inhibiting its function could also inhibit transcriptional processes by preventing transcriptional elongation and termination from taking place. In addition, a proportion of stalled RNAPII might escape the degradation which could be regulated by elongation factors and deubiquitinating enzymes leading to resumption of the RNAPII transcription. This RNAPII escape from the stalling site was recently shown to occur with a stalled RNAPII that arose independently of DNA-damage (Karakasili *et al.*, 2014). Recruitment of factors that would allow RNAPII to escape from the stalling site could be controlled by the activity of the proteasome; hence inhibiting the proteasome would downregulate transcription, as seen in this chapter. The proteasome at the *FXN* gene in FRDA might function in (i) degrading the RNAPII and (ii) promoting the escape of RNAPII from the stalling site and (iii) regulate both transcriptional elongation and termination. More studies are required to address the precise role of the proteasome on *FXN* gene regulation.

Additionally, it is noteworthy that a previous study using proteasome inhibitor reported accumulation of the frataxin protein (Rufini *et al.*, 2015). Also, it is unclear in the Rufini study whether there was any additional effect on *FXN* transcription at the doses used - either transcription was not affected or minimally leaving enough mRNA to be translated into FXN protein. In addition, the observed accumulation could be explained by a long half-life of the frataxin protein (~50h) (K. Y. Li *et al.*, 2008) compared to the *FXN* RNA transcript (~8h).

Another key finding in this chapter is upregulation of pericentromeric and centromeric satellite repeats expression with *in vivo* proteasome inhibition in both cerebellum and heart tissue in male mice. On the other hand, in female mice, the effect of the proteasome inhibition on the expression of pericentromeric and centromeric satellite repeats was found to be tissue-dependent, with a small upregulation and downregulation detected in cerebellum and heart tissues respectively. Although females and males contain nearly identical DNA sequences, a significant proportion of genes have been reported to be differentially expressed between sexes in various tissues such as liver, brain, adipose, muscle (Clodfelter *et al*., 2006; Dewing, Shi, Horvath, & Vilain, 2003; Gomez-Abellan *et al.,* 2012; Trabzuni *et al.,* 2013; Welle, Tawil, & Thornton, 2008; X. Yang *et al.,* 2006). Data from the GCMD lab has recently found that the expression not only of genes, but also of the basal level of the heterochromatin repeats differs between males and females (Unpublished data, MSc thesis Marta Mauri, MPhil thesis Raquel SIlva). This sexual dimorphism on (i) the basal level of the repeat expression and (ii) the response to proteasome inhibition could potentially indicate either difference in the mechanism or abundance of factors that regulate the transcriptional repression of heterochromatic repeats between genders as well as different tissues.

The role of the proteasome in regulation of the heterochromatic repeats is analysed in the following chapters.

In summary the results in this chapter suggest that:

- The proteasome was found by ChIP to bind along the *FXN* gene in a pattern that resembles H3K9me3 heterochromatin. This finding would be consistent with the hypothesis that in FRDA proteasomal degradation of a stalled RNAPII might contribute to *FXN* silencing. However, proteasome inhibition in tissue culture instead of upregulating *FXN* was found to downregulate *FXN* transcription whereas the expression of the gene remains largely unaffected by in vivo proteasome inhibition. Thus the proteasome might have pleiotropic effects on *FXN* expression. Thus, RNAPII degradation might take place in patient cells due to higher levels of proteasome recruited to the locus which might also regulate escape of RNAPII from pausing and further elongation of transcription.
- That the proteasome may also play a role in silencing of constitutive heterochromatin was investigated by proteasome inhibition *in vivo* where this was found to upregulates pericentromeric and centromeric satellite repeat expression.

3.4 Contributions

Treatment of YG8 mice with PS341 was performed by Dr M. Pook at Brunel University. RNA extraction from YG8 mice tissues and further analysis was performed by Theona Natisvili. Everything else in this chapter was performed by Theona Natisvili.

CHAPTER 4: Effects of proteasome inhibition and the cell cycle on regulation of constitutive heterochromatin

4.1 Introduction

In the previous chapter, *in vivo* proteasome inhibition was shown to increase the levels of transcripts derived from pericentromeric major and centromeric minor satellite repeats in male mice (Figure 3.11), suggesting a potential role for the proteasome in repression of heterochromatic repeats. In order to investigate this further, the effects of proteasome inhibition was assessed in this chapter on several regions including pericentromeric major satellite, centromeric minor satellites and the two most common retrotransposons, LINE L1 and SINE B1 in NIH3T3 cells, a well-studied mouse embryonic fibroblast cell line. This cell line was chosen as, in contrast to the primary cells or lymphoblastoid cell lines is easier to grow and transfect for knockdown experiments and is derived from a male mouse (supplementary figure S1).

Several studies have shown that proteasome inhibition induces cell-cycle arrest in various cell types. The phase of this cell cycle arrest is dependent on the cell type as well as the properties of the proteasome inhibitor (Adams *et al*., 1999a; Bonvini, Zorzi, Basso, & Rosolen, 2007; Ling *et al.,* 2003; Machiels *et al.,* 1997). The mitotic cell cycle is a highly regulated process consisting of four consecutive phases that is Gap 1 (G1), Synthesis (S), Gap 2 (G2) and Mitosis (M) (Darzynkiewicz, Bedner, & Smolewski, 2001). Regulation of cell cycle is important for proper cell growth and proliferation (Gerard & Goldbeter, 2014). Cell cycle is known to play an important role in regulating chromatin structure (Ma, Kanakousaki, & Buttitta, 2015), which could potentially impact on chromatin associated processes such as transcription of heterochromatin repeats. More specifically two events during cell cycle are known to cause major changes in chromatin structure (Ma *et al.,* 2015). These events are:

(i) Incorporation of new histones into newly synthesized DNA during S-phase and re-establishment of post-translational histone modifications

(ii) The transcriptional machinery and chromatin associated proteins disassociate from chromatin during mitosis. In addition the chromatin detaches from the nuclear lamina.

Major features of chromatin changes during the different phase of the cell cycle are shown in Figure 4.1. Therefore in this chapter, cell cycle dependent regulation of heterochromatic repeats was analysed in order to exclude any possible effect of the proteasome treatment due to cell cycle skewing.

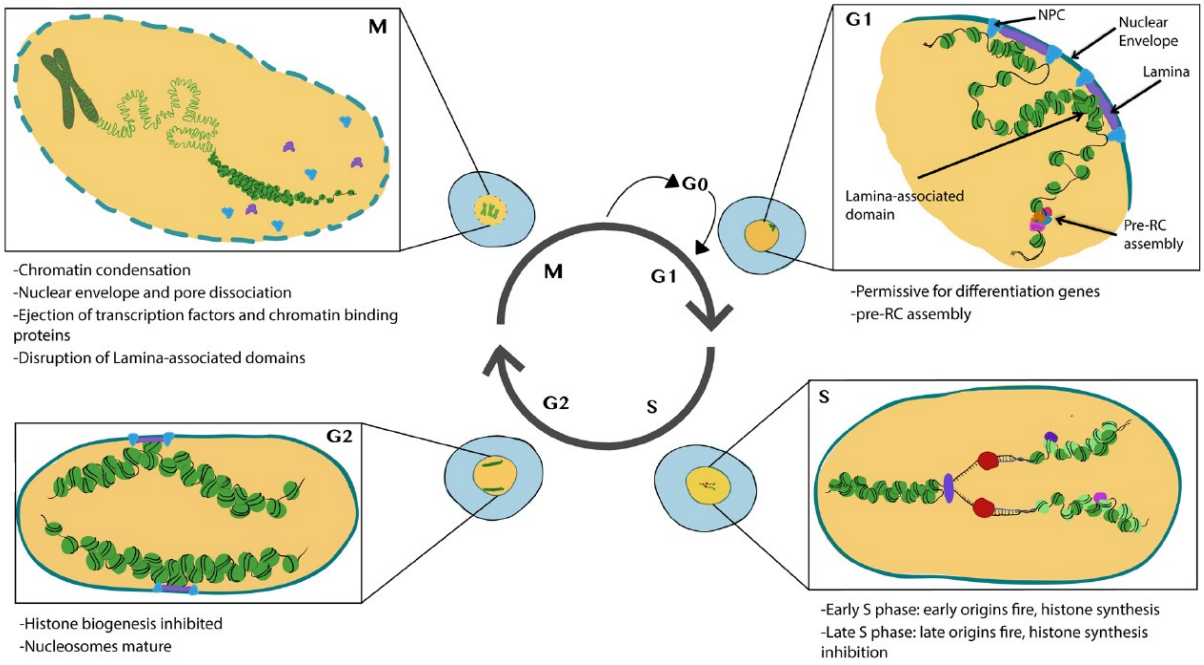


Figure 4.1: Proposed model for structural changes of chromatin during the different phases (G1, S, G2, M) of the cell cycle (Ma *et al*., 2015). Cells during G1 display interaction of some regions of chromatin (predominantly heterochromatin) with the nuclear envelope and assembly of pre-replication complexes (pre-RCs) at euchromatic regions. During S phase DNA is replicated and newly synthesized (light green) and recycled (dark green) histones bind to DNA forming nucleosomes which in turn form nascent chromatin. At this stage histone 'writers' and 'readers' (see Introduction) associate with nascent chromatin in order to re-establish the appropriate histone code. During G2 phase nucleosomes mature and histone biogenesis is inhibited. During mitosis transcription factors and chromatin binding proteins dissociate from the chromatin, which becomes highly condensed. The nuclear envelope disassembles and lamina-associated domains are disrupted. Adapted and modified from (Ma *et al.,* 2015).

The aims for this chapter were:

- To assess the effect of proteasome inhibition and the cell cycle on the transcription of major satellite, minor satellite, LINE L1 and SINE B1 elements.
- To determine the effect of proteasome inhibition on the general structure of constitutive heterochromatin.
- To investigate the effect of proteasome inhibition and the cell cycle on the distribution of the number of chromocentres per cell.

4.2 Results

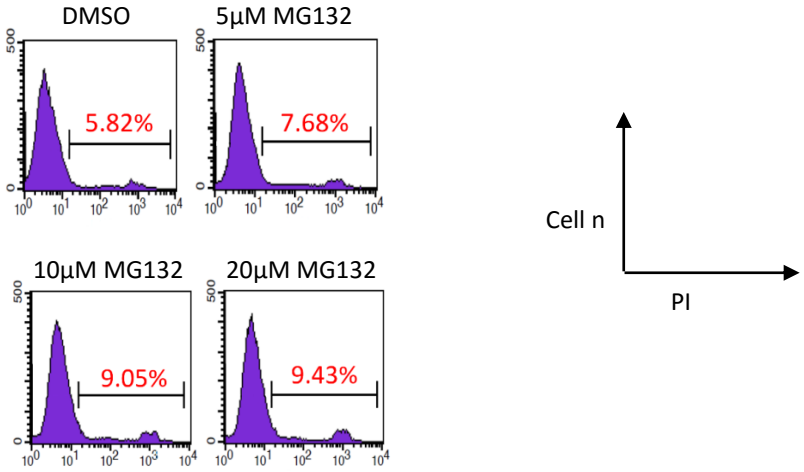
4.2.1 Proteasome inhibition results in the upregulation of major satellite repeat expression

In order to investigate whether transcriptional activity of heterochromatic repeats is controlled by the proteasome, NIH3T3 cells were treated with an inhibitor that blocks the proteolytic activity of the 20S core subunit. The effect of proteasome inhibition on transcript level of pericentromeric major satellite, centromeric minor satellite, LINE L1 and SINE B1 were analyzed in NIH3T3 cells. Cells were treated with different concentrations (5µM, 10µM and 20µM) of the proteasome inhibitor MG132, and changes in transcript levels were measured by quantitative real time PCR (Q-RT-PCR) during an 8h time course.

Effect of the proteasome inhibition on cell survival and morphology.

Propidium iodide (PI) staining followed by FACS analysis revealed that an 8h incubation in 5µM, 10µM and 20µM MG132 did not substantially affect cell survival. The treatment showed a dose dependent minor increase in the proportion of cell death (Figure 4.2A). Furthermore only minor morphological changes were observed in the cultures during the treatments, with a small proportion of cells showing characteristic cell shrinkage (Figure 4.2B). This observed cell shrinkage could be an indicator of early event of apoptosis, (J. Liu, Lee, Galbiati, Kitsis, & Lisanti, 2001), which was previously shown to be caused by proteasome inhibition in multiple cells lines (Wojcik, 2002).

A



B

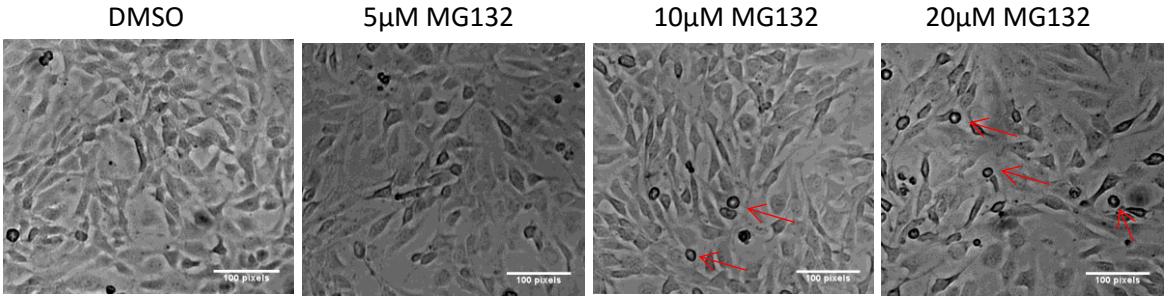


Figure 4.2: Proteasome inhibition leads to only minor morphological changes during the time course of treatment. NIH3T3 cells were treated with 5µM, 10µM and 20µM MG132. (A) Proteasome inhibition results in only 4% increase in cell death as estimated by uptake of PI. PI staining was performed on DMSO (Untreated) and MG132 treated cells for 8h, followed by FACS analysis to measure the percentage of dead cells. The intensity of the PI signal is shown on the X axes and the percentages of PI–positive cells that provides an estimate of the proportion of dead cells are shown in red. (B) Representative phase contract images of NIH3T3 cell cultures after treatment with MG132 for 8h. Arrows indicate the cells exhibiting shrinkage.

4.2.2 Effect of the proteasome inhibition on transcription of heterochromatic repeats

A significant increase in transcript level of major satellite repeat was observed upon MG132 treatment. The increase was dose dependent reaching 3, 5 and 10 fold upregulation when compared to DMSO, when treated with 5µM, 10µM and 20µM MG132, respectively. Furthermore reduction of minor satellite repeat transcript level was identified with 5µM and 10µM MG132, with no change at 20µM of treatment. A 1.2-fold increase in transcript level of SINE B1 repeat was also observed with all MG132 treatments, reaching statistically significant upregulation only at 8h of treatment. No statistically significant changes were found in expression of LINE L1 (Figure 4.3).

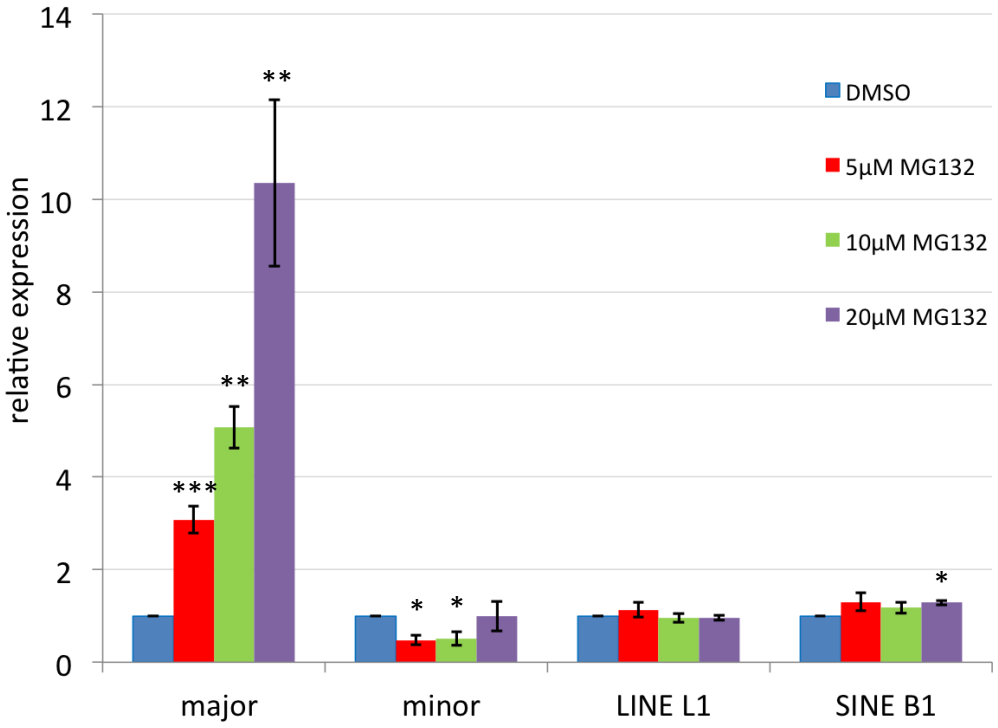


Figure 4.3: Proteasome inhibition results in increased transcript level of major satellite repeat. NIH3T3 cells were treated with 5µM, 10µM and 20µM MG132 and transcript levels of major satellite, minor satellite, LINE L1 and SINE B1 were measured by q-RT-PCR. The relative expression was normalised against spike and shows fold change relative DMSO. Error bars indicate SEs of six biological replicates. * $p<0.05$, ** $p<0.001$, *** $p<0.0001$ (Student 't' test)

This result suggests a role for the proteasome in regulating the transcript levels of major satellite repeats, the major component of pericentromeric heterochromatin. Whether the observed upregulation is occurring at the transcriptional level or post-transcriptional level will be analysed in the following sections. Firstly it was important to investigate whether the effect of the proteasome inhibition on the cell cycle might contribute to the upregulation of major satellite expression observed here.

4.2.3 Cell cycle dependent transcription of heterochromatic repeats

Previous studies have shown that proteasome inhibition induces cell-cycle arrest in various cell types. The phase of this cell cycle arrest is dependent on the cell type as well as the properties of the proteasome inhibitor (Adams *et al*., 1999a; Bonvini *et al.,* 2007; Ling *et al.,* 2003; Machiels *et al.,* 1997).

Although it was shown in mouse C127 cells that expression of major satellite repeats is cell cycle dependent (J. Lu & Gilbert, 2007), there is a paucity of studies examining such cell cycle dependent transcription. More specifically the authors identified one population of abundant, large, heterogeneous major satellite repeat transcripts late in G1 phase, with their synthesis decreasing during mid S phase. Also they showed another population of small major satellite repeat transcripts that were synthesized exclusively during mitosis and quickly reducing during mitotic exit (J. Lu & Gilbert, 2007). On the other hand the expression of minor satellite repeats was found to peak during G2/M phase of the cell cycle (Ferri *et al.*, 2009). There was no available data found for the LINE L1 and SINE B1 in mammalian system. More detailed analysis of the cell cycle dependent regulation of transcription of heterochromatic repeats was therefore needed in order to exclude any possible effect of the proteasome treatment due to changes in proportion of cells in different stages of cell cycle.

In order to confirm the expression of the major and minor satellite repeats in G1/S and G2/M phases respectively and identify any cell cycle effects on the expression of LINE L1 and

SINE B1 in NIH3T3 cells, counterflow centrifugal elutriation was performed for cell synchronization (Banfalvi, 2008). This is a biophysical cell separation technique in which the living cells are separated based on differences in cell size and sedimentation density, as the cell size is generally correlating with the cell cycle stage. During the elutriation process unfractionated cells enter the elutriation chamber where centrifugal force and counterflow of elutriation fluids retain the cells within the chamber. Gradient increase of the flow rate elutes cells from the chamber starting from smaller cells and followed by larger ones (Banfalvi, 2008) The schematic view of the principal of cell synchronisation by centrifugal elutriation is shown in Figure 4.4. This cell separation technique was used primarily because it offers the advantage of selection of cells during the whole cell cycle and does not affect the metabolism of cells (Banfalvi, 2008). By contrast, the previous studies (Ferri *et al*., 2009; J. Lu & Gilbert, 2007) used either chemical inhibition or a combination of chemical inhibition and mechanical shake off to synchronize the cells. Chemical inhibition was shown to lead quite often to perturbation of the cell metabolism (Darzynkiewicz, Halicka, Zhao, & Podhorecka, 2011; J. Gong, Traganos, & Darzynkiewicz, 1995; Kung, Zetterberg, Sherwood, & Schimke, 1990; Pardee & Keyomarsi, 1992; Urbani, Sherwood, & Schimke, 1995). It is worth mentioning that the main drawback of the centrifugal elutriation method is moderate dispersion of synchrony from the fractions obtained in the mid-late S, G2 and M phases during the elutriation process, resulting in enrichment of cells in specific cell cycle stage rather than complete synchronization. Best synchrony with elutriation is achieved in the G1 phase of the cell cycle (Banfalvi, 2008), the phase where major satellite repeats were previously found to be expressed.

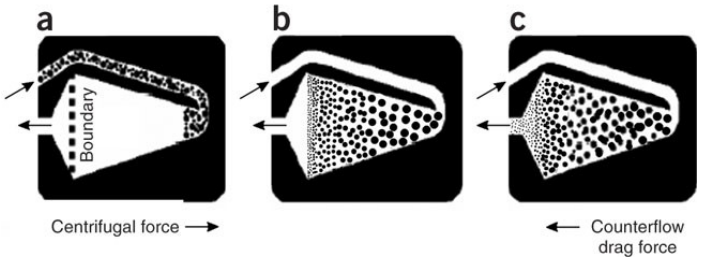


Figure 4.4: A schematic view of the principal of cell synchronisation by centrifugal elutriation. (a) Whole unfractionated cell population enters in the elutriation chamber. (b) Centrifugal force and counterflow drag force of elutriation fluid retain the cells within the chamber. (c) Gradient increase of flow rate elutes the cells based on their size, starting from smaller cells first followed by larger ones. Adapted from (Banfalvi, 2008).

Following cell elutriation part of the eluted material was stained with PI followed by FACS in order to check the efficiency of the elutriation process; the remaining part was used for RNA extraction followed by q-RT-PCR, in order to investigate the expression of the repeats in different phases of the cell cycle.

FACS analysis showed five cell fractions obtained by elutriation, each exhibiting different cell cycle profiles (Figure 4.5). More details regarding the fractions obtained are shown in material and methods. Representative images of the cell cycle profile of each fraction including the non-elutriated (control) are shown in Figure 4.5A. Analysis of the cell cycle distribution of the control revealed that 60%, 20% and 18% were in G1/G0, S and G2/M phase of the cell cycle respectively. Elutriated fraction 1 showed good separation of G1/G0 phase where 92% of the cells were in this stage of the cell cycle. Furthermore good separation was obtained for the G2/M phase in fraction 5 where 75% of the cells were within this phase. Fraction 3 showed the best enrichment for cells in S phase which was 33%. Fraction 2 gave a similar percentage of cells in G1 as in non-elutriated material, with a modest increase (7%) and decrease (5%) in S and G2/M phases respectively. Lastly, fraction 4 gave a threefold increase of cells in G2 phase reaching 53% relative to the control (Figure 4.5B).

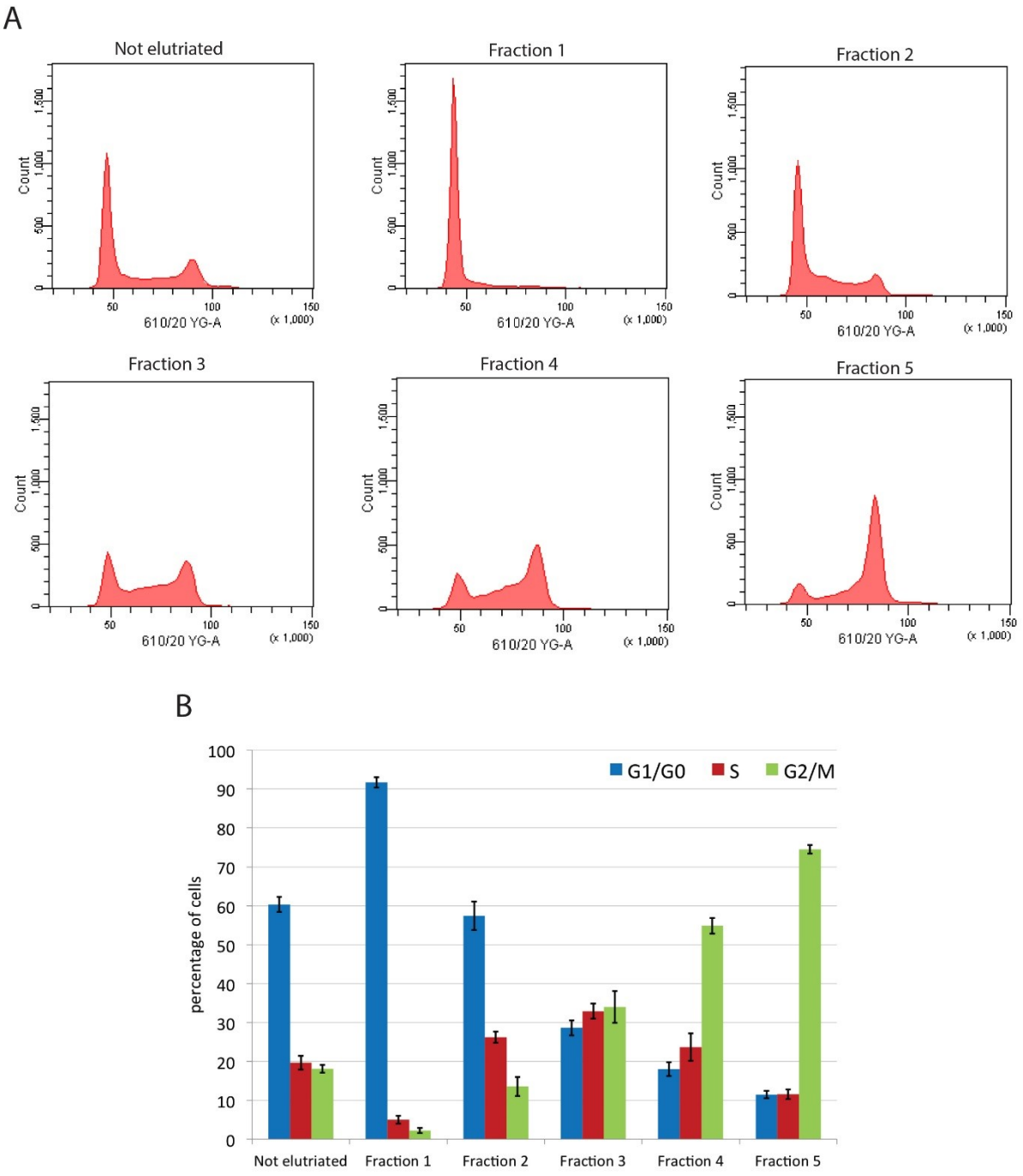


Figure 4.5: Cell fractions, enriched at specific phases of the cell cycle were obtained by centrifugal elutriation. (A) Representative images of the FACS profiles after PI staining showing non-elutriated and five different fractions of elutriated material. (B) Cell cycle distribution of each fraction is shown as percentage of cells acquired. Error bars =SEs obtained from at least 3 biological replicates.

The expression of the repeats analysed by q-RT-PCR revealed changes in the expression of the major and minor satellite repeats, whereas LINE L1 and SINE B1 expression remained constantly similar throughout the different cell fractions (Figure 4.6).

More specifically the expression of the major satellite repeat showed a statistically significant increase in fraction 1, which represents the majority of cells in G1/G0 phase of the cell cycle. Furthermore a minor increase in the transcript levels was observed in fraction 3 which has the highest enrichment of the cells in S phase of the cell cycle. Also a reduction of the expression of the major satellite was detected in fractions 4 and 5 which represent the fractions where the majority of cells are in the G2/M phase of the cell cycle (Figure 4.6A). Thus, this result indicates cell cycle dependent regulation of the expression of the major satellite repeats in NIH3T3 cell lines, with the expression of the transcript occurring primarily in the G1 phase of the cell cycle. Similar observations were reported in the previous study in mouse C127 cells (J. Lu & Gilbert, 2007).

In contrast, the expression of minor satellite repeat with respect to cell cycle was substantially different from that of major satellite repeat. There was a statistically significant reduction of the transcript levels in fractions 1 and 2, fractions which contain either greatly depleted or decreased amounts of cells in G2/M phase respectively. An increase of minor satellite repeat expression levels occurred in fractions 4 and 5, fractions enriched with cells in G2/M phase of the cell cycle (Figure 4.6B). This result demonstrates cell cycle dependent regulation of minor satellite transcript level in the examined cells, with the expression occurring in the G2/M phase of the cell cycle, consistent with a previously published study using murine erythroleukemic (MEL) and NIH3T3 cell lines (Ferri *et al*., 2009). The expression of LINE L1 and SINE B1 was also examined, with only minor changes of the transcript levels occurring in the different fractions (Figure 4.6C, 4.6D). The results suggest cell cycle independent transcription of these retrotransposons in NIH3T3 cell lines.

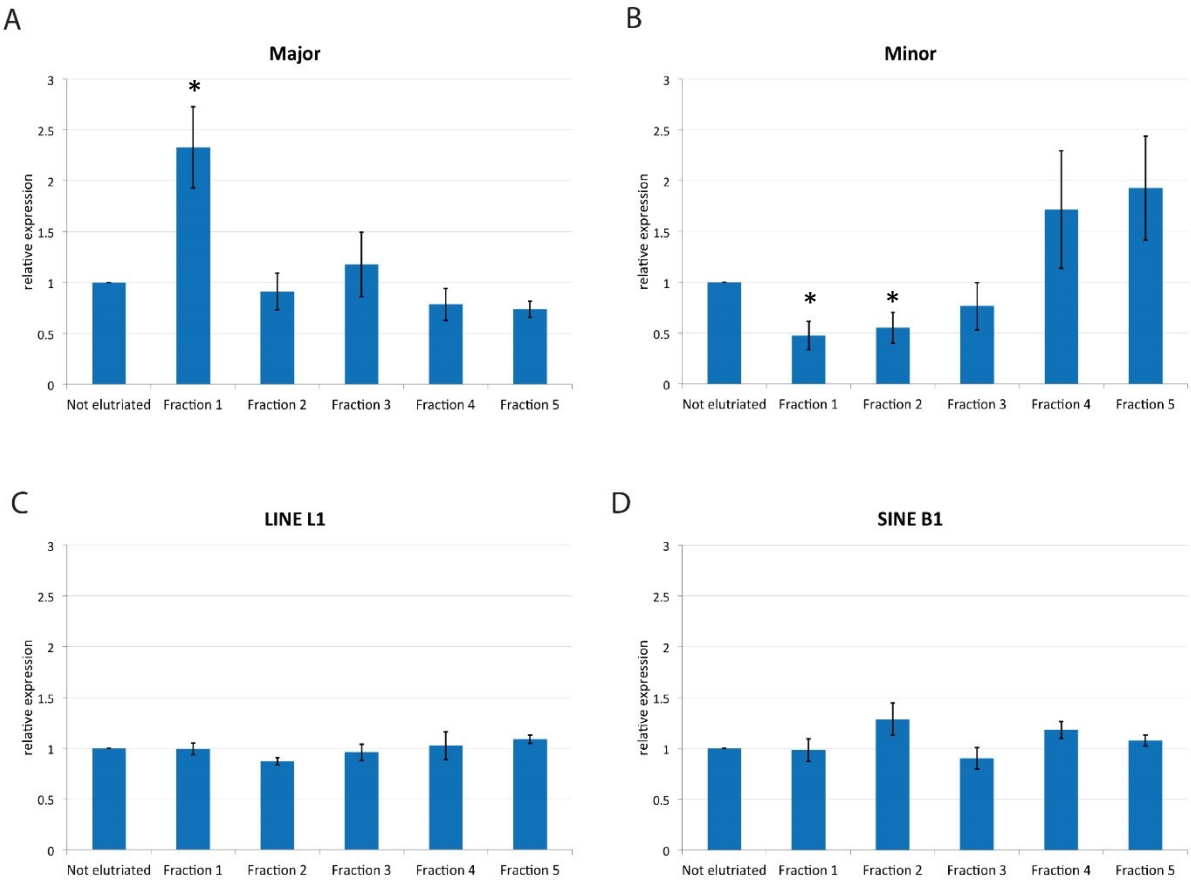


Figure 4.6: Cell cycle regulated expression of the major and minor satellite repeats. NIH3T3 cells were separated with centrifugal elutriation into five fractions, each enriched with cells in different phases of the cell cycle and transcript levels of the major (A), minor (B), LINE L1 (C) and SINE B1 (D) was measured by q-RT-PCR. The relative expression was normalised against endogenous control (GAPDH) and is shown relative to RNA levels obtained with non-elutriated cells. Error bars indicate SEs of at least 3 biological replicates. *$p<0.05$ (Student's 't' test)

4.2.4 Cell cycle independent expression of major satellite repeat and SINE B1 upon proteasome inhibition.

In order to assess whether the increase in major satellite transcripts was due to the proteasome inhibition rather than cell cycle dysregulation, the cell cycle profile following proteasome inhibition treatment was analysed, concomitant with the expression of the repeats. NIH3T3 cells were treated for 1h, 2h, 4h and 8h with MG132 (final concentration 20μM) dissolved in DMSO and PI staining was performed followed by FACS to analyse the proportion of cells at different cell cycle stages. A minimum of 10 000 events were acquired. In parallel RNA was extracted and q-RT-PCR was performed to analyse the expression of the repeats.

FACS analysis revealed alteration in the cell cycle profile upon proteasome inhibition, primarily after 8h of MG132 treatment, with only minor changes occurring in the control (DMSO) (Figure 4.7A). More specifically, MG132 treatment resulted in a decrease of the proportion of cells within G1/G0 phase of the cell cycle, compared to DMSO, reaching statistically significant reduction only after 8h of treatment (Figure 4.7B). Furthermore there was a gradual increase of cells within G2/M phase which was apparent after 1h of treatment, showing a 3% increase at 1h treatment, followed by 7% increase for both 2h and 4h with a further 22% increase at 8h, compared to the untreated (Figure 4.7D). No change was observed for the cell population within S phase for 1h and 2h of treatment, while a minor increase (4%) was identified at 4h and 8h of treatment (Figure 4.7C).

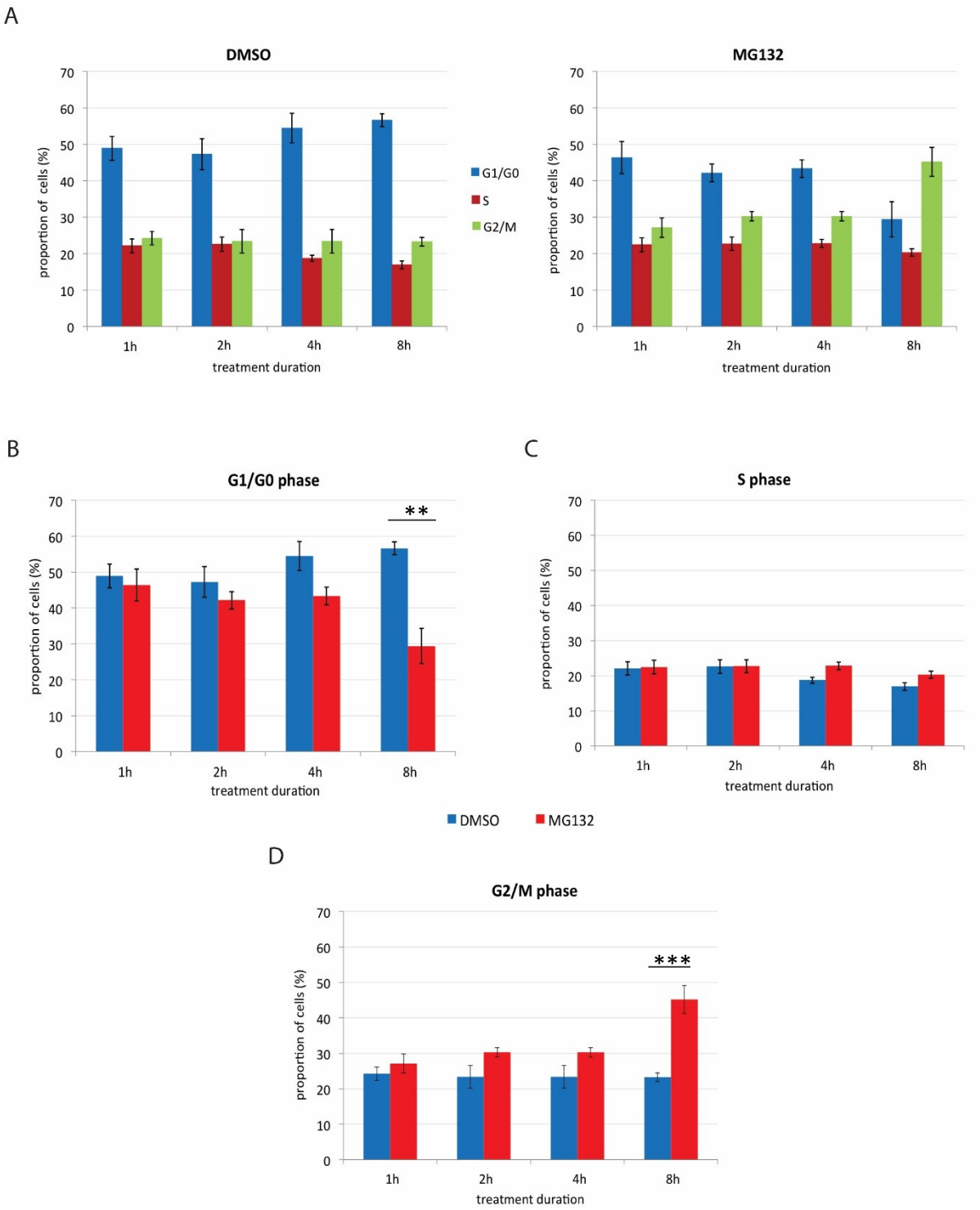


Figure 4.7 : The effect of proteasome inhibion on the cell cycle of NIH3T3 cells. NIH3T3 cells were treated with DMSO or 20µM MG132 for 1h, 2h, 4h and 8h followed by PI staining and FACS analysis. Proportion (%) of acquired cells in G1/G0 phase (B), S phase (C) and G2/M phase (D) are shown for treated (MG132) and untreated (DMSO) cells. **p<0.001, ***p<0.0001 (Student's 't' test)

The RNA expression analysis of a time course treatment with 20μM MG132 showed 8 and 16 fold upregulation of the major satellite repeat expression at 4h and 8h of treatment respectively, with no change at 1h and 2h of treatment, compared to untreated (DMSO) (Figure 4.8A). Furthermore, only minor changes were observed in the expression of the minor satellite repeat throughout the treatment period, with the highest, 1.2 fold increase, occurring at 8h of treatment (Figure 4.8B). Relatively moderate levels of upregulation of SINE B1 were observed at all time points of treatment, reaching a statistically significant, 1.2 and 1.7 fold increase, of the transcript level at 4h and 8h of treatment respectively, compared to untreated (Figure 4.8D). Additionally, only minor changes were displayed in the expression of the LINE L1 at all the time points examined (Figure 4.8C).

Taken together these results suggest that upregulation of the expression of the major satellite transcripts and SINE B1 upon proteasome inhibition is not a consequence of cell cycle dysregulation. Major satellite repeat was shown to be expressed primarily in the G1 phase of the cells cycle (Figure 4.6A), whereas the proteasome inhibition stalls the cells in G2/M phase (Figure 4.7A). Similarly SINE B1 expression was not shown here to be regulated by the cell cycle hence any stalling upon proteasome inhibition should not affect its expression. However, it is worth mentioning that the small upregulation of the minor satellite repeat at 8h of treatment could possibly be due to the cell-cycle stalling effect of proteasome inhibition, since the expression of minor satellite was higher in G2/M phase where proteasome inhibition cell-cycle stalling is taking place.

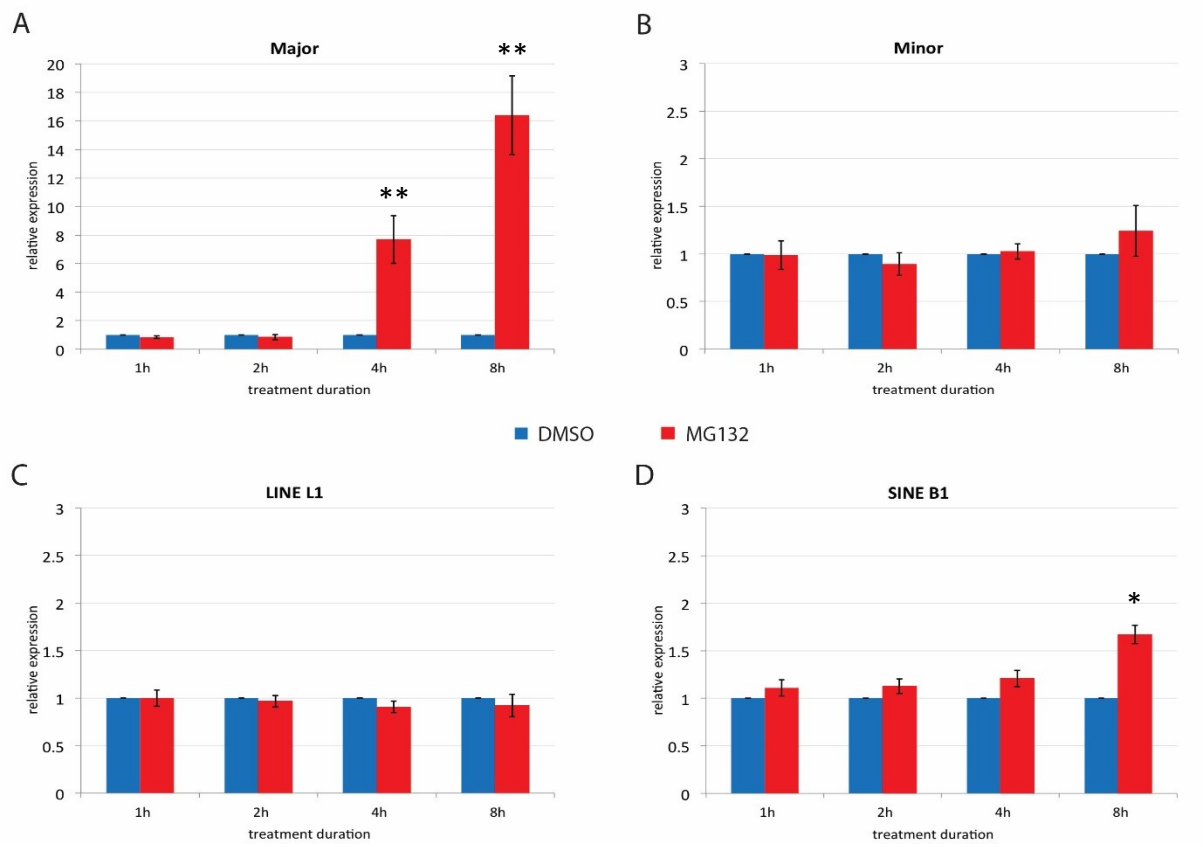


Figure 4.8: A time course of the effect of proteasome inhibition in the expression of major satellite (A), minor satellite (B), LINE L1 (C) and SINE B1 (D) repeats. NIH3T3 cells were treated with 20µM MG132 for 1h, 2h, 4h and 8h followed by RNA extraction and q-RT-PCR. The relative expression was normalised against spike and shows fold change relative DMSO. Error bars indicate SEs of at least 10 biological replicates. *p<0.05, **p<0.001 (Student's 't' test)

4.2.5 Transcription dependent increase of major satellite repeat expression upon proteasome inhibition

So far the results presented in this chapter suggest that proteasome inhibition upregulates major satellite repeat expression in the cell. However, this upregulation could be due to an increase of the transcription or to an inhibition of major satellite transcript degradation. Either of these would result in accumulation of the RNA transcript in the cell. In order to analyse this further, transcriptional inhibition was performed concomitant with proteasome inhibition. Two RNA polymerase inhibitors were used to block the transcription, DRB and ActD. As mentioned in chapter 3, DRB is CDK9 kinase inhibitor which associates with the positive elongation factor b (P-TEFb) and prevents Ser2 phosphorylation of the RNAPII C-terminal domain (Chodosh *et al*., 1989; Ip *et al.,* 2011; Marshall, Peng, Xie, & Price, 1996). This leads to disruption of the transcriptional progress by inhibiting the transition from transcriptional initiation to elongation (Bensaude, 2011). On the other hand, ActD intercalates into DNA and stabilizes topoisomerase-I DNA covalent complexes thereby preventing the progression of all three RNA polymerases (Bensaude, 2011; Trask & Muller, 1988).

Initially, NIH3T3 cells were treated with either 20µM MG132, 100µM DRB or both 100µM DRB and 20µM MG132 for 1h, 2h, 4h and 8h. DRB treatment alone was used to assess the efficiency of RNAP II inhibition and its effect on the repeat transcription (control). RNA was extracted followed by cDNA synthesis and transcript levels of the repeats were analysed by qPCR using the same primers as previous experiments.

Ongoing transcription by RNAPII was found to be effectively inhibited as the short lived c-myc transcript was strongly reduced after 1h of treatment with DRB (Figure 4.9A).

Proteasome inhibition resulted in a 5 and 16 fold increase in the major satellite repeat expression at 4h and 8h of treated cells respectively compared to untreated cells, confirming previously obtained results. This increase was no longer seen in cells treated concomitantly with MG132 and DRB (Figure 4.9B), suggesting that upregulation of the expression of the major satellite repeat is dependent upon transcription rather than stabilisation of the transcript. Notably, the DRB treatment alone led to an initial decrease in major satellite repeat transcripts at 1h and 2h of treatment as might be expected,

surprisingly this was followed by a 1.5 and 3.5 fold increase at 4h and 8h of treatment respectively (Figure 4.9b, 4.10). This result is unexpected since it is thought that the major satellite repeat is exclusively transcribed by RNAP II (J. Lu & Gilbert, 2007; Rudert *et al*., 1995; Valgardsdottir *et al.*, 2005) which has been inhibited by DRB and therefore suggests a possible role of other RNA polymerases. Clearly one way of testing this hypothesis would be to inhibit all RNA polymerases by ActD and observe its effect on the transcription levels (see below Figure 4.11).

Consistent with the previously described results (Figure 4.3, 4.8), the minor satellite and LINE L1 transcripts were not significantly affected by proteasome inhibition. However, DRB treatment resulted in significant reduction of both minor satellite and LINE L1 transcripts at all time points examined (Figure 4.9C and 4.9D) consistent with their transcription being dependent on RNAPII. Furthermore, a moderate level (1.5 fold) of upregulation of SINE B1 expression was observed after 8h of MG132 treatment compared to untreated cells. Similar levels of upregulation were also obtained with concomitant MG132 and DRB treatment whilst 50% reduction with only DRB treatment (Figure 4.9E). It is noteworthy that SINE B1 are predominantly transcribed by RNAPIII (Dridi, 2012; Williams, Tamburic, & Astell, 2004), therefore the upregulation upon MG132 and DRB treatment may still be the result of an effect on transcription mediated by RNAPIII.

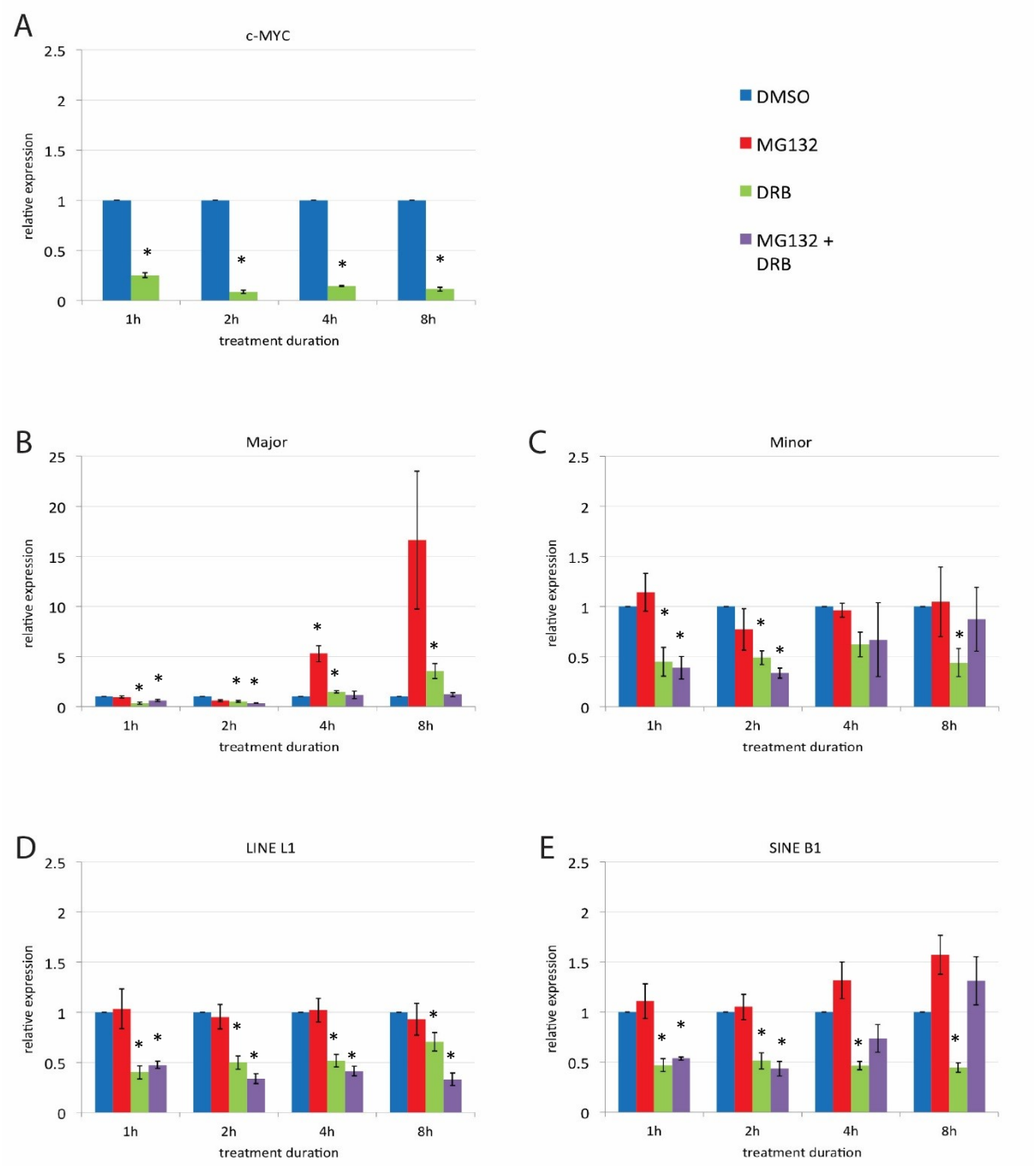


Figure 4.9: A time course showing the effect of proteasome and/or RNAPII inhibition on the expression of *c-MYC* (A), major satellite (B), minor satellite (C), LINE L1 (D) and SINE B1 (E) repeats. NIH3T3 cells were treated with either 20µM MG132, 100µM DRB or both 100µM DRB and 20µM MG132 for 1h, 2h, 4h and 8h followed by RNA extraction and q-RT-PCR. The relative expression was normalised against 'spiked' RNA (see methods) and is shown as fold change relative to DMSO. Error bars indicate SEs of at least 3 biological replicates. *p<0.05 (Student's 't' test).

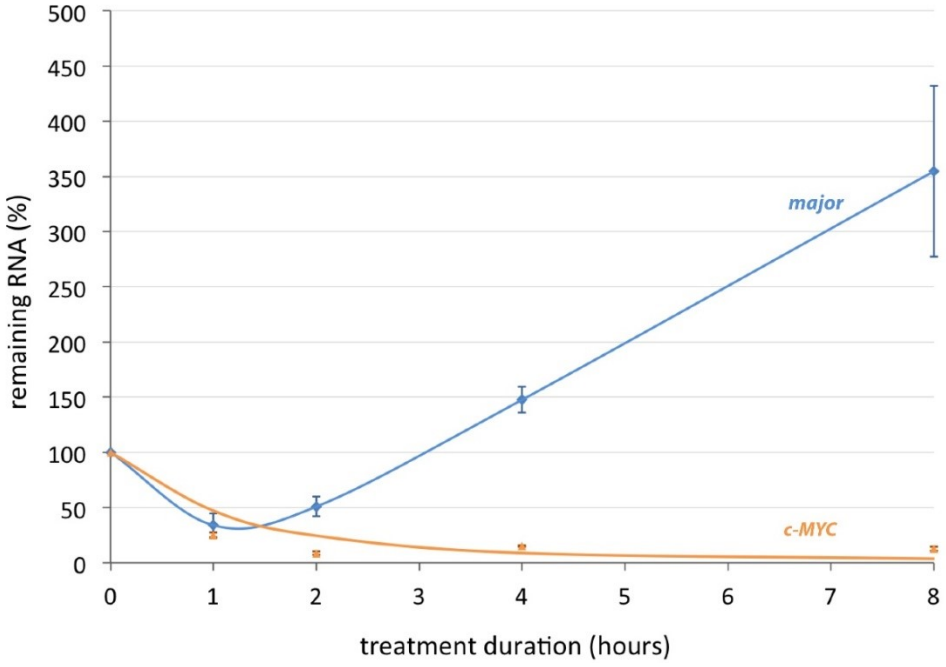


Figure 4.10: A time course showing the effect of RNAPII inhibition on the expression of *c-MYC* (A) and major satellite repeat (B). NIH3T3 cells were treated with 100µM DRB for 1h, 2h, 4h and 8h followed by RNA extraction and q-RT-PCR. The relative expression was normalised against spike and shows fold change relative to DMSO. Error bars indicate SEs of at least 3 biological replicates.

In order to confirm the transcription-dependent upregulation of the major satellite transcripts and potentially uncover the pathway of SINE B1 transcript accumulation upon proteasome inhibition, NIH3T3 cells were treated with either 20µM MG132, 20µg/ml ActD or both 20µg/ml ActD and 20µM MG132 for 1h, 2h, 4h and 8h. ActD treatment alone was used to assess the efficiency of inhibition of all three RNA polymerases (RNAPI, II and III) and to determine the RNA half-life of the major satellite, minor satellite, LINE L1 and SINE B1 transcripts using kinetic studies of RNA decay. In a similar approach as above, RNA was extracted followed by cDNA synthesis and transcript levels of the repeats were analysed by qPCR using the same primers as previous experiments.

Consistent with effective inhibition of transcription there was an exponential decay of all analysed transcripts. As expected, the c-MYC mRNA was degraded rapidly with a half-life of

approximately 20min (Gondran, Amiot, Weil, & Dautry, 1999). Half-lifes of approximately 150min, 70min, 60min and 80min was measured for major, minor, LINE L1 and SINE B1 RNAs respectively (Figure 4.11A). To our knowledge this is the first formal measurement of these half-lifes and the half-life of the major satellite repeat is longer than we had anticipated based upon a previous estimate which was less than 1 hour although this was based upon RNA FISH (J. Lu & Gilbert, 2007).

Consistent with the previous results, proteasome inhibition resulted in a 5 and 14 fold increase in major satellite repeat expression following 4h and 8h of MG132 treatment respectively compared to untreated. This increase was blocked in cells treated concomitantly with both MG132 and ActD (Figure 4.11B), indicating that their upregulation in response to MG132 was transcription dependent (compare in Figure 4.11A MG132 and MG132+ActD). Strikingly, the upregulation at 8h seen following treatment with the RNAPII-specific inhibitor DRB (Figure 4.9B) did not occur when all forms of RNAP were inhibited with ActD treatment (Figure 4.11B). It is tempting to speculate that RNAPI or III might be able to substitute for RNAPII in transcribing major satellite after 8h of RNAPII inhibition (Figure 4.9B and 4.11B). Interestingly a similar result was obtained for the SINE B1 element, suggesting that MG132 induced upregulation at the level of transcription leading to the accumulation of these transcripts after 8h of treatment with proteasome inhibitor (Figure 4.11E). Inhibition of RNAPI, II and III by ActD had a profound effect (Figure 4.11E) whereas the selective RNAPII inhibitor DRB was ineffective (Figure 4.9E). This result is consistent with RNAPIII being the predominant polymerase transcribing the SINE B1 element as previously suggested (Dridi, 2012; Williams *et al*., 2004).

Furthermore, proteasome inhibition resulted in only minor changes in minor satellite and LINE L1 expression, whilst ActD and concomitant MG132 and ActD significantly diminished the transcript levels (Figure 4.11C, 4.11D).

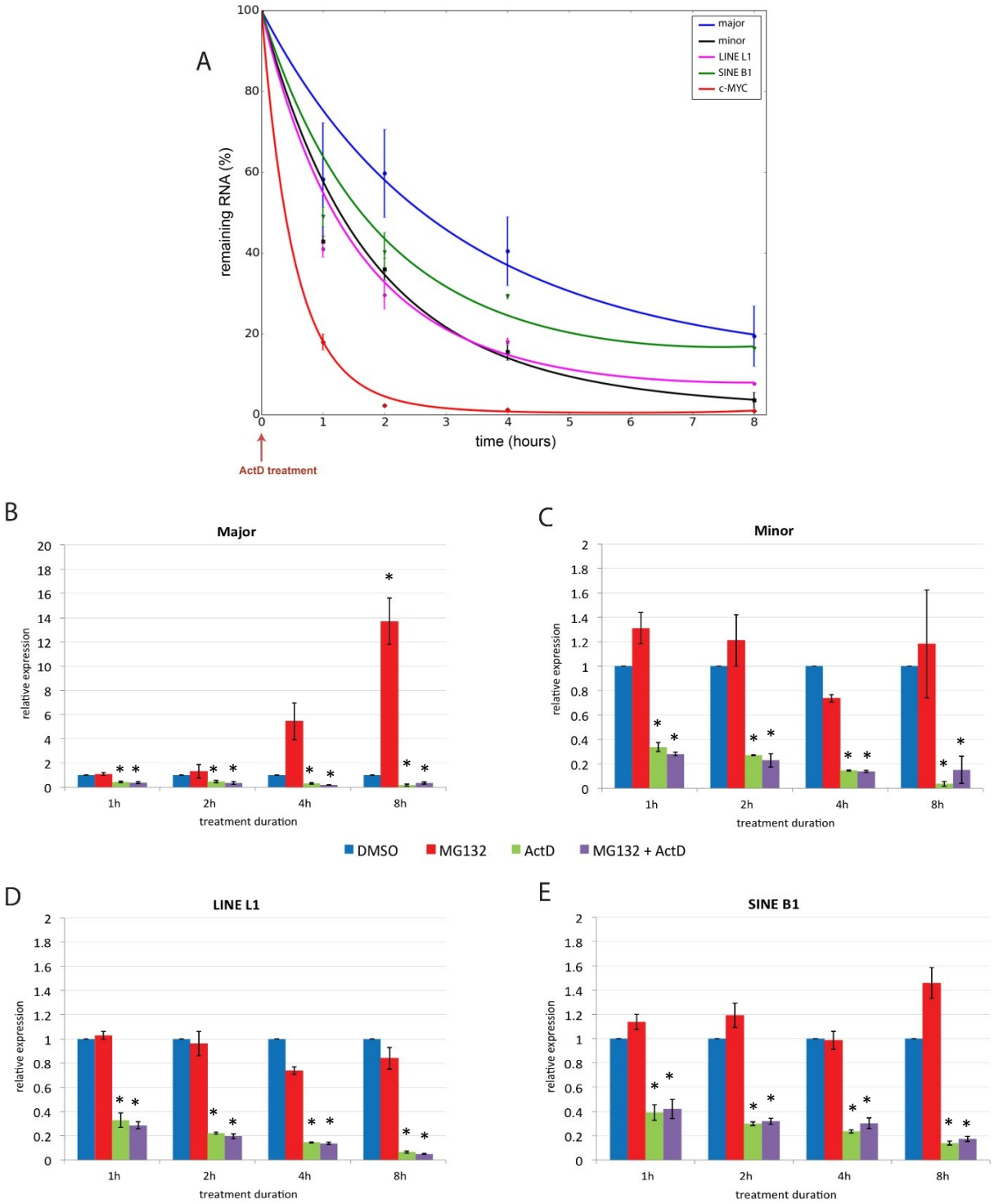


Figure 4.11: A time course showing the effect of proteasome and/or all RNA polymerases (RNAPI, II and III) inhibition on the expression of major satellite (B), minor satellite (C), LINE L1 (D) and SINE B1 (E) repeats. (A) Represents best fitted exponential decay curve obtained with nonlinear regression for half-life calculations of *c-MYC*, major, minor, LINE L1 and SINE B1 transcripts. NIH3T3 cells were treated with either 20µM MG132, 20µg/ml ActD or both 20µg/ml ActD and 20µM MG132 for 1h, 2h, 4h and 8h followed by RNA extraction and q-RT-PCR. The relative expression was normalised against spike and shows fold change relative to DMSO. Error bars indicate SEs of 3 biological replicates. *p<0.05 (Student's 't' test).

4.2.6 RNA FISH analysis confirms the increase transcription of the major satellite repeat upon proteasome inhibition

RNA fluorescent in situ hybridization (RNA FISH) was undertaken to validate at the single cell level, the upregulation of the major satellite repeat transcription upon proteasome inhibition. This imaging technique has been a successful method to optically detect single RNA molecules in fixed but otherwise intact cells, determining both presence and spatial location of the transcript within the cell (Femino, Fay, Fogarty, & Singer, 1998). This is especially important due to the presence of the 42 intergenic major satellite repeat sequences interspersed in the mouse genome outside of pericentromeric heterochromatin (Bulut-Karslioglu *et al*., 2012), that cannot be easily discriminated by q-RT-PCR. Moreover, RNA FISH is able to display the location of the transcript hence providing evidence of their transcription site (Levsky, Shenoy, Pezo, & Singer, 2002; Osborne *et al.,* 2004).

Here NIH3T3 cells, seeded on polylysine coated coverslips, were treated for 2h, 4h and 8h with 20μM MG132 and processed by RNA FISH using a probe set that was complementary to the major satellite repeat sequence and stained with DAPI (4',6-diamidino-2-phenylindole; which binds to the minor groove of DNA). The RNA binding specificity was determined by digesting the cells with RNAse prior to hybridization with the probe step.

As shown in figure 4.12, proteasome inhibition resulted in a gradual and dramatic increase of the major satellite repeat signal from the MG132 treated cells at 4h and 8h, compared to DMSO only, whilst no significant change was observed at 2h of treatment. Furthermore, no signal was detected with RNAse digestion of both treated and untreated cells, indicating dependency on the presence of RNA. It is worth mentioning that the RNAse digestion was performed for each time point; however the data is shown only upon 8h of treatment with MG132 and DMSO.

In order to investigate the origin of the major satellite repeat transcripts (intergenic or pericentromeric) upon proteasome inhibition, multiple mid-zone z-section images were taken with confocal microscopy (Figure 4.13) and 3D images were reconstructed using Velocity software (Figure 4.14). The overall analysis of multiple z-section images confirmed the upregulation of the major satellite repeat transcripts upon 4h of treatment with

proteasome inhibitor MG132, compared to untreated (Figure 4.13B, 4.14B), whereas only minor changes occurred at 2h (Figure 4.13A, 4.14A).

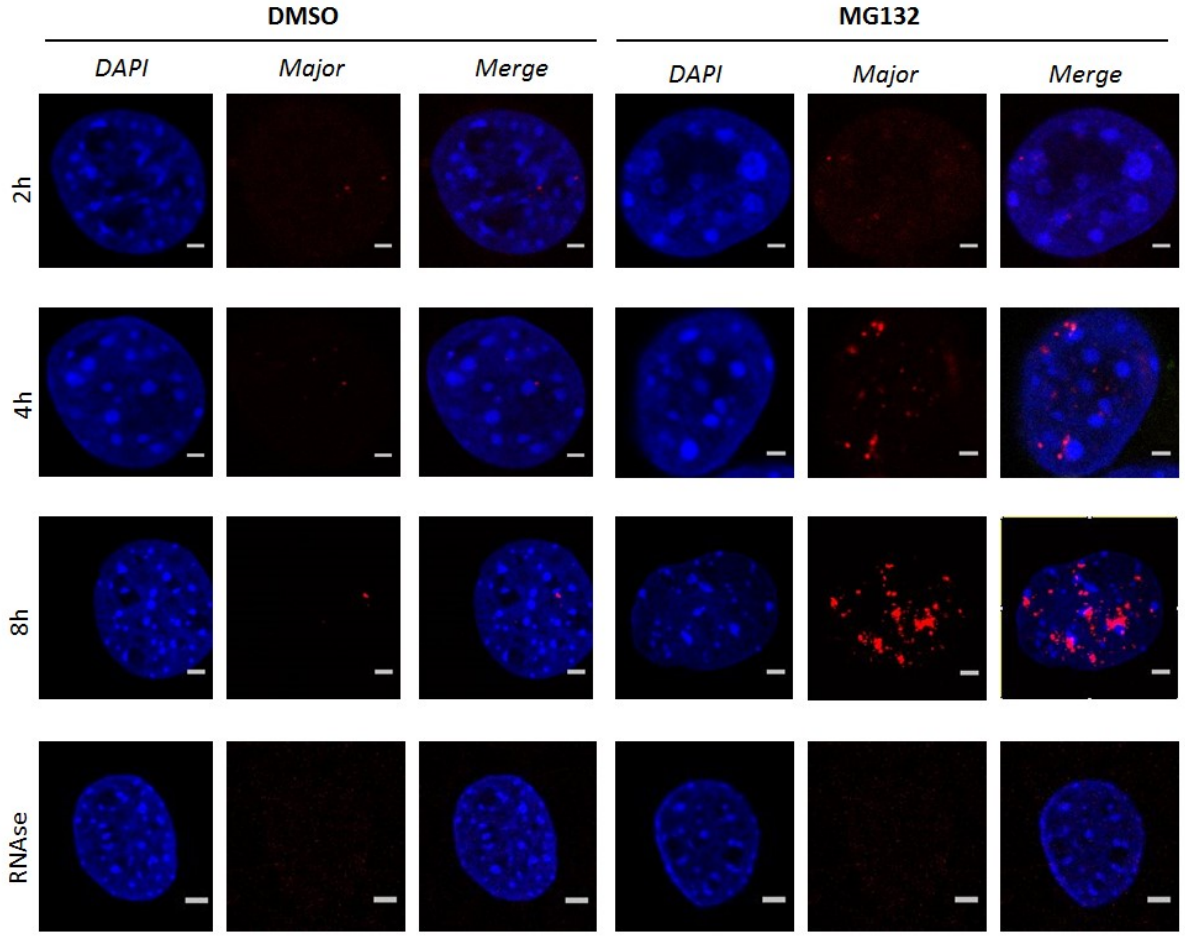


Figure 4.12: RNA–FISH analysis of major satellite repeat transcription upon proteasome inhibition. NIH3T3 cells were treated with 20µM M132 for 2h, 4h and 8h and were subjected to RNA-FISH analysis with mouse major satellite probe. Representative single z-section images for DAPI (blue), major (red) and merge are shown for 2h, 4h and 8h with DMSO and MG132 treatment. Negative control of hybridization was conducted with RNAse treatment. Scale bar 2µm.

The number of transcription sites detected per cell upon proteasome inhibition was highly heterogeneous (compare MG132_1 and MG132_2 in figure 4.13B, 4.14B). A clear signal of probe hybridization to the major satellite was revealed surrounding or within a proportion of DAPI-dense heterochromatin regions with the morphology characteristic of so-called chromocentres (Guenatri *et al*., 2004) (see more in the general introduction, Figure 1.8). In addition, the signal was also identified coming from areas of nucleus lacking chromocentres (Figure 4.13B, 4.14B), suggesting either the partial transcription from intergenic major satellite DNA sequences or it might reflect the migration of the transcript from the chromocentres.

Notably, there was a very small number of major satellite hybridization signals detected in most of the untreated (DMSO) cells, primarily surrounding or within the chromocentres (Figure 4.12, 4.13A, 4.14A). This clearly suggests the presence of major satellite repeat transcripts within the cells and confirms the previous studies of the transcription of pericentromeric heterochromatic repeats (Eymery, Horard, *et al*., 2009; Hall *et al.,* 2012).

Overall the RNA-FISH analysis is consistent with the observation of upregulation of major satellite repeat transcription upon proteasome inhibition, confirming previously obtained results using q-RT-PCR (Figure 4.3, 4.8A). Thus, RNA-FISH analysis indicates that proteasome inhibition leads to upregulation of RNA transcripts originating from major satellite DNA within pericentromeric heterochromatin, although it does not exclude the intergenic origin or their combination.

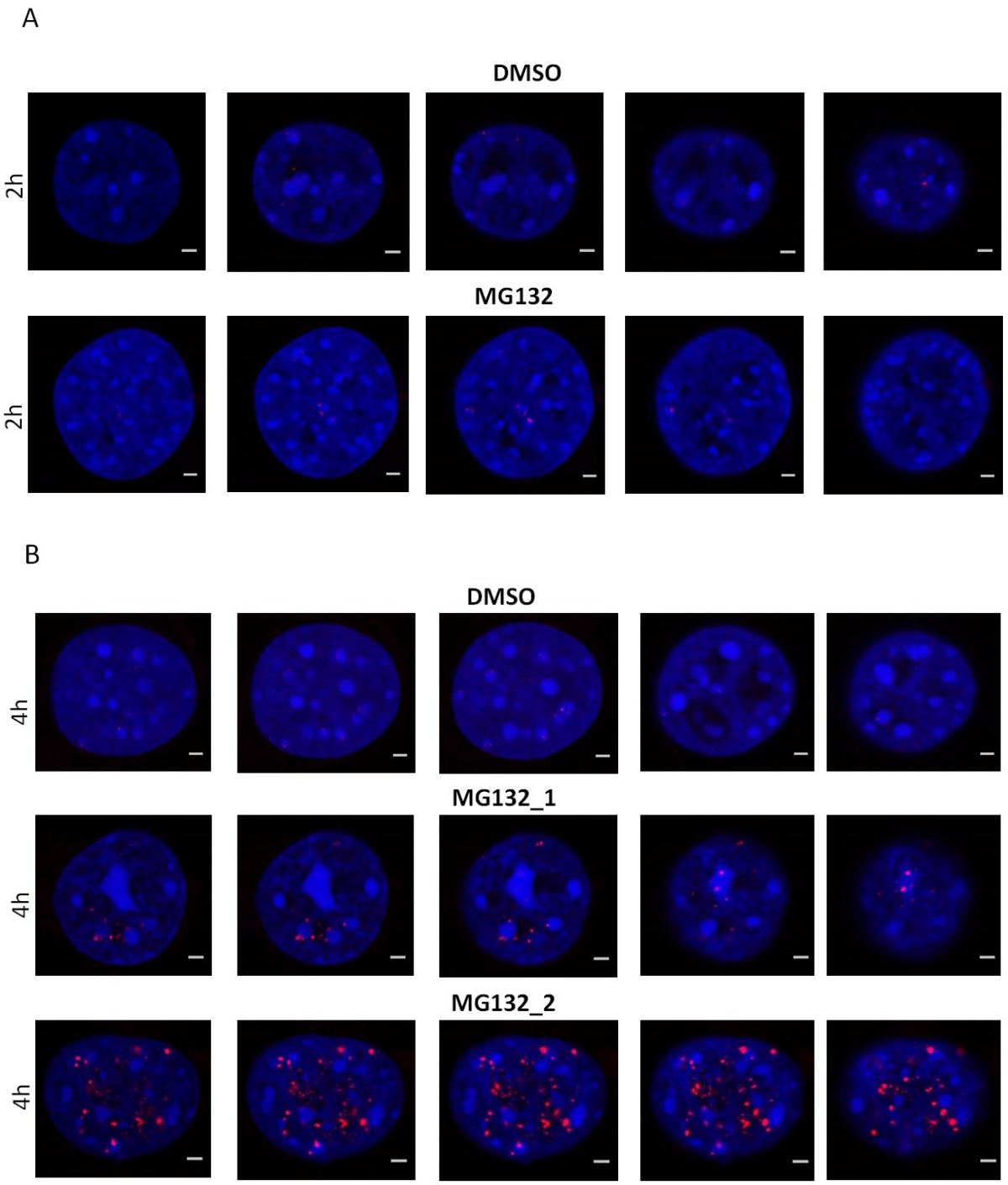


Figure 4.13: RNA-FISH analysis of major satellite transcription sites in cells upon proteasome inhibition. NIH3T3 cells treated with 20µM MG132 and DMSO only for 2h and 4h were subjected to RNA-FISH analysis with mouse major satellite probe set. Representative mid-zone confocal z-sections merged images for DAPI (blue) and major (red) are shown for 2h (A) and 4h (B) treatment with DMSO and MG132. Scale bar 2µm.

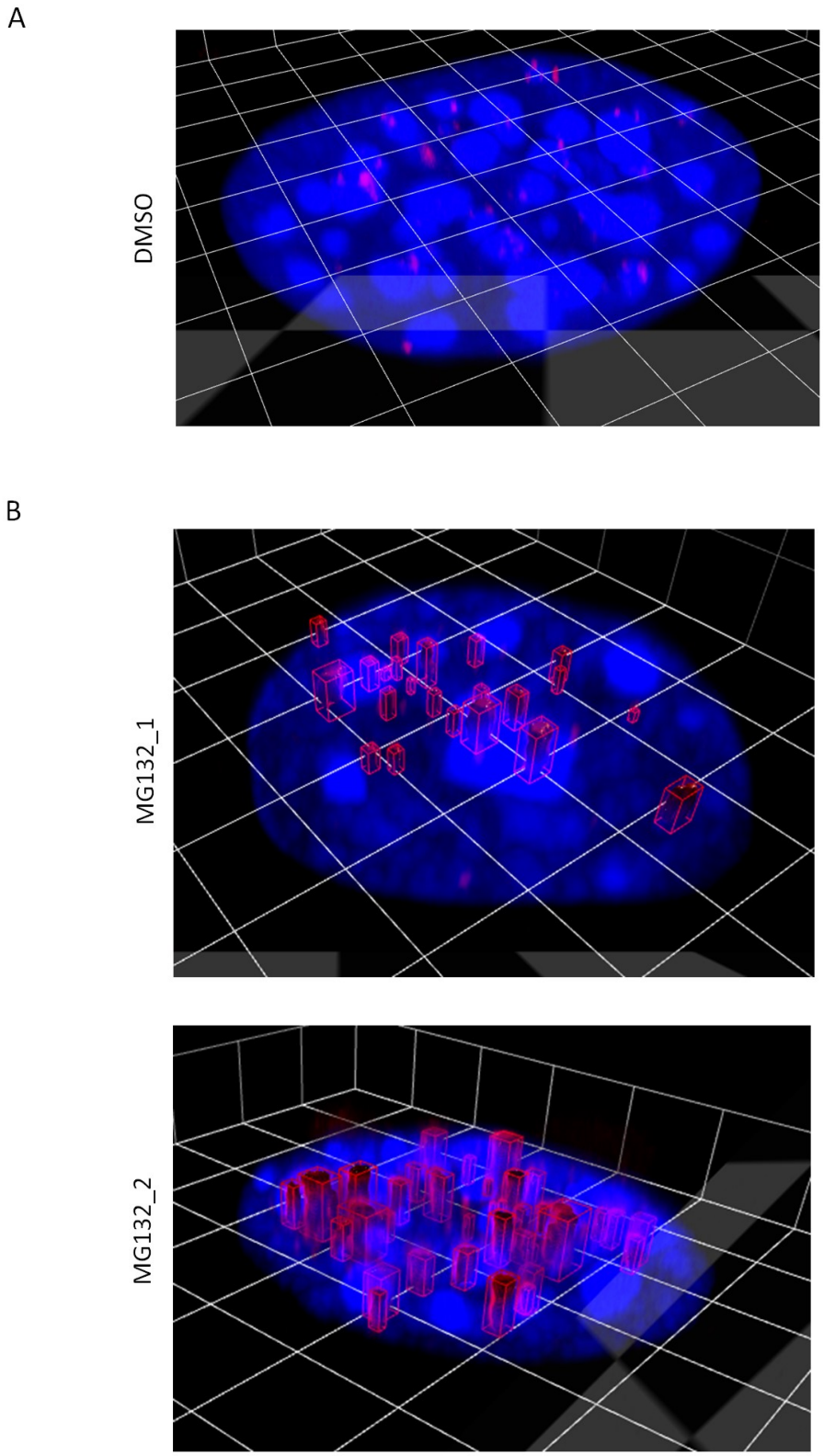


Figure 4.14: Representative 3D images obtained following RNA-FISH using Velocity software for NIH3T3 cells treated with DMSO (A) and MG132 (B) for 4h with probe against major satellite repeat transcript. DAPI is shown in blue and major satellite repeat transcript in red.

4.2.7 No change in the main heterochromatic/euchromatic histone modification marks on the major satellite repeat locus upon proteasome inhibition

The above data demonstrates the upregulation of transcription from major satellite repeat upon proteasome inhibition. In order to assess whether this upregulation might also impair the chromatin signature of pericentromeric heterochromatin, histone posttranslational modifications were analysed by ChIP.

ChIP was performed using antibodies against the repressive histone modification H3K9me3 and activating marks H3K4me3, H3K36me3 and H3ac on NIH3T3 cells after 20μM MG132 treatment for 4h. Immunoprecipitated material was quantified using qPCR with the same primers as those used in the previous experiment. Additionally primers against the promoter and gene body of the housekeeping gene GAPDH and the brain-specific gene MOG (myelin oligodendrocyte glycoprotein) were used as positive and negative control for the euchromatic regions respectively.

According to the q-PCR analysis, the H3K9me3, which is primarily associated with pericentromeric heterochromatin was highly enriched on major satellite repeat, as previously shown (Martens *et al*., 2005) and was reduced in all the remaining regions examined (Figure 4.15A). The absence of H3K9me3 from the minor satellite repeat, which forms the centromere was expected since centromeres are characterised by the centromere-specific histone H3 variant CENP that is occasionally interrupted by nucleosome containing H3K4me2 (Masumoto, Masukata, Muro, Nozaki, & Okazaki, 1989; D. K. Palmer, O'Day, Trong, Charbonneau, & Margolis, 1991; Purgato *et al.,* 2015; Stimpson & Sullivan, 2011). Additionally, in somatic cells, silencing of the retro-elements including LINE L1 and SINE B1 is thought to be achieved predominantly by DNA methylation, whilst histone modification marks appear to play only a minor role (Bierhoff, Postepska-Igielska, *et al.,* 2014), explaining the relatively low level of the H3K9me3 at the examined retro-element regions. The treatment of cells with proteasome inhibitor did not result in significant changes in H3K9me3 enrichment on the major satellite repeat, compared to untreated; or any of the remaining examined regions (Figure 4.15A).

Overall, a balance between repressive and activating histone modifications regulates the expression of many genes and non-coding RNAs. As the main repressive mark (H3K9me3)

was not altering upon proteasome inhibition on the major satellite repeat loci, accompanied by the upregulation of their expression, next the activating histone modification marks were analysed.

As expected, the highly conserved H3K4me3, which is found on the promoters of actively transcribed genes (Santos-Rosa *et al*., 2002; X. D. Zhao *et al.,* 2007) displayed high levels of enrichment on the promoter of the GAPDH gene. In contrast, both heterochromatic regions (major, minor, LINE L1 and SINE B1) and an inactive gene (MOG) showed much lower levels of H3K4me3 (Figure 4.15B). Interestingly, whilst previous studies have correlated the level of H3K4me3 at the gene promoter with their transcriptional activity (Gu & Lee, 2013), amongst the repeat regions examined, the major satellite repeats revealed the highest enrichment for H3K4me3. No significant change of the level of H3K4me3 was observed on the major satellite repeat locus upon proteasome inhibition. Similar levels of the mark were also obtained in all the remaining regions examined (Figure 4.15B).

H3K36me3 is a well-known mark associated with elongating RNA polymerase II (Ser2P) and appears on the gene bodies of actively transcribed genes (Chae, Danko, & Kraus, 2015; M. A. Hahn, Wu, Li, Hahn, & Pfeifer, 2011). The analysis of immunoprecipitated chromatin by H3K36me3 antibody revealed high enrichment of this mark on the GAPDH gene bodies and low levels in the heterochromatic repeats as well as the inactive MOG gene (Figure 4.15C). The treatment of the cell with MG132 did not alter the relative enrichment status either on major satellite repeat, centromeric repeat, retrotransposons or the inactive gene (Figure 4.15C).

In addition, histone acetylation levels that correlate with a transcriptionally active status of chromatin (Hebbes *et al*., 1988; Roh, Cuddapah, & Zhao, 2005) were examined upon proteasome treatment. Overall histone H3 acetylation (K9, K14, K18, K23 and K27) were demonstrated to be increased on the GAPDH gene body and reduced in heterochromatic and inactive regions, with no change on the level of this modification upon proteasome inhibition (Figure 4.15D)

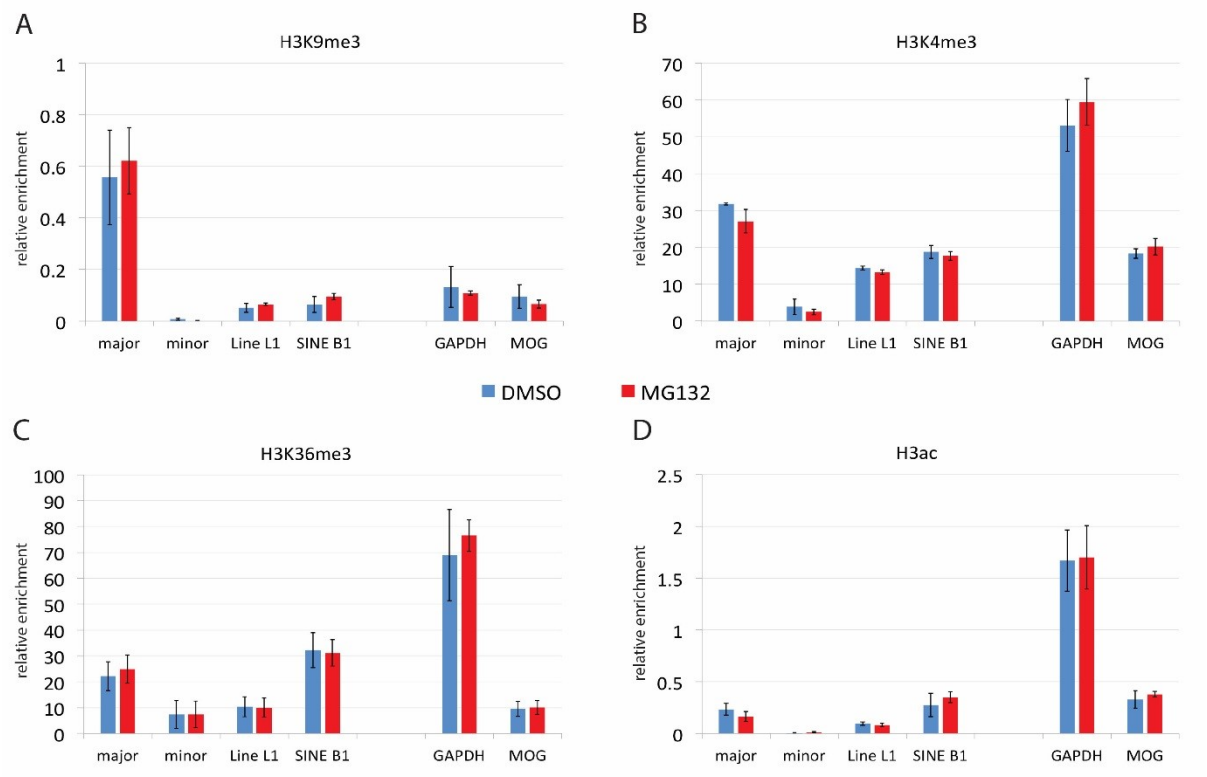


Figure 4.15: The proteasome treatment does not affect the global chromatin histone modification marks on the repetitive elements. NIH3T3 cells were treated with 20µM MG132 for 4h and underwent ChIP – qPCR against repressive mark H3K9me3 (A) and activating marks H3K4me3 (B), H3K36me3 (C) and H3ac (D). ChIP signal is shown as relative enrichment to H3 with background (no antibody) subtraction. Error Bars represent SEM, n=3.

In summary, results in this section showed that proteasome inhibition did not have any net effect on four histone modifications (1 repressive and 3 activating) marks investigated on the major satellite repeat locus. The lack of effect might seem surprising given that proteasome inhibition led to significantly increased transcription of the repeats. One possible explanation might relate to the proportion of repeat sequences that have been activated by inhibiting the proteasome. The RNA FISH experiment indicates that the number of repeats or heterochromatic clusters that are transcriptionally activated might be a very small proportion of the total and therefore any chromatin changes would be diluted by the majority of DNA sequences which are not expressing the transcript (see discussion).

4.2.8 No change of H3K9me3 distribution on the pericentromeric heterochromatin foci (chromocentres) upon proteasome inhibition

Chromatin Immunoprecipitation showed no significant change on the heterochromatic mark H3K9me3 on the major satellite repeat locus upon treatment with proteasome inhibition. To further validate this result, NIH3T3 cells were treated for 4h with proteasome inhibitor MG132 (final concentration 20µM) followed by Immunofluorescence (IF) analysis. Paraformaldehyde fixed and permeabilised cells were stained with DAPI (blue) and H3K9me3 (red) antibody and analysed by confocal microscope. As expected the DAPI staining clearly visualised the pericentromeric heterochromatin foci (chromocentres) (Figure 4.16) which is formed by the coalescence of the major satellites within the nucleus (see introduction Figure 1.8). The H3K9me3 signal overlapped well with these heterochromatic foci with no significant change occurring between treated and untreated samples (Figure 4.16).

This result suggests that proteasome inhibition does not change the repressive histone modification mark H3K9me3 on the chromocentres, confirming previously obtained results by ChIP (Figure 4.15A).

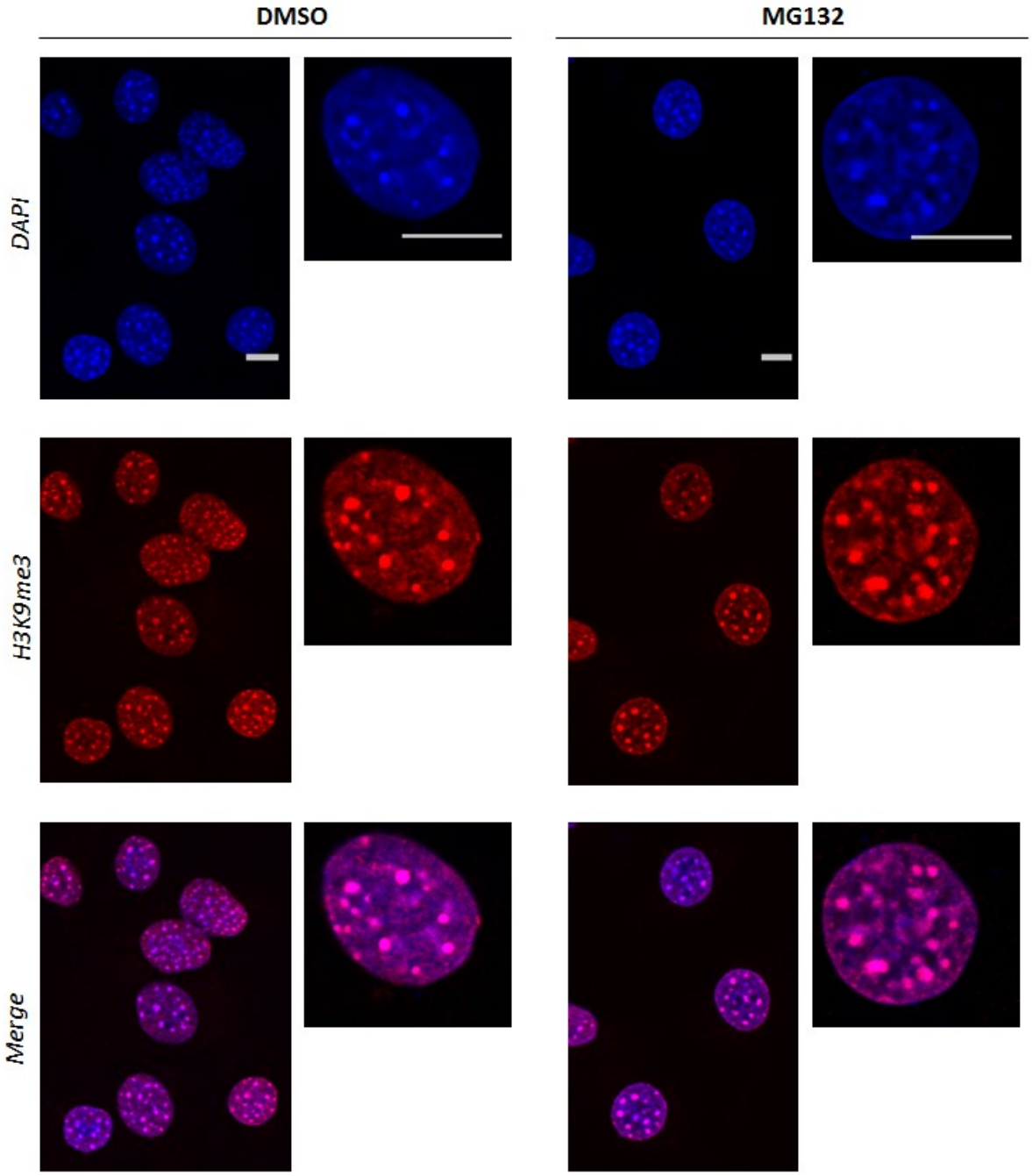


Figure 4.16: Proteasome inhibition does not affect H3K9me3. NIH3T3 cells were treated with 20µM MG132 for 4h and immunolabeled with H3K9me3 antibody (red) and stained with DAPI (blue). Scale bar 10µm.

4.2.9 Alteration of the HP1α in the cells upon proteasome inhibition

Both the chromatin immunoprecipitation and immunofluorescence experiments upon treatment of NIH3T3 cells with MG132 revealed no change in the histone modification signature at the major satellite repeat locus which forms the pericentromeric heterochromatin. However the histone modifications are not the only factors regulating the pericentromeric heterochromatin. According to previous studies structural proteins such as HP1, predominantly HP1α and HP1β, are essential factors too, involved in the chromatin condensation and maintenance of stable heterochromatin domains (Azzaz *et al*., 2014; Cheutin *et al.,* 2003). HP1α was previously shown to play a role in transcriptional gene silencing by changing the nucleosome packaging and preventing the accessibility of transcription factors for their binding sites (Azzaz *et al.,* 2014; Danzer & Wallrath, 2004; Hiragami & Festenstein, 2005; Nielsen *et al.,* 2001).

Therefore the effect of proteasome inhibition on the localisation and distribution of HP1α was evaluated by immunofluorescence microscopy. IF was performed on NIH3T3 cells after treatment with the proteasome inhibitor MG132 with a final concentration of 20μM for 4h and 8h. Paraformaldehyde fixed and permeabilised cells were stained with DAPI (blue) and HP1α (green) antibody and analysed by confocal microscope. As expected, for all the samples and time points, DAPI staining highlighted pericentromeric heterochromatin domains. In the untreated cells, the HP1α proteins were highly accumulated in the DAPI dense stained regions, confirming their localisation on the pericentromeric heterochromatin. Interestingly, the treatment of cells with MG132 for both time points showed a dispersed distribution of the HP1α protein throughout the nucleus, clearly reducing the accumulation within the DAPI dense regions (Figure 4.17, 4.18).

Whilst the distribution of HP1α was clearly changing upon treatment of NIH3T3 cells with proteasome inhibitor, total HP1α levels remained similar between treated and untreated cells, as shown by western blot (Figure 4.19).

The results in this section suggest that proteasome inhibition leads to displacement of HP1α from pericentromeric heterochromatin, without visible changes in the DAPI dense staining domains. This observation is consistent with previous studies where loss of HP1 proteins from pericentromeric heterochromatin was not sufficient to disrupt the DAPI dense stained

regions and H3K9me3 in such heterochromatin domains (Mateos-Langerak *et al.*, 2007; Mosch *et al.*, 2011).

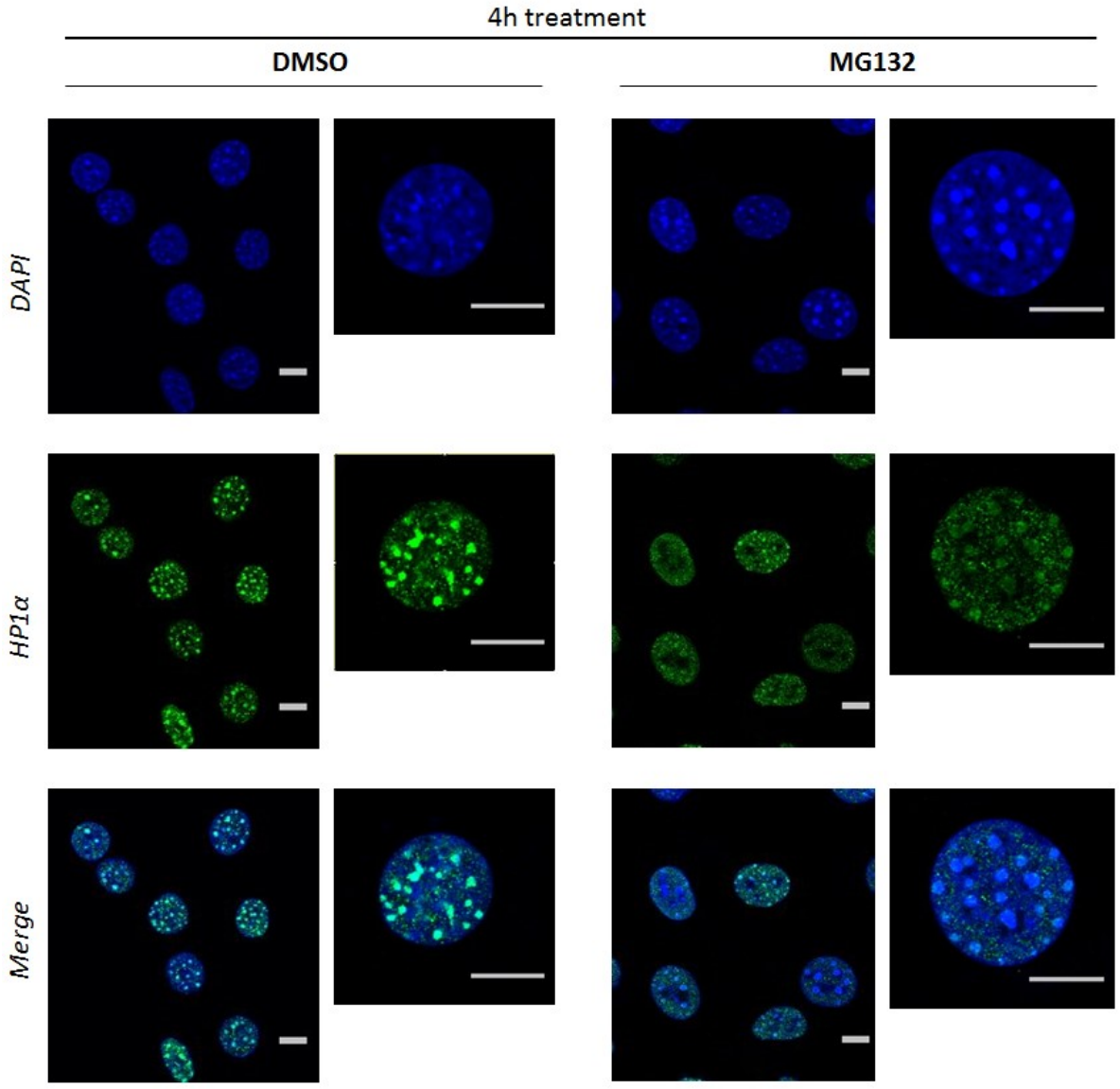


Figure 4.17: HP1α distibution change upon 4h of proteasome inhibition. NIH3T3 cells were treated with 20µM MG132 for 4h and immunolabeled with HP1α antibody (green) and stained with DAPI (blue). Scale bar 10µm.

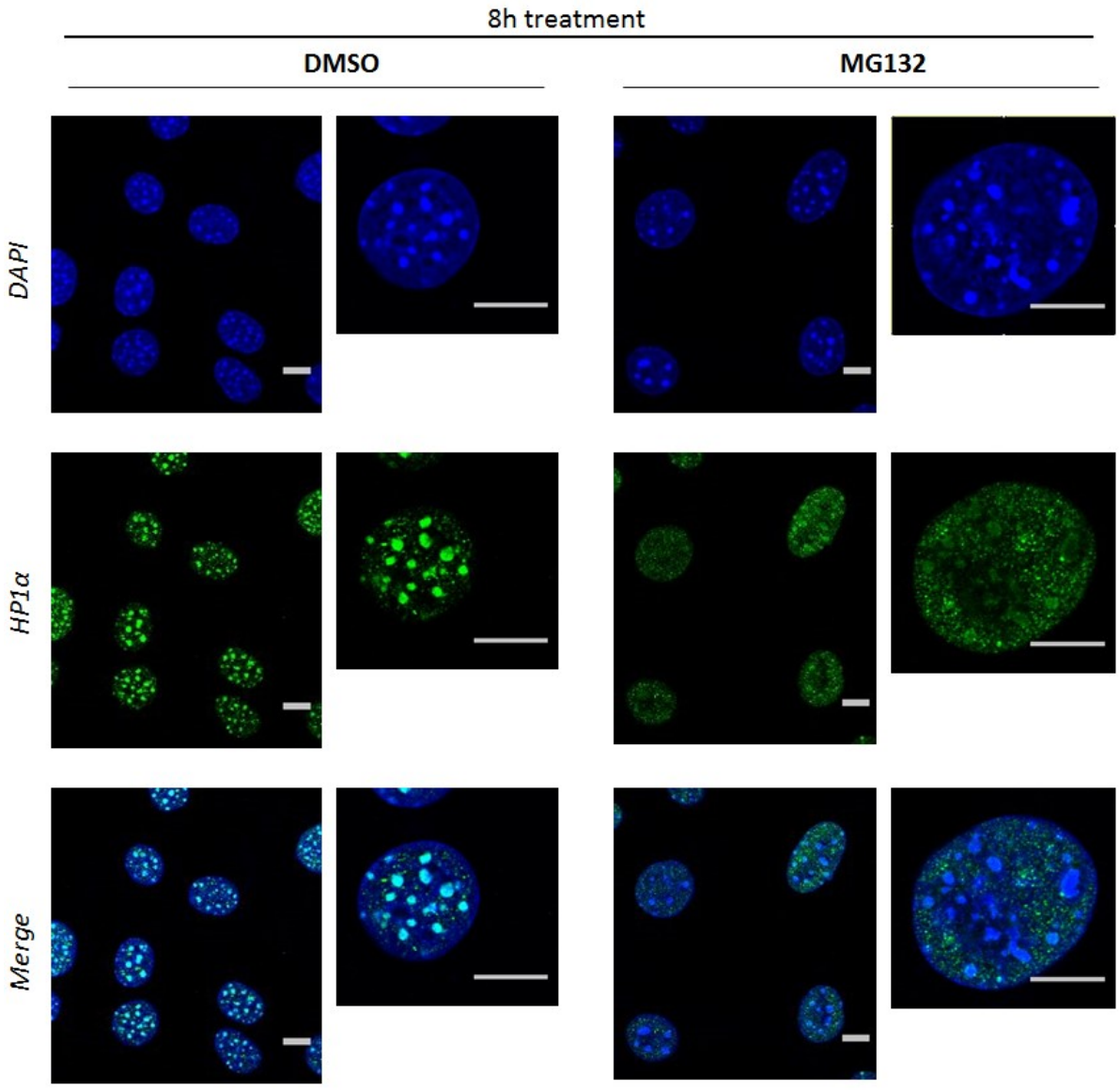


Figure 4.18: HP1α distibution change upon 8h of proteasome inhibition. NIH3T3 cells were treated with 20µM MG132 for 8h and immunolabeled with HP1α antibody (green) and stained with DAPI (blue). Scale bar 10µm.

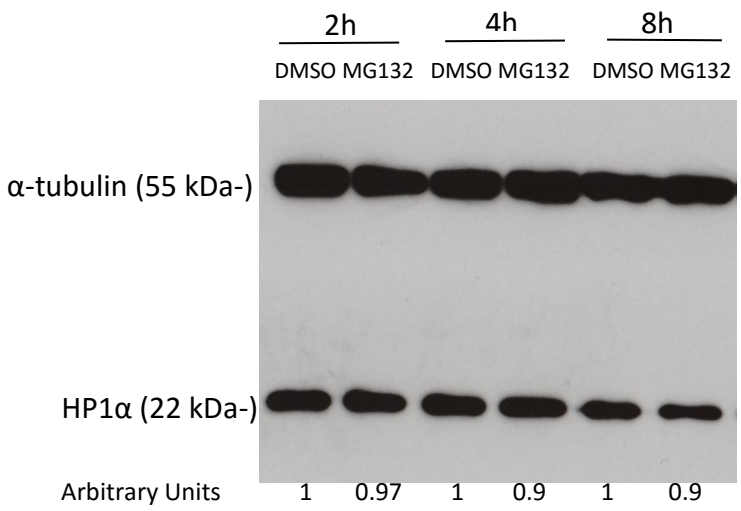


Figure 4.19: Total HP1α protein levels remain similar upon proteasome inhibition. NIH3T3 cells were treated with 20μM MG132 for 2h, 4h an 8h. Total cell lysate was probed with antibody against HP1α (~22 kDa) and α-tubulin (~55kDa) that served as a loading control.

Finally, it is also noteworthy that all HP1 proteins were previously shown to be regulated by cell cycle. Specifically it was revealed that HP1 proteins were released from chromatin during the M phase of the cell cycle, while H3K9me3 levels remained unaffected (Fischle *et al*., 2005). This is relevant because proteasome inhibition results in cell cycle dysregulation and stalling of the cells in G2/M phase (Figure 4.7A). However following 2h and 4h treatment with MG132, only minor effects on the cell cycle were observed (see Figure 4.7A), whereas HPIα shows a clear change in its distribution in the vast majority of cells visualised (Figure 4.17). Therefore the observed displacement of HP1α is unlikely to be a result of the cell cycle effect of the proteasome inhibitor treatment.

As HP1α release from the DAPI dense stained regions precedes the upregulation of the major satellite repeat transcription, it is tempting to speculate this step might be necessary to permit access of the transcriptional machinery to the heterochromatin.

4.2.10 Proteasome inhibition leads to an increased number of heterochromatic domains (chromocentres) in NIH3T3 cells

The immunofluorescence imaging of the chromocentres (visualised by DAPI staining) from fixed cells treated with proteasome inhibitor did not reveal any visible structural changes. Considering that major satellite repeats are located at these regions and from a previous study where these clusters were affected with concomitant major satellite upregulation (Zhu *et al*., 2011), it was further investigated whether the treatment of NIH3T3 cells with proteasome inhibitor could also affect the number of chromocentres. In order to acquire cells in a high-throughput method, an imaging flow cytometer (ImageStream X) was used. The ImagestreamX allows acquisition of a single cell image of each individual live cell, which is further processed using the IDEAS analysis software.

As before, NIH3T3 cells were treated for 2h, 4h and 8h with either DMSO or MG132 (final concentration 20μM). Cells were collected and stained with DRAQ5 (5μM). DRAQ5 is a far red fluorescent DNA dye that easily penetrates through the lipid bilayer of live cell membranes and can allow visualisation of the highly condensed regions of heterochromatin that correspond to the chromocentres, in a similar manner to DAPI, with the advantage that DRAQ5 is less toxic for living cells (Yuan *et al*., 2004). A minimum of 20 000 events were collected for each sample. The gating and analysis strategy that was applied aimed at gating live single cells, in focus and stained with DRAQ5. This strategy allowed exclusion of those cells that were morphologically entering cell death, visible by granularity and cell morphology on brightfield (further explained in supplementary figure S2)

Figure 4.20A illustrates representative images from the time course treatment described, both in brightfield and DRAQ5 channels. Figures 4.20B, 4.21B and 4.21C present the effect of the proteasome inhibition on the distribution of the number of chromocentres per cell, which presents a normally distributed data. More specifically, the treatment of the cells with MG132 for 2h resulted in a shift of the distribution towards the right, compared to DMSO only. This indicates that there was an increased number of the intranuclear DRAQ5 stained foci per cell (average frequency 18 to 20) (Figures 4.20B, 4.21C). A further gradual shift to the right was observed at 4h and 8h of MG132 treatment, compared to DMSO, which indicates an additional increase in the number of DRAQ5 stained foci per cell (average frequency 18 to 22 for both time points) (Figures 4.20B, 4.21D).

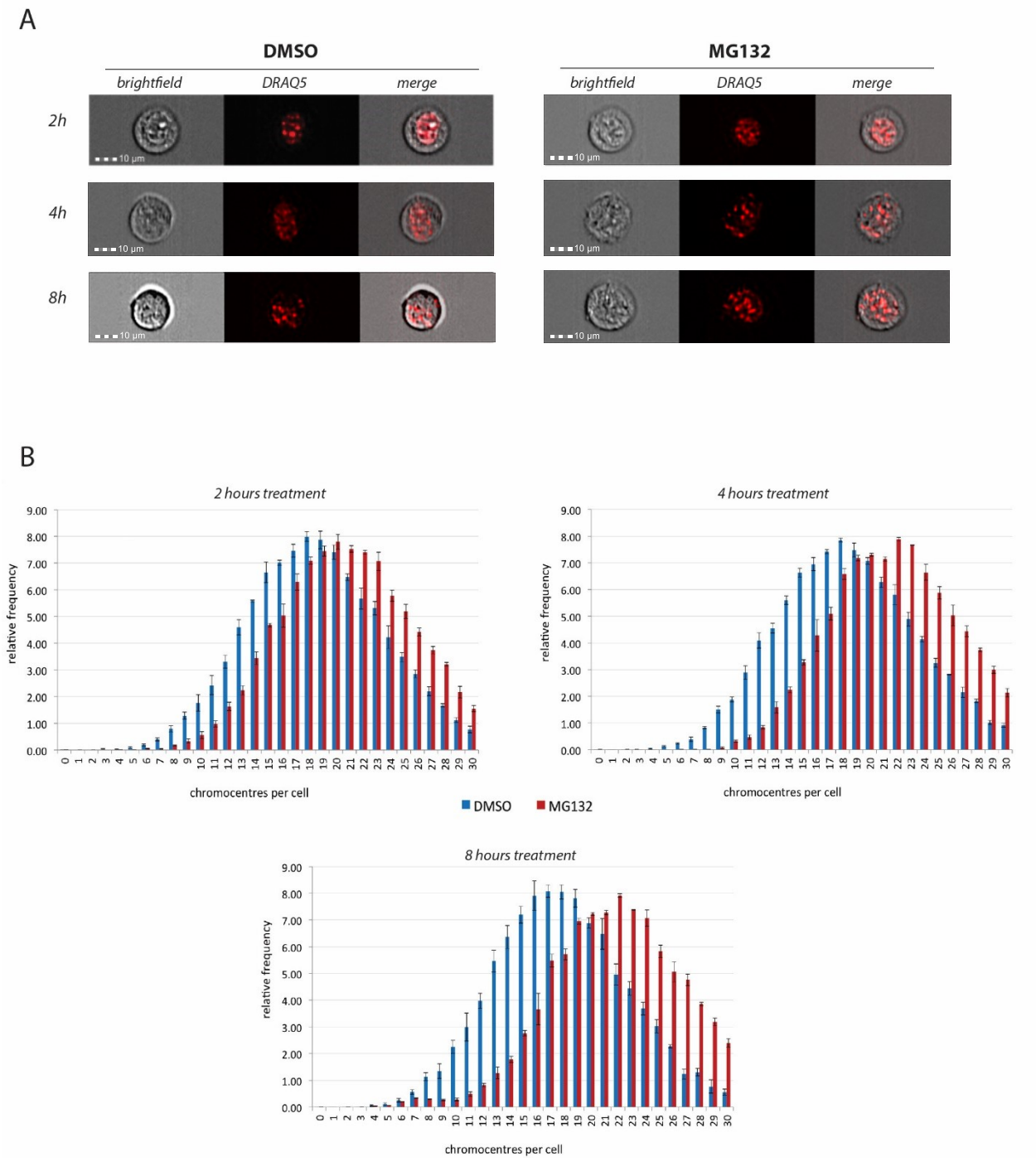


Figure 4.20: The distribution of the number of chromocentres per cell is increased by proteasome inhibition. NIH3T3 cells were treated with 20µM MG132 for 2h, 4h and 8h followed by DRAQ5 staining and imaging using ImageSteamX. (A) Representative images from brightfield and DRAQ5 channels for each time point of the treatment. (B) Analysis of the number of DRAQ5 stained foci using IDEAS software upon treatment with cells with MG132 for each time point. Error bars indicate SEs of 3 biological replicates.

While the treatment with only the vehicle (DMS0) over the studied time points did not alter the overall distribution of the chromocentres (Figure 4.21A), a shift in the distribution and an increase in the number of chromocentres per cell was already apparent after 2h of MG132 treatment (Figure 4.21B).

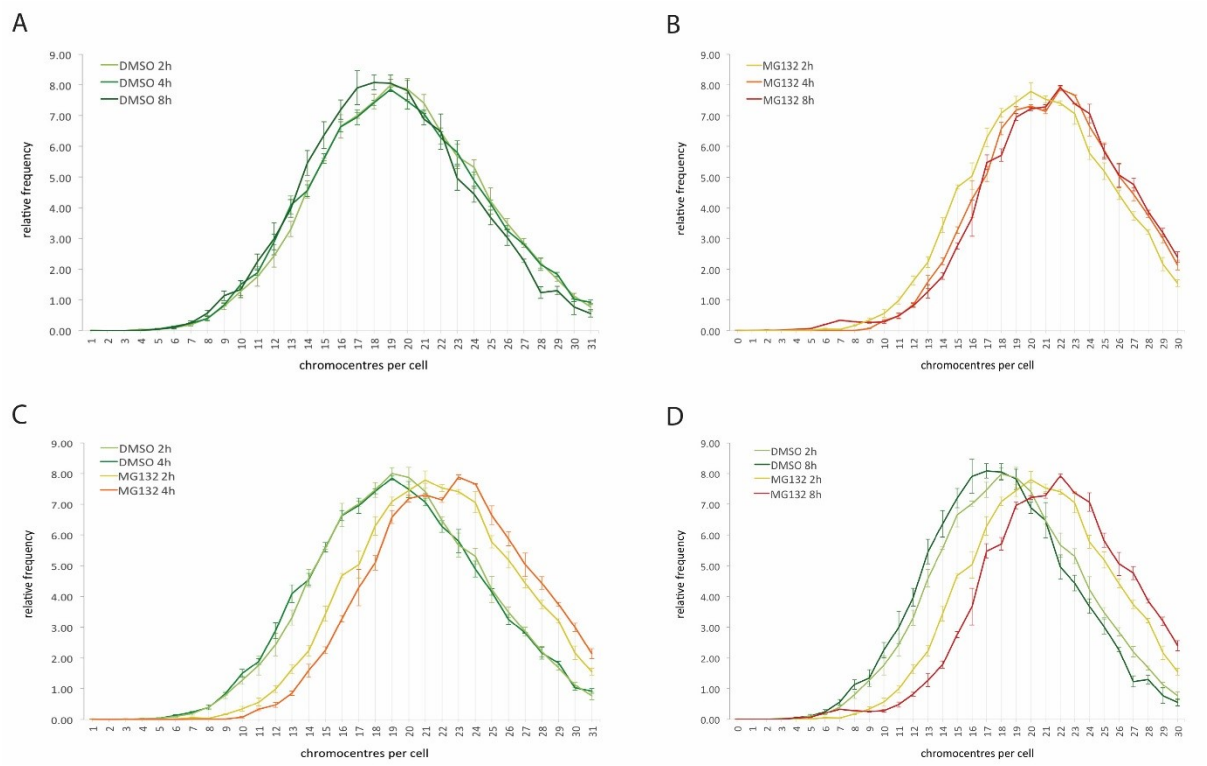


Figure 4.21: Comparison of the distribution of the number of chromocentres per cell upon proteasome inhibition. NIH3T3 cells were treated with 20µM MG132 or DMSO for 2h, 4h and 8h followed by DRAQ5 staining and analyses by ImageStreamX. (A) No change of the distribution of the chromocentres with DMSO treatment for 2h, 4h and 8h. (B) Increase in the number of chromocentres per cell upon treatment of cells with MG132. (C) Shift of the distribution of the number of chromocentres per cell to the right following treatment of cells for 2h and 4h with MG132, compared to DMSO. (D) Shift of the distribution of the number of chromocentres per cell to the right following treatment of cells for 2h and 8h with MG132, compared to DMSO. Error bars represent SEs of 3 biological replicates.

4.2.11 Cell cycle regulated changes of the number of chromocentres

The previous results suggested that proteasome inhibition increases the number of heterochromatic foci per cell, potentially affecting the structural organisation of the chromocentres. Considering that treatment of cells with proteasome inhibitor caused cell cycle dysregulation, it was therefore important to investigate the effect of the cell cycle on the chromocentre distribution.

In order to assess the cell cycle effect on the changes of the number of chromocentres, NIH3T3 cells were sorted using counterflow centrifugal elutriation. The process was conducted using constant centrifugal force and gradient increase of flow rate. A proportion of the eluted material was stained with PI followed by FACS to check the efficiency of the elutriation process; the remaining cells were stained with DRAQ5 and imaged with ImageStreamX, as previously described.

Representative images of the cell cycle profile of each fraction including the non–elutriated (control) are shown in Figure 4.22A. As expected, the control revealed 60%, 20% and 20% cells in G1/G0, S and G2/M phase of the cell cycle respectively. Elutriated fraction 1 showed high separation of G1/G0 phase where 92% of the cells were at this stage of the cell cycle. Moreover competent separation was achieved for the G2/M phase in fraction 5 where 71% of the cells were within this phase. Both fraction 2 and cells that had not been elutriated had similar cell cycle profiles. Lastly, fraction 4 was enriched for cells within G2/M phase reaching 58% (Figure 4.22B).

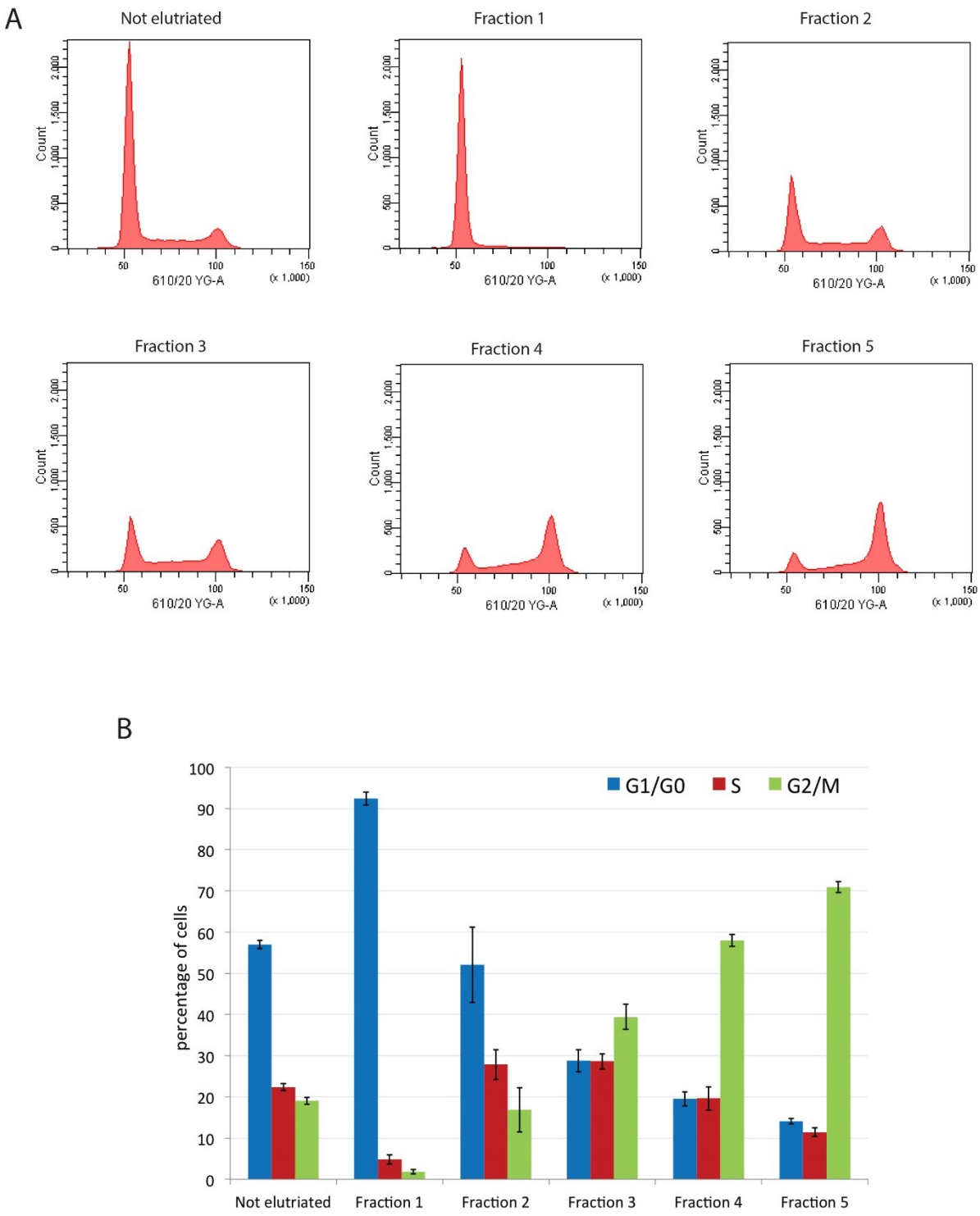
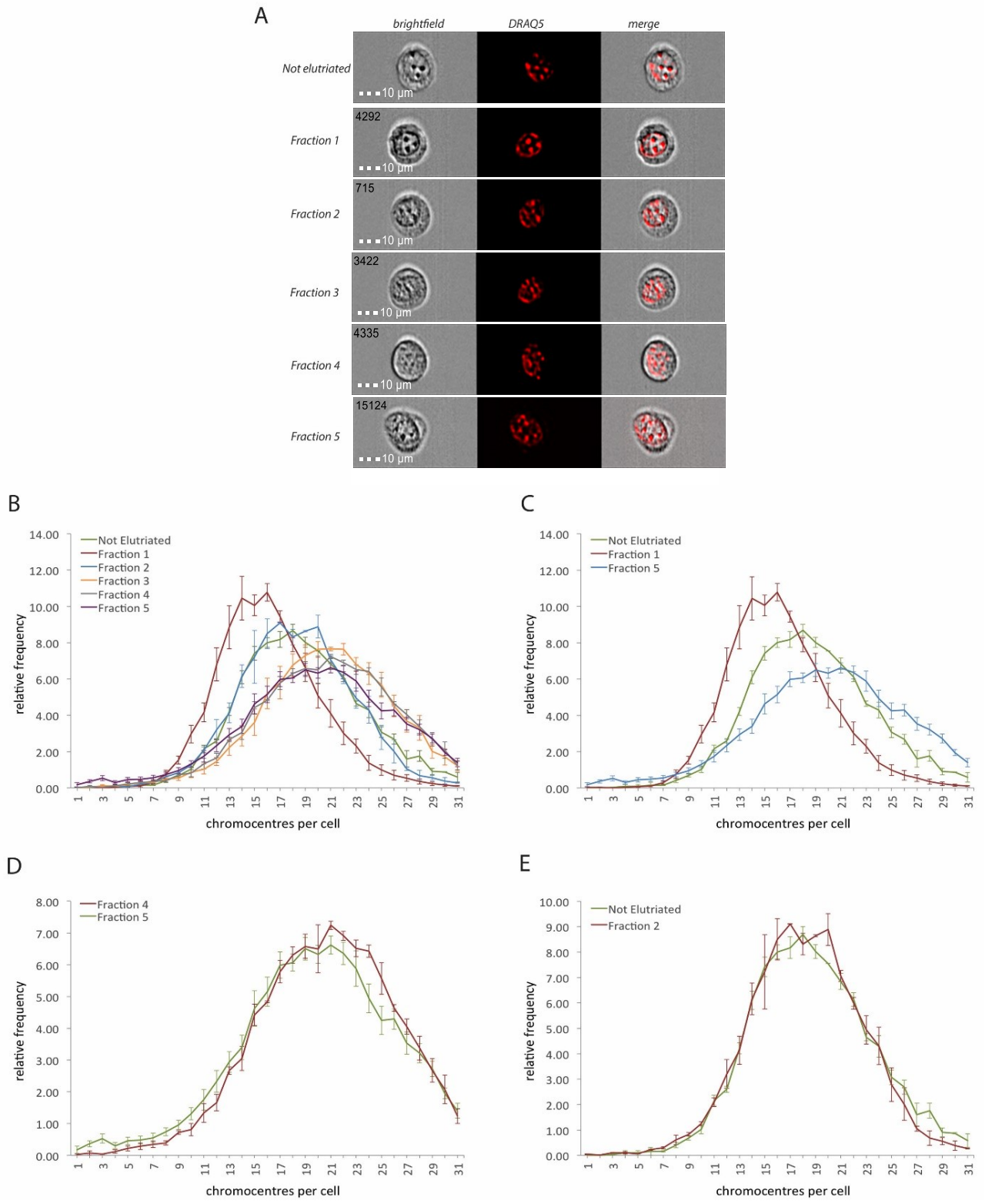


Figure 4.22: Cell fractions, enriched at specific phases of the cell cycle were obtained by centrifugal elutriation. (A) Representative images of the FACS profiles after PI staining showing non-elutriated and five different fractions of elutriated material. (B) Cell cycle distribution of each fraction is shown as a percentage of cells acquired. Data represent SEs of at least 2 biological replicates.

The ImageStreamX gating and analysis strategy was performed as previously with a minimum of 20 000 acquired events. Figure 4.23A illustrates representative images for the non-elutriated and all the fractions mentioned both in the brightfield and DRAQ5 channels. As shown in Figure 4.23B, the cell cycle affects the distribution of the chromocentres per cell. In more detail, fraction 1 which represents the cells in G1/G0 phase of the cell cycle presented a shift of the distribution towards the left, compared to the non-elutriated, meaning there was a decreased number of DRAQ5 stained foci per cell (average frequency 18 to 16) (Figure 4.23B, 4.23C). On the contrary fractions 4 and 5 representing the fractions highly enriched with G2/M phase of the cell cycle showed a shift of the distribution towards the right, compared to non-elutriated cells, indicating an increase of the number of chromocentres per cell (average frequency 18 to 21) (Figure 4.23B, 4.23C 4.23D). As expected, fraction 2 had a similar cell cycle profile as non –elutriated cells and showed no change in the chromocentre distribution compared to the non -elutriated cells (Figure 4.23D).

These results indicate cell cycle mediated regulation of the chromocentre distribution within the cell, with reduced number in G1/G0 phase and increased in G2/M phase of the cell cycle. This might make sense from a biological perspective as during G2/M the chromosomes are condensed and the centromeres separating to enable attachment of mitotic spindles to the individual chromosomes at the centromere (Cleveland, Mao, & Sullivan, 2003; Guenatri *et al*., 2004).



See next page for figure legend

Figure 4.23: Chromocentre distribution is affected by cell cycle. Not elutriated and fractions with different cell cycle profile were stained with DRAQ5 and imaged using ImageSteeamX. (A) Representative images from brightfield and DRAQ5 channels for not elutriated and each fraction containing cells with different cell cycle profiles. (B) Analysis of heterochromatic foci in all the fractions and not elutriated cells. (C) Analysis of heterochromatic foci in not elutriated, fraction 1 and fraction 5. (D) Analysis of heterochromatic foci in fraction 4 and fraction 5. (E) Analysis of heterochromatic foci in not elutriated and fraction 2. Error bars indicate SEs of at least 2 biological replicates.

4.2.12 Analysis of the effect of cell cycle perturbations due to proteasome inhibition on the number of chromocentres per cell.

According to the presented results, the distribution of chromocentres was affected by cell cycle and proteasome inhibition. Considering that proteasome inhibition caused cell cycle partial arrest in G2/M, it was necessary to investigate whether the changes on the chromocentres observed were directly caused by the treatment or indirectly caused by cell cycle skewing, or potentially a combination of both. Treatment of cells for 4h with proteasome inhibitor dramatically increased the number of chromocentres per cell (Figures 4.20, 4.21), with only a relatively minor effect on the cell cycle, (Figure 4.7) indicating that the increase in chromocentre number appears to be independent of skewing of the cell cycle towards G2/M. To formally analyse this in more depth, the similarity function between (i) cell cycle profile of different fractions obtained by elutriation and (ii) cell cycle profile upon proteasome inhibition after 4h and 8h was compared – these measurements were obtained from PI staining. The similarity function was defined as the Euclidian distance (Lele, 1993) between average values for the percentage number of cells in each phase of the cell cycle (G1/G0, S, G2/M) in the examined groups (more details regarding the analysis is shown in material and methods). The distances obtained from this analysis are shown in Table 1, where the minimum distance indicates highest similarity.

As expected, the cell cycle profile upon treatment with DMSO gave the highest degree of similarity between the samples that had not been elutriated (Figure 4.22, table 3). On the

contrary, treatment of cells with MG132 for 4h and 8h gave cell cycle profiles similar to those obtained with fraction 2 and fraction 3 respectively (table 3). Notably fraction 2 and the not-elutriated sample gave very similar cell cycle profiles and in turn similar numbers of chromocentres per cell (Figures 4.22, 4.23).

	Not-elutriated	**Fraction 1**	**Fraction 2**	**Fraction 3**	**Fraction 4**	**Fraction 5**
4h DMSO	**6.2**	45.8	11.5	31.9	49.2	62.8
4h MG132	17.7	59.5	**16.8**	18.2	36.7	51.3
8h DMSO	**6.9**	43.4	13.5	34.3	50.9	64.1
8h MG132	38.1	78.0	37.1	**10.1**	16.2	31.2

Table 3: Euclidian distances between cell cycle profile upon proteasome inhibition and different fractions of elutriated and not elutriated material obtained from PI staining. The lower the value the higher the similarity. The smallest values indicating the highest similarity are shown in bold.

Next, the chromocentre distributions, previously analysed by ImageStreamX, were compared between cells treated with either DMSO or MG132 for 4h and 8h and the fractions from the elutriated or not-elutriated material with the highest degree of similarity in respect of their cell cycle profile (Figure 4.24).

In all DMSO treated samples analysed, the number of chromocentres per cell was highly similar compared with not-elutriated samples (Figures 4.24A, 4.24B). This result was expected as DMSO treatment had no effect on cell cycle distribution (data not shown).

As illustrated in Figures 4.24C and 4.24D, a clear difference in the distribution of the number of chromocentres per cell was observed after 4h and 8h of MG132 treatment, relative to fractions 2 and 3 respectively. Notably, the difference was more pronounced at 4h of treatment when compared with 8h of MG132 treatment (Figures 4.24C, 4.24D). These

results suggest an effect of the proteasome inhibition on the regulation of the heterochromatic foci within the nucleus, rather than solely an indirect effect secondary to skewing of the cell cycle. However, to investigate this further, cells could be treated with the proteasome inhibitor followed by elutriation and Imagestream analysis, in order to determine at what cell cycle stage/s the increase in the number of chromocentres per cell occurs.

Overall the results presented in this section imply that the effect of proteasome inhibition on the distribution of the number of chromocentres per cell does not appear to be solely secondary to cell cycle skewing (Figure 4.21C, 4.21D) and correlated with transcriptional upregulation of the major satellite repeats which in itself might loosen the association of centromeres with each other during interphase.

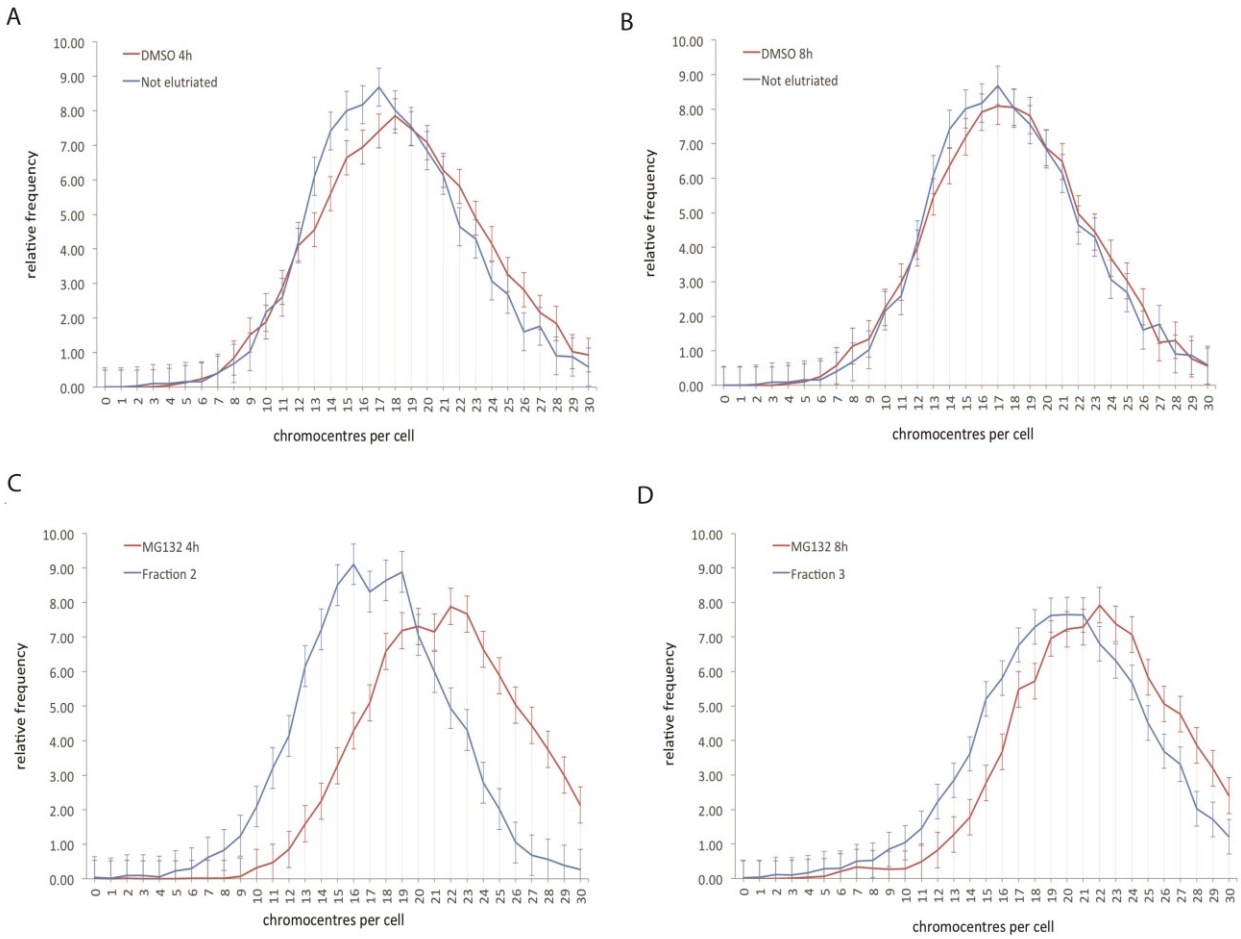


Figure 4.24: Comparison of distributions of the number of chromocentres per cell. Elutriation samples were compared with samples treated with MG132 or DMSO for 4h and 8h. Those with the most similar cell cycle profiles (Table 3) are compared. (A, B) Cells treated with vehicle only (DMSO) and not-elutriated cells, have very similar overlapping distributions of chromocentres per cell as well as cell cycle profiles (C, D). After 4h and 8h of proteasome inhibition there is an increase in chromocentres (the distribution shifts to the right) despite having similar cell cycle profiles obtained in fraction 2 and fraction 3 respectively of the elutriation.

4.3 Discussion

4.3.1 Cell cycle mediated regulation of heterochromatic repeats

Chromatin in proliferating cells is highly dynamic and each phase of the cell cycle was shown to induce changes in chromatin structure and accessibility (Figure 4.1). These changes could impact numerous chromatin associated processes such as gene expression. The effect of cell cycle has previously been extensively studied in the context of DNA replication and cell division. However, so far, only few studies investigated the effect of the cell cycle in the regulation of transcription of repetitive elements. In this chapter, pericentromeric major satellite repeats and centromeric minor satellite repeats were shown to be preferentially transcribed during G1 and G2/M phases of the cell cycle respectively, consistent with previous studies (Ferri *et al*., 2009; J. Lu & Gilbert, 2007). The expression of LINE L1 and SINE B1 retrotransposons was found to be unaffected by the cell cycle. It is worth mentioning that in this thesis, the analysis of the expression levels of these repeat transcripts, in contrast to the previous studies was performed without use of any chemical inhibitor to arrest the cell cycle, which could potentially cause stress or alter the metabolism of cells and induce unintended expression of the repeats.

The cell cycle regulated expression of pericentromeric satellite repeats prior to the DNA replication process which takes place during S phase might play a role in (i) reassembling the high order heterochromatin structure and/or (ii) regulating heterochromatin replication. Studies in fission yeast, where heterochromatin is known to be repressed by an RNA interference mechanism (see more information in the general introduction) have reported transcription of pericentromeric repeats to peak during early S phase of the cell cycle (E. S. Chen *et al*., 2008; Kloc, Zaratiegui, Nora, & Martienssen, 2008)**.** Rapid processing of these transcripts into siRNA was shown to promote H3K9me2 and recruitment of Swi6 (homologue to HP1) and hence re-establishment of heterochromatin regions after the replication process (Kloc *et al*., 2008). In mammalian cells, transcription of pericentromeric major satellite repeats was identified to gradually increase during the course of G1, reaching a peak in late G1 phase of the cell cycle (J. Lu & Gilbert, 2007). In contrast to *S. Pombe*, the synthesis of these transcripts was shown to decrease from early S phase and was found to be substantially reduced by mid S phase, which coincides with the timing of replication of

pericentromeric heterochromatin (J. Lu & Gilbert, 2007) . Consistently, in this thesis, the transcription of major satellite repeats was found to take place predominantly during the G1 phase of the cell cycle. It is important to mention that here, the methodology that was used to synchronise cells (centrifugal elutriation) did not allow isolation of a highly enriched population of cells in S phase. Therefore the limitation of this technique to synchronize the entire population of cells in S phase could explain the only slight increase of major satellite repeat expression found relative to unsynchronized cells. In both yeast and mammalian cells, transcription of pericentromeric repeats was shown to precede heterochromatin replication (J. Lu & Gilbert, 2007; Zaratiegui *et al*., 2011). The induction of pericentromeric repeat transcription in different phases could be explained by differences between the mammalian and fission yeast cell cycle and the different times of heterochromatin replication. The cell cycle of yeast consists of a very short G1 phase (Gomez & Forsburg, 2004; Knutsen *et al*., 2011), whereas in mammals the G1 is typically the longest phase of the cell cycle (Donjerkovic & Scott, 2000; Harper & Brooks, 2005). In fission yeast, heterochromatin replicates in early S phase (S. M. Kim, Dubey, & Huberman, 2003) whereas in mammals the replication takes place during late S phase of the cycle (N. Collins *et al*., 2002; Fuss & Linn, 2002; Lima-de-Faria & Jaworska, 1968; Nakayasu & Berezney, 1989; O'Keefe, Henderson, & Spector, 1992). Additionally, it is noteworthy that there are clear differences in pericentromeric heterochromatin repression and pericentromeric transcription between the two systems. Firstly, while the classic siRNA (21-25nt) mediated pathway plays an important role in heterochromatin repression in fission yeast (T. Volpe & Martienssen, 2011; T. A. Volpe *et al.,* 2002; Zofall & Grewal, 2006), there is still no or little evidence for the existence of such RNAs in mammalian cells (F. Wang *et al.*, 2006). However, some studies suggest that the binding of HP1α to pericentromeric regions is dependent on non-siRNA-sized pericentromeric transcripts (Maison *et al.,* 2011; Muchardt *et al.,* 2002). Secondly while cell cycle regulated transcription of pericentromeric repeats was disrupted in fission yeast Clr4 (homologue to SUV39H1/2) mutants (E. S. Chen *et al.,* 2008), in mammalian cells their transcription during G1 phase was shown to be independent of SUV39H1/2 activity (J. Lu & Gilbert, 2007).

On the other hand, the presence of minor satellite transcripts during the G2/M phase of the cell cycle is most likely to be important for proper kinetochore formation during mitosis.

Indeed, α-satellite transcripts were shown to be an integral component of the kinetochore structure in human cells (L. H. Wong *et al*., 2007). Moreover, in mouse cells, minor satellite transcripts were found to recruit and tether the M-phase specific chromosomal passenger complex (CPC), consisting of Aurora Kinase B (AUKB), INCENP and Survivin, to centromeric chromatin (F. L. Chan & Wong, 2012). The same study also showed that minor satellite transcripts enhance the activity of AUKB, a protein important in the microtubule-kinetochore attachment, spindle checkpoint, and cytokinesis (Fu, Bian, Jiang, & Zhang, 2007).

Further studies are required in order to elucidate whether the transcription derived from pericentromeric and centromeric regions is a regulated process or a consequence of a dynamic regulation of the heterochromatin structure mediated by the cell cycle in mammalian systems. As the highly condensed structure of heterochromatin can inhibit the transcription of repetitive elements by blocking the access of essential factors, the 'leaky' heterochromatin that could possible arise during late G1 (just prior the DNA replication) and G2/M (prior or during the cell division) phases of the cell cycle might provide a "window of opportunity" for RNAPII and the transcriptional machinery to access the underlying DNA sequences. However, it is not clear if the transcription of the major and minor satellite repeats at G1 and G2/M phases of the cell cycle is a direct regulatory process regulated by the cell cycle or an indirect process secondary to changes in heterochromatin structure. It would now be interesting to analyse which factors associate with repetitive DNA sequences to drive the transcription and further analyse the functional consequences of perturbing the transcription of these endogenous repeats on cell cycle progression.

As mentioned in the introduction, pericentromeric major satellite repeats from different chromosomes are known to physically associate to form chromocentres (Figure 1.8). Previous studies have shown that the number of chromocentres differs during the different cytogenetic stages of cell division i.e interphase, prophase, anaphase and metaphase, with a significant increase occurring from prophase and reaching a maximum number during metaphase (Guenatri *et al*., 2004). In this chapter, the number of chromocentres per cell was quantified in live cells within each phase of the cell cycle and was shown to reduce in G1 phase compared to S, G2/M phases. Similarly, Bartholdi in 1991 showed an increased number of dispersed chromocentres during S and G2/M phase relative to G1 phase, without

measuring the absolute difference (Bartholdi, 1991). Consistently another study reported an increased number of chromocentres per nucleus during S phase compared to G0 in multiple cells including fibroblast, ES cells and macrophages (Mayer *et al*., 2005). So far, studies have measured the number of chromocentres in fixed cells stained either with DAPI or anti-centromere antibody, which could potentially induce alterations in chromocentre structure and number. Indeed, examining the distribution of the number of chromocentres per cell in an unsynchronised population of paraformaldehyde fixed and living cells revealed distinct differences, with fixed cells showing an overall decrease in the number of chromocentres per cell relative to living cells (data not shown).

Why does the number of chromocentres per cell increase during S and G2/M phase of the cell cycle? The increased number of chromocentres suggests de-clustering of the chromocentres. Interestingly, a previous study (Ito *et al*., 2014) found a correlation between chromocentre de-clustering and disruption of association of heterochromatin with the nuclear lamina, an important structural change of chromatin observed during S and G2/M phases (see more in the introduction of this chapter, Figure 4.1). Hence, de-clustering of chromocentres could potentially facilitate: (i) the accessibility of the replication machinery to the underlying DNA sequence of the pericentromere during S phase of the cell cycle and (ii) the assembly of kinetochore and separation of sister chromatids during mitosis.

A summary of the cell cycle regulated transcription of heterochromatin and distribution of the number of chromocentres per cell in mammals is shown in Figure 4.25.

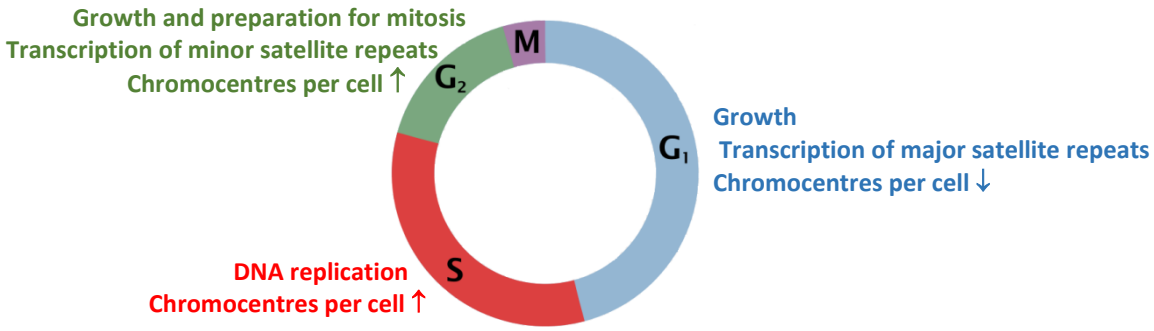


Figure 4.25: Summary of cell cycle effects on the transcription of pericentromeric and centromeric repeats and distribution of the number of chromocentres per cell. Transcription of major satellite repeats was detected in G1 phase of the cell cycle, whereas transcription of minor satellite repeats was found in G2/M phase. The number of chromocentres per cell was lower in G1 phase of the cell cycle relative to S and G2/M phases.

4.3.2 The effect of proteasome inhibition in regulation of transcription of heterochromatic repeats

Mammalian cells have evolved multiple complex mechanisms to repress the transcription of repetitive elements. It is generally accepted that heterochromatinisation (see more in the general introduction) of repetitive regions is the main physical barrier for restricting the accessibility of the transcriptional machinery to repetitive DNA sequences. Over the last decade, progress in the analysis of the chromatin structure has uncovered many epigenetic properties of heterochromatin and the mechanisms that initiate and maintain heterochromatin formation is under intense investigation. Mis-regulation of heterochromatic repeat expression has been reported to have deleterious effects on chromosome segregation and genome stability. For example ectopic overexpression of satellite repeats was shown to cause impaired mitosis, centromere amplification, lack of sister-chromatid cohesion and increased DNA double-strand breaks (Bouzinba-Segard *et al*., 2006; Zhu *et al.,* 2011). Expression of interspersed repeats LINEs and SINES and their further insertion into new genomic loci was found to lead to insertional mutagenesis, increased

DNA double-strand breaks and genomic rearrangements such as deletions, duplication and inversions (Cordaux & Batzer, 2009; deHaro *et al*., 2014). Additionally, absence of the *SUV39H* gene was found to significantly reduce the levels of H3K9me3 from pericentromeric heterochromatin, downregulate the satellite repeats expression (Lehnertz *et al.,* 2003; Muramatsu, Singh, Kimura, Tachibana, & Shinkai, 2013) and induce various chromosomal instabilities including aneuploidies, presence of so called "butterfly" chromosomes and aberrant chromosome segregation (A. H. Peters *et al*., 2001). To date multiple factors such as ubiquitin E3 ligase BRCA1 (Zhu *et al*., 2011), the histone demethylase KDM2A (Frescas *et al*., 2008), transcription factors Pax3 and Pax9 (Bulut-Karslioglu *et al*., 2012) were identified to silence satellite repeats in mammalian systems, indicating that a variety of functionally distinct cellular components might contribute to the regulation of heterochromatin. Data presented in this chapter suggests that the multisubunit enzymatic complex, the proteasome, might facilitate transcriptional silencing of pericentromeric repeats.

In this chapter, proteasome inhibition was shown using two independent techniques (RNA-FISH and q-RT-PCR) to cause dose-dependent, transcription-dependent and cell-cycle independent upregulation of major satellite repeat expression. This transcriptional upregulation clearly indicates a loss of repression in constitutive heterochromatin and suggests that the proteasome acts as a transcriptional repressor of pericentromeric repeats in mouse cells. However, at this point it is worth mentioning that the effect of proteasome inhibition could not be entirely restricted to the pericentromeric regions, as the effect might also take place at 42 intergenic major satellite repeats which were previously mapped and identified to be interspersed throughout the mouse genome (Bulut-Karslioglu *et al*., 2012). One way of confirming the origin of these transcripts would be by performing RNA sequencing after treatment of cells with proteasome inhibitor. Additionally, RNA interference-mediated depletion of each proteasomal subunit will elucidate which are required for transcriptional activation of major satellite repeats.

Notably, while proteasome inhibition showed significant effects on the major satellite repeat expression, centromeric minor satellite repeats and retrotransposon LINE L1 were largely unaffected. On the other hand, a small albeit significant transcriptional activation of SINE B1 elements was shown to occur specifically at high-dose and prolonged treatment of the cells with proteasome inhibitor. This increase of SINE B1 expression could partly explain

the downregulation of housekeeping gene transcription with proteasome inhibition, as previous studies have shown that various SINE transcripts including SINE B2 and Alu (homologue to SINE B1) function as transacting transcriptional repressors which block mRNA synthesis by directly associating with RNAPII (Allen, Von Kaenel, Goodrich, & Kugel, 2004; Espinoza, Allen, Hieb, Kugel, & Goodrich, 2004; Mariner *et al*., 2008).

Why is it that proteasome inhibition specifically upregulates pericentromeric repeat transcription rather than centromeric repeats? As mentioned in the general introduction, the chromatin structure of centromeres differs significantly from pericentromeres and euchromatin by incorporating a highly specialised variant of histone H3 (B. E. Black & Bassett, 2008; Guse *et al*., 2011; Hori *et al.,* 2013; Perpelescu & Fukagawa, 2011; Warburton *et al.,* 1997). On the other hand LINE L1 and SINE B1 elements are thought to be predominantly repressed by DNA methylation including hypermethylation of their promoter regions (see general introduction section 3.1.3). Therefore these different categories of repetitive elements appear to be repressed in distinct ways and proteasome inhibition might compromise (via an direct or indirect manner) the overall heterochromatin organisation of pericentromeric regions leaving the centromeric repeats unaffected. Indeed, in this thesis, proteasome inhibition was shown to cause displacement of HP1α, a bona-fide pericentromeric heterochromatin associated protein (see general introduction section 2.2.2), from chromocentres. In contrast, no obvious changes in the distribution and enrichment of H3K9me3, which serves as a platform for HP1 recruitment to chromatin, were identified. Interestingly, a previous study has shown global histone hyperacetylation and hypomethylation in the liver of rats following treatment with proteasome inhibitor (Oliva *et al*., 2009). Furthermore, treatment of multiple myeloma (MM) cells with proteasome inhibitor was found to downregulate HDACs expression accompanied by global histone hyperacetylation (Kikuchi *et al.,* 2010). In this thesis the levels of histone modifications associated with open chromatin structure and active transcription including H3 panacetylation, H3K36me3 and H3K4me3 were also examined and found to be unaffected at satellite repeats after proteasome inhibition. A possible explanation for the observed stable levels of histone modifications could be due to transcriptional activation of a very small proportion of the total major satellite repeats, which are represented approximately 10 000 times in each chromosome (Garagna, Zuccotti, Capanna, & Redi,

2002). Hence chromatin immunoprecipitation that was used to examine these histone modifications might not be able to detect such small variations.

Consistent with the findings presented here, various studies have attributed transcriptional activation of pericentromeric repeats to either partial or full dissociation of HP1 from pericentromeric regions without any changes in H3K9me3 levels. For example knockdown of the lysine-specific demethylase 2A (KDM2A) which specifically demethylates H3K36me2 in cell lines was shown to delocalise the HP1 from chromocentres and this was correlated with derepression of pericentromeric repeat expression but no change in H3K9me3 levels (Frescas *et al*., 2008). Another study has also reported that mutation of histone variant H3.3 at an early stage of development resulted in increased accumulation of major satellite repeat transcripts which was accompanied by displacement of HP1 from chromocentres (Santenard *et al.,* 2010). Moreover, another interesting example comes from BRCA1-deficient cells, where a significant reduction in the number of HP1 positive foci and loss of ubiquitylation of histone H2A (H2Aub) apparently induced activation of major and minor satellite repeat transcription (Zhu *et al.,* 2011). Finally HP1α/β double knockout MEF cells were shown to upregulate major satellite repeat expression, without affecting the localization of H3K9me3 (Mosch *et al.,* 2011).

As the release of HP1 from chromatin during M phase of the cell cycle was shown to be dependent on H3 serine 10 phosphorylation (H3S10ph) (Fischle *et al.*, 2005; Hirota, Lipp, Toh, & Peters, 2005), it would be interesting to assess the level of this modification mark on the pericentromeric heterochromatin in the presence and absence of proteasome inhibitor. In addition, other histone modifications, such as H2Aub, mark associated with regulation of pericentromeric repeat expression and the heterochromatic H4K20me3 mark which was found to be increased at the distal estrogen receptor-α (*ESR1)* enhancer after proteasome inhibition (G. L. Powers, Rajbhandari, Solodin, Bickford, & Alarid, 2013) and therefore might be worth analysing at satellite repeats after treatment of cells with proteasome inhibitor.

A previous study has reported upregulation of major satellite repeat expression linked with a marked decrease of the number of chromocentres per cell upon deletion of BRCA1 gene in mice (Zhu *et al.,* 2011). In contrast, in this thesis transcriptional activation of major satellite repeats upon treatment of cells with proteasome inhibitor was accompanied by an increase of the number of chromocentres per cell far beyond than that induced by skewing of the cell

cycle. Of note, Zhu and colleagues used confocal microscopic images to count the chromocentres and based on the cell morphology and increased intensity of apoptotic marker caspase 3, the authors likely included a high number of apoptotic cells in their analysis. As apoptotic cells contain less chromocentres per cell, with an average frequency 1 spot per cell (data not shown); this could potentially have a major impact on the final calculation of the chromocentre number in a population of cells. On the other hand, we measured the chromocentres in each cell within a population of non-apoptotic cells (gating was used in order to exclude dead and apoptotic cells) using Imagestream. Therefore, differences in the technique and cell population used for the analysis could thus explain the discrepancy with our results. The increased number of chromocentres per cell suggests destabilisation of chromocentre structure, which in turn could reduce the compaction of heterochromatin and increase accessibility of the transcriptional machinery to the underlying DNA sequences. It would be very interesting to use the Imagestream analysis described here to analyse BRCA1 deficient mice and gate independently on the apoptotic versus non-apoptotic populations to analyse chromocentre numbers per cell.

The potential molecular mechanisms behind the upregulation of major satellite repeat expression with proteasome inhibition will be analysed and discussed in the following chapter (chapter 5).

Lastly it is important to mention that the proteasome inhibitor PS341 is currently used to treat patients with multiple myeloma (Bross *et al*., 2004; Field-Smith *et al.,* 2006; Meenaghan *et al.,* 2010a; Moreau *et al.,* 2012; Richardson *et al.,* 2005; San Miguel *et al.,* 2008). The anti-myeloma effects of the inhibitor were reported to mainly include inhibition of the nuclear factor kappa B (NFkB) activation though preventing the degradation of its inhibitor IkB, disruption of the cell cycle and induction of apoptosis (Hideshima *et al.,* 2002; Hutter et al., 2012; Ling *et al.,* 2002; Mitsiades *et al.,* 2002; Pham, Tamayo, Yoshimura, Lo, & Ford, 2003). Another anti-myeloma effect of PS341 could be upregulation of pericentromeric repeat transcription. This accumulation of satellite repeat transcripts is likely to cause genome instability, making a cell more prone to apoptosis. Furthermore as the use of the drug has been reported to have significant side effects including gastrointestinal disturbances, peripheral neuropathy and thrombocytopenia (Field-Smith *et al.*, 2006), it would be interesting to assess the levels of the pericentromeric repeat

transcripts in patients and correlate any side effects that might be due to the disruption of pericentromeric heterochromatin.

4.3.3 Possible role of RNAPI and/or RNAPIII in transcription of major satellite repeats

Transcription in eukaryotic cells is performed by three RNA polymerases, RNAPI, RNAPII and RNAPIII. RNAPI is known to transcribe ribosomal RNA genes (with an exception of 5S rRNA). RNAPII transcribes protein-coding genes (mRNA genes) and many noncoding RNA (ncRNA) such as microRNA (miRNA). RNAPIII transcribes tRNAs genes, 5S RNA, various small ncRNAs including U6 small nuclear RNA (U6 snRNA), 7SK RNA and H1 RNA (Dieci, Fiorino, Castelnuovo, Teichmann, & Pagano, 2007). There is evidence suggesting that different RNA polymerases can often work together to coordinate their target gene expression (Raha *et al*., 2010).

Considering that pericentromeric satellite repeats (i) do not harbour detectable promoter elements and (ii) lack sequence conservation (Saksouk *et al.,* 2015), it was difficult to predict which RNA polymerase mediated their transcription. Studies in yeast and mammalian cells have shown that transcription of pericentromeric repeats is driven by RNAPII (Djupedal *et al*., 2005; Kato *et al.,* 2005; J. Lu & Gilbert, 2007; Oya *et al.*, 2013). However, preliminary results in this thesis suggest a possible role of RNAPI and/or III in the transcription of major satellite repeats. It is worth mentioning that Lu and colleagues treated the cells with RNAPII inhibitor (DRB) for a short time course (1h) and observed a significant reduction of the levels of satellite repeat transcripts. Similarly, in this thesis, treatment of cells with RNAPII inhibitor for a short time course (<2h) strongly reduced the levels of major satellite repeat transcripts; only the prolonged treatment (>2h) caused accumulation of these transcripts in the cells.

Further studies are required in order to elucidate the possible function of RNAPI and RNAPIII in pericentromeric repeat transcription. This could be achieved by examining the binding of RNAPI and/or III on pericentromeric repeats in the presence and absence of RNAPII.

Furthermore, it would be interesting to assess the effect of the combinatory inhibition of RNAPI with RNAPII and RNAPIII with RNAPII on the levels of pericentromeric repeat transcription.

In summary the results in this chapter have further focused on the role of the proteasome in the regulation of pericentromeric repeat expression using proteasome inhibition which resulted in:

- Cell-cycle independent and transcription dependent upregulation of pericentromeric satellite repeat expression
- No change in the H3K9me3, H3K4me3, H3K36me3 and H3ac levels at major satellite repeats
- Delocalisation of HP1α from chromocentres
- Increased number of chromocentres per cell that would be unlikely to be simply accounted for by cell cycle skewing towards G2/M.

These findings suggested that proteasome activity might be required for maintaining the stability of heterochromatin clusters within cells and the pericentromeric localisation of a key component of heterochromatin, HP1α, as well as silencing of the pericentromeric repeats. Based on the sequence of events following proteasome inhibition it appears that HP1α delocalises first followed by disaggregation of centromeric clusters and upregulation of transcription of pericentromeric repeats. Interestingly, there were no changes in the histone modifications examined (see discussion).

4.4 Contributions

Theona Natisvili performed all the experiments. Ms Giulia Emmanueli provided help for RNA-FISH experiment and acquiring microscope images. Ms Raquel Silva provided help with the ImageStream experiment.

CHAPTER 5: Investigating the molecular mechanism of the major satellite repeat transcriptional upregulation upon proteasome inhibition

5.1 Introduction

In the previous chapter it was shown that proteasome inhibition upregulates the transcription of major satellite repeats. This is accompanied by release of HP1α from pericentromeric heterochromatin and an increase in the number of chromocentres per cell. As the proteasome participates in a large number of cellular pathways and controls the steady-state level of many proteins it is difficult to distinguish between direct involvement of the proteasome on the transcription of the pericentromeric repeat and indirect effects mediated by a protein whose level is controlled by the proteasome activity. Additionally, accumulation of misfolded proteins due to proteasome inhibition is known to trigger cell stress responses (Boyault *et al*., 2007; Bush, Goldberg, & Nigam, 1997; Goldberg, 2003; Johnston, Ward, & Kopito, 1998; Kawazoe, Nakai, Tanabe, & Nagata, 1998; Mathew, Mathur, & Morimoto, 1998; Obeng *et al.,* 2006; Rao & Bredesen, 2004) therefore a component from the cell stress pathway could also be responsible for the de-repression of the major satellite repeat. Therefore the main goal of this chapter was to investigate the molecular mechanism for transcriptional upregulation upon proteasome inhibition. More specifically the aims of this chapter were:

- To analyse the possible proteasome recruitment to the repetitive elements and the effect upon proteasome inhibition
- To examine the effect of the proteasome inhibition on RNAPII recruitment to the repeats
- To investigate the activation of the cell stress pathway and the role of HSF1 in the transcriptional upregulation of major satellite repeats upon proteasome inhibition.

5.2 Results

5.2.1 Investigation of proteasome binding in heterochromatic repeats

The first step to assess whether the proteasome is directly involved in the repression of major satellite repeats was to investigate the distribution of the proteasome in the nucleus and more specifically the possible binding of the proteasome to the pericentromeric regions.

Numerous studies have shown the presence of the proteasome in the nucleus of eukaryotic cells (Mengual *et al*., 1996; A. Palmer, Mason, Paramio, Knecht, & Rivett, 1994; J. M. Peters, Franke, & Kleinschmidt, 1994; Rivett, Palmer, & Knecht, 1992; Wojcik, Paweletz, & Schroeter, 1995) and its recruitment to various regions of the chromatin including centromeres (Kitagawa *et al.,* 2014a), yeast telomeres (Geng & Tansey, 2012) and sites of cryptic transcriptional initiation (Szutorisz *et al.,* 2006).

To confirm the nuclear localisation of the proteasome in NIH3T3 cell lines and to investigate whether the proteasome is co-localized with heterochromatin antibodies against the β6 subunit of the 20S proteasomal particle were employed. As expected the immunofluorescence analysis revealed a diffuse presence of the proteasome throughout the cells, with the signal coming from both, the cytoplasm and the nucleus. However, the 20S proteasomal particle was found to be relatively excluded from heterochromatin domains represented by DAPI dense stained region (Figure 5.1).

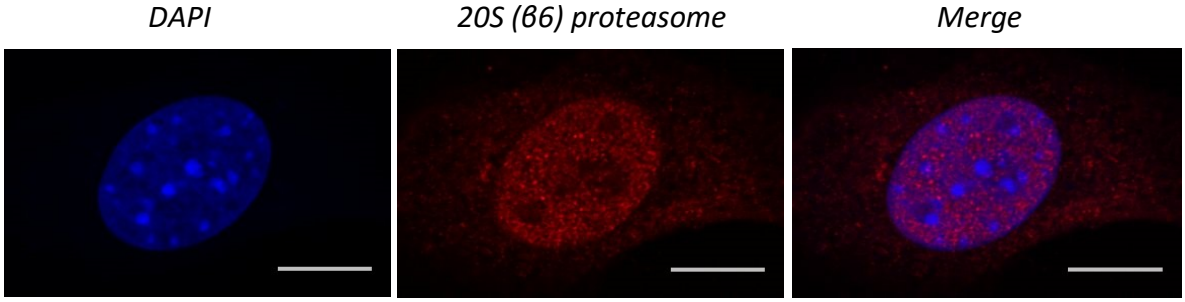


Figure 5.1: Proteasome distribution within the cell. NIH3T3 cells were immunolabeled with 20S Proteasomal particle antibody (red) and stained with DAPI (blue). Scale bar 10µm.

To further validate these results, ChIP was performed with the same antibody used for the immunofluorescence experiment and immunoprecipitated material was quantified using qPCR with primers against major, minor, LINEL1 and SINEB1 heterochromatin regions. Additionally primers against *GAPDH* and *MOG* genes were used as controls, representing transcriptionally active and inactive regions respectively.

As illustrated in Figure 5.2, the analysis of immunoprecipitated material by qPCR showed binding of the proteasome in all the examined regions to a similar extent, with the exception of minor satellite repeats, where significantly lower levels of enrichment were detected.

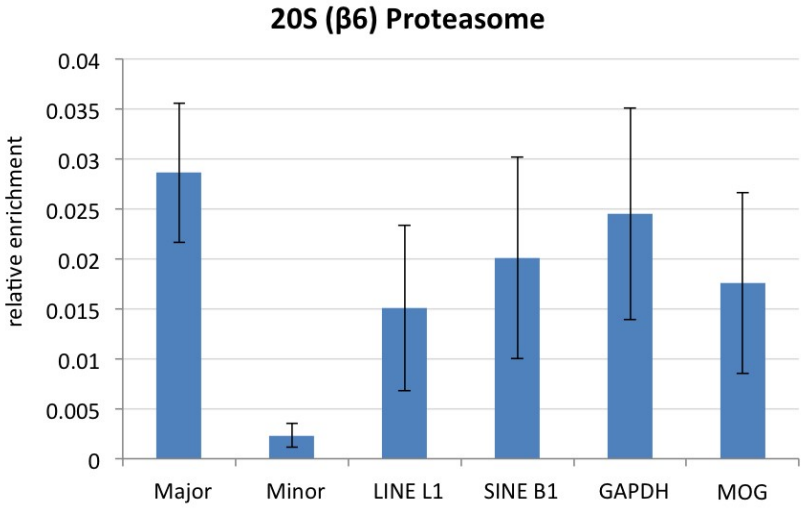


Figure 5.2: Proteasome subunit β6 is recruited to heterochromatic regions, active gene (GAPDH) and inactive gene (MOG) in NIH3T3 cells measured by ChIP-qPCR. Enrichment level is presented relative to input. Error bars SEM, n=3 biological replicates.

Chromatin immunoprecipitation revealed high levels of the 20S proteasome on the major satellite repeats sequences whereas the immunofluorescence showed exclusion from the DAPI-dense regions where this sequence is known to reside. This difference might be explained by how the techniques differ. For example in the case of immunofluorescence the proteasome appeared excluded from the DAPI –dense regions which could be due to the physical inaccessibility of the antibody to the proteasome epitope when it is packaged into highly compacted regions such as heterochromatin whereas chromatin immunoprecipitation is performed on sonicated chromatin.

5.2.2 Small overall increase of 20S proteasome binding on various chromatin regions upon proteasome inhibition

Transcriptional activation of the major satellite repeats upon proteasome inhibition (shown in the previous chapter) and binding of the proteasome to the major satellite repeats in the absence of the proteasome inhibition raised the question as to what happens to the proteasome binding upon proteasome inhibition? To address this question, NIH3T3 cells were treated with DMSO or proteasome inhibitor MG132 at a final concentration of 20μM for 4h followed by ChIP. In a similar approach to that explained in the previous section, immunoprecipitated material was analysed by qPCR using primers against major, minor, LINE L1 and SINE B1 heterochromatin regions as well as *GAPDH* and *MOG*.

According to the qPCR analysis, in the absence of proteasome inhibition, uniform binding of the β6 subunit of the 20S proteasome was observed on major satellite repeats, LINE L1, SINE B1 as well as active *GAPDH* and inactive *MOG* genes. A significantly smaller enrichment was also observed for the minor satellite repeats (Figure 5.3), consistent with the previous ChIP experiment (Figure 5.2). When NIH3T3 cells were treated with MG132 a slight increase of proteasome binding was identified for all the examined regions (Figure 5.3). This is in agreement with a previous study (Szutorisz *et al*., 2006) where proteasome inhibition was revealed to increase the proteasome binding at the intergenic regions in ES cells; this increase varied amongst the different proteasomal subunits with β6 20S and RPN12 19S proteasome showing the largest increase of binding while the α4 and β4 subunits were not affected by proteasome inhibition (Szutorisz *et al.,* 2006).

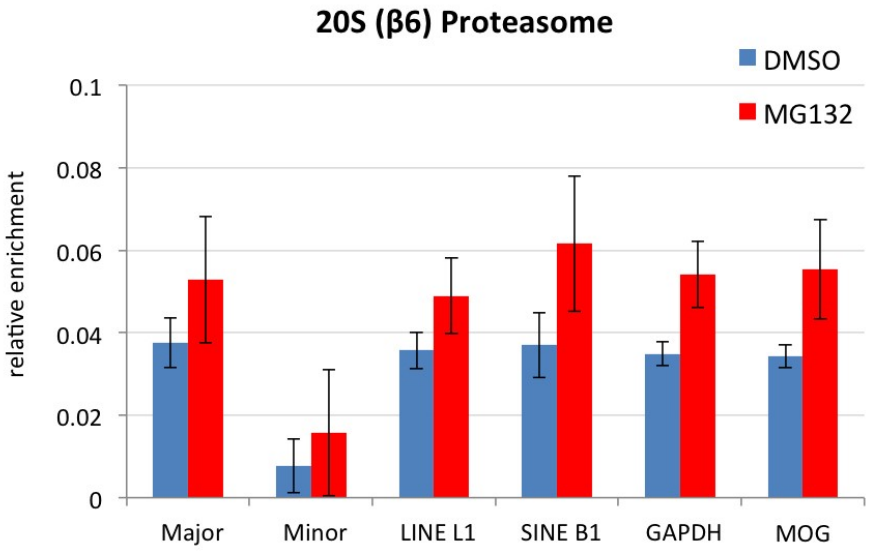


Figure 5.3: Proteasome inhibition induces slight overall increase of proteasome binding on heterochromatin regions, active gene (GAPDH) and inactive gene (MOG). NIH3T3 cells were treated with DMSO or MG132 at a final concertation of 20µM for 4h followed by ChIP-qPCR. Enrichment level is presented relative to input. Error bars SEM, n=3 biological replicates.

5.2.3 The effect of proteasome inhibition on distribution and binding of RNAPII in heterochromatin regions

Despite the formation of highly condensed chromatin at repetitive elements, RNAPII might still access the underlying DNA sequences causing transcriptional activation of the repeats. However, it has been suggested that it is important that the level of transcription of endogenous repetitive sequences remains low, as high transcription derived from repetitive elements might lead to various diseases including cancer (Criscione, Zhang, Thompson, Sedivy, & Neretti, 2014; Eymery, Horard, *et al*., 2009; Ting *et al.,* 2011). Given that the proteasome had been proposed to degrade RNAPII in the case of transcription-coupled repair (K. B. Lee *et al.,* 2002; Somesh *et al.*, 2005; Wilson *et al.,* 2013) and to prevent cryptic transcription (Szutorisz *et al.,* 2006), we hypothesised therefore that the proteasome might also contribute to the repression of the transcription of repetitive elements by actively degrading the RNAPII bound to the repeats. Hence inhibition of proteasome activity might be expected to increase the transcription of repeats, as seen in the previous chapter (chapter 3).

In previous sections, the proteasome was shown by ChIP to bind to the major satellite repeats which is abundant in pericentromeric heterochromatin. One possible hypothesis for the recruitment of the proteasome to chromatin is through recognition of its ubiquitinated substrates. A number of chromatin associated substrates can become polyubiquitinated including histones, RNAPII, transcriptional factors and co-factors and ultimately become a target for proteasome dependent degradation (Beaudenon, Huacani, Wang, McDonnell, & Huibregtse, 1999; C. Chen *et al.*, 2005; Fuchs & Ronai, 1999; Karakasili *et al.,* 2014; Z. Liu, Oughtred, & Wing, 2005; Mitsui & Sharp, 1999; Ouni, Flick, & Kaiser, 2011; R. K. Singh, Kabbaj, Paik, & Gunjan, 2009; Vinas-Castells *et al.*, 2010; S. P. Wang *et al.,* 2009; Zenke-Kawasaki *et al.*, 2007). One example is polyubiquitination and degradation of stalled RNAPII during transcription coupled DNA repair by the ubiquitin-proteasome system (Anindya *et al.*, 2007; Ghosh-Roy, Das, Chowdhury, Smerdon, & Chaudhuri, 2013; K. B. Lee *et al.,* 2002; Somesh *et al.,* 2005; Somesh *et al.,* 2007; Wilson *et al.,* 2013). A similar mechanism, of active removal of the RNAPII by the proteasome, could potentially take place in heterochromatin regions thereby reducing the chances for transcription to occur. In order to investigate this hypothesis, NIH3T3 cells were treated with DMSO or proteasome inhibitor MG132 at a final

concentration of 20μM for 4h and the levels of S5P-RNAPII and S2P-RNAPII were measured by ChIP-qPCR in various heterochromatic regions including major satellite, minor satellite, LINE L1 and SINE B1. Additionally primers against the promoter and gene body of the *GAPDH* gene were used as positive controls for S5P-RNAPII and S2P-RNAPII respectively and primers for *MOG* gene were used as a negative control for both forms of RNAPII.

As expected, S5P-RNAPII and S2P-RNAPII were found to be enriched at the promoter and the gene body of *GAPDH* respectively with a small decrease upon proteasome inhibition (Figure 5.4) which is consistent with the downregulation of GAPDH expression albeit not statistically significant (data not shown). In contrast to *GAPDH*, the levels of both forms of RNAPII were lower at heterochromatic regions and the inactive *MOG* gene and virtually unaffected upon treatment of cells with proteasome inhibitor (Figure 5.4).

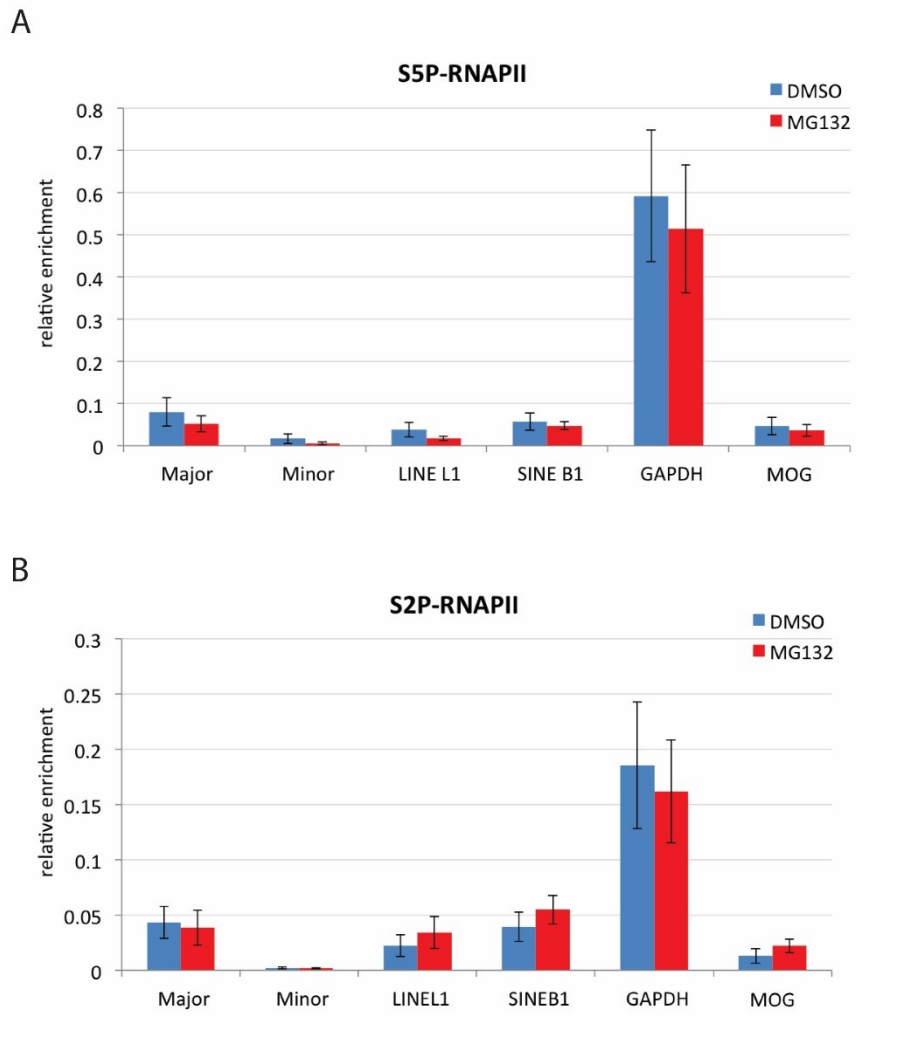
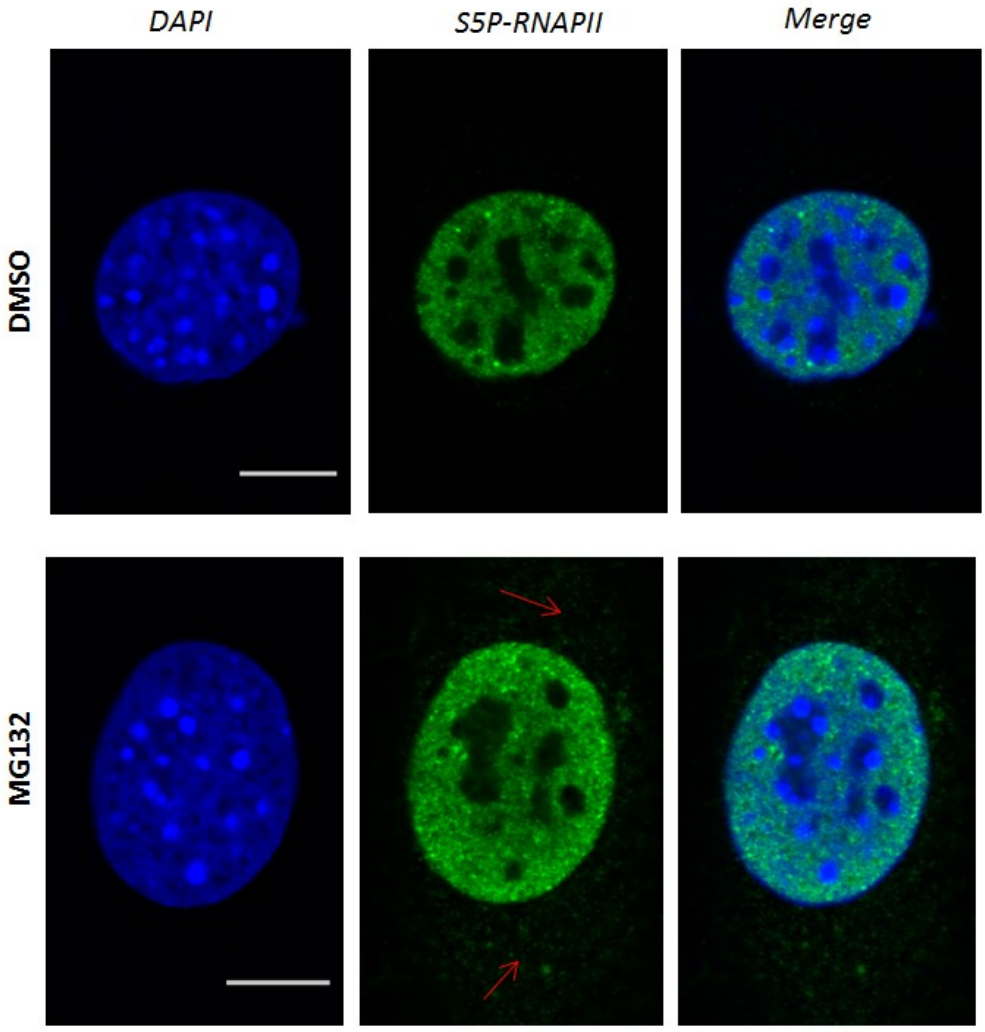


Figure 5.4: S2P-RNAPII and S5P-RNAPII binding on the heterochromatic repeats were unaffected by proteasome inhibition. NIH3T3 cells were treated with DMSO or MG132 at a final concentration of 20µM for 4h followed by ChIP-qPCR. Enrichment level is presented relative to input after background (no antibody) subtraction. Error bars SEM, n=4-7.

To further validate these results, NIH3T3 cells were treated with DMSO or MG132 at a final concentration of 20µM for 4h followed by IF using DAPI and antibodies against S5P-RNAPII and S2P-RNAPII. The analysis of IF images showed that firstly the signals from S5P-RNAPII and S2P-RNAPII antibodies were largely excluded from heterochromatin domains identified by DAPI dense stained regions in both treated and untreated cells (Figure 5.5A, 5.6A). Secondly, while in the untreated cells the signal from S5P-RNAPII antibody was confined to the nucleus, the treatment of cells with proteasome inhibitor caused appearance of the

signal within the cytoplasm (Figure 5.5A). Lastly, the proteasome inhibition was found to increase the overall intensity for both phosphorylated forms of RNAPII within the nucleus (Figure 5.5B, 5.6B). This result is consistent with the western blot presented previously (Chapter 3, Figure 3.7) and a previous study (Kinyamu & Archer, 2007).

A



B

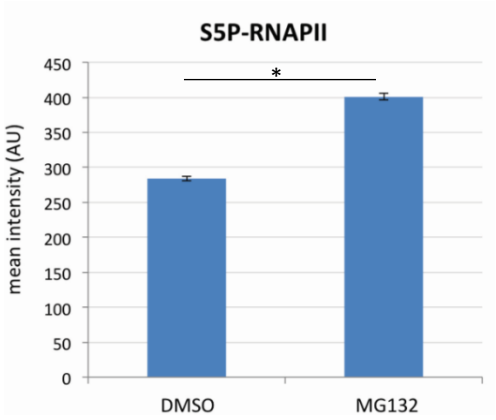
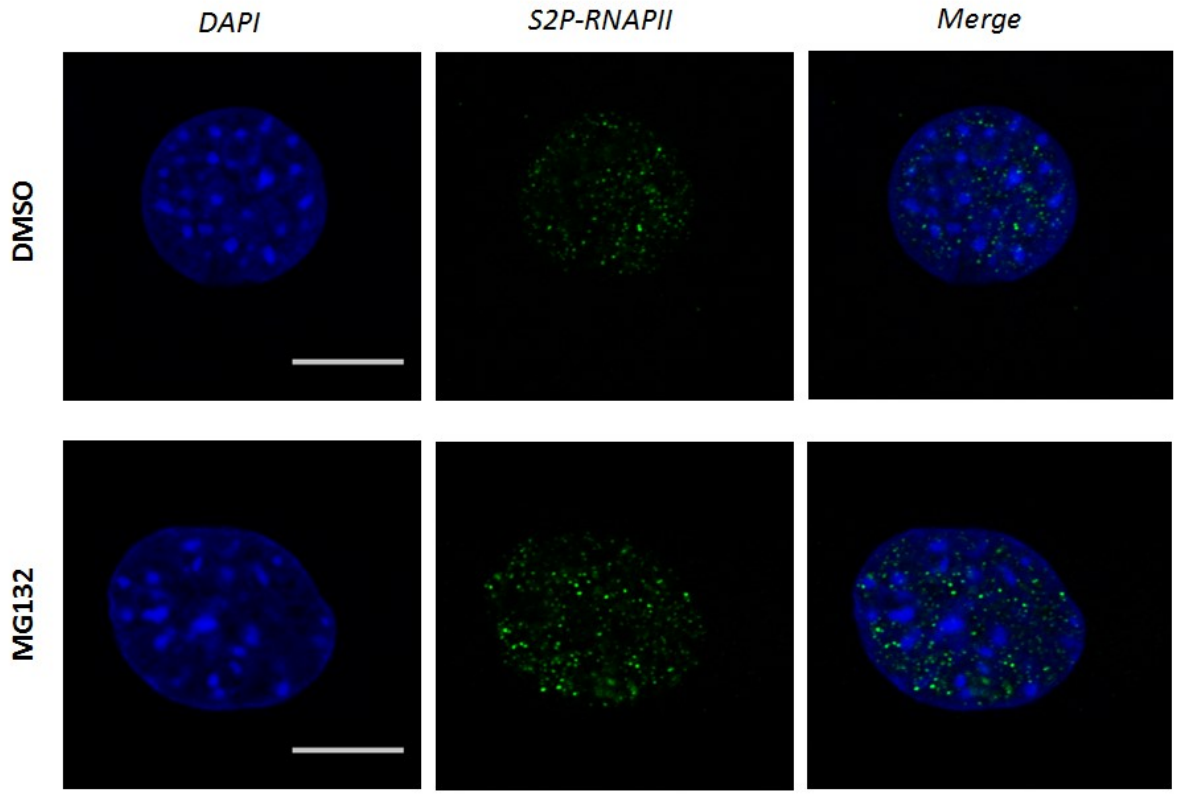


Figure 5.5: Immunofluorescence analysis for S5P-RNAPII upon proteasome inhibition. NIH3T3 cells were treated with MG132 at a final concentration of 20µM for 4h following by IF using DAPI and antibody against S5P-RNAPII. (A) Representative IF images. Scale bar 10µM. Arrows represent the signal coming from the cytoplasm. (B) Analysis of the mean nuclear intensity. Error bars SEM n = 332 and 508 cells for DMSO and MG132 respectively. AU represents Arbitrary Units. *$p<0.05$ (Student's 't' test)

A



B

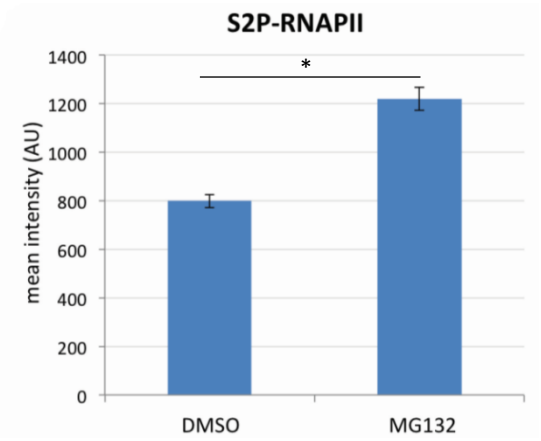


Figure 5.6: Immunofluorescence analysis for S2P-RNAPII upon proteasome inhibition. NIH3T3 cells were treated with MG132 at a final concentration of 20µM for 4h following by IF using DAPI and antibody against S2P-RNAPII. (A) Representative IF images. Scale bar 10µM (B) Analysis of the mean nuclear intensity. Error bars SEM n = 88 and 72 cells for DMSO and MG132 respectively. AU represents Arbitrary Units. *p<0.05 (Student's 't' test).

5.2.4 Proteasome inhibition induces activation of the cell stress response pathway in NIH3T3 cells

Several studies have shown that proteasome inhibition induces cell stress and activates the heat shock pathway (Bush *et al*., 1997; Kawazoe *et al.,* 1998; Stangl *et al.,* 2002; Zaarur, Gabai, Porco, Calderwood, & Sherman, 2006). Considering that various cellular stresses were also shown in several human studies to activate the transcription of pericentromeric satellite repeats (Eymery, Horard, *et al.,* 2009; Jolly *et al.,* 1997; Rizzi *et al.,* 2004; Valgardsdottir *et al.,* 2008), it was hypothesized here that proteasome inhibition could potentially upregulate the transcription of murine major satellite repeats though activating the cell stress pathway. In order to investigate this hypothesis, firstly it was essential to confirm the activation of the cell stress pathway with the concentration of the inhibitor and the duration of treatment used throughout this thesis in NIH3T3 cells. Therefore, NIH3T3 cells were treated with proteasome inhibitor MG132 at a final concentration of 20µM for 2h, 4h and 8h. Part of the sample was lysed and used to assess the activation of HSF1 by western blot; the remaining was used for RNA extraction followed by cDNA synthesis and qPCR with primers against mRNA transcript of heat shock protein *HSP70* gene. Additionally NIH3T3 cells were treated with DMSO, 5µM, 10µM and 20µM of MG132 for 8h followed by RNA extraction, cDNA synthesis and qPCR with primers against mRNA transcripts of major heat shock proteins encoding genes *HSP70* and *HSP90*.

As illustrated in Figure 5.7A, activation of HSF1 indicated by an increase of the molecular size which is likely to occur due to the phosphorylation of HSF1, as previously shown (Metzler *et al*., 2003; Sarge, Murphy, & Morimoto, 1993) was already apparent from 2h of MG132 treatment and maintained at 4h and 8h of treatments. As HSF1 is a transcription factor required for transcriptional activation of heat shock protein genes (Kroeger, Sarge, & Morimoto, 1993; Morimoto, 1998; Sarge *et al*., 1993; Trinklein, Chen, Kingston, & Myers, 2004), a dramatic time dependent increase of the expression of *HSP70* was observed upon treatment of cells with proteasome inhibitor compared to the untreated control (DMSO) (Figure 5.7B). In addition, a highly significant dose-dependent upregulation of *HSP70* and *HSP90* expression were also detected upon treatment of cells with different concentrations of MG132 relative to untreated (Figure 5.7C).

These results confirm the activation of the cell stress pathway (also known as heat shock pathway) upon proteasome inhibition in NIH3T3 cells.

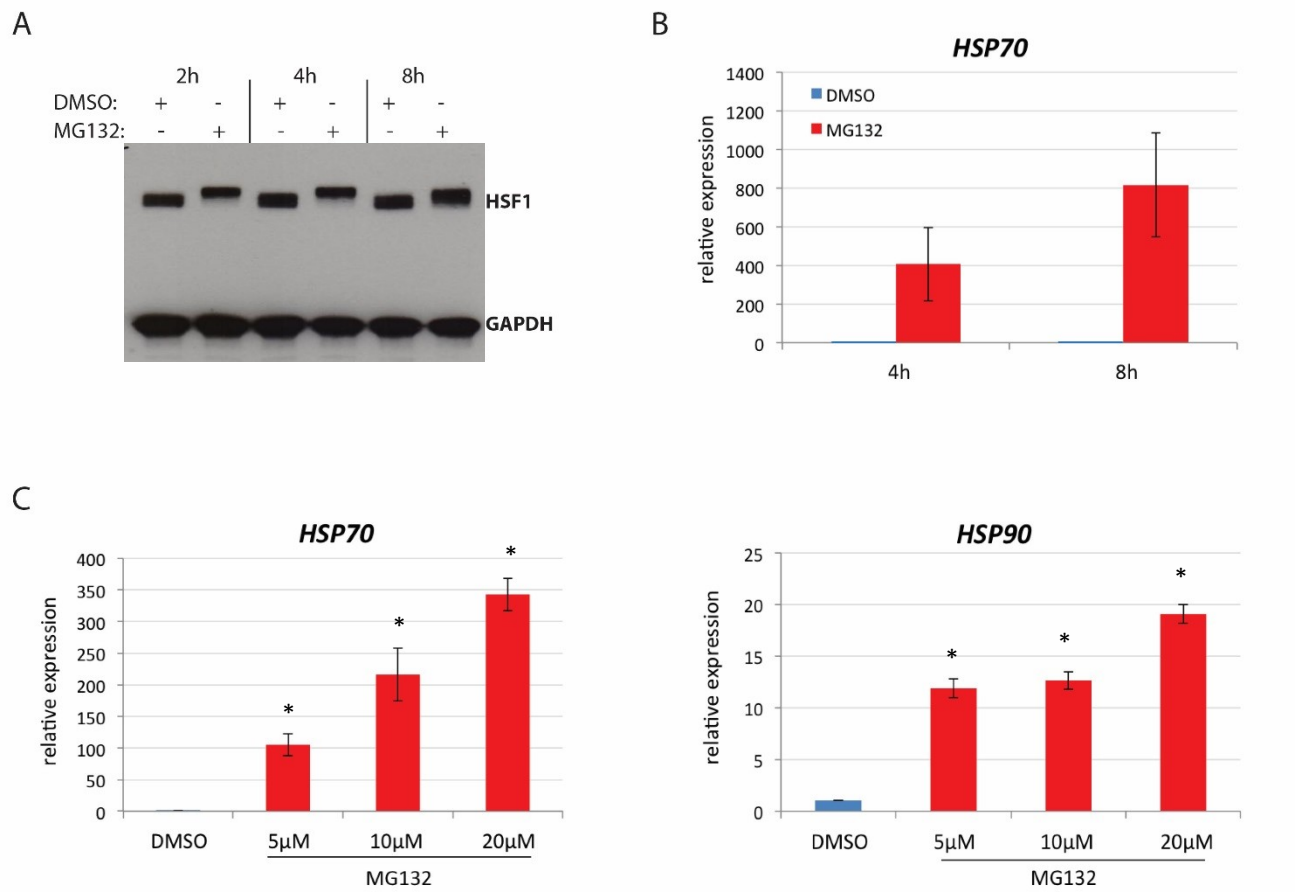


Figure 5.7: Activation of the cell stress response pathway upon treatment of cells with proteasome inhibitor MG132. NIH3T3 cells were treated with 20µM MG132 for 2h, 4h and 8h (A and B) as well as 5µM, 10µM and 20µM MG132 for 8h (C). (A) Activation of HSF1 factor upon proteasome inhibition (see text): Total cell lysate was probed with antibody against HSF1 (~75kDa) and GAPDH (~38kDA) that was serving as a loading control. (B) Time-dependent upregulation of *HSP70* expression upon proteasome inhibition: Upon 4h and 8h of DMSO or 20µM MG132 treatment, RNA was extracted followed by q-RT-PCR with primers specific to HSP70 mRNA transcript. The relative expression was normalised against spike and fold change shown relative to DMSO. Error bars SEM, n=3. (C) Dose-dependent upregulation of *HSP70* and *HSP90* expression: Upon 5µM, 10µM and 20µM MG132 for 8h, RNA was extracted followed by q-RT-PCR with primer against *HSP70* and *HSP90* mRNA transcript. The relative expression was normalised against spike and fold change shown relative to DMSO. Error bars SEM, n=6. *p<0.05 (Student's 't' test).

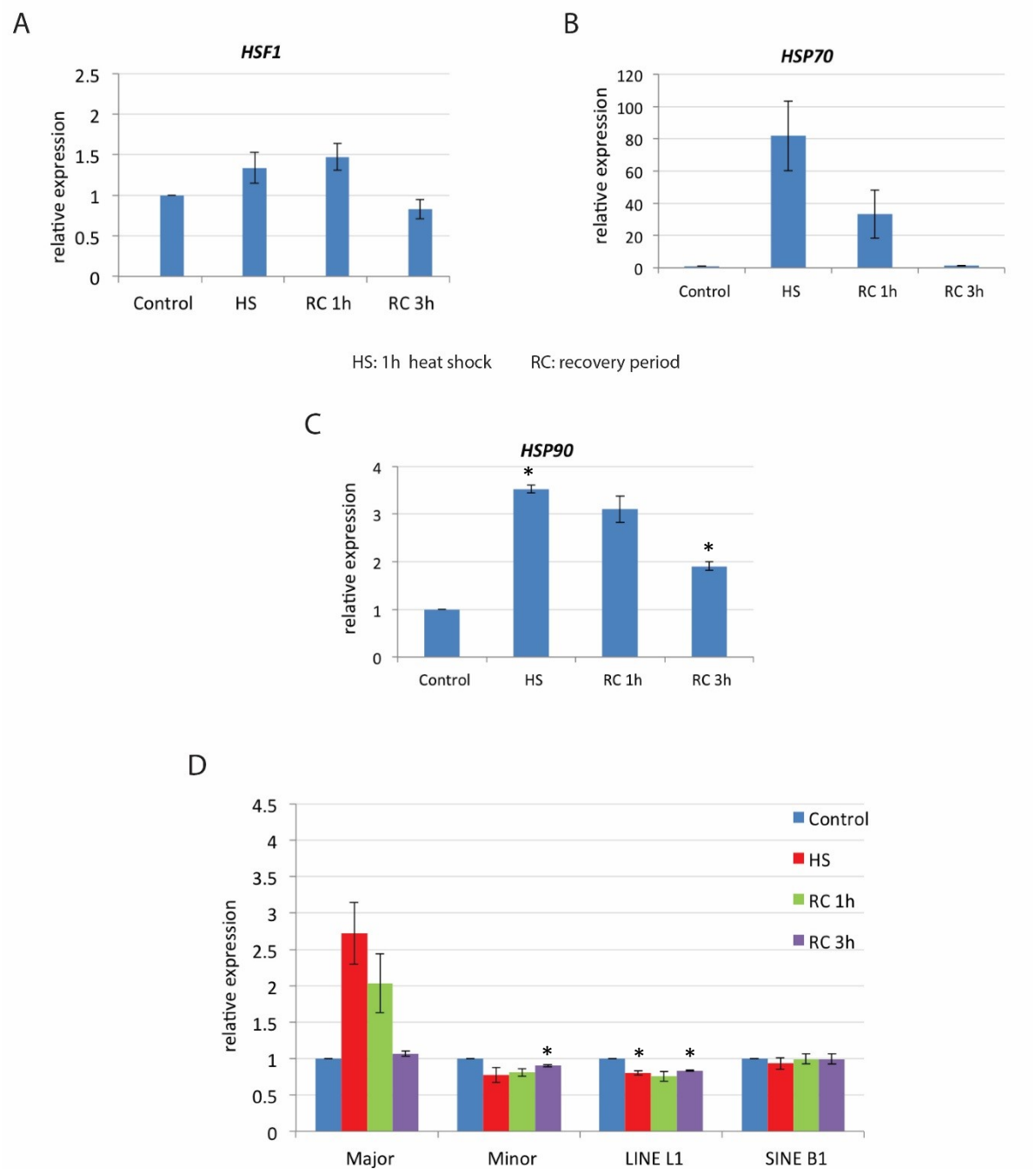
5.2.5 Heat shock activates the transcription of major satellite repeats in NIH3T3 cells

It was shown here that proteasome inhibition upregulated the expression of major satellite repeats (chapter 4) and could also activate the heat shock pathway (see above). Previous experiments by others had predominantly focused on the effect of the heat shock in upregulating the specific subset of pericentromeric satellite repeats in human cells. Here we examined, for the first time, whether heat shock itself could upregulate a range of repetitive elements in mice including the predominant pericentromeric major satellite repeats.

Here NIH3T3 cells were heat shocked for 1h at 43^{O}C or maintained at 37^{O}C (control). The heat shocked cells were then returned to 37^{O}C for 1h and 3h (recovery). From each time point (Control, Heat shocked, Recovery 1h, Recovery 3h) RNA was extracted followed by cDNA synthesis and qPCR with primers against heterochromatic regions of pericentromeric major satellite, centromeric minor satellite, retrotransposons LINE L1 and SINE B1. Furthermore the levels of HSF1, HSP70 and HSP90 mRNA transcripts were also examined by specific exon-exon junction primers.

The results of the q-PCR analysis are illustrated in Figure 5.8. The expression of HSF1 was slightly increased (~1.3 fold) 1h immediately after the heat shock and was maintained at similar levels 1h after recovery before dropping to the initial levels at 3h of recovery (Figure 5.8A). Furthermore, as expected, the expression of *HSP70* was dramatically increased by ~80 fold upon heat shock compared to the control and was subsequent reduced to ~30 fold after 1h of recovery and completely abolished by 3h of recovery (Figure 5.8B). Similarly to HSP70, HSP90 mRNA was significantly upregulated upon heat shock and sustained at similar levels 1h after recovery followed by some reduction at 3h of recovery. In contrast to *HSP70*, the levels of *HSP90* transcripts were constantly maintained throughout the heat shock and the recovery time points were significantly higher relative to the control (Figure 5.8C). Interestingly, the heat shocked NIH3T3 cells specifically expressed the major satellite repeats ~ 2.7 fold higher compared to the control (Figure 5.8D) which is in agreement with previous studies of pericentromeric satellite repeat expression in human cells (Eymery, Horard, *et al.,* 2009; Rizzi *et al.,* 2004; Valgardsdottir *et al.,* 2008). Furthermore, the levels of major satellite transcripts were kept on average ~2 fold higher at 1h of recovery relatively to control and were reduced to the initial level only after 3h of recovery (Figure 5.8D). In contrast to the major satellite, the minor satellite and LINE L1 transcripts were reduced by

~10-20% during the heat shock and throughout the recovery periods compared to the control whereas SINE B1 remained unaffected (Figure 5.8D). In conclusion, of the repeats examined the upregulation in expression levels due heat shock was restricted to the major satellite repeat sequences.



See next page for figure legend

Figure 5.8: Effect of the heat shock on the expression of (A) *HSF1*, (B) *HSP70*, (C) *HSP90* and (D) heterochromatic repeats including major, minor, LINE L1 and SINE B1. NIH3T3 cells were heat shocked for 1h at 43^{o}C followed by 1h and 3h of recovery at 37^{o}C. For each time point RNA was extracted and q-RT-PCR was performed. The relative expression was normalised against spike and is shown as fold change relative DMSO. HS indicates the Heat shock and RC represents the recovery. Error bars SEM, n=3 biological replicates. *p<0.05 (Student's 't' test).

5.2.6 Suppression of the cell stress response abolishes the transcriptional activation of major satellite repeats upon proteasome inhibition

Considering that the cell stress and more specifically activated HSF1 was shown to cause transcription of pericentromeric Satellite III repeats in the human cells (Jolly *et al*., 2004a; Valgardsdottir *et al.,* 2008), investigation was needed to assess the potential role of the HSF1 transcription factor in transcriptional activation of the major satellite repeats upon proteasome inhibition in the mouse genome. Clearly, one way of investigating that would be to inhibit simultaneously HSF and the proteasome and observe its effect on transcription levels of major satellite repeats. So NIH3T3 cells were treated with either DMSO (vehicle) or proteasome inhibitor MG132 and HSF1 inhibitor Quercetin. Quercetin (3,3',4',5,7-pentahydroxyflavone) is a flavonoid that suppresses the cell stress response in the presence of various stressors by affecting several steps of the HSF1 activation pathway, including hyperphosporylation, DNA binding and transcriptional activity (O. Gonzalez *et al.,* 2009; M. V. Powers & Workman, 2007; Zanini *et al.,* 2007).

Initially Quercetin (100µM) was added to the culture medium of NIH3T3 cells and 4 hours later MG132 (20µM) was added. This was done in order to give some time for the HSF1 inhibition to take place before the proteasome inhibition. After the addition of MG132, cells were treated for an additional 4 hours in the presence of both drugs. RNA was extracted followed by cDNA synthesis and transcript levels of the repeats were analysed by qPCR using the same primers for the DNA repeat sequences as in the previous experiments. Additionally, primers against mRNA transcripts of *HSF1* and *HSP70* were used as a control for the effect of the treatments.

The effects of both proteasome and HSF1 inhibition are shown in Figure 5.9A and 5.9B. The proteasome inhibition upregulated the expression of *HSF1* by ~2.3 fold whereas Quercetin and concomitant treatment of cells with Quercetin and MG132 reduced the *HSF1* transcript levels by 40% and 50% respectively relative to DMSO. Furthermore, the HSP70 mRNA transcript levels were found to be dramatically increased by ~530 fold with MG132 treatment while simultaneous treatment of cells with Quercetin and MG132 showed only ~44 fold increase compared to DMSO, resulting in 92% reduction in the expression of HSP70 relative to MG132 treatment (Figure 5.9B).

Importantly, while proteasome inhibition increased the major satellite transcripts level by ~3.6 fold, concomitant treatment of cells with MG132 and Quercetin caused only ~1.5 fold increase relative to DMSO, which represents a similar level obtained by Quercetin treatment alone (Figure 5.9C). This result suggests that HSF1 is required for the transcriptional activation of major satellite repeats upon proteasome inhibition.

Additionally a slight reduction of the level of minor satellite transcript was detected upon treatment of cells with Quercetin with further decrease with the combination of both proteasome and HSF1 inhibition. Lastly only minor changes were observed on the expression of LINE L1 and SINE B1 with all the treatments (Figure 5.9C). The results indicate that proteasome inhibition requires activation of HSF1 in order to specifically upregulate major satellite repeats expression.

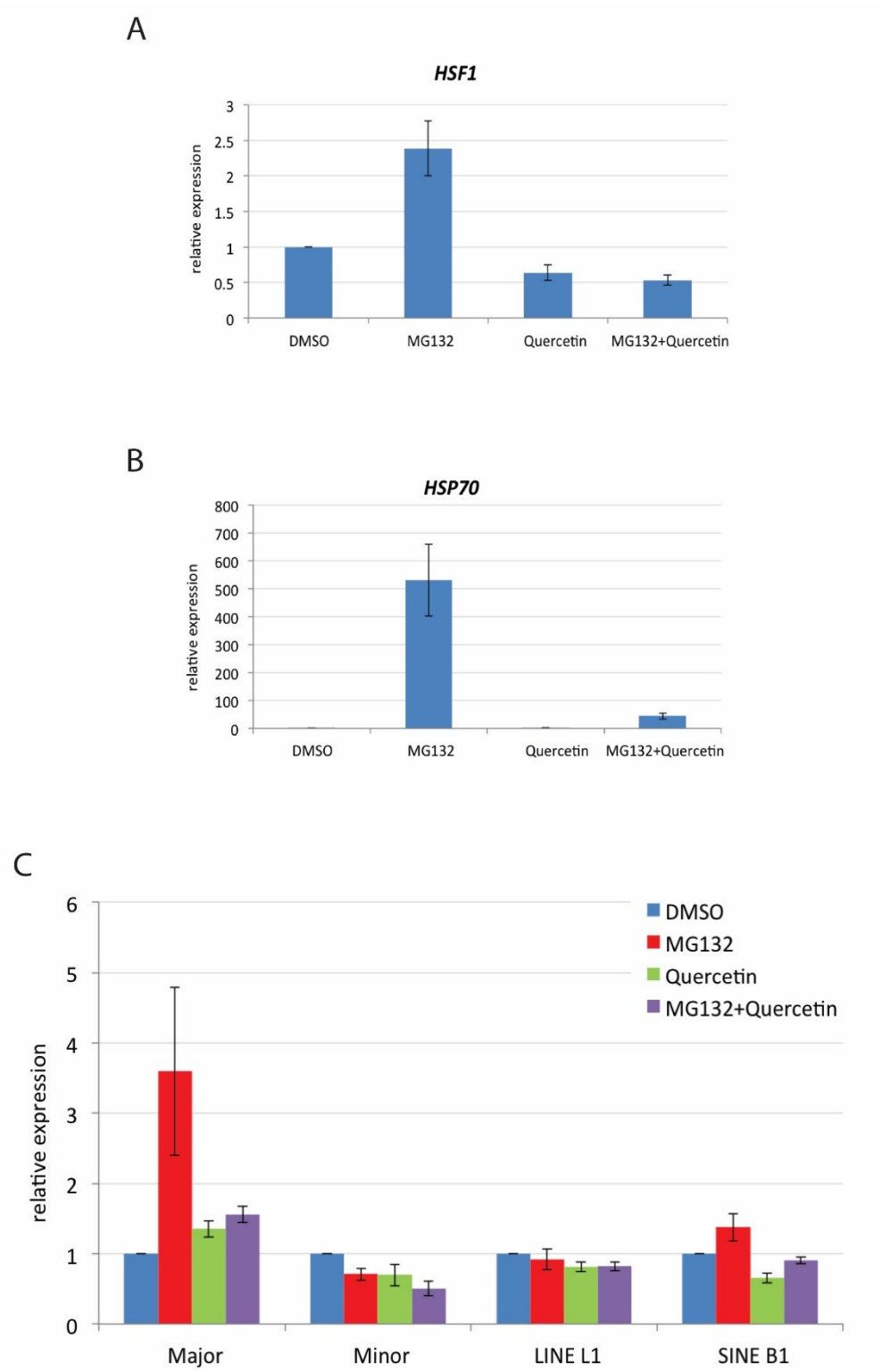


Figure 5.9: The effect of HSF1 and proteasome inhibition on the expression of (A) HSF1, (B) HSP70 and (C) heterochromatic repeats. NIH3T3 cells were treated with proteasome inhibitor MG132 in the presence and absence of HSF1 inhibitor Quercetin (4h with 100µM Quercetin only followed by 4h with 20µM Mg132 + 100µM Quercetin). RNA was extracted followed by q-RT-PCR. The relative expression was normalised against spike and is shown as fold change relative DMSO. Error bars SEM, n=3 biological replicates.

5.2.7 HSF1 binds to major satellite repeats upon proteasome inhibition

In order to investigate whether HSF1 transcription factor might operate directly at pericentromeric and centromeric heterochromatin regions, the canonical recognition sequence of the HSF1 was aligned to the major satellite and minor satellite consensus sequence respectively. Interestingly, the analysis of the alignment revealed a high homology of the HSF1 binding to a portion of major satellite repeat (Figure 5.10A, Supplementary figure S3), indicating that HSF1 transcription factor might directly associate with pericentromeric heterochromatin. In contrast, no apparent consensus HSF1 binding site was found within the minor satellite repeat expression of which is unaffected by proteasome inhibition (Supplementary figure S3).

To further investigate the binding of HSF1 to major satellite repeats, NIH3T3 cells were treated with DMSO (control) or proteasome inhibitor MG132 at a final concentration of 20μM for 4h followed by ChIP using antibody specific to HSF1. The immunoprecipitated material was analysed by qPCR with primers against major and minor satellite repeats as well as primer against the promoter regions of *HSP70* which was used as a positive control for HSF1 binding as HSF1 has been shown previously to bind here (Abravaya, Phillips, & Morimoto, 1991; Fujimoto, Takii, Hayashida, & Nakai, 2015; Ostling *et al*., 2007; Westerheide *et al.,* 2009).

As expected, the treatment of cells with MG132 showed an enrichment of HSF1 on the promoter regions of *HSP70* gene (Figure 5.10B). Importantly HSF1 enrichment was also found on the major satellite repeats upon proteasome inhibition whereas no signal was detected on the minor satellite repeats (Figure 5.10B). This result correlates well with the alignment analysis and indicates that HSF1 appeared to be recruited to pericentromeric heterochromatin through binding to the major satellite repeats upon proteasome inhibition.

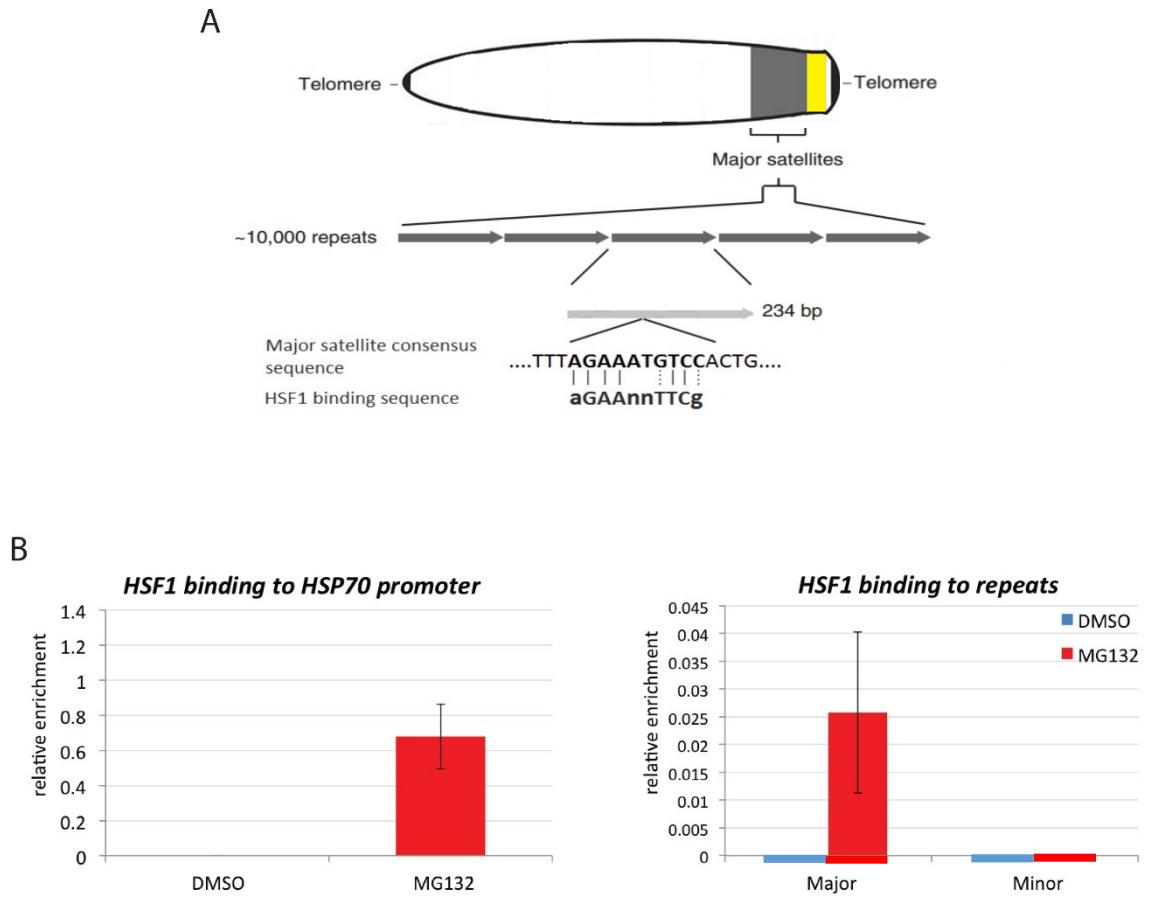


Figure 5.10: Transcription factor HSF1 binds to major satellite repeats upon proteasome inhibition. (A) Alignment of a portion of the pericentromeric major satellite consensus sequence with the canonical binding sequence of the HSF1 transcription factor. (B) ChIP-qPCR analysis of HSF1 binding on the major and minor satellite repeats upon treatment of NIH3T3 cells with DMSO or 20µM MG132 for 4h. The promoter region of *HSP70* served as a control for HSF1 binding. ChIP signal is shown as enrichment relative to input after background (no antibody – see methods) subtraction. Error Bars represent SEM, n=3 biological replicates.

5.2.8 Transduction of NIH3T3 cells enhance the activation of transcription of major satellite repeats upon proteasome inhibition

So far, the results in this chapter suggest that transcriptional activation of major satellite repeats upon proteasome inhibition, are mediated by the transcription factor HSF1. The function of Quercetin was previously proposed to be cell-type specific as well as to depend on the type and the condition of stress applied (R. K. Hansen, Oesterreich, Lemieux, Sarge, & Fuqua, 1997). For example in HeLa, HepG2 and COLO 320DM cells, Quercetin was shown to (i) inhibit the DNA-binding of HSF1 to the HSE (ii) reduce the protein level of HSF1, predominantly of the phosphorylated form of HSF1 and (iii) reduce the expression of HSF1 and HSF2 (Hosokawa *et al*., 1992; Nagai, Nakai, & Nagata, 1995; A. Sharma, Meena, & Bhat, 2010). Quercetin has also been shown to inhibit several protein kinases (Levy, Teuerstein, Marbach, Radian, & Sharoni, 1984; Matter, Brown, & Vlahos, 1992). Therefore, in order to rule out potential non-specific effects of Quercetin, the effect of stable HSF1 knockdown, followed by treatment with proteasome inhibitor was examined in NIH3T3 cells.

The stable HSF1 knockdown in NIH3T3 cells was performed by using 3 different lentiviral pGIPZ-HSF1 shRNA expression constructs. In parallel identical lentiviral vectors containing either a non-targeting 'scrambled'-shRNA or an empty vector with no shRNA insertion were used as controls for the procedure. The shRNA expressing cells and the infection efficiency of lentivirus were monitored by fluorescence microscopy 48h after infection, as pGIPZ vectors contain TurboGFP and shRNA as part of a single transcript (Supplementary figures S4 and S5).

To assess the efficiency of the knockdown, HSF1 mRNA expression and protein levels were analysed in puromycin selected NIH3T3 cells. For the HSF1 mRNA expression analysis, RNA was extracted followed by cDNA synthesis and qPCR with primers against HSF1 mRNA transcript; the HSF1 protein levels were detected by western blot using antibody specific to HSF1. As illustrated in Figure 5.11A and 5.11B, q-RT-PCR and western blot data revealed that transduction with HSF1-shRNA 1, 2 and 3 resulted in similar decreases in HSF1 mRNA and protein levels by approximately 80%, 60% and 45% respectively compared to the uninfected control. On the other hand the levels of both HSF1 mRNA and proteins were largely unaffected by transduction with the scrambled shRNA and the empty vector (Figure 5.11A, 5.11B).

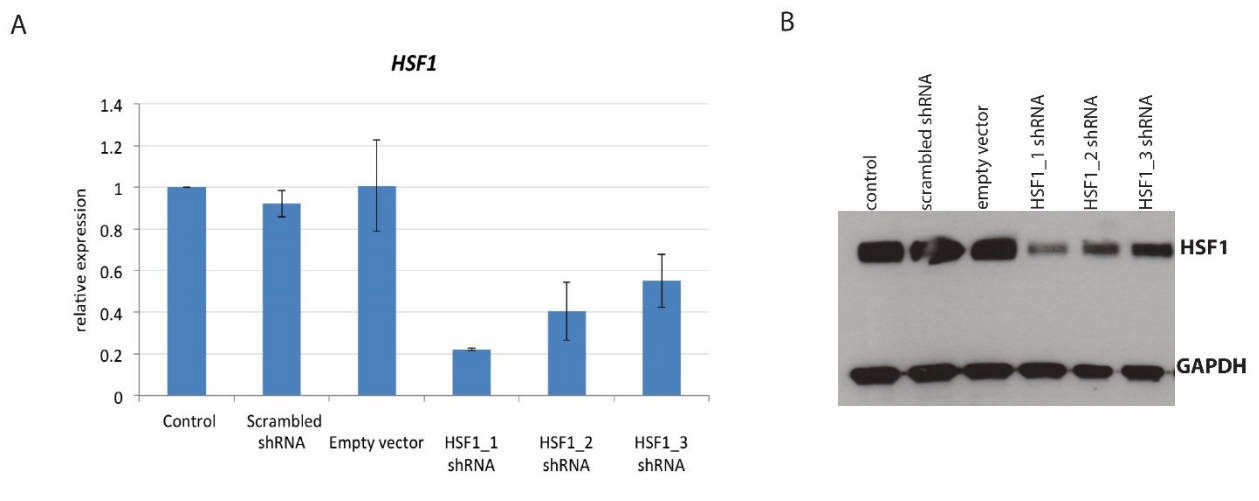
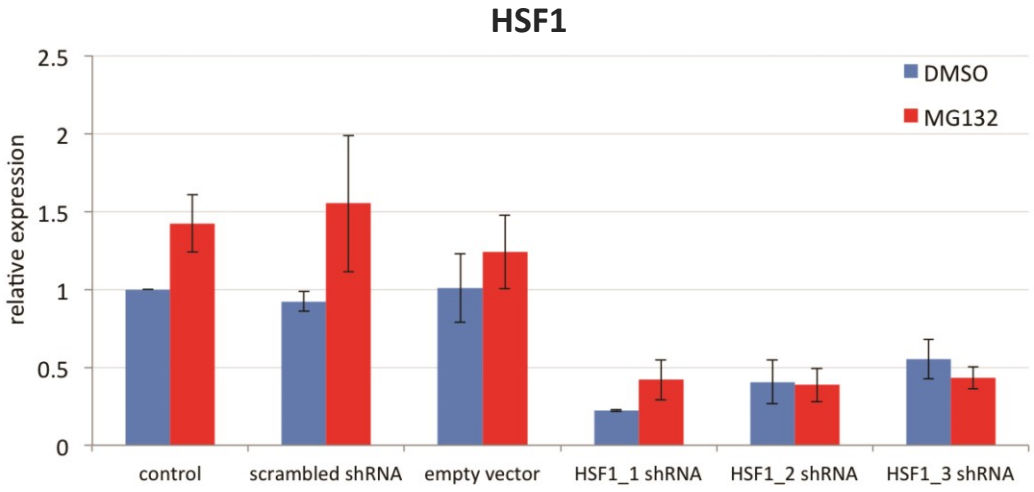


Figure 5.11: HSF1 knockdown in NIH3T3 cells. (A) HSF1 mRNA expression levels in uninfected and in puromycin selected NIH3T3 cells analysed by q-RT-PCR after transduction with HSF1-specific shRNA (shRNA 1, 2, 3), scramble shRNA and empty vector. The relative HSF1 mRNA expression was normalised against spiked in RNA and is shown as fold change relative to uninfected control. Error bars represent SEM, n=3 biological replicates. (B) Representative image of HSF1 protein levels in uninfected and puromycin selected NIH3T3 cells analysed by western blot after infection with HSF1-specific shRNA (shRNA 1, 2, 3), scrambled shRNA and empty vector. GAPDH served as a loading control.

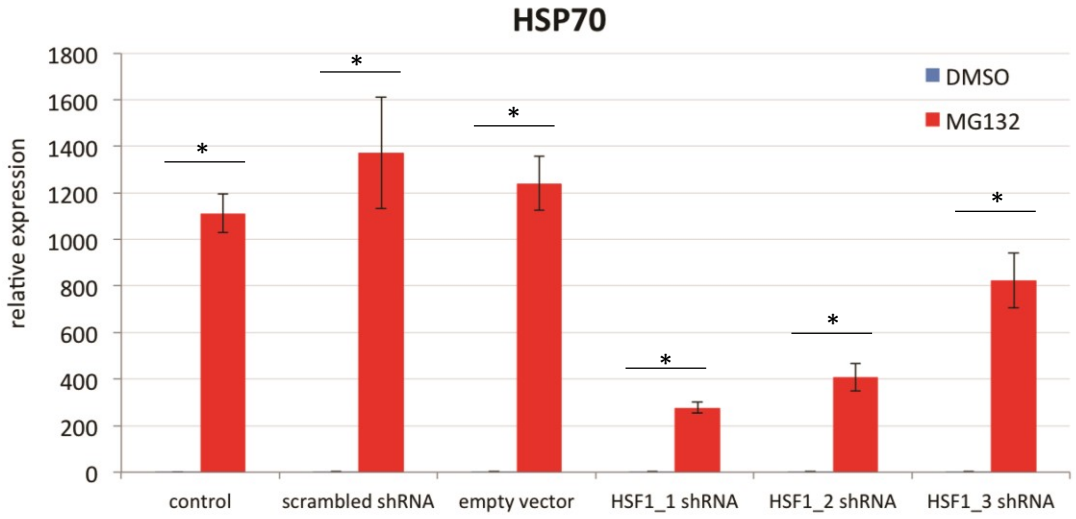
Having confirmed the HSF1 knockdown, uninfected NIH3T3 cells, HSF1 knockdown (HSF1 shRNA 1, 2, 3) cells and controls with scrambled shRNA and empty vector were treated with DMSO or proteasome inhibitor MG132 at a final concentration of 20µM for 4h. RNA was extracted followed by cDNA synthesis and qPCR with primers against HSF1 and HSP70 mRNA transcript as well as major satellite repeat transcript. Although the levels of HSF1 correlated well with the upregulation of *HSP70* gene expression upon treatment of cells with MG132 (Figure 5.12A, 5.12B), surprisingly no correlation was found between the extent of HSF1 knockdown and the expression of major satellite repeats upon proteasome inhibition (Figure 5.12A, 5.12C). However, transduction and selection with puromycin for ~10 days of the control shRNA and empty vector both resulted in an increased response to MG132 treatment relative to untransduced cells. So it is possible that in addition to the effect of HSF1 knockdown, the cells were already 'primed' by the stress of transduction for major satellite upregulation. Thus, the experiment is potentially confounded by this additional effect of transduction. Interestingly, similar but much less pronounced effects were seen

with *HSP70* upregulation in the non-targeting controls. Thus the presence of MG132 resulted in upregulation of major satellite repeat expression as shown in the previous chapter; however the levels were observed on average to be higher in all the lentivirus transduced cells, including HSF1 shRNA, Scramble shRNA and Empty Vector compared to uninfected cells (Figure 5.12C).

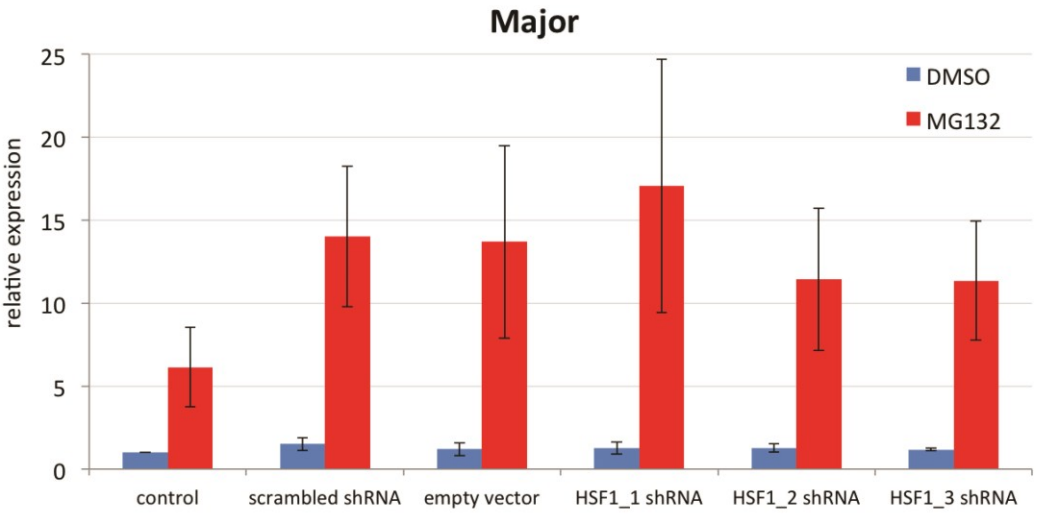
A



B



C



See next page for figure legend

Figure 5.12: The effect of the HSF1 knockdown in the expression of major satellite repeats followed by treatment of NIH3T3 cells with proteasome inhibitor. NIH3T3 uninfected cells, HSF1 knockdown cells with HSF1 shRNA, scramble shRNA and empty vector were treated with DMSO or 20μM MG132 for 4h. The expression of (A) *HSF1*, (B) *HSP70* and (C) major satellite were analysed by q-RT-PCT. The levels of HSF1 and HSP70 served as a control for the knockdown and the function of HSF1. The relative expression was normalised against spike and is shown as fold change against uninfected with DMSO only treated, which was set as 1. Error bars represent SEM n=3 biological replicates. *$p<0.05$ (Student's 't' test).

5.2.9 The HSF1 knockout partially reduced the expression of major satellite repeats upon proteasome inhibition in immortalized mouse embryonic fibroblasts (iMEFs)

Given that the knockdown experiment for HSF1 was partially confounded by non-targeting effects (see above) of the procedure is was decided to adopt a knockout approach. For this we collaborated with Professor A. Nakai (Japan) who kindly supplied us with immortalised MEF (iMEFs) derived from knockout and wildtype mice (see more in materials and methods). The absence of HSF1 in HSF1 null (-/-) iMEFs was confirmed by western blot (Figure 5.13A).

RNA was extracted from the HSF1+/+ and HSF1-/- cells, followed by cDNA synthesis and qPCR with primers against various heterochromatin repeats including major satellite and minor satellite repeats, LINE L1 and SINE B1. No significant difference in the expression levels of major satellite repeat, LINE L1 and SINE B1 was revealed between wild type and HSF1 knockout cells (Figure 5.13B). However, on average a ~2 fold increase of the expression of minor satellite repeats was found in HSF1-/- compared to the wild type albeit not statistically significant (Figure 5.13B). Minor satellite upregulation was not seen with Quercetin treatment (see Figure 5.9C) or proteasome inhibition (see Figure 4.3, 4.8B) and was not investigated further.

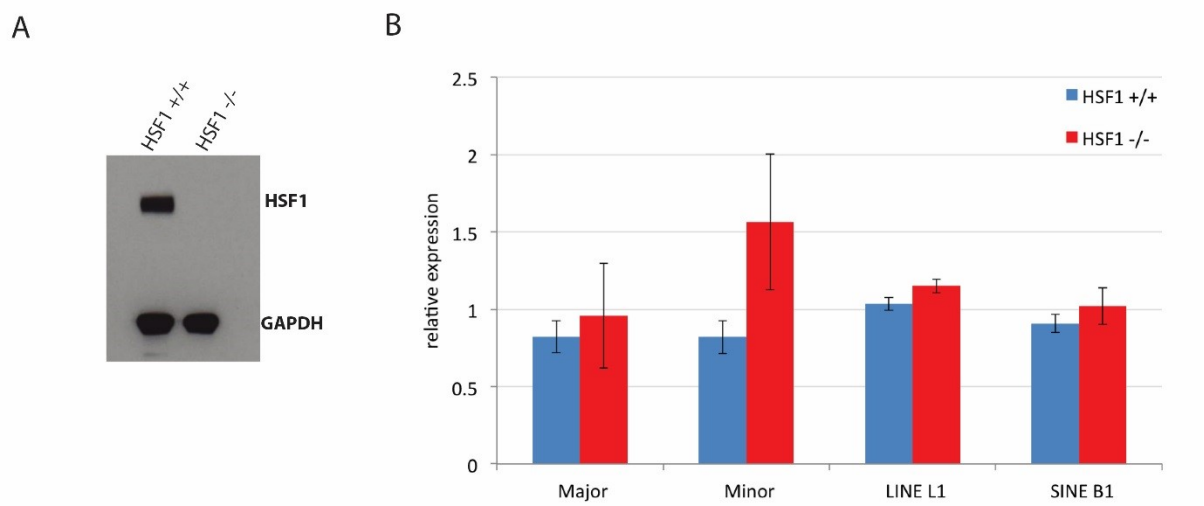


Figure 5.13: The basal heterochromatic repeats expression levels in HSF1 wild type (+/+) and HSF1 null (-/-) iMEFs. (A) The HSF1 is absent in HSF1-/- iMEFs. Total cell lysate from HSF1+/+ and HSF1-/- was blotted with antibody against HSF1 and GAPDH that served as a loading control. (B) The expression levels of major satellite, minor satellite, LINE L1 and SINE B1 in HSF1+/+ and HSF1-/- cells analysed by RNA extraction followed by q-RT-PCR. The relative expression was normalised against GAPDH and is shown as fold change against HSF1+/+. Error bars represent SEM n=4 biological replicates.

Next, the HSF1+/+ and HSF1-/- iMEFs were treated with DMSO (vehicle) or MG132 at a final concentration of 5μM, 10μM and 20μM for 4h. RNA was extracted, followed by cDNA synthesis and qPCR with primers against *HSP70* and major satellite repeats. As expected, in the wild type cells, the expression of *HSP70* was dramatically and dose-dependently increased upon treatment of cells with MG132, compared to the untreated control. On the contrary, in HSF1 knockout cells, the upregulation of *HSP70* was completely abolished upon proteasome inhibition (Figure 5.14A). The transcriptional activation of major satellite repeats upon MG132 treatment was apparent in both wild type and HSF1 knockout cells as illustrated in Figure 5.14B. However, the level of this upregulation on average was approximately doubled in the wild type cells compared to the HSF1 knockout cells within each treatment concentration (Figure 5.14B), suggesting that HSF1 has a partial function on the regulation of the pericentromeric major satellite repeat transcription upon proteasome

inhibition. Notably, in the wild type cells the major satellite repeat transcription was found to negatively correlate with the dose of the proteasome inhibitor, reaching ~19 -, 14 - and 10 - fold increase with 5μM, 10μM and 20μM MG132 treatment respectively, relative to the untreated control (Figure 5.14B). On the contrary, in NIH3T3 cells the upregulation of the major satellite transcription upon proteasome treatment was shown to be dose–dependent (Figure 4.3). There is no clear explanation for this difference however it might reflect cell-type specific differences. Nevertheless, deletion of HSF1 partially inhibited the upregulation of major satellite repeat expression upon proteasome inhibition. It is possible that other HSFs are responsible for the remaining upregulation seen, this is not the case for *HSP70* (see discussion).

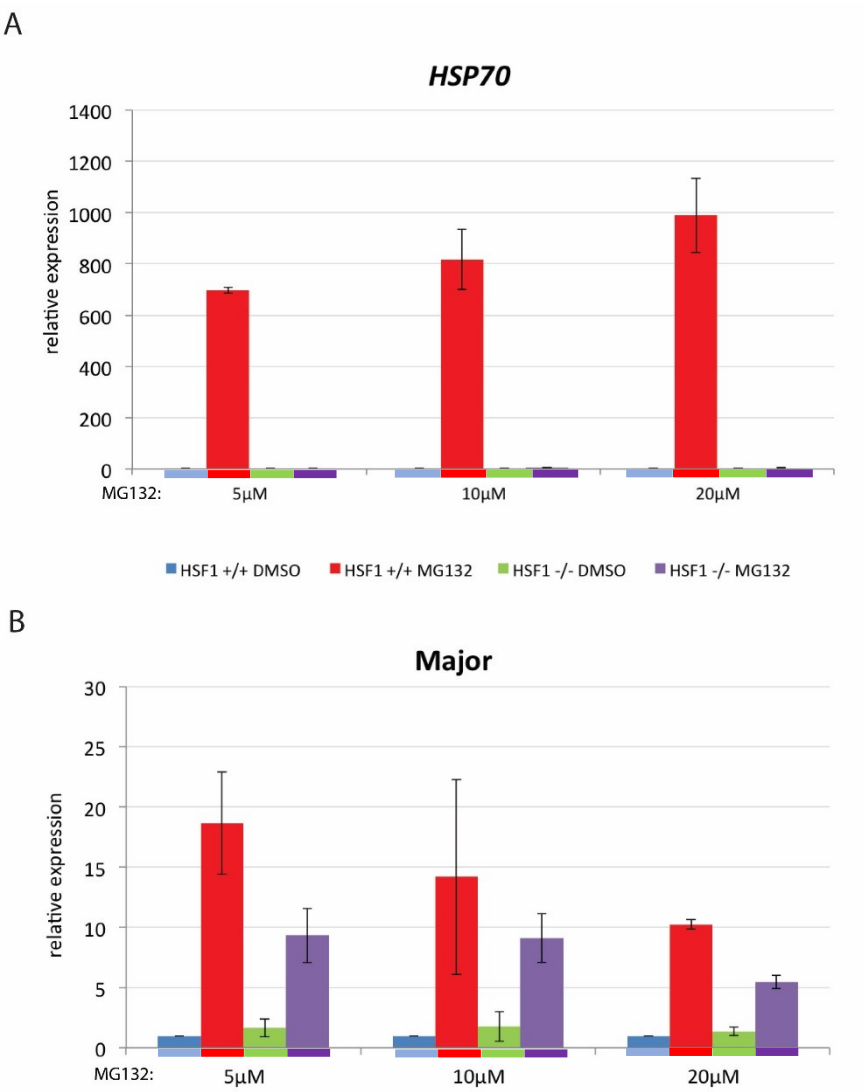


Figure 5.14: The effect of the proteasome inhibition on the expression of (A) HSP70 and (B) major satellite repeats in wild type and HSF1 knockout cells. HSF1+/+ and HSF1-/- iMEFs were treated with DMSO or 5µM, 10µM and 20µM MG132 for 4h followed by RNA extraction and q-RT-PCR. The relative expression was normalised against spike and is shown as fold change relative to DMSO. Error bars represent SEM n=2-3 biological replicates.

5.3 Discussion

In this chapter, two hypotheses were proposed to explain the transcriptional activation of pericentromeric satellite repeats with proteasome inhibition. These hypotheses were: i) degradation of RNAPII by the proteasome and (ii) activation of heat shock pathway, which in turn facilitates expression of major satellite repeats. The next sections will discuss this in more detail.

5.3.1 Does proteasome mediate the degradation of RNAPII at major satellite repeats leading to its transcriptional activation?

As mentioned in chapter 3, the proteasome was shown to bind to the *FXN* gene and degrade the stalled S2P-RNAPII in the presence of expanded GAA repeats. In the chapter the total levels of S2P- and S5P RNAPII and their binding at heterochromatic repeats were analysed in the presence and absence of the proteasome inhibitor in order to assess whether a similar mechanism might operate to degrade RNAPII on repetitive DNA elements and thereby facilitate transcriptional silencing. Here, both S2P- and S5P-RNAPII were shown to accumulate by treating the cells with proteasome inhibitor, consistent with previous study (Kinyamu & Archer, 2007). This observed increase in the total levels of S2P and S5P-RNAPII with proteasome inhibition could indicate prevention of degradation of both forms of RNAPII when inhibiting the catalytic proteasomal activity. Serine 5 phosphorylation of RNAPII was previously shown *in vitro* to inhibit polymerase ubiquitylation and further degradation (Somesh *et al*., 2005) suggesting that S2P-RNAPII is the target for proteasome-dependent degradation at the RNAPII stalling site. This was consistent with the finding that S2P-RNAPII is apparently degraded by the proteasome at the RNAPII stalling site in the *FXN* gene (see chapter 4). Additional studies have also shown that RNAPII marked by S2P becomes a target for proteasome mediated degradation, which is an important process in transcription-coupled DNA repair (K. B. Lee *et al.,* 2002; Somesh *et al.,* 2007). In mammalian cells, ubiquitylation and degradation of hyperphosphorylated RNAPII was shown to be mediated by E3 ligases NEDD4 and Smurf1 (Anindya *et al.,* 2007). Of note Anindya and colleagues analysed RNAPII with an antibody (4H8) which according to the authors recognises both phosphorylated and unphosphorylated RNAPII. However, some studies

argue against the specificity of this antibody, suggesting the monoclonal 4H8 antibody recognises only S5P-RNAPII (Alder *et al*., 2010; Stock *et al.,* 2007). In addition, a fraction of ubiquitylated S5P-RNAPII mediated by BRCA1/BARD1 was shown to be degraded by the proteasome (Starita *et al*., 2005). Therefore, it is tempting to speculate that cells might have evolved different mechanisms to degrade stalled RNAPII, whether it is marked by S5P or S2P. At this point it is worth mentioning that not all the ubiquitylation pathways lead to RNAPII degradation (Daulny *et al.,* 2008; K. B. Lee & Sharp, 2004; Mikhaylova *et al.,* 2008). For example in yeast, RING finger ubiquitin-ligase Asr1 was shown to ubiquitylate S5P-RNAPII resulting in ejection of Rpb4/7 subunits and inhibition of polymerase activity (Daulny *et al.,* 2008). Alternatively, the accumulation of the hyperphosphorylated RNAPII could be attributed to inhibition/deactivation of the phosphatases that remove phosphate groups from RNAPII. Dephosphorylation of RNAPII CTD is catalysed mainly by (i) Ssu72 which targets specifically S5P and S7P- RNAPII (Hausmann, Koiwa, Krishnamurthy, Hampsey, & Shuman, 2005; Krishnamurthy, He, Reyes-Reyes, Moore, & Hampsey, 2004; Reyes-Reyes & Hampsey, 2007; D. W. Zhang *et al*., 2012) and (ii) Fcp1 which is specific for S2P-RNAPII (Cho, Kobor, Kim, Greenblatt, & Buratowski, 2001; Ghosh, Shuman, & Lima, 2008). In future experiments, to investigate whether the accumulation of S2P and S5P-RNAPII is due to effects of the proteasome inhibition on the stability and function of RNAPII CTD phosphatases, cells could be treated with phosphatase inhibitor concomitant with proteasome inhibitor followed by analysis of the levels of both forms of RNAPII within the nucleus.

In contrast to an increase in total levels of S2P and S5P-RNAPII, the binding of both phosphorylated forms of RNAPII to pericentromeric major satellite repeats which was analysed by ChIP, were found to be unaffected by proteasome inhibition. Although this could be considered surprising, as upregulation these repeats was found to be dependent on RNAPII mediated transcription (chapter 4), one explanation for similar levels of RNAPII at pericentromeric repeats DNA would be that the proteasome inhibition resulted in increased kinetics of transcription which might not be detected by examining steady state levels. Another possible explanation could be due to the transcriptional activation of a relatively small fraction of the total amount of repeat units (~10 000 per each chromosome). Hence, detection of RNAPII by ChIP in such a small proportion of repeat units may not be possible

by ChIP. Furthermore the absence of S2P- and S5P-RNAPII from chromocentres which was analysed by IF after treatment of cells with proteasome inhibitor, would suggest that repeats are activated from the outer surface of the chromocentres. This is consistent with the RNA-FISH results shown in the previous chapter (chapter 4), where the majority of major satellite repeat transcripts were detected surrounding the chromocentres.

The presence of the proteasome at major satellite repeats revealed by ChIP would support the hypothesis of RNAPII degradation. In contrast to the ChIP results presented here, proteomics of isolated chromatin segments (PICh), which is a protocol that directly detects the steady-state protein composition of the chromatin (Dejardin & Kingston, 2009), did not shown any specific enrichment of the proteasome subunits on the pericentromeric major satellite repeats in mouse ESCs (Saksouk *et al*., 2014). On the other hand, recruitment of the proteasome was previously shown at telomeres (Geng & Tansey, 2012), which is also predominantly repressed and consists of telomeric satellite repeats (Blackburn, 1991; Zakian, 2012). Furthermore, analysis by ChIP of proteasome binding in mouse thymocytes showed higher enrichment of the proteasome at heterochromatic repeats and inactive genes, compared to active genes (Yandim, 2012). Lastly, it is noteworthy that the absence of co-localisation of the proteasome with chromocentres determined by IF could indicate, similarly to RNAPII, that binding of the proteasome also occurs at the outer surface of the chromocentres.

Based on the evidence presented in this chapter, it is not clear whether RNAPII is degraded by the proteasome at major satellite repeats and further studies are required in order to examine this hypothesis. As RNAPII needs to be ubiquitinated in order to be recognised and degraded by the proteasome (Anindya *et al*., 2007; Beaudenon *et al.,* 1999; Harreman *et al.*, 2009; Ratner, Balasubramanian, Corden, Warren, & Bregman, 1998), one approach would be to knockdown the E3 ligases that were shown to add ubiquitin to RNAPII (eg. NEDD4, AIP4, Smurf1, Smurf2, WWP1, and WWP2) (Anindya *et al.,* 2007; Ingham, Gish, & Pawson, 2004) and analyse the transcript levels of major satellite repeats as well as ubiquitinated RNAPII. Furthermore, in yeast, disassembly and removal of ubiquitinated RNAPII from a DNA damage site which is followed by proteasome mediated degradation was shown to be facilitated by AAA ATPase Cdc48 and its adaptor proteins Ufd1, NP14, Ubx4/5 (Verma, Oania, Fang, Smith, & Deshaies, 2011). Considering that (i) degradation of RNAPII is

evolutionarily conserved and (ii) the process of removal of stalled RNAPII is similar between DNA–damage dependent and independent pathways (Karakasili *et al*., 2014), homologues of Cdc48 factors might also be present in mammalian cells and facilitate degradation of RNAPII at various regions of the genome. If such homologues are present in mammals, it would be interesting to investigate whether their activity is implicated in removal of ubiquitinated RNAPII from pericentromeric repeats. Finally recruitment of the proteasome to the pericentromeric chromatin and the effect on its inhibition could be further assessed by the Histone Association Assay (HAA) which is essentially western blot analysis of ChIP material which permits the quantification of the relative amount of cellular protein bound to chromatin (Ricke & Bielinsky, 2004).

5.3.2 Proteasome inhibition partly upregulates major satellite repeat transcription by activating the heat shock stress pathway

As mentioned in the introduction, various cellular stresses were previously shown to induce pericentromeric repeat transcription specifically in human cells (see Figure 1.11). Among them heat shock is the best studied and was shown in human cells to activate pericentromeric Satellite III transcription at 9q12 pericentromeric region of chromosome 9 which in turn forms a central core for the formation of a nuclear stress body (see more in the general introduction). Notably Eymery and colleagues further demonstrated in 2010 that secondary nuclear stress bodies could also arise from the transcription of pericentromeric Satellite II and Satellite III repeats at various chromosomes in heat shocked tumour cell lines (Eymery, Souchier, Vourc'h, & Jolly, 2010). Furthermore, heat-shocking both normal and cancer cell lines resulted in increased levels of pericentromeric satellite transcripts but no change in centromeric transcription was detected (Eymery, Horard, *et al*., 2009). Consistently, in this thesis heat shock was shown to cause a marked increase of mouse pericentromeric major transcript levels whereas centromeric minor transcripts

remained largely unaffected or slightly decreased in mouse cells, indicating evolutionary conservation in the response to the heat shock. Similar to minor satellite repeats, retrotransposon LINE L1 elements were found to be unaffected. Furthermore, in contrast to previous studies (Allen *et al*., 2004; Fornace & Mitchell, 1986; T. H. Li, Spearow, Rubin, & Schmid, 1999; Mariner *et al*., 2008) where heat shock was shown to also upregulate both human Alu elements and mouse SINE B1 and SINE B2 transcription, no such effect was found in this thesis. One possible explanation for this discrepancy, at least in NIH3T3 cells could be due to the difference in the heat shock temperature, as a previous study (Allen *et al*., 2004) used a higher temperature (~3^{o}C difference) to induce stress.

Considering that the stress response is evolutionarily highly conserved among different species (Kultz, 2003, 2005), proteasome inhibition which is known to induce accumulation of misfolded proteins and activate the stress pathway (Boyault *et al*., 2007; Bush *et al.,* 1997; Goldberg, 2003; Johnston *et al.,* 1998; Kawazoe *et al.,* 1998; Mathew *et al.,* 1998; Obeng *et al.,* 2006; Rao & Bredesen, 2004), which was also confirmed in this thesis, was analysed and shown to be largely responsible for transcriptional activation of major satellite repeats. Based on the data that (i) HSF1 binds to major satellite repeats, (ii) treatment of cells with both HSF and proteasome inhibitors reduces major satellite repeat upregulation and (iii) treatment of HSF1 knockout MEFs only partly induces transcriptional activation of major satellite repeats; it is tempting to speculate that HSF1 together with other HSFs (eg HSF2, HSF3) could mediate the expression of the pericentromeric repeats in mice upon proteasome inhibition. Interestingly, in human cells, HSF2 was shown to form a heterotrimer with HSF1 and activate Satellite III expression upon heat shock (Sandqvist *et al*., 2009). Furthermore, the HSF3, present in mouse and absent in human cells, was shown to activate the expression of non-classical heat shock genes including the PDZ domain–containing protein (PDZK3) in response to heat shock (Fujimoto *et al.,* 2010). If HSF3 could bind to the major satellite repeat it would be another candidate.

Curiously, knockdown of HSF1 presented in this thesis was not capable of inhibiting the upregulation of pericentromeric repeats in response to proteasome inhibition whereas HSF1 knockout and inhibition of HSF could inhibit this response in mouse fibroblasts. One possibility is that in the knockdown experiment transduction of both controls with lentivirus resulted in persistent upregulation of repeat expression following proteasome inhibition

indicating that the cells may have primed an additional chronic stress pathway which circumvents the requirement for HSF1 in specifically upregulating the pericentromeric repeats. However at this point it is worth mentioning that in a previous study in human cells HSF1 knockdown inhibited heat-shock induced upregulation of pericentromeric repeats (Eymery, Horard, *et al*., 2009).

The similarities between the chromatin structural changes that take place as a result of both heat shock and proteasome inhibition suggest a common mechanism. For example, in non-heat shocked HeLa and MCF-7 cells HP1β and HP1α were found to be accumulated at chromocentres respectively, whereas in heat shocked cells HP1β and HP1α were shown to display a rather homogenous nuclear distribution (Eymery, Horard, *et al.,* 2009; Velichko, Kantidze, & Razin, 2011). This is consistent with the results presented in this thesis (chapter 4), where proteasome inhibition induced clear delocalisation of HP1α from chromocentres. Notably, both HP1α and HP1β are known to be repressors of pericentromeric heterochromatin (Mosch *et al.,* 2011). Another example comes from *Drosophila melanogaster,* where heat shock was shown to induce marked redistribution and concentration of H3S10P at heat shock genes which form microscopically visible puffs on polytene chromosomes while the levels of H3 and H4 acetylation marks were largely unaffected (Nowak & Corces, 2000). The authors suggested that H3S10P is required for transcriptional activation of heat shock genes. Consistently, in this thesis treatment of cells with proteasome inhibition did no substantially change the levels of H3 acetylation (chapter 4). Considering that (i) H3S10P was shown to mediate HP1 disassociation from the chromatin (Fischle *et al.,* 2005; Hirota *et al.,* 2005) and (ii) proteasome inhibition was shown in this thesis to delocalise HP1 from chromocentres, it would therefore be interesting to analyse the levels of H3S10P in pericentromeric regions in the presence and absence of the proteasome inhibitor. On the other hand, extensive analysis of changes of the histone modifications after heat shock in HeLa and MEFs (Fritah *et al.,* 2009) revealed strikingly different results from the heat-shock puffs on *Drosophila melanogaster* polytene chromosomes. More specifically Fritah and colleagues reported that in Hela cells and MEFs heat shock induces (i) global histone deacetylation, (ii) reduction of H3S10P and H4K20me3 levels and (iii) no obvious changes on H3K4me2, H3K4me3, H3K36me1, H3K36me3, H3K9me1, H3K9me2, H3K9me3 levels. Similarly, in another study histone (H2A, H2B, H3,

and H4) acetylation levels were also increased in stress-induced HSF1 granules and no change was found in H3S10P levels (Jolly *et al*., 2004b). These differences might relate in some way to the structural differences between the polytene chromosomes versus human chromosomes (Alberts, 2002). With reference to the results presented here following proteasome inhibition the fibroblast derived cells showed no changes in histone modification in common with the *Drosophila melanogaster* studies rather than the human studies. Moreover, these changes were previously seen in HSF1 granules, where acetylation was analysed by immunofluorescence in human but not mouse cells (Jolly *et al.,* 2004b). This agrees with the results presented here in that no such granules were detected in murine cells (data no shown). It is possible however, that the failure to detect histone acetylation by IF or ChIP in the studies presented here reflects the possibility that only a small fraction of the pericentromeric repeats are affected. A similar argument could be applied to the lack of change in most histone modifications found in human cells following heat shock.

Further studies are required in order to confirm the role of HSFs in regulation of pericentromeric repeats in mice. For example, knockdown of HSF2 in HSF1 knockout mice would assess whether HSF2 is required for the activation of the repeat transcription. Finally it is noteworthy to mention that transcriptional activation of human Satellite III under osmotic stress was shown to be independent of HSF1 and dependent on TonEBP transcription factor (Valgardsdottir *et al*., 2008). That study suggested that different stresses activate transcription of pericentromeric repeats via distinct transcription factors as was suggested by our study of lentiviral transduction which seemed to result in bypass of HSF1 dependent transcriptional activation of pericentromeric repeats following proteasome inhibition. Therefore, stress induced through inactivation of proteasome function could also operate through transcription factors other than HSFs.

Following on from the findings presented in Chapter 4 this chapter examined the molecular mechanisms whereby proteasome inhibition might lead to de-repression and disorganisation of pericentromeric heterochromatin. The main findings were as follows:

- The proteasome was found by ChIP to bind to the pericentromeric repeats consistent with its potential role in regulating transcription e.g by degradation of stalled RNAPII.
- Inhibition of the proteasome led to accumulation of RNAPII within the nucleus by immunofluorescent microscopy but there was no increase in RNAPII detectable by ChIP on pericentromeric repeats which argues against significant degradation of RNAPII at this location. However, this highlights the need for further investigation between RNAPII degradation and pericentromeric silencing.
- Proteasome inhibition led to upregulation of pericentromeric repeat expression which was apparently dependent on activation of the heat shock pathway.

5.4 Contributions

Theona Natisvili performed all the experiments. Ms Giulia Emanuelli helped acquiring confocal images. Lorenzo Orietti analysed the binding of HSF1 to major and minor satellite repeats.

CHAPTER 6: CONCLUSION

In order to understand how heterochromatin is silenced in a mammalian system, this PhD study initially focused on the pathologically silenced *FXN* gene and then pursued silencing of classical heterochromatin elements, including pericentromeric, centromeric satellite repeats and LINE L1 and SINE B1 retrotransposons.

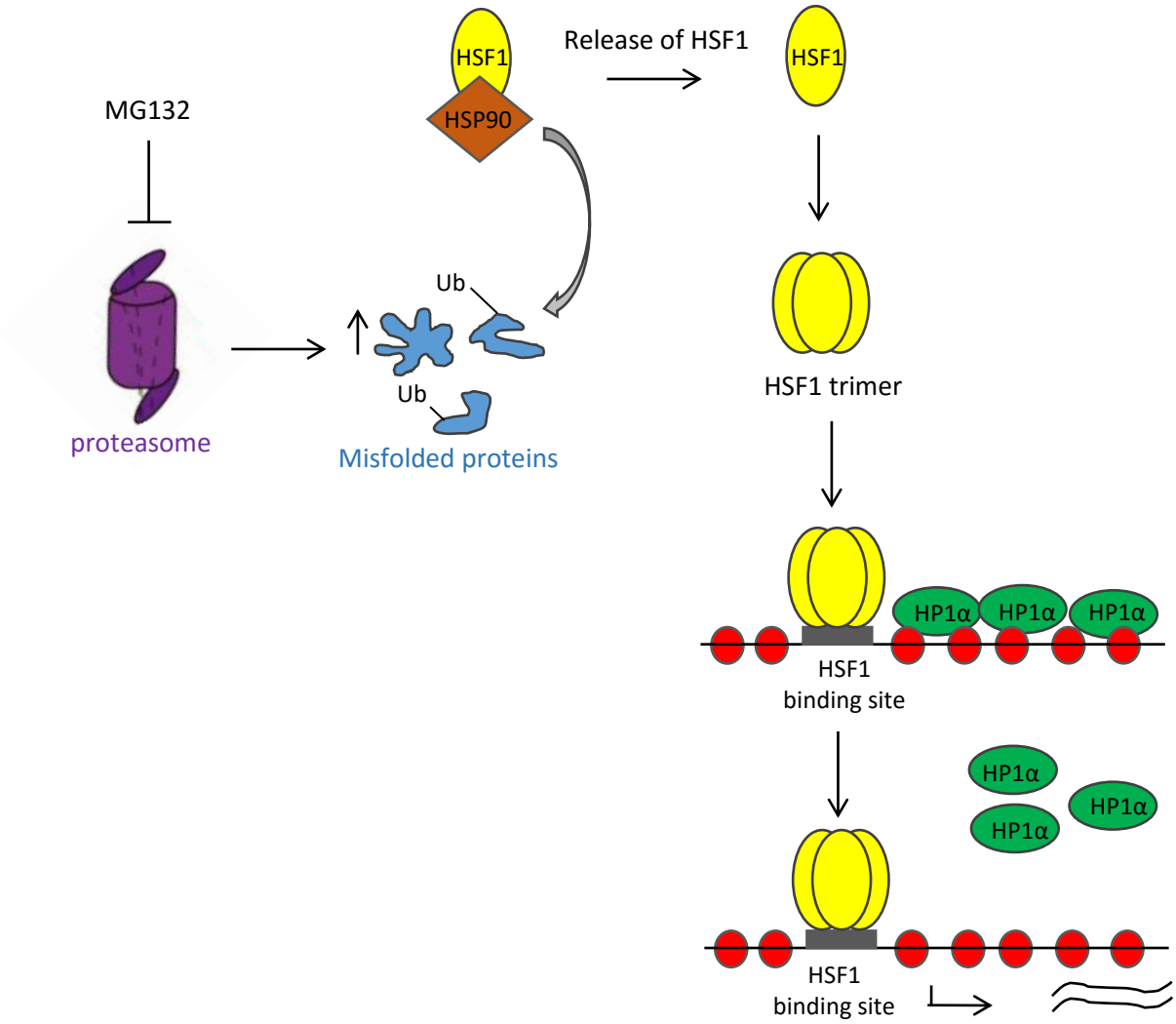
Here, nicotinamide was shown to reduce the heterochromatic mark H3K9me3 at the pathologically silenced *FXN* gene and upregulate its expression *in vivo* in patients with FRDA. This study suggested that altering a chromatin state by targeting epigenetic modifiers such as HDACs could provide a potential therapeutic avenue for FRDA and potentially a range of other diseases where the chromatin state of a causative gene is altered (eg. Fragile X syndrome, myotonic dystrophy).

Another interesting phenomenon explored in this thesis was the role of the proteasome in the regulation of the *FXN* gene in FRDA. Here the proteasome was found to bind along the *FXN* gene, which was further confirmed to be heterochromatinised in cells derived from FRDA patients. This binding was shown to be at higher levels in patient cells and is consistent with the hypothesis, that in FRDA, proteasomal degradation of a stalled RNAPII might contribute to pathological *FXN* silencing. Instead, it was found that inhibition of the proteasome downregulated *FXN* transcription in cell lines, whereas the expression of the gene remained largely unaffected by proteasome inhibition in mice. This result might be explained by differences in the inhibitor used, the dose and bioavailability. Therefore the transcriptional effects of proteasome function might be pleiotropic, causing not only degradation of stalled RNAPII but also efficient transcriptional elongation of the *FXN* gene as has been suggest in yeast studies. Furthermore, inhibition of proteasome function was shown to result in upregulation of pericentromeric repeats transcripts which was dependent on ongoing transcription and appeared to be independent of cell-cycle perturbations. This transcriptional activation was found to be accompanied by changes in heterochromatin structure including delocalisation of HP1α from chromocentres and disruption of chromocentre clusters. Further investigation revealed that the mechanism underlying repression of murine pericentromeric repeats was apparently dependent on activation of the heat shock pathway, analogous to what was previously shown for various cellular

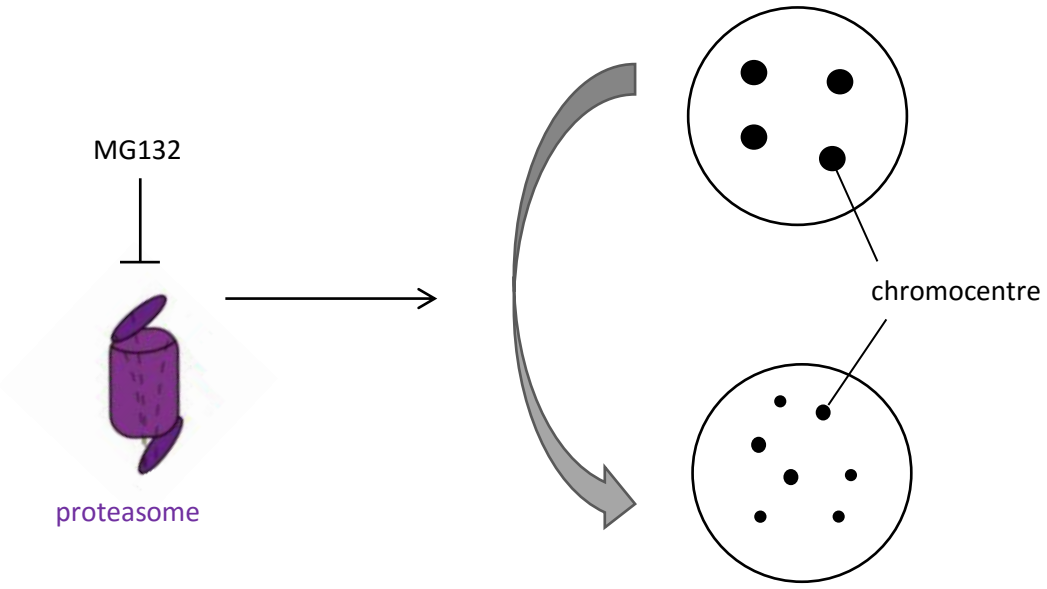
stresses in activating sub-classes of pericentromeric repeats in human cells (Eymery, Callanan, *et al*., 2009; Eymery *et al.,* 2010; Jolly *et al.,* 2004b; Valgardsdottir *et al.,* 2008). In this thesis the investigation was restricted to HSF1, which was shown previously to mediate heat shock dependent activation of sub-classes of pericentromeric repeats in human cells (Eymery, Callanan, *et al.,* 2009; Eymery *et al.,* 2010) and was shown to partly mediate transcription of murine pericentromeric repeats. However, as different stresses were suggested to activate different transcription factors (Valgardsdottir *et al.,* 2008), other factors might also be activated by proteasome inhibition and mediate transcription of mouse pericentromeric repeats. Further studies are required to analyse this hypothesis.

In summary proteasome inhibition was shown here to regulate both transcription of the *FXN* and *c-myc* genes and repression of pericentromeric heterochromatin the latter of which was at least partially dependent on an intact heat shock pathway. The data presented here suggests a model whereby proteasome inhibition activates HSF1 which invades heterochromatin, evicts HP1α which leads to disaggregation of centromeric clusters and activation of transcription of pericentromeric repeats (Figure 6.1).

A



B



See next page for figure legend

Figure 6.1: Model of pericentromeric major satellite repeat activation with proteasome inhibition. (A) Inhibition of the proteasome by MG132 results in accumulation of misfolded and ubiquitynated proteins causing the release of HSF1 from the HSF1-HSP90 complex followed by HSF1 activation. The activated HSF1 (trimer) binds to its binding sequence within the major satellite repeat unit causing the release of HP1α from pericentromeres which becomes more accessible to the transcriptional machinery. The figure represents HSF1 only although other HSFs may also be involved. (B) Proteasome inhibition by MG132 results in disaggregation of chromocentres thereby causing alteration of centromeric clusters structure.

CHAPTER 7: MATERIALS AND METHODS

7.1 Cell lines

All cell lines were incubated at 37 °C in a humidified atmosphere of 5% CO_2.

EBV-transformed cell lines

Epstein-Barr virus (EBV)-transformed human lymphoblastoid cell lines derived from healthy individuals or FRDA patients were used in chapter 3.

GM14926: Healthy 38 years old Caucasian male, GAA repeat in normal range (6-34 repeats)

GM15850: Caucasian male with no age of onset specified, harbours 650 and 1030 GAA repeats on either alleles, blood sample taken at the age of 13 (FRDA_1)

GM16234*: Caucasian* female with onset at 20 years, harbour 580 and 1030 GAA repeats on either alleles, blood sample taken at the age of 39 (FRDA_2)

All EBV cell lines were obtained from Corriell Cell Repositories indicating the repeat lengths for each cell line.

Culture conditions: All EBV cells lines were routinely cultured in RPMI medium with L-glutamine (PAA laboratories GmbH) supplemented with Foetal bovine serum (Sigma) (10% v/v), Penicillin/Streptomycin (GIBCO ®) (1% v/v) and GlutamixTM-I 100x (GIBCO ®) (1% v/v). The cell number was adjusted between 0.2-0.5 x 10^6 cells/ml during the culture.

NIH3T3 cell line

NIH3T3 which is a standard mouse embryonic fibroblast cell line were used throughout the Chapter 4 and 5. This cell line was a kind gift from Dr Phill Wise (Imperial College London)

***Culture conditions*:** NIH3T3 cells were routinely cultured in Dulbecco's modified Eagle's medium (DMEM) with L--glutamine (PAA laboratories GmbH) supplemented with Foetal bovine serum (Sigma) (10% v/v), Penicillin/Streptomycin (GIBCO ®) (1% v/v) and GlutamixTM-I 100x (GIBCO ®) (1% v/v).

Immortalised MEF HSF1+/+ and HSF-/-

The wild type (HSF1+/+) and HSF1 null (HSF1-/-) immortalised MEFs (iMEFs) were generated and kindly provided from Prof Akira Nakai, Yamaguchi University School of Medicine, Japan. More information regarding the cells can be found in (Takii *et al*., 2015a).

Culture conditions: iMEFs were routinely cultured in DMEM medium with L--glutamine (PAA laboratories GmbH) supplemented with Foetal bovine serum (Sigma) (10% v/v), Penicillin/Streptomycin (GIBCO ®) (1% v/v) and Glutamix^{TM}-I 100x (GIBCO ®) (1% v/v).

HEK293T cell line

Human Embryonic Kidney 293T cells were used for lentiviral production for the knockdown experiment. This cell line was provided by KC Tan Un at Hong Kong University.

Culture conditions: HEK293T were cultured in DMEM medium with L--glutamine (PAA laboratories GmbH) supplemented with Foetal bovine serum (Sigma) (10% v/v), Penicillin/Streptomycin (GIBCO ®) (1% v/v) and Glutamix^{TM}-I 100x (GIBCO ®) (1% v/v).

7.2 Transgenic YG8 mice containing human frataxin transgene (*hFXN*)

The YG8 frataxin transgenic mice were generated by rescuing frataxin null mice with YAC FRDA transgene which contains an entire *FXN* gene with GAA repeats. These mice have two copies of the FRDA gene with 90+190 repeats (Table 4). More details can be found in "GAA repeat instability in Friedreich ataxia YAC transgenic mice" by Al-Mahdawi *et al*., published in Genomics 2004 (Al-Mahdawi *et al.*, 2004).

Transgenic line	**YAC transgene integrity**	***FRDA* copy number**	**Founder GAA repeat length(s)**	**Range of GAA repeats in offspring**
YG8	Complete	2	190 + 90	<9 to 223

Table 4: Analysis of FRDA YG8 transgenic mouse line. Adapted from (Al-Mahdawi *et al.,* 2004)

7.3 Primary cells - Isolation of human peripheral blood mononuclear cells (PBMCs)

Human PBMCs were extracted from blood samples taken from FRDA patients and healthy individuals (full ethical approvals were obtained from the local ethics committees at the National Hospital for Neurology and Neurosurgery and the Hammersmith Hospital, London) using the Ficoll-Paque™ PLUS (GE Life Sciences). The blood samples (~ 10ml) were added into 50ml falcon tubes containing 10ml of Ficoll and the samples were centrifuged at 1500rpm in a benchtop centrifuge for 15min at room temperature. The interface buffy-coat containing PBMCs were transferred into new falcon tubes, diluted 2 fold with sterile PBS and centrifuged at 350g in a benchtop centrifuge for 15min at room temperature. The supernatant was discarded and the PBMCs pellet was either fixed for chromatin immunoprecipitation or stored in -80^{o}C for RNA extraction. Usually 1ml blood contained ~1-1.5X10^6 PBMCs.

7.4 Drug preparation and treatments

All drugs were prepared under sterile conditions under a cell culture-hood. The final drug concentrations are mentioned in the main text. MG132 (Sigma) was dissolved in DMSO to prepare a 20mM stock solution. A-amanitin (Sigma) was dissolved as 1mg/ml in culture medium. DRB (Sigma) was dissolved in DMSO to prepare a 10mM stock solution. ActD (Sigma) was dissolved in DMSO as 10mg/ml. PS341 (Velcade®, 3020µM) was kindly provided in a sterile bottle (in physiological saline) by Hammersmith Hospital (London) pharmacy. Quercetin (Sigma) was dissolved in DMSO to prepare a 100mM stock solution.

A total of 3X10^6 EBV-transformed human lymphoblastoid cells from lines GM14926, GM15850 and GM16234 (see above) were treated in 3ml culturing medium (1X10^6/ml). The NIH3T3 and iMEFs cell lines were initially seeded on coverslips in culture plates (0.5X10^6 cells in 60mm culture plate or 1.5X10^6 in 100mm culture plate) at least 20h before adding the drug directly into a confluent culture plate. All the cell line treatments were performed by incubating the cells at 37 °C in a humidified atmosphere of 5% CO_2. The treatment of YG8 mice with PS341 was performed by Dr Mark Pook at Brunel University and the frozen tissues were obtained and then analysed in this thesis.

7.5 Genotyping for gender determination in NIH3T3 and iMEFs

For genotyping 1X10^6 cells were lysed after overnight incubation at 55°C shaker in lysis buffer. The following day the DNA was extracted using phenol/chloroform. The genomic DNA was analysed by PCR, using the Biotaq PCR kit (Bioline) with primers designed that specifically amplify a region on exon 1 of the exclusively male *SRY* gene. The sequence of the primer is shown in Supplementary table S3. The PCR conditions used were: pre-heat at 94^{o}C for 2min, 30 cycles of 94^{o}C for 3min, 58^{o}C for 20 sec and 72^{o}C for 2min. Samples were run on a 3% gel at 140V for ~30min. The 194bp band is present only in males (Supplementary figure S1).

7.6 Phenol/chloroform DNA extraction

The DNA containing sample was vigorously mixed with an equal volume of phenol: chloroform. The sample was then centrifuged at 13000 rpm for 15 min at room temperature (RT) to separate the aqueous phase containing the DNA from the organic phase containing the proteins. The upper aqueous layer was transferred into a new tube and the DNA was precipitated by adding one tenth of sample volume of 3M sodium acetate (NaOAc pH=7) and 2.5X of the volume of 100% ethanol. The sample was incubated at -80°C for at least 1 hour followed by centrifugation at 13000 rpm for 30min at 4°C. The supernatant was discarded and the pellet was washed with 1ml of 70% ethanol. The sample was further centrifuged at 13000 rpm for 15min at 4°C and the pellet was air dried and resuspended in DEPC water. DNA concentration was assessed using NANODROP ® Spectrophotometer ND-1000 with ND-1000 v3.3.1 software.

7.7 Chromatin immunoprecipitation (ChIP)

Chromatin Immunoprecipitation was performed on chromatin derived from EBV lymphoblastoid cell lines or human PBMCs using the fast ChIP protocol described in (Nelson, Denisenko, & Bomsztyk, 2006), whereas in NIH3T3 cells the ChIP protocol used was that described in (Stock *et al*., 2007) both with some modifications.

ChIP on EBV cells/PBMCs

The chromatin in 18X10^6 EBV cells in 25ml RPMI medium was cross-linked by incubating with 1ml of 37% w/v formaldehyde (Sigma) (final concentration 1.42%) for 10min at RT. The cross-linking was quenched by adding 141µl of 1M glycine per 1ml culturing medium (final concentration of glycine 125mM) followed by 5min incubation at RT. The incubation was followed by centrifugation at 2000g, 5min at 4^{o}C. The fixed cell pellet was washed 2X with cold PBS and stored at -80^{o}C.

PBMCs were isolated from human blood as described previously and resuspendend in PBS. The cross-linking was performed by adding 40µl 37% w/v formaldehyde per 1ml of PBS (final concentration 1.42%) and incubating for 15min at RT. The fixing was quenched by adding 141µl of 1M glycine per 1ml culturing medium (final concentration of glycine 125mM) followed by 5min incubation at RT. The incubation was followed by centrifugation at 2000g, 5min at 4^{o}C. The fixed cell pellet was washed 2X with cold PBS and stored at -80^{o}C.

Lysis was carried out for both EBV cells and PBMCs by resuspending the pellet in 1ml IP buffer containing proteasome inhibitor cocktail and PMSF (IP++ buffer) and pipetting up and down several times. This was followed by centrifugation at 12000g for 2min at 4°C. The pellet was washed once more with IP+++ buffer. The nuclear pellet was then resuspended in 1ml IP++ buffer and sheared by sonication with the Bioruptor (Diagenode) for 1h, high energy (with intervals of 30sec on, 30sec off). Next, the sonicated chromatin was centrifuged twice at 12000g for 15min at 4°C. Sheared chromatin in supernatant was snap-frozen in liquid nitrogen and stored at -80°C. The sonication efficiency was visualised by reverse crosslinking 100µl of sheared chromatin, DNA extraction using phenol/chloroform and run on a 1.5% agarose gel.

For immunoprecipitation, specific amounts of different antibodies (Supplementary table S4) were added to 200µl aliquot of sheared chromatin. One 200µl aliquot was used as a no-antibody mock IP in order to monitor the non-specific binding (background). Furthermore 50µl of sonicated chromatin material (input) was stored in -20^{o}C. Binding efficiency of the antibodies to their target epitopes was enhanced by incubating the samples in Biorupter (Diagenode) for 45 min, low energy (with interval of 30sec on, 30 sec off). Subsequently each sample was centrifuged at 12000g for 10min at 4^{o}C. The top 180µl of material was mixed with pre -washed 50µl Dynabeads ® Protein G (Invitrogen) and incubated overnight

on a rotating wheel at 4°C. Next day, the beads bound to antibody-chromatin complexes were washed six times with IP buffer and the DNA was isolated using 110µl Chelex-100 (10% w/v) (BIO-RAD) per sample. Beads bound to antibody-chromatin complex and Chelex-100 was mixed gently and heated 2X at 95°C for 7min with vortex in between. Then the samples were centrifuged at 12000g for 2min 4°C and the 80µl supernatant was transferred into a new tube. 200µl of sterile water was added to the Dynabeads, vortex and centrifuged at 12000 g for 2 minutes at 4°C. The supernatant (200µl) was pooled with that previously obtained to make a final total of 280µl of ChIP DNA. The pre-stored input sonicated chromatin material (50µl) was mixed with 150µl 100% ethanol, incubated for 2min at RT and centrifuged at 12000g for 10min at 4°C. The pellet was then washed with 1ml of 70% ethanol. Upon centrifugation at 12000g for 5min at 4°C, the supernatant was discarded and the DNA was purified by using 110µl Chelex-100 (10% w/v) in the same way as with the ChIP samples described above.

The DNA obtained was analysed by quantitative real time polymerase chain reaction (qPCR).

ChIP on NIH3T3 cells

The chromatin in 1X10^7 NIH3T3 cells were fixed by adding 540µl of 37% w/v formaldehyde (Sigma) directly to the 150mm culture dish containing 20ml of DMEM medium (final concentration of formaldehyde 1%) and incubating for 10min at 37°C. The formaldehyde fixation was quenched by adding 2820µl 1M glycine (final concentration of glycine 125mM) and incubating for 5min at RT. The cells were then washed 3X with cold PBS before the lysis. Lysis was carried out by adding 10ml of Swelling buffer (the NP-40 concentration was increased from 0.1% to 2.5% compared to the original protocol) containing protease inhibitor cocktail and PMSF to the cells and incubating for 10min at 4°C. Next, cells were collected by scraping and lysed using a Dounce homogenizer with a “Tight” pestle (~250 strokes). The lysed material was centrifuged at 3000g, for 5min at 4°C. The nuclear pellet was resuspended in 1ml Sonication buffer (containing protease inhibitor cocktail and PMSF) and sheared by sonication using a Bioruptor (Diagenode) for 20min, high energy (with intervals of 0.5min on, 0.5 min off). The sonicated chromatin was centrifuged twice at 15000g for 15min at 4°C. Sheared chromatin in supernatant was snap-frozen in liquid nitrogen and stored in -80°C. The sonication efficiency was visualised by reverse crosslinking

50µl of sheared chromatin, DNA was extracted using phenol/chloroform and run on a 1.5% agarose gel.

For Immunoprecipitation, specific amounts of different antibodies (Supplementary table S4) were added to 200µl aliquots of sheared chromatin. One 200µl aliquot was used as a no-antibody mock IP in order to monitor the non-specific binding (background). Furthermore 10µl of sonicated chromatin material (input) was stored in -20^{o}C. Binding efficiency of the antibodies to their target epitopes was enhanced by incubating the samples in a Biorupter (Diagenode) for 40 min, low energy (with intervals of 30sec on, 30 sec off). Subsequently each sample was centrifuged at 12000g for 10min at 4^{o}C. The top 180µl of material was mixed with pre-washed 50µl Dynabeads Protein G (Invitrogen) or pre-washed 50µl Dynabeads Protein M (Invitrogen) specifically for the S2P-RNAPII antibody and incubated overnight on a rotating wheel at 4^{o}C. Next day, Protein G Dynabeads bound to antibody–chromatin complexed was washed by rotating for 5min at 4^{o}C with 1ml of Sonication buffer, 1ml Wash buffer A, 1ml Wash Buffer B and two times with 1ml of TE Buffer. Protein M Dynabeads bound to antibody-chromatin complexes were washed by rotating for 5min at 4^{o}C with the following buffer: twice with 1ml Sonication buffer, once with 1ml IgM antibody wash buffer and twice with 1ml TE buffer. The recovery of DNA from the immunoprecipitated protein/DNA complexes was performed using the Ipure Kit (Diagenode) following the manufacturer's instructions.

The DNA obtained was analysed by qPCR.

7.8 Total RNA extraction

Total RNA from EBV lympoblastoid cell lines/PBMCs, NIH3T3 cell line, HSF1+/+ and HSF1-/- Immortalised MEFs and mouse cerebellum/heart tissues was isolated using TRIZOL® Reagent (Invitrogen).

The EBV cells/PBMCs were collected by centrifuge and resuspended in 1ml of Trizol. For the RNA extraction from the NIH3T3 cells and immortalised MEFs, lysis was performed by adding Trizol directly into the culture dish (1 ml per 10 cm2). For tissue samples, frozen tissue was homogenised using the IKA ultra-turrax T25 homogeniser with 1ml Trizol. Next, the samples were incubated at room temperature for 5 minutes. 200 µl chloroform per 1 ml

Trizol was added, mixed by 20sec shaking and incubated for 5 minutes at room temperature. Samples were then centrifuged at 12000g, for 15min at 4°C and the aqueous phase was transferred to a fresh tube. The pink organic phase was used to extract protein when necessary. Next, 500µl of isopropanol per 1ml of Trizol was added to the retained aqueous phase, mixed by vortex and incubated at room temperature for 10 minutes. Followed the incubation, the samples were centrifuged at 12000g for 15min at 4°C. Supernatant was removed and the pellet was washed by adding 1ml of 70% ethanol per 1ml of Trizol. Samples were vortex and centrifuged at 7500g for 5min at 4°C. Supernatant was removed and the RNA pellet was briefly air dried, followed by DNase treatment using a DNA free kit (Ambion). This was performed by adding 40µl master mix containing 33µl RNase free water, 2µl Superase, 4µl 10X DNaseI buffer and 1µl DNaseI followed by 20-30 min incubation at 37°C. 4µl of inactivation reagent was then added and mixed with each sample, followed by incubation at room temperature for 2min and centrifuged at 10000g for 2min at 4°C. 35µl supernatant containing isolated RNA was retained for cDNA synthesis. RNA concentration was assessed using a NANODROP ® Spectrophotometer ND-1000 with ND-1000 v3.3.1 software. The quality of RNA was determined by running a 1% agarose gel. RNA was stored at -80°C.

7.9 Complementary DNA (cDNA) synthesis

Total RNA isolated was reverse transcribed into transcribed into complementary DNA with ThermoScript kit (Invitrogen) following the manufacturer's instructions. For each reaction, 50-250ng of random hexamers (primer) and 2µl of 10mM dNTP mix was mixed with 2.2µg of RNA and sterile water was added to make total volume of 12ul. For all the samples treated with proteasome inhibitor, 0.03µg of a 'spike' RNA with a unique sequence (generously provided by N. Dillon) was added per reaction as previously described (Szutorisz *et al*., 2006). The reaction mixture was incubated for 5 min at 65°C and then placed on ice. Subsequently 1µl sterile DEPC-treated water, 4µl of 5X cDNA synthesis buffer, 1µl of 0.1M DTT, 1µl of ThermoScriptTM reverse transcriptase (15U/µl) and 1µl RNAseOUT (ThermoFischer) were added to each reaction mix giving final volumes of 20µl. Next, the

samples were incubated at 25°C for 10 minutes, 50°C for 50 minutes, 5 minutes at 85°C and finally 30 seconds at 4°C. Samples were stored at - 20°C. cDNA samples were diluted 7 fold and analysed by qPCR.

7.10 Quantitative real time polymerase chain reaction (qPCR)

qPCR was performed to analyse products generated by chromatin immunoprecipitation (ChIP) using the SYBR® Green Jumpstart™ Taq ReadyMix™ (Sigma-Aldrich®) or SensiMix™ (Bioline) in low-profile 96-well white PCR plates (BIORAD). A single qPCR reaction composed by 10µl of SYBR® Green Jumpstart™ Taq ReadyMix (Sigma) or 10µl SensiMix™, 5µl primer mix containing 1mM of specific forward primer and 1mM of specific reverse primer (detailed primer sequences are shown in supplementary tables S2, S3) and 5µl DNA sample giving a total volume of 20µl. cDNA samples were prepared in triplicate and ChIP samples in duplicate. The PCR reaction was run using Chromo4 DNA engine (MRJ) with Opticon Monitor 3 (BioRad) software. The following PCR programmes were used for specific purposes:

qPCR program for ChIP analysis:

Initial step:	95℃	10min	(incubation)
40 cycles:	95℃	30sec	(denaturation)
	58℃	30sec	(annealing)
	72°C	30sec	(extension)
	Plate Read		
	80°C	1sec	
	Plate Read		
	82°C	1sec	
	Plate Read		
	85°C	1sec	
	Plate Read		

Melting curve read from 70℃ to 96℃, read every 0.5℃ - hold 1sec

qPCR program for RNA expression analysis:

Initial step:	94℃	2min	(incubation)
40 cycles:	94℃	30sec	(denaturation)
	58℃	30sec	(annealing)
	72°C	30sec	(extension)
	Plate Read		
	80°C	1sec	
	Plate Read		
	82°C	1sec	
	Plate Read		
	85°C	1sec	
	Plate Read		

Melting curve read from 70℃ to 95℃, read every 0.5℃ - hold 1sec

At the end of the amplification reaction, the threshold was arbitrarily set on the linear part of the logarithmic scale and the cycle threshold (Ct) values were imported from Opticon Monitor 3 to MS excel software upon checking the melting curves.

All the relative RNA expression analysis was calculated using delta/delta-Ct method, in which the obtained Ct values were normalised to spike or housekeeping genes *GAPDH or HPRT*. The RNA expression analysis for all of the samples treated with proteasome inhibitor MG132 were normalised to spike as the treatment of cells with proteasome inhibitor caused a clear reduction of the examined housekeeping gene (*GAPDH, HPRT, BACTIN*) expression (data not shown). For all the remaining samples, (including mouse treated with PS341) the Ct values were normalised to *GAPDH* or *HPRT* (clinical trial). Normalisation to spike or *GAPDH*/*HPRT* was used (i) to improve the accuracy of quantification and (ii) as an internal control to correct for potential differences in reverse transcription efficiency.

The ChIP analysis was calculated using delta/delta-Ct method in which the obtained Ct values were normalised to histone H3 occupancy or input along the examined locus. This value was further subtracted from the signal obtained from the no-antibody control. For the clinical trial, to internally control for variation in ChIP efficiency, enrichment levels were normalised against those obtained from heterochromatic ALRsat repeats for H3K9me3 whereas normalisation for H3 pan-acetylation was performed by using the average enrichment levels of active housekeeping genes *GAPDH, ALDOA, HMBS* and *HPRT*.

The RNA half-lives were calculated after normalising to housekeeping genes, using a nonlinear regression model of multi-phase exponential decay which was run on MS Excel (PC, 2011) to obtain the best fit parameters. Fitted values were then plotted in Python (version 3.5) along with actual values which were represented as dots with error bars.

7.11 Analysis of frataxin protein

The organic pink phase containing protein was obtained after Trizol extraction of RNA. Frataxin (FXN) protein was quantified using Frataxin Dipstick Assay Kit (Mitosciences), following the manufacturer's instructions. Absolute FXN values were obtained as pg using a standard curve generated by the recombinant FXN protein (Mitosciences #MSF42). Total protein concentrations were analysed using QuantiPro™ BCA assay kit (Sigma). Final FXN protein values calculated as pg of FXN per 1 µg of total protein.

7.12 Western blot

For adherent cells (~3X10^6), culture medium was aspirated from the culture plate and cells were washed 1X with PBS. The lysis of cells was performed by adding 500µl RIPA buffer directly to the culture plate followed by incubation for 5min at 4^{o}C. Next, cells were gently scraped off the plate using a cell scraper and the cell lysate was transferred to an Eppendorf tube. The tube was then centrifuged at 12000g for 15min at 4^{o}C and the supernatant was collected and stored at -20^{o}C.

For EBV cell lines, 10X10^6 cells were transferred to an Eppendorf tube and washed 2X with PBS. The lysis of EBV cells was performed by resuspending the cell pellet in 500µl of ice cold lysis buffer followed by rotation for 10min at 4^{o}C. The sample was centrifuged at 12000g for 15min at 4^{o}C and the supernatant was collected and stored in -20^{o}C.

The protein concentration for each sample was determined by Bradford dye colorimetric assay (Bio-rad), following the manufacturer's instructions. The protein concentration was calculated based on a standard curve of Bovine Serum Albumin (BSA) dilution standards.

For protein denaturation, lysate samples with specific amounts of protein were mixed with 6X Laemmli buffer (Alfa Aesar) followed by incubation at 100°C for 10min. 5-10µg of protein

and 5-10µl of Precision Plus Protein Dual colour Standard (Bio-Rad) molecular weight marker were loaded on a Polyacrylamide Gel (SDS-PAGE gel). The gel was then run in 1X running buffer (Bio-Rad) at 150 Volts.

When the electrophoresis was completed, the proteins were electrotransferred from the SDS-PAGE gel to 0.2µm nitrocellulose membrane (Bio-Rad) (for HSF1) or methanol pre-washed PVDF membrane (GE Healthcare) (for HP1α and RNAPII) in the presence of Transfer buffer containing 0%-0.05% SDS. After transfer, the membrane was blocked in TBST+5% non-fat milk (for HSF1), PBST+5% non-fat milk (for HP1α), blocking buffer+5% non-fat milk (for RNAPII) for 1h at RT. Next, the membrane was incubated with an appropriate dilution of the primary antibody (Supplementary table 3) in TBST+5% BSA (for HSF1), PBST+5% non-fat milk (for HP1α) and blocking buffer+5% non-fat milk (for RNAPII) on a rocking platform overnight at 4^{o}C. Next day, the membrane was washed 3 times for 15min at RT each with TBST (For HSF1), PBST (for HP1α) or 1h at RT with blocking buffer+5% non-fat milk (for RNAPII). Subsequently, the secondary antibody conjugated with Horse Radish Peroxidase (HRP) was added at an appropriate dilution (see supplementary table S4) in TBST+5% non-fat milk (for HSF1), PSBT+5% non-fat milk (for HP1α), blocking buffer+5% non-fat milk (for RNAPII) and incubated for 1h at RT. Following incubation, the membrane was washed 3 times for 15min at RT each with TBST (for HSF1), PBST (for HP1α) or 2 times for 30 min in RT with blocking buffer and PBST (for RNAPII). The presence of HRP on the membrane was then detected using ECL Plus Western Blotting Detection Reagents (GE Healthcare) using the manufacturer's instructions.

7.13 Propidium Iodide (PI) staining for cell cycle analysis

Adhering cells were trypsinised, washed with PBS and 1X10^6 cells and were resuspendend in 100µl of PBS. Drop by drop, cells were added into 1ml of ice cold 70% ethanol (pre-stored at -20^{o}C) and incubated overnight at -20^{o}C. The following day, the sample was centrifuged at 600g for 5min at 4^{o}C and supernatant was discarded. The fixed cell pellet was washed once with PBS and centrifuged at 600g for 5min at 4^{o}C. Subsequently, the pellet was resuspended in 250µl PBS containing 5µl RNAse A (10mg/ml) and incubated at 37^{o}C for 30min. Then cells were washed with 1ml PBS, spun down and resuspended in 350µl Propidium Iodide (PI)

solution (50µg/ml) (Millipore). Cells were analysed with fluorescent activated cell sorter (FACS) LSR (10000 events per sample) and gated according to single-cell population and to DNA content representative of the cell cycle.

7.14 Counterflow centrifugal elutriation

Cell cycle separation was conducted using an elutriation system with JE-5.0 elutriator rotor (Beckmann Coulter Inc) equipped with Avanti J-26 XP centrifuge (Beckmann Coulter Inc) and a pump. This system consists of a device that uses constant centrifugal force and gradually increases the counterflow rate in order to separate cells based on their size, which correlates well with the cell cycle stage (Banfalvi, 2008).

2X10^8 cells were harvested and washed twice with Elutriation buffer. In order to obtain a single cell suspension the cell pellet was resuspended in 40ml Elutriation buffer and passed twice through an 18-gauge needle (25G) syringe. Next, the sample was loaded into the pre-assembled elutriation chamber. Throughout the elutriation process the centrifuge was maintained at a constant speed of 1700rpm at 4^{o}C. To obtain elutriation fractions, the flow rate of the elutriation buffer (regulated by a pump connected to the chamber) was increased from 8ml/min to 20ml/min by 1ml/min increments. Consecutively 200ml effluent volumes were collected from the centrifuge for each flow rate and cells were pelleted by centrifugation at 300g for 5min at 4^{o}C. To assess the quality of synchronization in each elutriated fractions, cells were stained with PI followed by FACS analysis (see above). Based on the cell cycle profile similarity, elutriation fractions were further pooled and categorised into 5 different fractions. From each fraction (i) RNA was isolated followed by q-RT-PCR and/or (ii) cells were stained by DRAQ5 followed by imaging using Imagestream. The experimental workflow is shown in Figure 7.1.

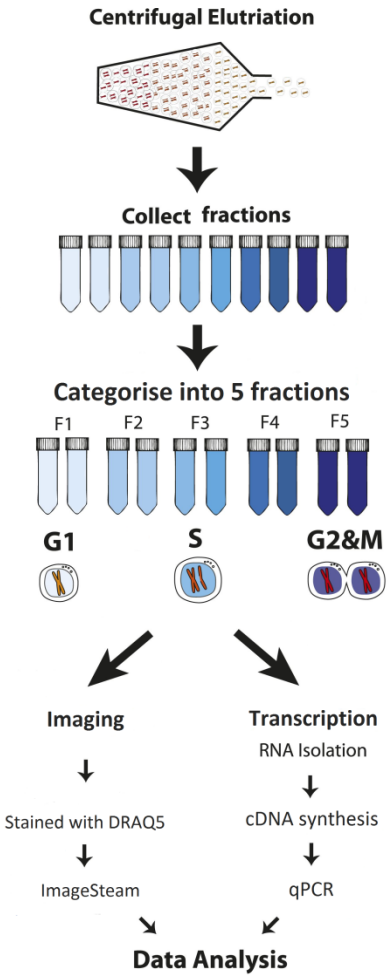


Figure 7.1: Experiment workflow for elutriation. NIH3T3 cells were harvested and fractionated by cell size using centrifugal elutriation. The different fractions obtained were pooled and categorised based on their cell cycle similarity which was measured by PI staining into 5 distinct fractions. From each fraction RNA was extracted followed by q-RT-PCR or/and the cells were stained with DRAQ5 followed by imaging using Imagestream. The image was adapted and modified from (Ly *et al*., 2014)

7.15 Immunofluorescence

NIH3T3 cells were grown and treated when necessary, directly on coverslips placed into a culture plate. Subsequently coverslips were transferred from culture plate to petri dish and washed twice with cold PBS. To fix the cells, coverslips were incubated in 4% paraformaldehyde (PFA) diluted in PBS containing 0.1% (v/v) Triton X100 for 15 min at RT. Following incubation, the fixative was aspirated and coverslips were washed with 2XPBS for

three times and 1XPBS twice. Next, fixed cells were permeabilised with 0.5% (v/v) Triton X100 diluted in PBS for 30min at RT. This was followed by three washes in 1X PBS and incubation of coverslips in 20mM Glycine dissolved in PBS for 30min at RT. Then the non-specific antibody binding sites were blocked by incubating the coverslips in PBS+ blocking solution for 1h at RT. Subsequently, cells on the coverslip were incubated with 80µl of primary antibody appropriately diluted (Supplementary table S4) in PBS+ in a dark humidified chamber overnight at 4^{o}C. On the following day, the coverslips were washed by immersing in 3 consecutive cups containing PBS+. Next, cells were incubated in fluorochrome-conjugated (Alexa488 or Alexa568) secondary antibody diluted to the required concentration in 1XPBS for 1h at RT in a dark humidified chamber. Coverslips were washed by immersing in 9 consecutive cups containing PBS. Each washed coverslip was further incubated with DAPI diluted in 1:1000 in PBS for 15min at RT in the dark. Finally the coverslips were washed three times in 1XPBS for 3min each and mounted on the microscope slides using Vectashield mounting medium (Vector Laboratories).

Images were acquired with Leica Microsystems SP5 confocal microscope and Leica FISH microscope. Analysis of images was performed by Fiji Image J software.

7.16 RNA *in situ* hybridization (RNA-FISH)

RNA *in situ* hybridization (RNA-FISH) was performed using ViewRNA^{TM} ISH Cell Assay kit (Affymetrix Panomics) following the manufacturer's instructions. The images were acquired with a 63X oil-immersion lens using a Leica Microsystems SP5 confocal microscope. Analysis of images was performed by Fiji Image J software.

RNA probe:

Major satellite RNA probe set was designed and produced by Panomics (Affymetrix) probe developers. This probe was *V00846* – Mouse Satellite DNA sequence – type 1 (conjugated with Alexa546).

7.17 Chromocentre cluster analysis by Imagestream X

The ImageStreamX (Amnis, Seattle, Washington) is a combination of a flow cytometer and a digital fluorescence microscope that allows living cells to be directly imaged individually in suspension.

5X10^5 cells were pelleted and washed twice in cold PBS containing 1mM EDTA and 0.02% (w/v) Sodium Azide (PBS++). Next cells were resuspended in 100µl of 1µM DRAQ5 dissolved in PBS++. Samples were placed on ice and kept in the dark until imaging. 20000 cells were collected at 40X magnification using 658nm laser wavelength. Results were quantitated using the associated Image Data Exploration and Analysis software (IDEAS Amnis). After single cell and DRAQ5 fluorescence gating, the number of chromosome clusters per cell was determined by computing the intensity of localized bright spots within the image that were greater than 2.75 pixels in radius. Results were transferred to Microsoft Office Excel 2013, and plotted for analysis. Detailed analysis of the gating strategy is shown in Supplementary figure S2.

7.18 Lentivirus-mediated short hairpin RNA (shRNA) knockdown

HSF1 shRNAs, Scramble shRNA (unspecific shRNA) cloned into the pGIPZ vector as well as pGIPZ vector without any shRNA (GE Dharmacon) were provided as E.coli stock cultures. A single colony from each stock culture was picked and streaked on a different petri dish containing LB Agar growth medium supplemented with 100µg/ml Ampicillin. The petri dishes were incubated overnight at 30^{o}C. Following incubation, a single colony was tooth-picked from each dish and placed into a 15ml snap falcons containing 2ml Low salt LB medium supplemented with 100µg/ml Ampicillin and 25µg/ml Zeocin. Samples were incubated on a shaking platform overnight at 30^{o}C. Next day, 500µl of each sample was used to extract the vector DNA using a MiniPrep kit (Qiagen) according to the manufacturer's instructions. Constructs were then digested with SacII restriction enzymes and run out on a gel. If the digestion pattern was as expected (band sized: 1259 bp, 2502 bp, 7927 bp), 500µl of "snap" culture samples were transferred into 2L flasks containing 500ml Low salt LB with 100µg/ml Ampicillin. Cultures were then incubated on a shaking platform (~150rpm) overnight at 30^{o}C. The following day samples were centrifuged at 5000

rpm for 15min at 4^{o}C. The constructs were purified using High-speed Maxi extraction kit (Qiagen) following the manufacturer's instructions and further checked via SacII digestion.

Lentivirus particles were produced in the HEK293T cell line culture in 100mm culture dishes. The transfection of HEK293T cells was performed using transfection mix containing 20µg of construct, 2µg of the envelope vector (pMD2.G), 8µg of packaging vector (psPAX2) and 90µl of polymer PEI (1mg/ml) in a final volume of 1ml. The mix was initially incubated for 20min at RT before adding to HEK293T cells. Cells were then incubated with transfection mix for 5h at 37^{o}C. Following incubation, the mix was replaced with fresh DMEM culture medium and incubated overnight at 37^{o}C. The following day medium was again replaced with 8ml of fresh DMEM culture medium. 48h after transfection, cells were examined for GFP under the fluorescence microscope (Supplementary figure S4) and if a green signal was detected, the medium from culture dish was collected and filtered in a 0.45µm filter. ~7 ml of virus containing medium was supplemented with PEG to a final concentration of 8µg/ml. The mix was used to transduce NIH3T3 cells cultured in a 6-well plate (~1X10^5 cells per well). After an overnight incubation, the medium was replaced. 48h after infection, cells were examined for GFP under the fluorescence microscope (Supplementary figure S5) and if green signal was detected, transduced cells were then selected with 2µg/ml of puromycin.

7.19 Materials and Reagents

1X Phosphate buffered saline (PBS): 171mM NaCl, 3.3M KCl, 10.1mM Na_2PO_4, 1.8 mM KH_2PO_4

Tris-buffered saline (TBS): 50 mM Tris-Cl, pH 7.5, 150 mM NaCl

Lysis buffer for genotyping: 0.1M Tris HCl (pH 8.0), 5mM EDTA (pH 8.0), 0.2M NaCl, 0.2% SDS, proteinase K (Roche,200 µg/ml, freshly added each time)

IP buffer: 150 mM NaCl, 50 mM Tris-HCl (pH 7.5), 5 mM EDTA, NP-40 (0.5% vol/vol), Triton X-100 (1.0% vol/vol). When necessary, add freshly 0.5µl P8430 Protease inhibitor cocktail (Sigma) and 5µl 0.1M PMSF in isopropanal per 1 ml of IP buffer.

Swelling buffer: 25 mM HEPES pH 7.9, 1.5 mM $MgCl_2$, 10mM KCl, 2.5% NP-40. Adjust pH to 7.9. When necessary, add freshly 0.5µl P8430 Protease inhibitor cocktail (Sigma) and 5µl 0.1M PMSF in isopropanal per 1 ml of Swelling buffer.

Sonication buffer: 50 mM HEPES pH 7.9, 140 mM NaCl, 1mM EDTA, 1% Triton X-100, 0.1% Na-deoxycholate, 0.1% SDS. Adjust pH to 7.9. When necessary, add freshly 0.5µl P8430 Protease inhibitor cocktail (Sigma) and 5µl 0.1M PMSF in isopropanal per 1 ml of Sonication buffer.

Wash buffer A: 50 mM HEPES pH 7.9, 500 mM NaCl, 1mM EDTA, 1% Triton X-100, 0.1% Na-deoxycholate, 0.1% SDS. Adjust pH to 7.9

Wash buffer B: 20 mM Tris pH 8.0, 1 mM EDTA, 250 mM LiCl, 0.5% NP-40, 0.5% Na-deoxycholate. Adjust pH to 8.0.

IgM antibody wash buffer: 2 mM Tris pH 8.0, 0.02 mM EDTA, 50 mM LiCl, 0.1% NP-40, 0.1% Na-deoxycholate. Adjust pH to 8.0

TE buffer: 10 mM Tris pH 8.0, 1mM EDTA

RIPA buffer: 50mM Tris pH 8.0, 150mM NaCl, 0.5% Na-deoxycholate, 1% NP-40, 0.1% SDS. Freshly were added 0.5µl P8430 Protease inhibitor cocktail (Sigma) and 5µl 0.1M PMSF in isopropanal per 1 ml of RIFA buffer.

Lysis buffer (western blot): 50mM Tris-HCl pH 7.5, 1mM EDTA, 10% glycerol, 50mM NaF, 5mM sodium pyrophosphate, 1% Triton. Add freshly 1mM DTT (stock 1M, 1:1000 dilution), 0.1mM PMSF (stock 0.1M, 1:1000 dilution), Na_3VO_4 in a 1:100 dilution.

Running buffer: 25 mM Tris pH8.3, 190 mM glycine, 0.1% SDS

Transfer buffer: 25mM Tris pH 8.3, 190mM glycine. Add freshly 20% (v/v) methanol and if necessary 0-0.05% (v/v) SDS.

Blocking buffer: 10mM Tris HCl pH8, 150mM NaCl, 0.1% Tween 20

PBST: 0.1% (v/v) Tween 20 in 1X PBS

TBST: 0.1% (v/v) Tween 20 in 1X TBS

Elutriation buffer: 3.4mM EDTA and 1% FBS in 1X PBS.

PBS+ Blocking Solution: 1%BSA, 10% Casein, 5% Fish Skin Gelatin in 1X PBS. pH7.8-8.

APPENDIX

SUPPLEMENTARY FIGURES

Supplementary figure 1

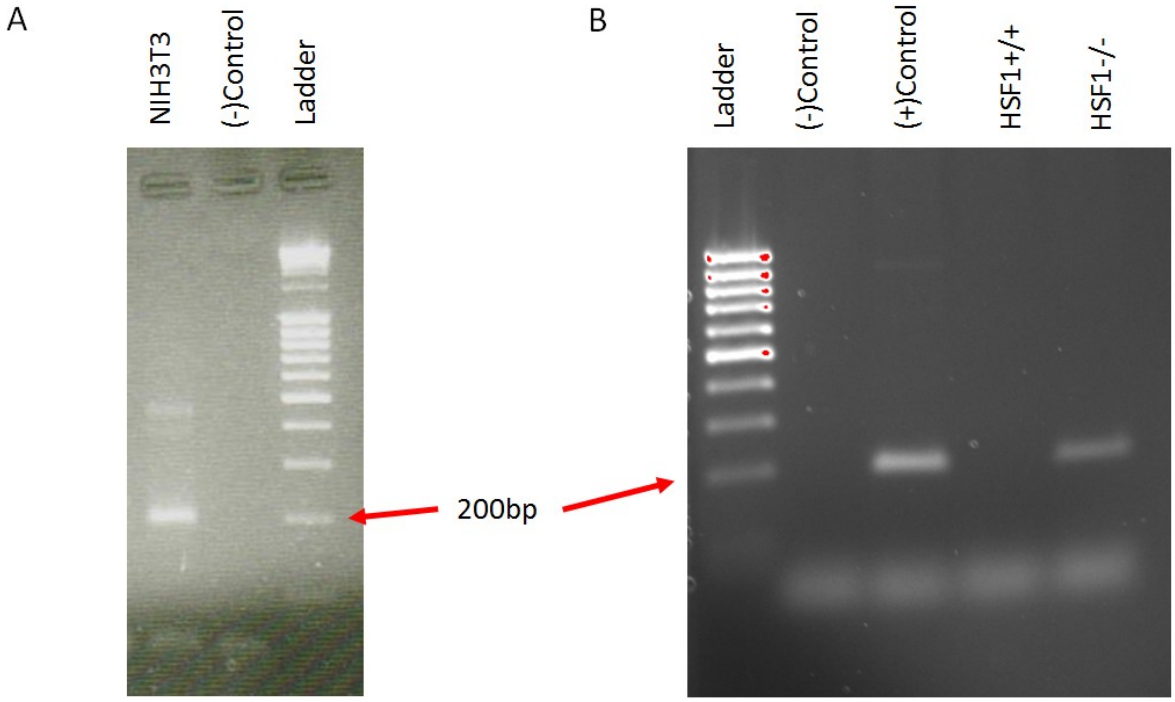


Figure S1: Sex determination in (A) NIH3T3 cells and (B) HSF1+/+ and HSF1-/- iMEFs. Lane ladder represent DNA size marker (MassRuler, Fermentas); lane (-) control represent the negative control (reaction with all the reagents except the genomic material); lane (+)control represent a positive PCR reaction from the genomic DNA derived from a known male mouse. The presence of 194bp band indicated male sex *SRY* gene (NIH3T3 and HSF1-/-), whereas the absence of the band shows female (HSF1+/+) sex.

Supplementary figure 2

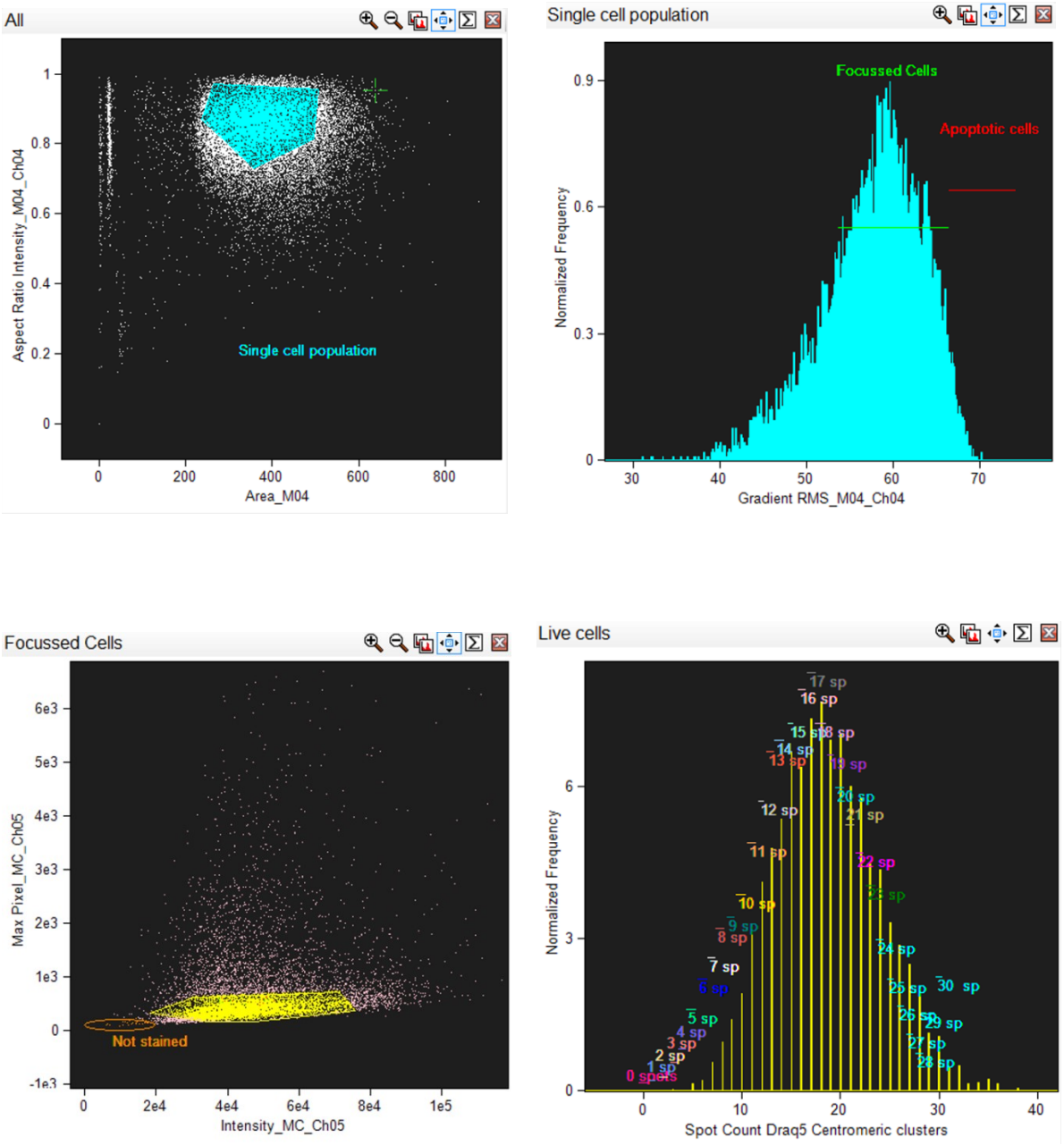


Figure S2: Gating strategy for the ImageStreamX analysis. The single cell population was gated, followed by gating of focused cells and further gating of stained cells. The number of chromocentres was determined by computing the intensity of localized bright spots within the image that were 2.75 pixels in radius. Results were transferred to Microsoft Office Excel 2013 and plotted for analysis.

Supplementary figure 3

A

```
CLUSTAL O(1.2.1) multiple sequence alignment

major      GGACCTGGAATATGGCGAGAAAACTGAAAATCACGGAAAATGAGAAATACACACTTTAGG
mHSF1      ------------------------------------------------------------

major      ACGTGAAATATGGCGAGGAAAACTGAAAAAGGTGGAAAATTTAGAAATGTCCACTGTAGG
mHSF1      ----------------------------------------aGAAnnTTCg--------
                                                   ****   **

major      ACGTGGAATATGGCAAGAAAACTGAAAATCATGGAAAATGAGAAACATCCACTTGACGAC
mHSF1      ------------------------------------------------------------

major      TTGAAAAATGACGAAATCACTAAAAAACGTGAAAAATGAGAAATGCACACTGAA
mHSF1      ----------------------------------------------------
```

B

```
CLUSTAL O(1.2.1) multiple sequence alignment

Minor      TTGTAGAACAGTGTATATCAATGAGTTACAATGAGAAACATGGAAAATGATAAAAACCAC
mHSF1      ------------------------------------------------------------

Minor      ACTGTAGAACATATTAGATGAGTGAGTTACACTGAAAAACACATTCGTTGGAAACGGGAT
mHSF1      ------------------------------------aGAAnnTTCg-------------
                                               *  *  ****


CLUSTAL O(1.2.1) multiple sequence alignment

Minor      TTGTAGAACAGTGTATATCAATGAGTTACAATGAGAAACATGGAAAATGATAAAAACCAC
mHSF1      ---------------------------------nGAAnnTTCnn----------------
                                            ***   *

Minor      ACTGTAGAACATATTAGATGAGTGAGTTACACTGAAAAACACATTCGTTGGAAACGGGAT
mHSF1      ------------------------------------------------------------
```

Figure S3: Alignment of a portion of (A) pericentromeric major satellite and (B) centromeric minor satellite consensus sequence with the canonical binding sequence of the HSF1 transcription factor. Capital letters define the most important bases and n=T, C, A or G.

Supplementary Figures 4 and 5

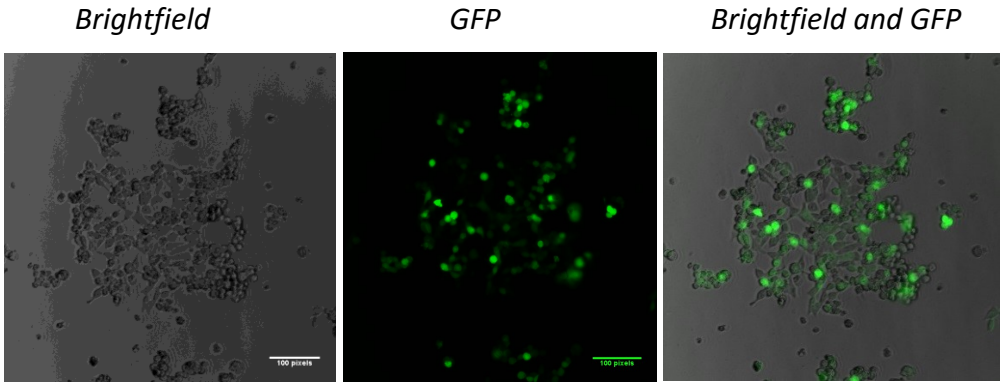


Figure S4: Representative images of the HEK293T transfection with shRNA vector containing GFP gene for assessing the efficiency of transduction. The GFP signal was checked 48h after transfection by fluorescence microscope.

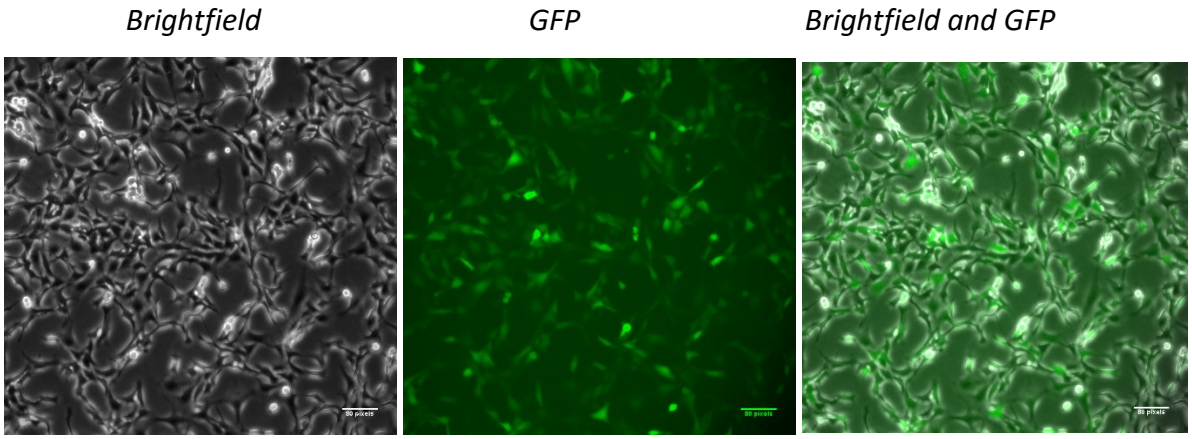


Figure S5: Representative images of NIH3T3 cells after lentiviral infection. The GFP signal was checked 48h after infection by fluorescence microscope.

SUPPLEMENTARY TABLES

Supplementary table 1: A summary from chromatin features of the *FXN* gene. Adapted and modified from (Yandim *et al*., 2013).

Region / Paper	**Promoter/5UTR**	**Upstream of GAA repeats**	**Downstream of GAA repeats**
Li *et al*., 2015		Fibroblast cell line H4K5ac ↓ H4K20me1 • H4K20me3 ↑	Fibroblast cell line H4K5ac ↓ H4K20me1 ↓ H4K20me3 ↑
Evans-Galea *et al*., 2012	Human Primary cells DNA methylation •	Human Primary cells DNA methylation ↑	Human Primary cells DNA methylation ↓
Kim *et al*., 2011	Lymphoblastoid cell lines H3K4me2 • H3K4me3 • H3K36me3 • H3K79me2 • H3K9ac • H3K14ac • H3K9me3 • H4K20m3 • H3K27me3 •	Lymphoblastoid cell lines H3K4me2 ↓ H3K4me3 ↓ H3K36me3 • H3K79me2 ↓ H3K9ac ↓ H3K14ac ↓ H3K9me3 ↑ H4K20m3 ↑ H3K27me3 ↑ HEK293 cell line inserted with GFP_(GAA)^ construct H3K9ac ↓ H3K14ac ↓ H3K9me3 ↑ H3K4me3 ↓ H3K79me2 ↓	Lymphoblastoid cell lines H3K4me2 • H3K4me3 • H3K36me3 • H3K79me2 ↓ H3K9ac • H3K14ac • H3K9me3 • H4K20me3 • H3k27me3 • HEK293 cell line inserted with GFP_(GAA)^ construct H3K9ac ↓ H3K14ac ↓ H3K9me3 ↑ H3K4me3 ↓ H3K79me2 ↓
Kumari *et al* . 2011	Lymphoblastoid cell lines H4K16ac ↓ H4K5ac ↓ H3K9ac • H3K14ac • H3K4me2 ↓ H3K36me3 •	Lymphoblastoid cell lines H4K16ac ↓ H4K5ac ↓ H3K9ac ↓ H3K14ac ↓ H3K4me2 ↓ H3K36me3 •	Lymphoblastoid cell lines H4K16ac ↓ H4K5ac ↓ H3K9ac ↓ H3K14ac ↓ H3K4me2 ↓ H3K36me3 ↓
Punga *et al*., 2010	Lymphoblastoid cell lines H3K9me3 • H3K4me2 • H3K36me3 •	Lymphoblastoid cell lines H3K9me3 ↑ H3K4me2 ↓ H3K36me3 ↓	Lymphoblastoid cell lines H3K9me3 ↑ H3K4me2 ↓ H3K36me3 ↓
De Biase *et al*., 2009	FRDA Fibroblast cell line H3K9me3 ↑ H3K27me3 ↑		

Al-Mahdawi *et al*., 2008	Human Brain tissue DNA methylation • H3K9ac • H3k14ac • H4K5ac • H4K8ac ↑ H4K12ac • H4K16ac • H3K9me2 ↑ H3K9me3 ↑ Human Heart tissue DNA methylation ↑ *FXN* transgenic mouse brain tissue DNA methylation • H3K9ac • H3K14ac • H4K5ac • H4K8ac • H4K12ac • H4K16ac ↑ H3K9me2 ↑ H3K9me3 ↑ *FXN* transgenic mouse heart tissue DNA methylation ↓	Human Brain tissue DNA methylation ↑ H3K9ac ↓ H3K14ac • H4K5ac • H4K8ac • H4K12ac • H4K16ac • H3K9me2 ↑ H3K9me3 ↑ Human Heart tissue DNA methylation ↑ Human cerebellar tissue DNA methylation ↑ *FXN* transgenic mouse cerebellar tissue DNA methylation ↑ *FXN* transgenic mouse brain tissue DNA methylation ↑ H3K9ac ↓ H3K14ac • H4K5ac • H4K8ac • H4K12ac H4K16ac ↑ H3K9me2 ↑ H3K9me3 ↑ *FXN* transgenic mouse heart tissue DNA methylation ↑	Human Brain tissue DNA methylation ↓ H3K9ac ↓ H3K14ac ↓ H4K5ac ↓ H4K8ac ↓ H4K12ac ↓ H4K16ac ↓ H3K9me2 ↑ H3K9me3 ↑ Human Heart tissue DNA methylation ↓ *FXN* transgenic mouse brain tissue DNA methylation • H3K9ac ↓ H3K14ac • H4K5ac • H4K8ac • H4K12ac H4K16ac ↑ H3K9me2 ↑ H3K9me3 ↑ *FXN* transgenic mouse heart tissue DNA methylation •
Soragni *et al* 2008		HEK293 cell line inserted with GFP_(GAA)^ construct H3K9ac ↓ H3K14ac ↓ H4K5ac ↓ H4K8ac ↓ H3K9me3 ↑	HEK293 cell line inserted with GFP_(GAA)^ construct H3K9ac ↓ H3K14ac ↓ H4K5ac ↓ H4K8ac ↓ H3K9me3 ↑
Herman *et al*., 2006	Lymphoblastoid cell lines H3K9ac • H3K14ac • H4K5ac • H4K8ac • H4K12ac • H4K16ac •	Lymphoblastoid cell lines H3K9ac ↓ H3K14ac ↓ H4K5ac ↓ H4K8ac ↓ H4K12ac ↓ H4K16ac ↓ H3K9me1 ↓ H3K9me2 ↑ H3K9me3 ↑	Lymphoblastoid cell lines H3K9ac ↓ H3K14ac • H4K5ac ↓ H4K8ac ↓ H4K12ac ↓ H4K16ac ↓

Supplementary table 2: List of primers for Chapter 2 and 3

Purpose	Primer name	primer sequence (5' to 3')
RNA expression	FXN_F (clinical trial)	CCCGCCGCGCAAGTTC
	FXN_R (clinical trial)	CTGCAAGGTCTTCAAAAAACTCTG
	FXN_F	ATGTCTCCTTTGGGAGTGGTGTCT
	FXN_R	CCCAGTCCAGTCATAACGCTTAGGT
	Primary FXN_F	AGCCCCACATTCTCAGACAC
	Primary FXN_R	ACGCACCAAAGGGTAACTTG
	YG8 mouse FXN_Ex3Ex4_F	ATGTCTCCTTTGGGAGTGGTGTCT
	YG8 mouse FXN_Ex3Ex4_F	CCCAGTCCAGTCATAACGCTTAGGT
	Human GAPDH_F	GGAGCGAGATCCCTCCAAAAT
	Human GAPDH_R	GGCTGTTGTCATACTTCTCATGG
	c_MYC_F	AAACACAAACTTGAACAGCTAC
	c_MYC_R	ATTTGAGGCAGTTTACATTATGG
	Mouse GAPDH_F	AACTTTGGCATTGTGGAAGG
	Mouse GAPDH_R	ACACATTGGGGGTAGGAACA
	Major_F	GACGACTTGAAAAATGACGAAATC
	Major_R	CATATTCCAGGTCCTTCAGTGTGC
	Minor_F	CATGGAAAATGATAAAAACC
	Minor_R	CATCTAATATGTTCTACAGTGTGG
	HPRT_F	CCCTGGCGTCGTGATTAGT
	HPRT_R	GAGCACACAGAGGGCTACAA
	Spike_F	GAGGGCCATACATGGTGGT
	Spike_R	CTCTAACCACTGGCGCCTTA
ChIP	FXN_UpsP1_F	GGGATTTCTTTTCCCCAGAG
	FXN_UpsP1_R	ACCTTGCAGGACACCAAAAC
	FXN_U2_F	CCCCACATACCCAACTGCTG
	FXN_U2_R	GCCCGCCGCTTCTAAAATTC
	FXN_Ex1_F	GGAGCAGCATGTGGACTCTC
	FXN_Ex1_R	CGGCGCGGATACTTACTG
ChIP	FXN_IntP1_F	CTCCCGGTTGCATTTACACT
	FXN_IntP1_R	GTGACAAGCATGGAGACAGC
	FXN_IntP2_F	CTGACCCGACCTTTCTTCCA
	FXN_IntP2_R	TGGGCGTCACCTTTATCTTC

	FXN_IntP3_F	GAAACCCAAAGAATGGCTGTG
	FXN_IntP3_R	TTCCCTCCTCGTGAAACACC
	FXN_IntP4_F	CTGGAAAAATAGGCAAGTGTGG
	FXN_IntP4_R	CAGGGGTGGAAGCCCAATAC
	FXN_IntP5_F	CCCTTGCACATCTTGGGTAT
	FXN_IntP5_R	GAGAAAAGGGTGGGGAAGAG
	FXN_IntP6_F	AGCCCCACATTCTCAGACAC
	FXN_IntP6_R	ACGCACCAAAGGGTAACTTG
	β_globin_F	GCTGGTGGTCTACCCTTGGA
	β_globin_R	AGGTTGTCCAGGTGAGCCAG
	GAPDH_ChIP_F	CACCGTCAAGGCTGAGAACG
	GAPDH_ChIP_R	ATACCCAAGGGAGCCACACC
	ALDOA_F	CTCCTCCCTGAAGAGCCTTT
	ALDOA_R	CCCTGCCCAACTTCAAATAG
	HMBS_F	CTCTGCGGAGACCAGGAGT
	HMBS_R	CGCTTGGAAAGTAGGCTGTG
	HPRT_ChIP_F	CCCTCAGGCGAACCTCTC
	HPRT_ChIP_R	CTGACTGCTCAGGAGGAGGA
	ALRsat_F	AACTCACAGAGTTGAACGATCC
	ALRsat_R	ACCTCAAAGCGGCTGAAAT

Supplementary table 3: List of primers for Chapter 4 and 5

	Primer name	primer sequence (5' to 3')
Genotyping	SRY_F	GCAGGTGGAAAAGCCTTACA
	SRY_R	GTCCCACTGCAGAAGGTTGT
RNA expression	Spike_F	GAGGGCCATACATGGTGGT
	Spike_R	CTCTAACCACTGGCGCCTTA
	GAPDH_F	AACTTTGGCATTGTGGAAGG
	GAPDH_R	ACACATTGGGGGTAGGAACA
	c_MYC_F	GCCCAAATCCTGTACCTCGTCC
	c_MYC_R	CTCTTCTCCACAGACACCACATCA
	HSP70_F	GGTGGTGCAGTCCGACATG
	HSP70_R	TTGGGCTTGTCGCCGT
	HSP90_F	AAAGGCAGAGGCTGACAAG
	HSP90-R	AGGGGAGGCATTTCTTCAGT
	HSF1_F	TGCTGGACATTCAGGAGCTT
	HSF1_R	AAGTAGGAGCTCTCCCCCAG
ChIP	promoter GAPDH_F	AGTCCGTATTTATAGGAACCCGGATGGTGG
	promoter GAPDH_R	ATGAGAGAGGCCCAGCTACTCGCGGCTTTA
	gene body GAPDH_F	GAGCCCTCCCTACTCTCTTGAAT
	gene body GAPDH_R	ACACCGCATTAAAACCAAGGA
	MOG_F	AATATCTGGCAAGGGTGACG
	MOG_R	TATGGTTACCGGGGACAGAG
	HSP70_F	CACCAGCACGTTCCCCA
	HSP70_R	CGCCCTGCGCCTTTAAG
RNA and ChIP	Major_F	GACGACTTGAAAAATGACGAAATC
	Major_R	CATATTCCAGGTCCTTCAGTGTGC
	Minor_F	CATGGAAAATGATAAAAACC
	Minor_R	CATCTAATATGTTCTACAGTGTGG
	LINEL1_F	TTTGGGACACAATGAAAGCA
	LINEL1_R	CTGCCGTCTACTCCTCTTGG
	SINEB1_F	GTGGCGCACGCCTTTAATC
	SINEB1_R	GACAGGGTTTCTCTGTGTAG

Supplementary table 4: List of Antibodies

Antibody/clone name	Purpose	Company	cat #
Histone H3	ChIP (6µg per sample)	Abcam	Ab1791
H3K9me3	ChIP (6µg per sample) IF (1:100)	Millipore	17-625
H3K4me3	ChIP (6µg per sample)	Abcam	Ab8580
H3K36me3	ChIP (3µg per sample)	Abcam	Ab9050
H3ac (K9+K14+K18+K23+K27)	ChIP (6µg per sample)	Abcam	Ab47915
HP1α	IF (1:50) WB (1:500)	Millipore Millipore	05689 MAB3446
HSF1	ChIP (10µg per sample) WB (1:1000)	Santa Cruz Cell Signalling	sc-9144X 4356
Proteasome 20S β6	ChIP (8µg per sample) IF (1:100)	Enzo Life	BML-PW9000
Proteasome 20S C2	ChIP (8µg per sample)	Abcam	Ab3325
S5P-RNAPII (4H8)	ChIP (8µg per sample) IF (1:1000) WB (1:10000)	Millipore	05-623
S2P-RNAPII (H5)	ChIP (18µg per sample) IF (1:50)	Covance	MMS-129R
RNAPII (8WG16)	WB (1:200)	Abcam	Ab817
Gapdh	WB (1:100000)	Abcam	Ab22555
α-Tubulin	WB (1:2000 and 1:10000)	Sigma	T5168
HRP-goat anti mouse	WB (1:20000)	Life Technologies	G21040
HRP-goat anti rabbit	WB (1:20000)	Santa Cruz	SC2004
Alexa488 Goat Anti-Mouse	IF (1:600)	Life Technologies	A11001
Alexa568 Goat Anti-Rabbit	IF (1:600 and 1:200)	Life Technologies	A11011

REFERENCES

Aagaard, L., Laible, G., Selenko, P., Schmid, M., Dorn, R., Schotta, G., . . . Jenuwein, T. (1999). Functional mammalian homologues of the Drosophila PEV-modifier Su(var)3-9 encode centromere-associated proteins which complex with the heterochromatin component M31. *Embo Journal, 18*(7), 1923-1938.

Abbas, T., Shibata, E., Park, J., Jha, S., Karnani, N., & Dutta, A. (2010). CRL4(Cdt2) Regulates Cell Proliferation and Histone Gene Expression by Targeting PR-Set7/Set8 for Degradation. *Molecular Cell, 40*(1), 9-21.

Abdul-Muneer, P. M. (2014). Application of microsatellite markers in conservation genetics and fisheries management: recent advances in population structure analysis and conservation strategies. *Genet Res Int, 2014*, 691759.

Abe, K., Naruse, C., Kato, T., Nishiuchi, T., Saitou, M., & Asano, M. (2011). Loss of Heterochromatin Protein 1 Gamma Reduces the Number of Primordial Germ Cells via Impaired Cell Cycle Progression in Mice. *Biology of Reproduction, 85*(5), 1013-1024.

Abravaya, K., Myers, M. P., Murphy, S. P., & Morimoto, R. I. (1992). The Human Heat-Shock Protein Hsp70 Interacts with Hsf, the Transcription Factor That Regulates Heat-Shock Gene-Expression. *Genes & Development, 6*(7), 1153-1164.

Abravaya, K., Phillips, B., & Morimoto, R. I. (1991). Heat shock-induced interactions of heat shock transcription factor and the human hsp70 promoter examined by in vivo footprinting. *Mol Cell Biol, 11*(1), 586-592.

Adams, J. (2003a). Potential for proteasome inhibition in the treatment of cancer. *Drug Discovery Today, 8*(7), 307-315.

Adams, J. (2003b). The proteasome: structure, function, and role in the cell. *Cancer Treat Rev, 29 Suppl 1*, 3-9.

Adams, J., Palombella, V. J., Sausville, E. A., Johnson, J., Destree, A., Lazarus, D. D., . . . Elliott, P. J. (1999a/b). Proteasome inhibitors: a novel class of potent and effective antitumor agents. *Cancer Res, 59*(11), 2615-2622.

Adelman, K., & Lis, J. T. (2012). Promoter-proximal pausing of RNA polymerase II: emerging roles in metazoans. *Nat Rev Genet, 13*(10), 720-731.

Adinolfi, S., Trifuoggi, M., Politou, A. S., Martin, S., & Pastore, A. (2002). A structural approach to understanding the iron-binding properties of phylogenetically different frataxins. *Hum Mol Genet, 11*(16), 1865-1877.

Adori, C., Low, P., Moszkovkin, G., Bagdy, G., Laszlo, L., & Kovacs, G. G. (2006). Subcellular distribution of components of the ubiquitin-proteasome system in non-diseased human and rat brain. *Journal of Histochemistry & Cytochemistry, 54*(2), 263-267.

Akerfelt, M., Henriksson, E., Laiho, A., Vihervaara, A., Rautoma, K., Kotaja, N., & Sistonen, L. (2008). Promoter ChIP-chip analysis in mouse testis reveals Y chromosome occupancy by HSF2. *Proc Natl Acad Sci U S A, 105*(32), 11224-11229.

Akerfelt, M., Morimoto, R. I., & Sistonen, L. (2010). Heat shock factors: integrators of cell stress, development and lifespan. *Nature Reviews Molecular Cell Biology, 11*(8), 545-555.

Al-Mahdawi, S., Pinto, R. M., Ismail, O., Varshney, D., Lymperi, S., Sandi, C., . . . Pook, M. (2008). The Friedreich ataxia GAA repeat expansion mutation induces comparable epigenetic changes in human and transgenic mouse brain and heart tissues. *Hum Mol Genet, 17*(5), 735-746. doi:10.1093/hmg/ddm346le, P., Carroll, C., Webster, Z., & Pook, M. (2004). GAA repeat instability in Friedreich ataxia YAC transgenic mice. *Genomics, 84*(2), 301-310.

Al-Mahdawi, S., Pinto, R. M., Varshney, D., Lawrence, L., Lowrie, M. B., Hughes, S., . . . Pook, M. A. (2006). GAA repeat expansion mutation mouse models of Friedreich ataxia exhibit oxidative stress leading to progressive neuronal and cardiac pathology. *Genomics, 88*(5), 580-590.

Al-Mahdawi, S., Sandi, C., Mouro Pinto, R., & Pook, M. A. (2013). Friedreich ataxia patient tissues exhibit increased 5-hydroxymethylcytosine modification and decreased CTCF binding at the FXN locus. *PLoS One, 8*(9), e74956.

Alastalo, T. P., Hellesuo, M., Sandqvist, A., Hietakangas, V., Kallio, M., & Sistonen, L. (2003). Formation of nuclear stress granules involves HSF2 and coincides with the nucleolar localization of Hsp70. *J Cell Sci, 116*(Pt 17), 3557-3570.

Alberti, S., Krause, S. M., Kretz, O., Philippar, U., Lemberger, T., Casanova, E., . . . Nordheim, A. (2005). Neuronal migration in the murine rostral migratory stream requires serum response factor. *Proceedings of the National Academy of Sciences of the United States of America, 102*(17), 6148-6153.

Alberts, B. J., A. Lewis, J. Raff, M. Roberts, K. Walter, P. . (2002). *The global structure of chromosomes* (4th edition ed.). Molecular Biology of the Cell.

Alcain, F. J., & Villalba, J. M. (2009). Sirtuin inhibitors. *Expert Opin Ther Pat, 19*(3), 283-294.

Alder, O., Lavial, F., Helness, A., Brookes, E., Pinho, S., Chandrashekran, A., . . . Azuara, V. (2010). Ring1B and Suv39h1 delineate distinct chromatin states at bivalent genes during early mouse lineage commitment. *Development, 137*(15), 2483-2492.

Ali, A., Bharadwaj, S., O'Carroll, R., & Ovsenek, N. (1998). HSP90 interacts with and regulates the activity of heat shock factor 1 in Xenopus oocytes. *Molecular and Cellular Biology, 18*(9), 4949-4960.

Allen, T. A., Von Kaenel, S., Goodrich, J. A., & Kugel, J. F. (2004). The SINE-encoded mouse B2 RNA represses mRNA transcription in response to heat shock. *Nature Structural & Molecular Biology, 11*(9), 816-821.

Allis, C. D., Jenuwein T, Reinberg D. (2007). Epigenetics.

Allshire, R. C., & Karpen, G. H. (2008). Epigenetic regulation of centromeric chromatin: old dogs, new tricks? *Nat Rev Genet, 9*(12), 923-937.

Allshire, R. C., Nimmo, E. R., Ekwall, K., Javerzat, J. P., & Cranston, G. (1995). Mutations derepressing silent centromeric domains in fission yeast disrupt chromosome segregation. *Genes Dev, 9*(2), 218-233.

Alper, B. J., Job, G., Yadav, R. K., Shanker, S., Lowe, B. R., & Partridge, J. F. (2013). Sir2 is required for Clr4 to initiate centromeric heterochromatin assembly in fission yeast. *Embo Journal, 32*(17), 2321-2335.

Amerik, A. Y., & Hochstrasser, M. (2004). Mechanism and function of deubiquitinating enzymes. *Biochimica Et Biophysica Acta-Molecular Cell Research, 1695*(1-3), 189-207.

Amin, J., Ananthan, J., & Voellmy, R. (1988). Key features of heat shock regulatory elements. *Mol Cell Biol, 8*(9), 3761-3769.

Amin, J., Fernandez, M., Ananthan, J., Lis, J. T., & Voellmy, R. (1994). Cooperative binding of heat shock transcription factor to the Hsp70 promoter in vivo and in vitro. *J Biol Chem, 269*(7), 4804-4811.

Andrulis, E. D., Neiman, A. M., Zappulla, D. C., & Sternglanz, R. (1998). Perinuclear localization of chromatin facilitates transcriptional silencing. *Nature, 394*(6693), 592-595.

Anheim, M., Mariani, L. L., Calvas, P., Cheuret, E., Zagnoli, F., Odent, S., . . . Koenig, M. (2012). Exonic Deletions of FXN and Early-Onset Friedreich Ataxia. *Archives of Neurology, 69*(7), 912-916.

Anindya, R., Aygun, O., & Svejstrup, J. Q. (2007). Damage-induced ubiquitylation of human RNA polymerase II by the ubiquitin ligase Nedd4, but not Cockayne syndrome proteins or BRCA1. *Molecular Cell, 28*(3), 386-397.

Aravin, A. A., Sachidanandam, R., Bourc'his, D., Schaefer, C., Pezic, D., Toth, K. F., . . . Hannon, G. J. (2008). A piRNA pathway primed by individual transposons is linked to de novo DNA methylation in mice. *Molecular Cell, 31*(6), 785-799.

Ardehali, M. B., Mei, A., Zobeck, K. L., Caron, M., Lis, J. T., & Kusch, T. (2011). Drosophila Set1 is the major histone H3 lysine 4 trimethyltransferase with role in transcription. *Embo Journal, 30*(14), 2817-2828.

Asher, G., Lotem, J., Sachs, L., Kahana, C., & Shaul, Y. (2002). Mdm-2 and ubiquitin-independent p53 proteasomal degradation regulated by NQ01. *Proceedings of the National Academy of Sciences of the United States of America, 99*(20), 13125-13130.

Asher, G., Tsvetkov, P., Kahana, C., & Shaul, Y. (2005). A mechanism of ubiquitin-independent proteasomal degradation of the tumor suppressors p53 and p73. *Genes Dev, 19*(3), 316-321.

Atkins, K. M., Thomas, L. L., Barroso-Gonzalez, J., Thomas, L., Auclair, S., Yin, J., . . . Thomas, G. (2014). The multifunctional sorting protein PACS-2 regulates SIRT1-mediated deacetylation of p53 to modulate p21-dependent cell-cycle arrest. *Cell Rep, 8*(5), 1545-1557.

Aucott, R., Bullwinkel, J., Yu, Y., Shi, W., Billur, M., Brown, J. P., . . . Singh, P. B. (2008). HP1-beta is required for development of the cerebral neocortex and neuromuscular junctions. *Journal of Cell Biology, 183*(4), 597-606.

Auld, K. L., Brown, C. R., Casolari, J. M., Komili, S., & Silver, P. A. (2006). Genomic association of the proteasome demonstrates overlapping gene regulatory activity with transcription factor substrates. *Molecular Cell, 21*(6), 861-871.

Avalos, J. L., Bever, K. M., & Wolberger, C. (2005). Mechanism of sirtuin inhibition by nicotinamide: altering the NAD(+) cosubstrate specificity of a Sir2 enzyme. *Mol Cell, 17*(6), 855-868.

Azzaz, A. M., Vitalini, M. W., Thomas, A. S., Price, J. P., Blacketer, M. J., Cryderman, D. E., . . . Shogren-Knaak, M. A. (2014). Human Heterochromatin Protein 1 alpha Promotes Nucleosome Associations That Drive Chromatin Condensation. *Journal of Biological Chemistry, 289*(10), 6850-6861.

Babcock, M., deSilva, D., Oaks, R., DavisKaplan, S., Jiralerspong, S., Montermini, L., . . . Kaplan, J. (1997). Regulation of mitochondrial iron accumulation by Yfh1p, a putative homolog of frataxin. *Science, 276*(5319), 1709-1712.

Babushok, D. V., & Kazazian, H. H., Jr. (2007). Progress in understanding the biology of the human mutagen LINE-1. *Hum Mutat, 28*(6), 527-539.

Bachman, K. E., Rountree, M. R., & Baylin, S. B. (2001). Dnmt3a and Dnmt3b are transcriptional repressors that exhibit unique localization properties to heterochromatin. *Journal of Biological Chemistry, 276*(34), 32282-32287.

Badugu, R., Yoo, Y., Singh, P. B., & Kellum, R. (2005). Mutations in the heterochromatin protein 1 (HP1) hinge domain affect HP1 protein interactions and chromosomal distribution. *Chromosoma, 113*(7), 370-384.

Baler, R., Welch, W. J., & Voellmy, R. (1992). Heat-Shock Gene-Regulation by Nascent Polypeptides and Denatured Proteins - Hsp70 as a Potential Autoregulatory Factor. *Journal of Cell Biology, 117*(6), 1151-1159.

Banfalvi, G. (2008). Cell cycle synchronization of animal cells and nuclei by centrifugal elutriation. *Nat Protoc, 3*(4), 663-673.

Bannister, A. J., & Kouzarides, T. (2011). Regulation of chromatin by histone modifications. *Cell Research, 21*(3), 381-395.

Bannister, A. J., Schneider, R., Myers, F. A., Thorne, A. W., Crane-Robinson, C., & Kouzarides, T. (2005). Spatial distribution of di- and tri-methyl lysine 36 of histone H3 at active genes. *Journal of Biological Chemistry, 280*(18), 17732-17736.

Bannister, A. J., Zegerman, P., Partridge, J. F., Miska, E. A., Thomas, J. O., Allshire, R. C., & Kouzarides, T. (2001). Selective recognition of methylated lysine 9 on histone H3 by the HP1 chromo domain. *Nature, 410*(6824), 120-124.

Bar-Nun, S., & Glickman, M. H. (2012). Proteasomal AAA-ATPases: Structure and function. *Biochimica Et Biophysica Acta-Molecular Cell Research, 1823*(1), 67-82.

Bartholdi, M. F. (1991). Nuclear distribution of centromeres during the cell cycle of human diploid fibroblasts. *Journal of Cell Science, 99 (Pt 2)*, 255-263.

Bartolo, C., Mendell, J. R., & Prior, T. W. (1998). Identification of a missense mutation in a Friedreich's ataxia patient: Implications for diagnosis and carrier studies. *American Journal of Medical Genetics, 79*(5), 396-399.

Bartova, E., Pachernik, J., Kozubik, A., & Kozubek, S. (2007). Differentiation-specific association of HP1alpha and HP1beta with chromocentres is correlated with clustering of TIF1beta at these sites. *Histochem Cell Biol, 127*(4), 375-388.

Beaudenon, S. L., Huacani, M. R., Wang, G., McDonnell, D. P., & Huibregtse, J. M. (1999). Rsp5 ubiquitin-protein ligase mediates DNA damage-induced degradation of the large subunit of RNA polymerase II in Saccharomyces cerevisiae. *Mol Cell Biol, 19*(10), 6972-6979.

Beckwith, R., Estrin, E., Worden, E. J., & Martin, A. (2013). Reconstitution of the 26S proteasome reveals functional asymmetries in its AAA plus unfoldase. *Nature Structural & Molecular Biology, 20*(10), 1164.

Bedford, M. T., & Richard, S. (2005). Arginine methylation: An emerging regulator of protein function. *Molecular Cell, 18*(3), 263-272.

Belancio, V. P., Hedges, D. J., & Deininger, P. (2008). Mammalian non-LTR retrotransposons: for better or worse, in sickness and in health. *Genome Res, 18*(3), 343-358.

Bell, O., Wirbelauer, C., Hild, M., Scharf, A. N. D., Schwaiger, M., MacAlpine, D. M., . . . Schubeler, D. (2007). Localized H3K36 methylation states define histone H4K16 acetylation during transcriptional elongation in Drosophila. *Embo Journal, 26*(24), 4974-4984.

Benetti, R., Gonzalo, S., Jaco, I., SChotta, G., Klatt, P., Jenuwein, T., & Blasco, M. A. (2007). Suv4-20h deficiency results in telomere elongation and derepression of telomere recombination. *Journal of Cell Biology, 178*(6), 925-936.

Bensaude, O. (2011). Inhibiting eukaryotic transcription: Which compound to choose? How to evaluate its activity? *Transcription, 2*(3), 103-108.

Bercovich, Z., Rosenberghasson, Y., Ciechanover, A., & Kahana, C. (1989). Degradation of Ornithine Decarboxylase in Reticulocyte Lysate Is Atp-Dependent but Ubiquitin-Independent. *Journal of Biological Chemistry, 264*(27), 15949-15952.

Bergmann, J. H., Jakubsche, J. N., Martins, N. M., Kagansky, A., Nakano, M., Kimura, H., . . . Earnshaw, W. C. (2012). Epigenetic engineering: histone H3K9 acetylation is compatible with kinetochore structure and function. *Journal of Cell Science, 125*(2), 411-421.

Bergmann, J. H., Rodriguez, M. G., Martins, N. M. C., Kimura, H., Kelly, D. A., Masumoto, H., . . . Earnshaw, W. C. (2011). Epigenetic engineering shows H3K4me2 is required for HJURP targeting and CENP-A assembly on a synthetic human kinetochore. *Embo Journal, 30*(2), 328-340.

Berkers, C. R., Verdoes, M., Lichtman, E., Fiebiger, E., Kessler, B. M., Anderson, K. C., . . . Galardy, P. J. (2005). Activity probe for in vivo profiling of the specificity of proteasome inhibitor bortezomib. *Nat Methods, 2*(5), 357-362.

Berndsen, C. E., & Wolberger, C. (2014). New insights into ubiquitin E3 ligase mechanism. *Nature Structural & Molecular Biology, 21*(4), 301-307.

Bhatt, S., Ashlock, B. M., Toomey, N. L., Diaz, L. A., Mesri, E. A., Lossos, I. S., & Ramos, J. C. (2013). Efficacious proteasome/HDAC inhibitor combination therapy for primary effusion lymphoma. *Journal of Clinical Investigation, 123*(6), 2616-2628.

Bhowmick, B. K., Takahata, N., Watanabe, M., & Satta, Y. (2006). Comparative analysis of human masculinity. *Genetics and Molecular Research, 5*(4), 696-712.

Biamonti, G. (2004). Nuclear stress bodies: a heterochromatin affair? *Nature Reviews Molecular Cell Biology, 5*(6), 493-498.

Biamonti, G., & Vourc'h, C. (2010). Nuclear stress bodies. *Cold Spring Harb Perspect Biol, 2*(6), a000695.

Bidichandani, S. I., Ashizawa, T., & Patel, P. I. (1997). Atypical Friedreich ataxia caused by compound heterozygosity for a novel missense mutation and the GAA triplet-repeat expansion. *American Journal of Human Genetics, 60*(5), 1251-1256.

Bierhoff, H., Dammert, M. A., Brocks, D., Dambacher, S., Schotta, G., & Grummt, I. (2014). Quiescence-Induced LncRNAs Trigger H4K20 Trimethylation and Transcriptional Silencing. *Molecular Cell, 54*(4), 675-682.

Bierhoff, H., Postepska-Igielska, A., & Grummt, I. (2014). Noisy silence Non-coding RNA and heterochromatin formation at repetitive elements. *Epigenetics, 9*(1), 53-61.

Bitterman, K. J., Anderson, R. M., Cohen, H. Y., Latorre-Esteves, M., & Sinclair, D. A. (2002). Inhibition of silencing and accelerated aging by nicotinamide, a putative negative regulator of yeast sir2 and human SIRT1. *J Biol Chem, 277*(47), 45099-45107.

Bjork, J. K., & Sistonen, L. (2010). Regulation of the members of the mammalian heat shock factor family. *Febs Journal, 277*(20), 4126-4139.

Black, B. E., & Bassett, E. A. (2008). The histone variant CENP-A and centromere specification. *Current Opinion in Cell Biology, 20*(1), 91-100.

Black, J. C., Van Rechem, C., & Whetstine, J. R. (2012). Histone Lysine Methylation Dynamics: Establishment, Regulation, and Biological Impact. *Molecular Cell, 48*(4), 491-507.

Blackburn, E. H. (1991). Structure and function of telomeres. *Nature, 350*(6319), 569-573.

Bolden, J. E., Peart, M. J., & Johnstone, R. W. (2006). Anticancer activities of histone deacetylase inhibitors. *Nat Rev Drug Discov, 5*(9), 769-784.

Bolzer, A., Kreth, G., Solovei, I., Koehler, D., Saracoglu, K., Fauth, C., . . . Cremer, T. (2005). Three-dimensional maps of all chromosomes in human male fibroblast nuclei and prometaphase rosettes. *Plos Biology, 3*(5), 826-842.

Bonvini, P., Zorzi, E., Basso, G., & Rosolen, A. (2007). Bortezomib-mediated 26S proteasome inhibition causes cell-cycle arrest and induces apoptosis in CD-30+ anaplastic large cell lymphoma. *Leukemia, 21*(4), 838-842.

Botuyan, M. V., Lee, J., Ward, I. M., Kim, J. E., Thompson, J. R., Chen, J. J., & Mer, G. (2006). Structural basis for the methylation state-specific recognition of histone H4-K20 by 53BP1 and Crb2 in DNA repair. *Cell, 127*(7), 1361-1373.

Bourn, R. L., Rindler, P. M., Pollard, L. M., & Bidichandani, S. I. (2009). E-coli mismatch repair acts downstream of replication fork stalling to stabilize the expanded (GAA.TTC)(n) sequence. *Mutation Research-Fundamental and Molecular Mechanisms of Mutagenesis, 661*(1-2), 71-77.

Bouzinba-Segard, H., Guais, A., & Francastel, C. (2006). Accumulation of small murine minor satellite transcripts leads to impaired centromeric architecture and function. *Proceedings of the National Academy of Sciences of the United States of America, 103*(23), 8709-8714.

Boyault, C., Zhang, Y., Fritah, S., Caron, C., Gilquin, B., Kwon, S. H., . . . Khochbin, S. (2007). HDAC6 controls major cell response pathways to cytotoxic accumulation of protein aggregates. *Genes Dev, 21*(17), 2172-2181.

Bradley, J. L., Blake, J. C., Chamberlain, S., Thomas, P. K., Cooper, J. M., & Schapira, A. H. V. (2000). Clinical, biochemical and molecular genetic correlations in Friedreich's ataxia. *Human Molecular Genetics, 9*(2), 275-282.

Brasher, S. V., Smith, B. O., Fogh, R. H., Nietlispach, D., Thiru, A., Nielsen, P. R., . . . Laue, E. D. (2000). The structure of mouse HP1 suggests a unique mode of single peptide recognition by the shadow chromo domain dimer. *EMBO J, 19*(7), 1587-1597.

Briggs, S. D., Bryk, M., Strahl, B. D., Cheung, W. L., Davie, J. K., Dent, S. Y. R., . . . Allis, C. D. (2001). Histone H3 lysine 4 methylation is mediated by Set1 and required for cell growth and rDNA silencing in Saccharomyces cerevisiae. *Genes & Development, 15*(24), 3286-3295.

Brill, S. J., & Sternglanz, R. (1988). Transcription-Dependent DNA Supercoiling in Yeast DNA Topoisomerase Mutants. *Cell, 54*(3), 403-411.

Brinkmeier, M. L., Geister, K. A., Jones, M., Waqas, M., Maillard, I., & Camper, S. A. (2015). The Histone Methyltransferase Gene Absent, Small, or Homeotic Discs-1 Like Is Required for Normal Hox Gene Expression and Fertility in Mice. *Biol Reprod*.

Brookes, E., & Pombo, A. (2009). Modifications of RNA polymerase II are pivotal in regulating gene expression states. *Embo Reports, 10*(11), 1213-1219.

Brookes, E., & Pombo, A. (2012). Code breaking: the RNAPII modification code in pluripotency. *Cell Cycle, 11*(7), 1267-1268.

Bross, P. F., Kane, R., Farrell, A. T., Abraham, S., Benson, K., Brower, M. E., . . . Pazdur, R. (2004). Approval summary for bortezomib for injection in the treatment of multiple myeloma. *Clin Cancer Res, 10*(12 Pt 1), 3954-3964.

Brouwer, J. R., Willemsen, R., & Oostra, B. A. (2009). Microsatellite repeat instability and neurological disease. *Bioessays, 31*(1), 71-83.

Brown, J. P., Bullwinkel, J., Baron-Luhr, B., Billur, M., Schneider, P., Winking, H., & Singh, P. B. (2010). HP1 gamma function is required for male germ cell survival and spermatogenesis. *Epigenetics & Chromatin, 3*.

Brueckner, F., & Cramer, P. (2008). Structural basis of transcription inhibition by alpha-amanitin and implications for RNA polymerase II translocation. *Nature Structural & Molecular Biology, 15*(8), 811-818.

Bruins, W., Zwart, E., Attardi, L. D., Iwakuma, T., Hoogervorst, E. M., Beems, R. B., . . . de Vries, A. (2004). Increased sensitivity to UV radiation in mice with a p53 point mutation at Ser389. *Molecular and Cellular Biology, 24*(20), 8884-8894.

Brunet, A., Sweeney, L. B., Sturgill, J. F., Chua, K. F., Greer, P. L., Lin, Y. X., . . . Greenberg, M. E. (2004). Stress-dependent regulation of FOXO transcription factors by the SIRT1 deacetylase. *Science, 303*(5666), 2011-2015.

Budworth, H., & McMurray, C. T. (2013). A brief history of triplet repeat diseases. *Methods Mol Biol, 1010*, 3-17.

Bulteau, A. L., O'Neill, H. A., Kennedy, M. C., Ikeda-Saito, M., Isaya, G., & Szweda, L. I. (2004). Frataxin acts as an iron chaperone protein to modulate mitochondrial aconitase activity. *Science, 305*(5681), 242-245.

Bulut-Karslioglu, A., Perrera, V., Scaranaro, M., de la Rosa-Velazquez, I. A., van de Nobelen, S., Shukeir, N., . . . Jenuwein, T. (2012). A transcription factor-based mechanism for mouse heterochromatin formation. *Nat Struct Mol Biol, 19*(10), 1023-1030.

Buscaino, A., Lejeune, E., Audergon, P., Hamilton, G., Pidoux, A., & Allshire, R. C. (2013). Distinct roles for Sir2 and RNAi in centromeric heterochromatin nucleation, spreading and maintenance. *Embo Journal, 32*(9), 1250-1264.

Bush, K. T., Goldberg, A. L., & Nigam, S. K. (1997). Proteasome inhibition leads to a heat-shock response, induction of endoplasmic reticulum chaperones, and thermotolerance. *Journal of Biological Chemistry, 272*(14), 9086-9092.

Bushnell, D. A., Cramer, P., & Kornberg, R. D. (2002). Structural basis of transcription: alpha-amanitin-RNA polymerase II cocrystal at 2.8 A resolution. *Proc Natl Acad Sci U S A, 99*(3), 1218-1222.

Byles, V., Chmilewski, L. K., Wang, J., Zhu, L. J., Forman, L. W., Faller, D. V., & Dai, Y. (2010). Aberrant Cytoplasm Localization and Protein Stability of SIRT1 is Regulated by PI3K/IGF-1R Signaling in Human Cancer Cells. *International Journal of Biological Sciences, 6*(6), 599-612.

Callinan, P. A., & Batzer, M. A. (2006). Retrotransposable elements and human disease. *Genome Dyn, 1*, 104-115.

Cammas, F., Herzog, M., Lerouge, T., Chambon, P., & Losson, R. (2004). Association of the transcriptional corepressor TIF1beta with heterochromatin protein 1 (HP1): an essential role for progression through differentiation. *Genes Dev, 18*(17), 2147-2160.

Campuzano, V., Montermini, L., Lutz, Y., Cova, L., Hindelang, C., Jiralerspong, S., . . . Koenig, M. (1997). Frataxin is reduced in Friedreich ataxia patients and is associated with mitochondrial membranes. *Human Molecular Genetics, 6*(11), 1771-1780.

Campuzano, V., Montermini, L., Molto, M. D., Pianese, L., Cossee, M., Cavalcanti, F., . . . Pandolfo, M. (1996). Friedreich's ataxia: autosomal recessive disease caused by an intronic GAA triplet repeat expansion. *Science, 271*(5254), 1423-1427.

Canzio, D., Larson, A., & Narlikar, G. J. (2014). Mechanisms of functional promiscuity by HP1 proteins. *Trends Cell Biol, 24*(6), 377-386.

Caron, A. Z., Haroun, S., Leblanc, E., Trensz, F., Guindi, C., Amrani, A., & Grenier, G. (2011). The proteasome inhibitor MG132 reduces immobilization-induced skeletal muscle atrophy in mice. *BMC Musculoskelet Disord, 12*, 185.

Carrard, G., Bulteau, A. L., Petropoulos, I., & Friguet, B. (2002). Impairment of proteasome structure and function in aging. *Int J Biochem Cell Biol, 34*(11), 1461-1474.

Carrozza, M. J., Li, B., Florens, L., Suganuma, T., Swanson, S. K., Lee, K. K., . . . Workman, J. L. (2005). Histone H3 methylation by Set2 directs deacetylation of coding regions by Rpd3S to suppress spurious intragenic transcription. *Cell, 123*(4), 581-592.

Castel, S. E., & Martienssen, R. A. (2013). RNA interference in the nucleus: roles for small RNAs in transcription, epigenetics and beyond. *Nature Reviews Genetics, 14*(2), 100-112.

Catalgol, B., & Grune, T. (2012). Proteasome and Neurodegenerative Diseases. *The Proteasomal System in Aging and Disease, 109*, 397-414.

Catic, A., Suh, C. Y., Hill, C. T., Daheron, L., Henkel, T., Orford, K. W., . . . Scadden, D. T. (2013). Genome-wide Map of Nuclear Protein Degradation Shows NCoR1 Turnover as a Key to Mitochondrial Gene Regulation. *Cell, 155*(6), 1380-1395.

Cavadini, P., O'Neill, H. A., Benada, O., & Isaya, G. (2002). Assembly and iron-binding properties of human frataxin, the protein deficient in Friedreich ataxia. *Human Molecular Genetics, 11*(3), 217-227.

Cedar, H., & Bergman, Y. (2009). Linking DNA methylation and histone modification: patterns and paradigms. *Nat Rev Genet, 10*(5), 295-304.

Cen, Y. (2010). Sirtuins inhibitors: the approach to affinity and selectivity. *Biochim Biophys Acta, 1804*(8), 1635-1644.

Chae, M., Danko, C. G., & Kraus, W. L. (2015). groHMM: a computational tool for identifying unannotated and cell type-specific transcription units from global run-on sequencing data. *BMC Bioinformatics, 16*, 222.

Chafin, D. R., Guo, H., & Price, D. H. (1995). Action of alpha-amanitin during pyrophosphorolysis and elongation by RNA polymerase II. *Journal of Biological Chemistry, 270*(32), 19114-19119.

Chan, F. L., Marshall, O. J., Saffery, R., Kim, B. W., Earle, E., Choo, K. H. A., & Wong, L. H. (2012). Active transcription and essential role of RNA polymerase II at the centromere during mitosis. *Proceedings of the National Academy of Sciences of the United States of America, 109*(6), 1979-1984.

Chan, F. L., & Wong, L. H. (2012). Transcription in the maintenance of centromere chromatin identity. *Nucleic Acids Research, 40*(22), 11178-11188.

Chan, P. K., Torres, R., Yandim, C., Law, P. P., Khadayate, S., Mauri, M., . . . Festenstein, R. (2013). Heterochromatinization induced by GAA-repeat hyperexpansion in Friedreich's ataxia can be reduced upon HDAC inhibition by vitamin B3. *Hum Mol Genet, 22*(13), 2662-2675.

Chang, C., Gonzalez, F., Rothermel, B., Sun, L. P., Johnston, S. A., & Kodadek, T. (2001). The Gal4 activation domain binds Sug2 protein, a proteasome component, in vivo and in vitro. *Journal of Biological Chemistry, 276*(33), 30956-30963.

Chang, Y. H., Ostling, P., Akerfelt, M., Trouillet, D., Rallu, M., Gitton, Y., . . . Mezger, V. (2006). Role of heat-shock factor 2 in cerebral cortex formation and as a regulator of p35 expression. *Genes & Development, 20*(7), 836-847.

Chantrel-Groussard, K., Geromel, V., Puccio, H., Koenig, M., Munnich, A., Rotig, A., & Rustin, P. (2001). Disabled early recruitment of antioxidant defenses in Friedreich's ataxia. *Human Molecular Genetics, 10*(19), 2061-2067.

Charlier, C., Lamaye, F., Thelen, N., & Thiry, M. (2009). Ultrastructural detection of nucleic acids within heat shock-induced perichromatin granules of HeLa cells by cytochemical and immunocytological methods. *Journal of Structural Biology, 166*(3), 329-336.

Chauhan, D., Hideshima, T., Mitsiades, C., Richardson, P., & Anderson, K. C. (2005). Proteasome inhibitor therapy in multiple myeloma. *Mol Cancer Ther, 4*(4), 686-692.

Chaves, S., Baskerville, C., Yu, V., & Reed, S. I. (2010). Cks1, Cdk1, and the 19S Proteasome Collaborate To Regulate Gene Induction-Dependent Nucleosome Eviction in Yeast. *Molecular and Cellular Biology, 30*(22), 5284-5294.

Chen, B., Ma, Y., Meng, R., Xiong, Z., Zhang, C., Chen, G., . . . Dong, Y. (2010). MG132, a proteasome inhibitor, attenuates pressure-overload-induced cardiac hypertrophy in rats by modulation of mitogen-activated protein kinase signals. *Acta Biochim Biophys Sin (Shanghai), 42*(4), 253-258.

Chen, C., Sun, X., Ran, Q., Wilkinson, K. D., Murphy, T. J., Simons, J. W., & Dong, J. T. (2005). Ubiquitin-proteasome degradation of KLF5 transcription factor in cancer and untransformed epithelial cells. *Oncogene, 24*(20), 3319-3327.

Chen, E. S., Zhang, K., Nicolas, E., Cam, H. P., Zofall, M., & Grewal, S. I. (2008). Cell cycle control of centromeric repeat transcription and heterochromatin assembly. *Nature, 451*(7179), 734-737.

Chen, J. M., Stenson, P. D., Cooper, D. N., & Ferec, C. (2005). A systematic analysis of LINE-1 endonuclease-dependent retrotranspositional events causing human genetic disease. *Hum Genet, 117*(5), 411-427.

Chen, Y., Barlev, N. A., Westergaard, O., & Jakobsen, B. K. (1993). Identification of the C-terminal activator domain in yeast heat shock factor: independent control of transient and sustained transcriptional activity. *EMBO J, 12*(13), 5007-5018.

Cheng, C., & Sharp, P. A. (2003). RNA polymerase II accumulation in the promoter-proximal region of the dihydrofolate reductase and gamma-actin genes. *Mol Cell Biol, 23*(6), 1961-1967.

Cheng, X., & Blumenthal, R. M. (2008). Mammalian DNA methyltransferases: a structural perspective. *Structure, 16*(3), 341-350.

Cheutin, T., McNairn, A. J., Jenuwein, T., Gilbert, D. M., Singh, P. B., & Misteli, T. (2003). Maintenance of stable heterochromatin domains by dynamic HP1 binding. *Science, 299*(5607), 721-725.

Chiodi, I., Biggiogera, M., Denegri, M., Corioni, M., Weighardt, F., Cobianchi, F., . . . Biamonti, G. (2000). Structure and dynamics of hnRNP-labelled nuclear bodies induced by stress treatments. *J Cell Sci, 113 (Pt 22)*, 4043-4053.

Chiodi, I., Corioni, M., Giordano, M., Valgardsdottir, R., Ghigna, C., Cobianchi, F., . . . Biamonti, G. (2004). RNA recognition motif 2 directs the recruitment of SF2/ASF to nuclear stress bodies. *Nucleic Acids Res, 32*(14), 4127-4136.

Cho, E. J., Kobor, M. S., Kim, M., Greenblatt, J., & Buratowski, S. (2001). Opposing effects of Ctk1 kinase and Fcp1 phosphatase at Ser 2 of the RNA polymerase II C-terminal domain. *Genes & Development, 15*(24), 3319-3329.

Chodosh, L. A., Fire, A., Samuels, M., & Sharp, P. A. (1989). 5,6-Dichloro-1-beta-D-ribofuranosylbenzimidazole inhibits transcription elongation by RNA polymerase II in vitro. *J Biol Chem, 264*(4), 2250-2257.

Choi, E. S., Stralfors, A., Castillo, A. G., Durand-Dubief, M., Ekwall, K., & Allshire, R. C. (2011). Identification of Noncoding Transcripts from within CENP-A Chromatin at Fission Yeast Centromeres. *Journal of Biological Chemistry, 286*(26), 23600-23607.

Choy, J. S., Acuna, R., Au, W. C., & Basrai, M. A. (2011). A role for histone H4K16 hypoacetylation in Saccharomyces cerevisiae kinetochore function. *Genetics, 189*(1), 11-21.

Chu, B. Y., Zhong, R., Soncin, F., Stevenson, M. A., & Calderwood, S. K. (1998). Transcriptional activity of heat shock factor 1 at 37 degrees C is repressed through phosphorylation on two distinct serine residues by glycogen synthase kinase 3 alpha and protein kinases C alpha, and C zeta. *Journal of Biological Chemistry, 273*(29), 18640-18646.

Chuang, D. M., Leng, Y., Marinova, Z., Kim, H. J., & Chiu, C. T. (2009). Multiple roles of HDAC inhibition in neurodegenerative conditions. *Trends in Neurosciences, 32*(11), 591-601.

Chutake, Y. K., Costello, W. N., Lam, C., & Bidichandani, S. I. (2014). Altered Nucleosome Positioning at the Transcription Start Site and Deficient Transcriptional Initiation in Friedreich Ataxia. *Journal of Biological Chemistry, 289*(22), 15194-15202.

Chutake, Y. K., Costello, W. N., Lam, C. C., Parikh, A. C., Hughes, T. T., Michalopulos, M. G., . . . Bidichandani, S. I. (2015). FXN Promoter Silencing in the Humanized Mouse Model of Friedreich Ataxia. *PLoS One, 10*(9), e0138437.

Clark, R. M., Dalgliesh, G. L., Endres, D., Gomez, M., Taylor, J., & Bidichandani, S. I. (2004). Expansion of GAA triplet repeats in the human genome: unique origin of the FRDA mutation at the center of an Alu. *Genomics, 83*(3), 373-383.

Cleveland, D. W., Mao, Y., & Sullivan, K. F. (2003). Centromeres and kinetochores: from epigenetics to mitotic checkpoint signaling. *Cell, 112*(4), 407-421.

Clodfelter, K. H., Holloway, M. G., Hodor, P., Park, S. H., Ray, W. J., & Waxman, D. J. (2006). Sex-dependent liver gene expression is extensive and largely dependent upon signal transducer and activator of transcription 5b (STAT5b): STAT5b-dependent activation of male genes and repression of female genes revealed by microarray analysis. *Mol Endocrinol, 20*(6), 1333-1351.

Clouaire, T., Webb, S., & Bird, A. (2014). Cfp1 is required for gene expression-dependent H3K4 trimethylation and H3K9 acetylation in embryonic stem cells. *Genome Biology, 15*(9).

Codd, R., Braich, N., Liu, J., Soe, C. Z., & Pakchung, A. A. (2009). Zn(II)-dependent histone deacetylase inhibitors: suberoylanilide hydroxamic acid and trichostatin A. *Int J Biochem Cell Biol, 41*(4), 736-739.

Collins, G. A., & Tansey, W. P. (2006). The proteasome: a utility tool for transcription? *Curr Opin Genet Dev, 16*(2), 197-202.

Collins, N., Poot, R. A., Kukimoto, I., Garcia-Jimenez, C., Dellaire, G., & Varga-Weisz, P. D. (2002). An ACF1-ISWI chromatin-remodeling complex is required for DNA replication through heterochromatin. *Nat Genet, 32*(4), 627-632.

Condo, I., Ventura, N., Malisan, F., Rufini, A., Tomassini, B., & Testi, R. (2007). In vivo maturation of human frataxin. *Hum Mol Genet, 16*(13), 1534-1540.

Cordaux, R., & Batzer, M. A. (2009). The impact of retrotransposons on human genome evolution. *Nat Rev Genet, 10*(10), 691-703.

Cossee, M., Durr, A., Schmitt, M., Dahl, N., Trouillas, P., Allinson, P., . . . Pandolfo, M. (1999). Friedreich's ataxia: Point mutations and clinical presentation of compound heterozygotes. *Annals of Neurology, 45*(2), 200-206.

Cotto, J., Fox, S., & Morimoto, R. (1997). HSF1 granules: a novel stress-induced nuclear compartment of human cells. *J Cell Sci, 110 (Pt 23)*, 2925-2934.

Cowieson, N. P., Partridge, J. F., Allshire, R. C., & McLaughlin, P. J. (2000). Dimerisation of a chromo shadow domain and distinctions from the chromodomain as revealed by structural analysis. *Curr Biol, 10*(9), 517-525.

Criscione, S. W., Zhang, Y., Thompson, W., Sedivy, J. M., & Neretti, N. (2014). Transcriptional landscape of repetitive elements in normal and cancer human cells. *BMC Genomics, 15*, 583.

Crowley, C. L., Payne, C. M., Bernstein, H., Bernstein, C., & Roe, D. (2000). The NAD+ precursors, nicotinic acid and nicotinamide protect cells against apoptosis induced by a multiple stress inducer, deoxycholate. *Cell Death Differ, 7*(3), 314-326.

Daniels, G. R., & Deininger, P. L. (1985). Repeat sequence families derived from mammalian tRNA genes. *Nature, 317*(6040), 819-822.

Dantuma, N. P., & Bott, L. C. (2014). The ubiquitin-proteasome system in neurodegenerative diseases: precipitating factor, yet part of the solution. *Frontiers in Molecular Neuroscience, 7*.

Danzer, J. R., & Wallrath, L. L. (2004). Mechanisms of HP1-mediated gene silencing in Drosophila. *Development, 131*(15), 3571-3580.

Darzynkiewicz, Z., Bedner, E., & Smolewski, P. (2001). Flow cytometry in analysis of cell cycle and apoptosis. *Semin Hematol, 38*(2), 179-193.

Darzynkiewicz, Z., Halicka, H. D., Zhao, H., & Podhorecka, M. (2011). Cell synchronization by inhibitors of DNA replication induces replication stress and DNA damage response: analysis by flow cytometry. *Methods Mol Biol, 761*, 85-96.

Daulny, A., Geng, F. Q., Muratani, M., Geisinger, J. M., Salghetti, S. E., & Tansey, W. P. (2008). Modulation of RNA polymerase II subunit composition by ubiquitylation. *Proc Natl Acad Sci U S A, 105*(50), 19649-19654.

Daulny, A., & Tansey, W. P. (2009). Damage control: DNA repair, transcription, and the ubiquitin-proteasome system. *DNA Repair (Amst), 8*(4), 444-448.

De Biase, I., Chutake, Y. K., Rindler, P. M., & Bidichandani, S. I. (2009). Epigenetic Silencing in Friedreich Ataxia Is Associated with Depletion of CTCF (CCCTC-Binding Factor) and Antisense Transcription. *PLoS One, 4*(11).

De Fazio, S., Bartonicek, N., Di Giacomo, M., Abreu-Goodger, C., Sankar, A., Funaya, C., . . . O'Carroll, D. (2011). The endonuclease activity of Mili fuels piRNA amplification that silences LINE1 elements. *Nature, 480*(7376), 259-U148.

De Zhu, J. (2005). The altered DNA methylation pattern and its implications in liver cancer. *Cell Res, 15*(4), 272-280.

Deaton, A. M., & Bird, A. (2011). CpG islands and the regulation of transcription. *Genes Dev, 25*(10), 1010-1022.

deHaro, D., Kines, K. J., Sokolowski, M., Dauchy, R. T., Streva, V. A., Hill, S. M., . . . Belancio, V. P. (2014). Regulation of L1 expression and retrotransposition by melatonin and its receptor: implications for cancer risk associated with light exposure at night. *Nucleic Acids Research, 42*(12), 7694-7707.

Deininger, P. L., & Batzer, M. A. (1999). Alu repeats and human disease. *Mol Genet Metab, 67*(3), 183-193.

Deininger, P. L., & Batzer, M. A. (2002). Mammalian retroelements. *Genome Res, 12*(10), 1455-1465.

Dejardin, J., & Kingston, R. E. (2009). Purification of proteins associated with specific genomic Loci. *Cell, 136*(1), 175-186.

Dembla-Rajpal, N., Seipelt, R., Wang, Q., & Rymond, B. C. (2004). Proteasome inhibition alters the transcription of multiple yeast genes. *Biochimica Et Biophysica Acta-Gene Structure and Expression, 1680*(1), 34-45.

Denegri, M., Chiodi, I., Corioni, M., Cobianchi, F., Riva, S., & Biamonti, G. (2001). Stress-induced nuclear bodies are sites of accumulation of pre-mRNA processing factors. *Mol Biol Cell, 12*(11), 3502-3514.

Denegri, M., Moralli, D., Rocchi, M., Biggiogera, M., Raimondi, E., Cobianchi, F., . . . Biamonti, G. (2002). Human chromosomes 9, 12, and 15 contain the nucleation sites of stress-induced nuclear bodies. *Mol Biol Cell, 13*(6), 2069-2079.

Denu, J. M., & Gottesfeld, J. M. (2012). Minireview series on sirtuins: from biochemistry to health and disease. *J Biol Chem, 287*(51), 42417-42418.

Dewannieux, M., Esnault, C., & Heidmann, T. (2003). LINE-mediated retrotransposition of marked Alu sequences. *Nat Genet, 35*(1), 41-48.

Dewing, P., Shi, T., Horvath, S., & Vilain, E. (2003). Sexually dimorphic gene expression in mouse brain precedes gonadal differentiation. *Brain Res Mol Brain Res, 118*(1-2), 82-90.

Dey, A., Chitsaz, F., Abbasi, A., Misteli, T., & Ozato, K., (2003). The double bromodomain protein Brd4 binds to acetylated chromatin during interphase and mitosis. *PNAS, 100(15),* 8758-63.

Dhasarathy, A., & Wade, P. A. (2008). The MBD protein family-Reading an epigenetic mark? *Mutation Research-Fundamental and Molecular Mechanisms of Mutagenesis, 647*(1-2), 39-43.

Didonna, A., & Opal, P. (2015). The promise and perils of HDAC inhibitors in neurodegeneration. *Ann Clin Transl Neurol, 2*(1), 79-101.

Dieci, G., Fiorino, G., Castelnuovo, M., Teichmann, M., & Pagano, A. (2007). The expanding RNA polymerase III transcriptome. *Trends in Genetics, 23*(12), 614-622.

Dietz, K. C., & Casaccia, P. (2010). HDAC inhibitors and neurodegeneration: At the edge between protection and damage. *Pharmacological Research, 62*(1), 11-17.

Dietzel, S., Zolghadr, K., Hepperger, C., & Belmont, A. S. (2004). Differential large-scale chromatin compaction and intranuclear positioning of transcribed versus non-transcribed transgene arrays containing beta-globin regulatory sequences. *J Cell Sci, 117*(Pt 19), 4603-4614.

Dillon, N. (2004). Heterochromatin structure and function. *Biol Cell, 96*(8), 631-637.

Dillon, N., & Festenstein, R. (2002). Unravelling heterochromatin: competition between positive and negative factors regulates accessibility. *Trends in Genetics, 18*(5), 252-258.

Djupedal, I., & Ekwall, K. (2009). Epigenetics: heterochromatin meets RNAi. *Cell Res, 19*(3), 282-295.

Djupedal, I., Portoso, M., Spahr, H., Bonilla, C., Gustafsson, C. M., Allshire, R. C., & Ekwall, K. (2005). RNA Pol II subunit Rpb7 promotes centromeric transcription and RNAi-directed chromatin silencing. *Genes & Development, 19*(19), 2301-2306.

Donjerkovic, D., & Scott, D. W. (2000). Regulation of the G1 phase of the mammalian cell cycle. *Cell Res, 10*(1), 1-16.

Dou, Y. L., Milne, T. A., Ruthenburg, A. J., Lee, S., Lee, J. W., Verdine, G. L., . . . Roeder, R. G. (2006). Regulation of MLL1 H3K4 methyltransferase activity by its core components. *Nature Structural & Molecular Biology, 13*(8), 713-719.

Dridi, S. (2012). Alu mobile elements: from junk DNA to genomic gems. *Scientifica (Cairo), 2012*, 545328.

Du, J. T., Campau, E., Soragni, E., Ku, S., Puckett, J. W., Dervan, P. B., & Gottesfeld, J. M. (2012). Role of Mismatch Repair Enzymes in GAA.TTC Triplet-repeat Expansion in Friedreich Ataxia Induced Pluripotent Stem Cells. *Journal of Biological Chemistry, 287*(35), 29861-29872.

Du, Y. Q., Topp, C. N., & Dawe, R. K. (2010). DNA Binding of Centromere Protein C (CENPC) Is Stabilized by Single-Stranded RNA. *Plos Genetics, 6*(2).

Dubois, M. F., Nguyen, V. T., Bellier, S., & Bensaude, O. (1994). Inhibitors of Transcription Such as 5,6-Dichloro-1-Beta-D-Ribofuranosylbenzimidazole and Isoquinoline Sulfonamide Derivatives (H-8 and H-7-Asterisk) Promote Dephosphorylation of the Carboxyl-Terminal Domain of Rna-Polymerase-Ii Largest Subunit. *Journal of Biological Chemistry, 269*(18), 13331-13336.

Durairaj, G., & Kaiser, P. (2014). The 26S proteasome and initiation of gene transcription. *Biomolecules, 4*(3), 827-847.

Durr, A., Cossee, M., Agid, Y., Campuzano, V., Mignard, C., Penet, C., . . . Koenig, M. (1996). Clinical and genetic abnormalities in patients with Friedreich's ataxia. *N Engl J Med, 335*(16), 1169-1175.

Eberhardy, S. R., & Farnham, P. J. (2001). c-Myc mediates activation of the cad promoter via a post-RNA polymerase II recruitment mechanism. *Journal of Biological Chemistry, 276*(51), 48562-48571.

Eckert, D., Buhl, S., Weber, S., Jager, R., & Schorle, H. (2005). The AP-2 family of transcription factors. *Genome Biology, 6*(13).

Ekwall, K. (2007). Epigenetic control of centromere behavior. *Annual Review of Genetics, 41*, 63-81.

Ellegren, H. (2000). Microsatellite mutations in the germline: implications for evolutionary inference. *Trends in Genetics, 16*(12), 551-558.

Elliott, P. J., Zollner, T. M., & Boehncke, W. H. (2003). Proteasome inhibition: a new anti-inflammatory strategy. *J Mol Med (Berl), 81*(4), 235-245.

Elsasser, S., Gali, R. R., Schwickart, M., Larsen, C. N., Leggett, D. S., Muller, B., . . . Finley, D. (2002). Proteasome subunit Rpn1 binds ubiquitin-like protein domains. *Nat Cell Biol, 4*(9), 725-730.

Enenkel, C. (2014). Proteasome dynamics. *Biochimica Et Biophysica Acta-Molecular Cell Research, 1843*(1), 39-46.

Enukashvily, N. I., Donev, R., Waisertreiger, I. S. R., & Podgornaya, O. I. (2007). Human chromosome 1 satellite 3 DNA is decondensed, demethylated and transcribed in senescent cells and in A431 epithelial carcinoma cells. *Cytogenetic and Genome Research, 118*(1), 42-54.

Enukashvily, N. I., & Ponomartsev, N. V. (2013). Mammalian satellite DNA: a speaking dumb. *Adv Protein Chem Struct Biol, 90*, 31-65.

Erales, J., & Coffino, P. (2014). Ubiquitin-independent proteasomal degradation. *Biochim Biophys Acta, 1843*(1), 216-221.

Erwin, J. A., Marchetto, M. C., & Gage, F. H. (2014). Mobile DNA elements in the generation of diversity and complexity in the brain. *Nat Rev Neurosci, 15*(8), 497-506.

Espinoza, C. A., Allen, T. A., Hieb, A. R., Kugel, J. F., & Goodrich, J. A. (2004). B2 RNA binds directly to RNA polymerase II to repress transcript synthesis. *Nature Structural & Molecular Biology, 11*(9), 822-829.

Everett, C. M., & Wood, N. W. (2004). Trinucleotide repeats and neurodegenerative disease. *Brain, 127*(Pt 11), 2385-2405.

Eymery, A., Callanan, M., & Vourc'h, C. (2009). The secret message of heterochromatin: new insights into the mechanisms and function of centromeric and pericentric repeat sequence transcription. *International Journal of Developmental Biology, 53*(2-3), 259-268.

Eymery, A., Horard, B., El Atifi-Borel, M., Fourel, G., Berger, F., Vitte, A. L., . . . Vourc'h, C. (2009). A transcriptomic analysis of human centromeric and pericentric sequences in normal and tumor cells. *Nucleic Acids Research, 37*(19), 6340-6354.

Eymery, A., Souchier, C., Vourc'h, C., & Jolly, C. (2010). Heat shock factor 1 binds to and transcribes satellite II and III sequences at several pericentromeric regions in heat-shocked cells. *Exp Cell Res, 316*(11), 1845-1855.

Ezzatizadeh, V., Pinto, R. M., Sandi, C., Sandi, M., Al-Mahdawi, S., Riele, H. T., & Pook, M. A. (2012). The mismatch repair system protects against intergenerational GAA repeat instability in a Friedreich ataxia mouse model. *Neurobiology of Disease, 46*(1), 165-171.

Fadloun, A., Le Gras, S., Jost, B., Ziegler-Birling, C., Takahashi, H., Gorab, E., . . . Torres-Padilla, M. E. (2013). Chromatin signatures and retrotransposon profiling in mouse embryos reveal regulation of LINE-1 by RNA. *Nature Structural & Molecular Biology, 20*(3), 332-338.

Falkenberg, K. J., & Johnstone, R. W. (2014). Histone deacetylases and their inhibitors in cancer, neurological diseases and immune disorders. *Nature Reviews Drug Discovery, 13*(9), 673-691.

Fang, J., Feng, Q., Ketel, C. S., Wang, H. B., Cao, R., Xia, L., . . . Zhang, Y. (2002). Purification and functional characterization of SET8, a nucleosomal histone H4-lysine 20-specific methyltransferase. *Current Biology, 12*(13), 1086-1099.

Fanti, L., Berloco, M., Piacentini, L., & Pimpinelli, S. (2003). Chromosomal distribution of heterochromatin protein 1 (HP1) in Drosophila: a cytological map of euchromatic HP1 binding sites. *Genetica, 117*(2-3), 135-147.

Fatyol, K., & Grummt, I. (2008). Proteasomal ATPases are associated with rDNA: The ubiquitin proteasome system plays a direct role in RNA polymerase I transcription. *Biochimica Et Biophysica Acta-Gene Regulatory Mechanisms, 1779*(12), 850-859.

Faulkner, G. J., Kimura, Y., Daub, C. O., Wani, S., Plessy, C., Irvine, K. M., . . . Carninci, P. (2009). The regulated retrotransposon transcriptome of mammalian cells. *Nature Genetics, 41*(5), 563-571.

Femino, A. M., Fay, F. S., Fogarty, K., & Singer, R. H. (1998). Visualization of single RNA transcripts in situ. *Science, 280*(5363), 585-590.

Feng, S., Cokus, S. J., Zhang, X., Chen, P. Y., Bostick, M., Goll, M. G., . . . Jacobsen, S. E. (2010). Conservation and divergence of methylation patterning in plants and animals. *Proc Natl Acad Sci U S A, 107*(19), 8689-8694.

Ferdous, A., Gonzalez, F., Sun, L. P., Kodadek, T., & Johnston, S. A. (2001). The 19S regulatory particle of the proteasome is required for efficient transcription elongation by RNA polymerase II. *Molecular Cell, 7*(5), 981-991.

Ferdous, A., Sikder, D., Gillette, T., Nalley, K., Kodadek, T., & Johnston, S. A. (2007). The role of the proteasomal ATPases and activator monoubiquitylation in regulating Gal4 binding to promoters. *Genes & Development, 21*(1), 112-123.

Ferri, F., Bouzinba-Segard, H., Velasco, G., Hube, F., & Francastel, C. (2009). Non-coding murine centromeric transcripts associate with and potentiate Aurora B kinase. *Nucleic Acids Res, 37*(15), 5071-5080.

Ferry, C., Gianni, M., Lalevee, S., Bruck, N., Plassat, J. L., Raska, I., Jr., . . . Rochette-Egly, C. (2009). SUG-1 plays proteolytic and non-proteolytic roles in the control of retinoic acid target genes via its interaction with SRC-3. *J Biol Chem, 284*(12), 8127-8135.

Feschotte, C., & Pritham, E. J. (2007). DNA transposons and the evolution of eukaryotic genomes. *Annual Review of Genetics, 41*, 331-368.

Festenstein, R., Pagakis, S. N., Hiragami, K., Lyon, D., Verreault, A., Sekkali, B., & Kioussis, D. (2003). Modulation of heterochromatin protein 1 dynamics in primary Mammalian cells. *Science, 299*(5607), 719-721.

Field-Smith, A., Morgan, G. J., & Davies, F. E. (2006). Bortezomib (Velcadetrade mark) in the Treatment of Multiple Myeloma. *Ther Clin Risk Manag, 2*(3), 271-279.

Filla, A., DeMichele, G., Cavalcanti, F., Pianese, L., Monticelli, A., Campanella, G., & Cocozza, S. (1996). The relationship between trinucleotide (GAA) repeat length and clinical features in friedreich ataxia. *American Journal of Human Genetics, 59*(3), 554-560.

Finch, J. T., & Klug, A. (1976). Solenoidal model for superstructure in chromatin. *Proc Natl Acad Sci U S A, 73*(6), 1897-1901.
Fischle, W., Tseng, B. S., Dormann, H. L., Ueberheide, B. M., Garcia, B. A., Shabanowitz, J., . . . Allis, C. D. (2005). Regulation of HP1-chromatin binding by histone H3 methylation and phosphorylation. *Nature, 438*(7071), 1116-1122.

Fischle, W., Wang, Y., Jacobs, S. A., Kim, Y., Allis, C. D., & Khorasanizadeh, S. (2003). Molecular basis for the discrimination of repressive methyl-lysine marks in histone H3 by Polycomb and HP1 chromodomains. *Genes Dev, 17*(15), 1870-1881.

Fleming, J. A., Lightcap, E. S., Sadis, S., Thoroddsen, V., Bulawa, C. E., & Blackman, R. K. (2002). Complementary whole-genome technologies reveal the cellular response to proteasome inhibition by PS-341. *Proceedings of the National Academy of Sciences of the United States of America, 99*(3), 1461-1466.

Fnu, S., Williamson, E. A., De Haro, L. P., Brenneman, M., Wray, J., Shaheen, M., . . . Hromas, R. (2011). Methylation of histone H3 lysine 36 enhances DNA repair by nonhomologous end-joining. *Proc Natl Acad Sci U S A, 108*(2), 540-545.

Fornace, A. J., & Mitchell, J. B. (1986). Induction of B2 Rna Polymerase-Iii Transcription by Heat-Shock - Enrichment for Heat-Shock Induced Sequences in Rodent Cells by Hybridization Subtraction. *Nucleic Acids Research, 14*(14), 5793-5811.

Foury, F., & Cazzalini, O. (1997). Deletion of the yeast homologue of the human gene associated with Friedreich's ataxia elicits iron accumulation in mitochondria. *Febs Letters, 411*(2-3), 373-377.

Frescas, D., Guardavaccaro, D., Kuchay, S. M., Kato, H., Poleshko, A., Basrur, V., . . . Pagano, M. (2008). KDM2A represses transcription of centromeric satellite repeats and maintains the heterochromatic state. *Cell Cycle, 7*(22), 3539-3547.

Fritah, S., Col, E., Boyault, C., Govin, J., Sadoul, K., Chiocca, S., . . . Vourc'h, C. (2009). Heat-shock factor 1 controls genome-wide acetylation in heat-shocked cells. *Mol Biol Cell, 20*(23), 4976-4984.

Fu, J., Bian, M., Jiang, Q., & Zhang, C. (2007). Roles of Aurora kinases in mitosis and tumorigenesis. *Mol Cancer Res, 5*(1), 1-10. doi:10.1158/1541-7786.

Fuchs, S. Y., & Ronai, Z. (1999). Ubiquitination and degradation of ATF2 are dimerization dependent. *Mol Cell Biol, 19*(5), 3289-3298.

Fujimoto, M., Hayashida, N., Katoh, T., Oshima, K., Shinkawa, T., Prakasam, R., . . . Nakai, A. (2010). A Novel Mouse HSF3 Has the Potential to Activate Nonclassical Heat-Shock Genes during Heat Shock. *Mol Biol Cell, 21*(1), 106-116.

Fujimoto, M., Izu, H., Seki, K., Fukuda, K., Nishida, T., Yamada, S., . . . Nakai, A. (2004). HSF4 is required for normal cell growth and differentiation during mouse lens development. *Embo Journal, 23*(21), 4297-4306.
Fujimoto, M., & Nakai, A. (2010). The heat shock factor family and adaptation to proteotoxic stress. *Febs Journal, 277*(20), 4112-4125.

Fujimoto, M., Takaki, E., Takii, R., Tan, K., Prakasam, R., Hayashida, N., . . . Nakai, A. (2012). RPA Assists HSF1 Access to Nucleosomal DNA by Recruiting Histone Chaperone FACT. *Molecular Cell, 48*(2), 182-194.

Fujimoto, M., Takii, R., Hayashida, N., & Nakai, A. (2015). Analysis of the heat shock factor complex in mammalian HSP70 promoter. *Methods Mol Biol, 1292*, 53-65.

Fukagawa, T., & Earnshaw, W. C. (2014). The centromere: chromatin foundation for the kinetochore machinery. *Dev Cell, 30*(5), 496-508.

Fuks, F., Hurd, P. J., Deplus, R., & Kouzarides, T. (2003). The DNA methyltransferases associate with HP1 and the SUV39H1 histone methyltransferase. *Nucleic Acids Res, 31*(9), 2305-2312.

Fuss, J., & Linn, S. (2002). Human DNA polymerase epsilon colocalizes with proliferating cell nuclear antigen and DNA replication late, but not early, in S phase. *J Biol Chem, 277*(10), 8658-8666.

Garagna, S., Zuccotti, M., Capanna, E., & Redi, C. A. (2002). High-resolution organization of mouse telomeric and pericentromeric DNA. *Cytogenetic and Genome Research, 96*(1-4), 125-129.

Garcia-Rubio, M. L., & Aguilera, A. (2012). Topological constraints impair RNA polymerase II transcription and causes instability of plasmid-borne convergent genes. *Nucleic Acids Research, 40*(3), 1050-1064.

Garrick, D., Fiering, S., Martin, D. I., & Whitelaw, E. (1998). Repeat-induced gene silencing in mammals. *Nat Genet, 18*(1), 56-59.

Gaubatz, J. W., & Cutler, R. G. (1990). Mouse Satellite DNA Is Transcribed in Senescent Cardiac-Muscle. *Journal of Biological Chemistry, 265*(29), 17753-17758.

Geng, F. Q., & Tansey, W. P. (2012). Similar temporal and spatial recruitment of native 19S and 20S proteasome subunits to transcriptionally active chromatin. *Proceedings of the National Academy of Sciences of the United States of America, 109*(16), 6060-6065.

Geng, F. Q., Wenzel, S., & Tansey, W. P. (2012). Ubiquitin and Proteasomes in Transcription. *Annual Review of Biochemistry, Vol 81, 81*, 177-201.

Gent, J. I., & Dawe, R. K. (2012). RNA as a Structural and Regulatory Component of the Centromere. *Annual Review of Genetics, Vol 46, 46*, 443-453.

Gerard, C., & Goldbeter, A. (2014). The balance between cell cycle arrest and cell proliferation: control by the extracellular matrix and by contact inhibition. *Interface Focus, 4*(3).

Ghosh-Roy, S., Das, D., Chowdhury, D., Smerdon, M. J., & Chaudhuri, R. N. (2013). Rad26, the transcription-coupled repair factor in yeast, is required for removal of stalled RNA polymerase-II following UV irradiation. *PLoS One, 8*(8), e72090.

Ghosh, A., Shuman, S., & Lima, C. D. (2008). The Structure of Fcp1, an Essential RNA Polymerase II CTD Phosphatase. *Molecular Cell, 32*(4), 478-490.

Gibson, T. J., Koonin, E. V., Musco, G., Pastore, A., & Bork, P. (1996). Friedreich's ataxia protein: phylogenetic evidence for mitochondrial dysfunction. *Trends Neurosci, 19*(11), 465-468.

Gillette, T. G., Gonzalez, F., Delahodde, A., Johnston, S. A., & Kodadek, T. (2004a/b). Physical and functional association of RNA polymerase II and the proteasome. *Proc Natl Acad Sci U S A, 101*(16), 5904-5909.

Gilmour, D. S., & Lis, J. T. (1986). RNA polymerase II interacts with the promoter region of the noninduced hsp70 gene in Drosophila melanogaster cells. *Molecular and Cellular Biology, 6*(11), 3984-3989.

Glickman, M. H., Rubin, D. M., Coux, O., Wefes, I., Pfeifer, G., Cjeka, Z., . . . Finley, D. (1998). A subcomplex of the proteasome regulatory particle required for ubiquitin-conjugate degradation and related to the COP9-signalosome and eIF3. *Cell, 94*(5), 615-623.

Glozak, M. A., & Seto, E. (2007). Histone deacetylases and cancer. *Oncogene, 26*(37), 5420-5432.

Goldberg, A. L. (2003). Protein degradation and protection against misfolded or damaged proteins. *Nature, 426*(6968), 895-899.

Gomes, C. M., & Santos, R. (2013). Neurodegeneration in Friedreich's ataxia: from defective frataxin to oxidative stress. *Oxid Med Cell Longev, 2013*, 487534.

Gomez-Abellan, P., Madrid, J. A., Lujan, J. A., Frutos, M. D., Gonzalez, R., Martinez-Augustin, O., . . . Garaulet, M. (2012). Sexual Dimorphism in Clock Genes Expression in Human Adipose Tissue. *Obesity Surgery, 22*(1), 105-112.

Gomez, E. B., & Forsburg, S. L. (2004). Analysis of the fission yeast Schizosaccharomyces pombe cell cycle. *Methods Mol Biol, 241*, 93-111.

Gondran, P., Amiot, F., Weil, D., & Dautry, F. (1999). Accumulation of mature mRNA in the nuclear fraction of mammalian cells. *FEBS Lett, 458*(3), 324-328.

Gonfloni, S., Iannizzotto, V., Maiani, E., Bellusci, G., Ciccone, S., & Diederich, M. (2014). P53 and Sirt1: Routes of metabolism and genome stability. *Biochemical Pharmacology, 92*(1), 149-156.

Gong, J., Traganos, F., & Darzynkiewicz, Z. (1995). Growth imbalance and altered expression of cyclins B1, A, E, and D3 in MOLT-4 cells synchronized in the cell cycle by inhibitors of DNA replication. *Cell Growth Differ, 6*(11), 1485-1493.

Gong, X. Q., Nedialkov, Y. A., & Burton, Z. F. (2004). alpha-amanitin blocks translocation by human RNA polymerase II. *Journal of Biological Chemistry, 279*(26), 27422-27427.

Gonzalez-Cabo, P., & Palau, F. (2013). Mitochondrial pathophysiology in Friedreich's ataxia. *Journal of Neurochemistry, 126*, 53-64.

Gonzalez, F., Delahodde, A., Kodadek, T., & Johnston, S. A. (2002). Recruitment of a 19S proteasome subcomplex to an activated promoter. *Science, 296*(5567), 548-550.

Gonzalez, O., Fontanes, V., Raychaudhuri, S., Loo, R., Loo, J., Arumugaswami, V., . . . French, S. W. (2009). The heat shock protein inhibitor Quercetin attenuates hepatitis C virus production. *Hepatology, 50*(6), 1756-1764.

Goodier, J. L., & Kazazian, H. H., Jr. (2008). Retrotransposons revisited: the restraint and rehabilitation of parasites. *Cell, 135*(1), 23-35.

Gopalakrishnan, S., Sullivan, B. A., Trazzi, S., Della Valle, G., & Robertson, K. D. (2009). DNMT3B interacts with constitutive centromere protein CENP-C to modulate DNA methylation and the histone code at centromeric regions. *Human Molecular Genetics, 18*(17), 3178-3193.

Gorisch, S. M., Wachsmuth, M., Toth, K. F., Lichter, P., & Rippe, K. (2005). Histone acetylation increases chromatin accessibility. *Journal of Cell Science, 118*(24), 5825-5834.

Gottlicher, M., Minucci, S., Zhu, P., Kramer, O. H., Schimpf, A., Giavara, S., . . . Heinzel, T. (2001). Valproic acid defines a novel class of HDAC inhibitors inducing differentiation of transformed cells. *EMBO J, 20*(24), 6969-6978.

Grabczyk, E., Mancuso, M., & Sammarco, M. C. (2007). A persistent RNA center dot DNA hybrid formed by transcription of the Friedreich ataxia triplet repeat in live bacteria, and by T7 RNAP in vitro. *Nucleic Acids Research, 35*(16), 5351-5359.

Grabczyk, E., & Usdin, K. (2000). The GAA*TTC triplet repeat expanded in Friedreich's ataxia impedes transcription elongation by T7 RNA polymerase in a length and supercoil dependent manner. *Nucleic Acids Res, 28*(14), 2815-2822.

Grandbastien, M. A. (2015). LTR retrotransposons, handy hitchhikers of plant regulation and stress response. *Biochim Biophys Acta, 1849*(4), 403-416.

Greene, E., Entezam, A., Kumari, D., & Usdin, K. (2005). Ancient repeated DNA elements and the regulation of the human frataxin promoter. *Genomics, 85*(2), 221-230.

Greene, E., Mahishi, L., Entezam, A., Kumari, D., & Usdin, K. (2007). Repeat-induced epigenetic changes in intron 1 of the frataxin gene and its consequences in Friedreich ataxia. *Nucleic Acids Res, 35*(10), 3383-3390.

Grewal, S. I., & Elgin, S. C. (2007). Transcription and RNA interference in the formation of heterochromatin. *Nature, 447*(7143), 399-406.

Grewal, S. I., & Jia, S. (2007). Heterochromatin revisited. *Nat Rev Genet, 8*(1), 35-46.

Grewal, S. I. S., & Moazed, D. (2003). Heterochromatin and epigenetic control of gene expression. *Science, 301*(5634), 798-802.

Groh, M., Lufino, M. M. P., Wade-Martins, R., & Gromak, N. (2014). R-loops Associated with Triplet Repeat Expansions Promote Gene Silencing in Friedreich Ataxia and Fragile X Syndrome. *Plos Genetics, 10*(5).

Groll, M., Bajorek, M., Kohler, A., Moroder, L., Rubin, D. M., Huber, R., . . . Finley, D. (2000). A gated channel into the proteasome core particle. *Nature Structural Biology, 7*(11), 1062-1067.

Groll, M., Ditzel, L., Lowe, J., Stock, D., Bochtler, M., Bartunik, H. D., & Huber, R. (1997). Structure of 20S proteasome from yeast at 2.4 angstrom resolution. *Nature, 386*(6624), 463-471.

Groll, M., Heinemeyer, W., Jager, S., Ullrich, T., Bochtler, M., Wolf, D. H., & Huber, R. (1999). The catalytic sites of 20S proteasomes and their role in subunit maturation: A mutational and crystallographic study. *Proceedings of the National Academy of Sciences of the United States of America, 96*(20), 10976-10983.

Gu, B. N., & Lee, M. G. (2013). Histone H3 lysine 4 methyltransferases and demethylases in self-renewal and differentiation of stem cells. *Cell and Bioscience, 3*.

Gualtieri, A., Andreola, F., Sciamanna, I., Sinibaldi-Vallebona, P., Serafino, A., & Spadafora, C. (2013). Increased expression and copy number amplification of LINE-1 and SINE B1 retrotransposable elements in murine mammary carcinoma progression. *Oncotarget, 4*(11), 1882-1893.

Guelen, L., Pagie, L., Brasset, E., Meuleman, W., Faza, M. B., Talhout, W., . . . van Steensel, B. (2008). Domain organization of human chromosomes revealed by mapping of nuclear lamina interactions. *Nature, 453*(7197), 948-951.

Guenatri, M., Bailly, D., Maison, C., & Almouzni, G. (2004). Mouse centric and pericentric satellite repeats form distinct functional heterochromatin. *Journal of Cell Biology, 166*(4), 493-505.

Guettouche, T., Boellmann, F., Lane, W. S., & Voellmy, R. (2005). Analysis of phosphorylation of human heat shock factor 1 in cells experiencing a stress. *BMC Biochem, 6*, 4.

Gui, C. Y., Ngo, L., Xu, W. S., Richon, V. M., & Marks, P. A. (2004). Histone deacetylase (HDAC) inhibitor activation of p21WAF1 involves changes in promoter-associated proteins, including HDAC1. *Proc Natl Acad Sci U S A, 101*(5), 1241-1246.

Gupta-Rossi, N., Six, E., LeBail, O., Logeat, F., Chastagner, P., Olry, A., . . . Brou, C. (2004). Monoubiquitination and endocytosis direct gamma-secretase cleavage of activated Notch receptor. *Journal of Cell Biology, 166*(1), 73-83.

Guse, A., Carroll, C. W., Moree, B., Fuller, C. J., & Straight, A. F. (2011). In vitro centromere and kinetochore assembly on defined chromatin templates. *Nature, 477*(7364), 354-358.

Haberland, M., Montgomery, R. L., & Olson, E. N. (2009). The many roles of histone deacetylases in development and physiology: implications for disease and therapy. *Nat Rev Genet, 10*(1), 32-42.

Haglund, K., Sigismund, S., Polo, S., Szymkiewicz, I., Di Fiore, P. P., & Dikic, I. (2003). Multiple monoubiquitination of RTKs is sufficient for their endocytosis and degradation. *Nature Cell Biology, 5*(5), 461-466.

Hahn, M., Dambacher, S., Dulev, S., Kuznetsova, A. Y., Eck, S., Worz, S., . . . Schotta, G. (2013). Suv4-20h2 mediates chromatin compaction and is important for cohesin recruitment to heterochromatin. *Genes & Development, 27*(8), 859-872.

Hahn, M. A., Wu, X., Li, A. X., Hahn, T., & Pfeifer, G. P. (2011). Relationship between gene body DNA methylation and intragenic H3K9me3 and H3K36me3 chromatin marks. *PLoS One, 6*(4), e18844.

Halabi, A., Ditch, S., Wang, J., & Grabczyk, E. (2012). DNA Mismatch Repair Complex MutS beta Promotes GAA.TTC Repeat Expansion in Human Cells. *Journal of Biological Chemistry, 287*(35), 29958-29967.

Hall, L. E., Mitchell, S. E., & O'Neill, R. J. (2012). Pericentric and centromeric transcription: a perfect balance required. *Chromosome Res, 20*(5), 535-546.

Halleck, M. S., & Gurley, L. R. (1981). Histone acetylation and heterochromatin content of cultured Peromyscus cells. *Exp Cell Res, 132*(1), 201-213.

Hamamoto, R., Furukawa, Y., Morita, M., Iimura, Y., Silva, F. P., Li, M. H., . . . Nakamura, Y. (2004). SMYD3 encodes a histone methyltransferase involved in the proliferation of cancer cells. *Nature Cell Biology, 6*(8), 731-740.
Hamazaki, J., Hirayama, S., & Murata, S. (2015). Redundant Roles of Rpn10 and Rpn13 in Recognition of Ubiquitinated Proteins and Cellular Homeostasis. *Plos Genetics, 11*(7).

Han, J. S. (2010). Non-long terminal repeat (non-LTR) retrotransposons: mechanisms, recent developments, and unanswered questions. *Mob DNA, 1*(1), 15.

Hansen, K. D., Timp, W., Bravo, H. C., Sabunciyan, S., Langmead, B., McDonald, O. G., . . . Feinberg, A. P. (2011). Increased methylation variation in epigenetic domains across cancer types. *Nat Genet, 43*(8), 768-775.

Hansen, R. K., Oesterreich, S., Lemieux, P., Sarge, K. D., & Fuqua, S. A. (1997). Quercetin inhibits heat shock protein induction but not heat shock factor DNA-binding in human breast carcinoma cells. *Biochem Biophys Res Commun, 239*(3), 851-856.

Harper, J. V., & Brooks, G. (2005). The mammalian cell cycle: an overview. *Methods Mol Biol, 296*, 113-153.

Harreman, M., Taschner, M., Sigurdsson, S., Anindya, R., Reid, J., Somesh, B., . . . Svejstrup, J. Q. (2009). Distinct ubiquitin ligases act sequentially for RNA polymerase II polyubiquitylation. *Proceedings of the National Academy of Sciences of the United States of America, 106*(49), 20705-20710.

Harrison, C. J., Bohm, A. A., & Nelson, H. C. (1994). Crystal structure of the DNA binding domain of the heat shock transcription factor. *Science, 263*(5144), 224-227.

Hassan, K. M. A., Norwood, T., Gimelli, G., Gartler, S. M., & Hansen, R. S. (2001). Satellite 2 methylation patterns in normal and ICF syndrome cells and association of hypomethylation with advanced replication. *Human Genetics, 109*(4), 452-462.

Hausmann, S., Koiwa, H., Krishnamurthy, S., Hampsey, M., & Shuman, S. (2005). Different strategies for carboxyl-terminal domain (CTD) recognition by serine 5-specific CTD phosphatases. *Journal of Biological Chemistry, 280*(45), 37681-37688.

Hawley, D. K., Wiest, D. K., Holtz, M. S., & Wang, D. G. (1993). Transcriptional Pausing, Arrest, and Readthrough at the Adenovirus Major Late Attenuation Site. *Cellular & Molecular Biology Research, 39*(4), 339-348.

Heard, E. (2005). Delving into the diversity of facultative heterochromatin: the epigenetics of the inactive X chromosome. *Current Opinion in Genetics & Development, 15*(5), 482-489.

Hebbes, T. R., Thorne, A. W., & Cranerobinson, C. (1988). A Direct Link between Core Histone Acetylation and Transcriptionally Active Chromatin. *Embo Journal, 7*(5), 1395-1402.

Hegde, A. N., & Upadhya, S. C. (2006). Proteasome and transcription: a destroyer goes into construction. *Bioessays, 28*(3), 235-239.
Heinemeyer, W., Fischer, M., Krimmer, T., Stachon, U., & Wolf, D. H. (1997). The active sites of the eukaryotic 20 S proteasome and their involvement in subunit precursor processing. *Journal of Biological Chemistry, 272*(40), 25200-25209.

Heinemeyer, W., Trondle, N., Albrecht, G., & Wolf, D. H. (1994). PRE5 and PRE6, the last missing genes encoding 20S proteasome subunits from yeast? Indication for a set of 14 different subunits in the eukaryotic proteasome core. *Biochemistry, 33*(40), 12229-12237.
Heitz, E. (1928). Das Heterochromatin der Moose. *Jahrb Wiss Botanik, 69*(762).

Hemeryck, A., Geerts, R., Monbaliu, J., Hassler, S., Verhaeghe, T., Diels, L., . . . De Coster, R. (2007). Tissue distribution and depletion kinetics of bortezomib and bortezomib-related radioactivity in male rats after single and repeated intravenous injection of C-14-bortezomib. *Cancer Chemotherapy and Pharmacology, 60*(6), 777-787.

Henikoff, S. (1998). Conspiracy of silence among repeated transgenes. *Bioessays, 20*(7), 532-535.

Herman, D., Jenssen, K., Burnett, R., Soragni, E., Perlman, S. L., & Gottesfeld, J. M. (2006). Histone deacetylase inhibitors reverse gene silencing in Friedreich's ataxia. *Nat Chem Biol, 2*(10), 551-558.

Hermann, A., Goyal, R., & Jeltsch, A. (2004). The Dnmt1 DNA-(cytosine-C5)-methyltransferase methylates DNA processively with high preference for hemimethylated target sites. *J Biol Chem, 279*(46), 48350-48359.

Hernandez-Pigeon, H., Laurent, G., Humbert, O., Salles, B., & Lautier, D. (2004). Degadration of mismatch repair hMutSalpha heterodimer by the ubiquitin-proteasome pathway. *Febs Letters, 562*(1-3), 40-44.

Heslop-Harrison, J. S., Brandes, A., & Schwarzacher, T. (2003). Tandemly repeated DNA sequences and centromeric chromosomal regions of Arabidopsis species. *Chromosome Res, 11*(3), 241-253.

Hideshima, T., Chauhan, D., Richardson, P., Mitsiades, C., Mitsiades, N., Hayashi, T., . . . Anderson, K. C. (2002). NF-kappa B as a therapeutic target in multiple myeloma. *J Biol Chem, 277*(19), 16639-16647.

Hiragami, K., & Festenstein, R. (2005). Heterochromatin protein 1: a pervasive controlling influence. *Cell Mol Life Sci, 62*(23), 2711-2726.

Hirota, T., Lipp, J. J., Toh, B. H., & Peters, J. M. (2005). Histone H3 serine 10 phosphorylation by Aurora B causes HP1 dissociation from heterochromatin. *Nature, 438*(7071), 1176-1180.

Hoane, M. R., Kaplan, S. A., & Ellis, A. L. (2006). The effects of nicotinamide on apoptosis and blood-brain barrier breakdown following traumatic brain injury. *Brain Research, 1125*, 185-193.

Holliday, R., & Pugh, J. E. (1975). DNA modification mechanisms and gene activity during development. *Science, 187*(4173), 226-232.

Holmberg, C. I., Hietakangas, V., Mikhailov, A., Rantanen, J. O., Kallio, M., Meinander, A., . . . Sistonen, L. (2001). Phosphorylation of serine 230 promotes inducible transcriptional activity of heat shock factor 1. *Embo Journal, 20*(14), 3800-3810.

Hon, G. C., Hawkins, R. D., & Ren, B. (2009). Predictive chromatin signatures in the mammalian genome. *Hum Mol Genet, 18*(R2), R195-201.

Hori, T., Shang, W. H., Takeuchi, K., & Fukagawa, T. (2013). The CCAN recruits CENP-A to the centromere and forms the structural core for kinetochore assembly. *J Cell Biol, 200*(1), 45-60.

Hori, T., Shang, W. H., Toyoda, A., Misu, S., Monma, N., Ikeo, K., . . . Fukagawa, T. (2014). Histone H4 Lys 20 Monomethylation of the CENP-A Nucleosome Is Essential for Kinetochore Assembly. *Developmental Cell, 29*(6), 740-749.

Horsman, M. R., Hoyer, M., Honess, D. J., Dennis, I. F., & Overgaard, J. (1993). Nicotinamide pharmacokinetics in humans and mice: a comparative assessment and the implications for radiotherapy. *Radiother Oncol, 27*(2), 131-139.

Hosokawa, N., Hirayoshi, K., Kudo, H., Takechi, H., Aoike, A., Kawai, K., & Nagata, K. (1992). Inhibition of the activation of heat shock factor in vivo and in vitro by flavonoids. *Mol Cell Biol, 12*(8), 3490-3498.

Huang, Q., & Figueiredo-Pereira, M. E. (2010). Ubiquitin/proteasome pathway impairment in neurodegeneration: therapeutic implications. *Apoptosis, 15*(11), 1292-1311.

Huang, T. T., & D'Andrea, A. D. (2006). Regulation of DNA repair by ubiquitylation. *Nat Rev Mol Cell Biol, 7*(5), 323-334.

Huang, Y., Liang, P. P., Liu, D., Huang, J. J., & Songyang, Z. (2014). Telomere regulation in pluripotent stem cells. *Protein & Cell, 5*(3), 194-202.

Huibregtse, J. M., Yang, J. C., & Beaudenon, S. L. (1997). The large subunit of RNA polymerase II is a substrate of the Rsp5 ubiquitin-protein ligase. *Proceedings of the National Academy of Sciences of the United States of America, 94*(8), 3656-3661.

Husnjak, K., Elsasser, S., Zhang, N. X., Chen, X., Randles, L., Shi, Y., . . . Dikic, I. (2008). Proteasome subunit Rpn13 is a novel ubiquitin receptor. *Nature, 453*(7194), 481-488.

Hutnick, L. K., Huang, X. H., Loo, T. C., Ma, Z. C., & Fan, G. P. (2010). Repression of Retrotransposal Elements in Mouse Embryonic Stem Cells Is Primarily Mediated by a DNA Methylation-independent Mechanism. *Journal of Biological Chemistry, 285*(27), 21082-21091.

Hutter, G., Rieken, M., Pastore, A., Weigert, O., Zimmermann, Y., Weinkauf, M., . . . Dreyling, M. (2012). The proteasome inhibitor bortezomib targets cell cycle and apoptosis and acts synergistically in a sequence-dependent way with chemotherapeutic agents in mantle cell lymphoma. *Ann Hematol, 91*(6), 847-856.

Imai, S., Armstrong, C. M., Kaeberlein, M., & Guarente, L. (2000). Transcriptional silencing and longevity protein Sir2 is an NAD-dependent histone deacetylase. *Nature, 403*(6771), 795-800.

Ingham, R. J., Gish, G., & Pawson, T. (2004). The Nedd4 family of E3 ubiquitin ligases: functional diversity within a common modular architecture. *Oncogene, 23*(11), 1972-1984.

Inoue, S., Nakase, H., Matsuura, M., Mikami, S., Ueno, S., Uza, N., & Chiba, T. (2009). The effect of proteasome inhibitor MG132 on experimental inflammatory bowel disease. *Clinical and Experimental Immunology, 156*(1), 172-182.

Inouye, S., Izu, H., Takaki, E., Suzuki, H., Shirai, M., Yokota, Y., . . . Nakai, A. (2004). Impaired IgG production in mice deficient for heat shock transcription factor 1. *Journal of Biological Chemistry, 279*(37), 38701-38709.

Ip, J. Y., Schmidt, D., Pan, Q., Ramani, A. K., Fraser, A. G., Odom, D. T., & Blencowe, B. J. (2011). Global impact of RNA polymerase II elongation inhibition on alternative splicing regulation. *Genome Res, 21*(3), 390-401.

Ito, S., Magalska, A., Alcaraz-Iborra, M., Lopez-Atalaya, J. P., Rovira, V., Contreras-Moreira, B., . . . Barco, A. (2014). Loss of neuronal 3D chromatin organization causes transcriptional and behavioural deficits related to serotonergic dysfunction. *Nat Commun, 5*, 4450.

Ivics, Z., & Izsvak, Z. (2010). Repetitive elements and genome instability. *Semin Cancer Biol, 20*(4), 197-199.

Izban, M. G., & Luse, D. S. (1991). Transcription on nucleosomal templates by RNA polymerase II in vitro: inhibition of elongation with enhancement of sequence-specific pausing. *Genes Dev, 5*(4), 683-696.

Jang, M.K. *et al*. (2005). The bromodomain protein Brd4 is a positive regulatory component of P-TEFb and stimulates RNA polymerase II-dependent transcription. *Mol.Cell* 19, 523–534.

Jamart, C., Raymackers, J. M., An, G. L., Deldicque, L., & Francaux, M. (2011). Prevention of Muscle Disuse Atrophy by Mg132 Proteasome Inhibitor. *Muscle & Nerve, 43*(5), 708-716.

Jariel-Encontre, I., Bossis, G., & Piechaczyk, M. (2008). Ubiquitin-independent degradation of proteins by the proteasome. *Biochimica Et Biophysica Acta-Reviews on Cancer, 1786*(2), 153-177.

Jeffreys, A. J. (1997). Spontaneous and induced minisatellite instability in the human genome. *Clinical Science, 93*(5), 383-390.

Jeffreys, A. J., Wilson, V., & Thein, S. L. (1985). Hypervariable Minisatellite Regions in Human DNA. *Nature, 314*(6006), 67-73.
Jenuwein, T., & Allis, C. D. (2001). Translating the histone code. *Science, 293*(5532), 1074-1080.

Jeppesen, P., Mitchell, A., Turner, B., & Perry, P. (1992). Antibodies to defined histone epitopes reveal variations in chromatin conformation and underacetylation of centric heterochromatin in human metaphase chromosomes. *Chromosoma, 101*(5-6), 322-332.

Jeppesen, P., & Turner, B. M. (1993). The Inactive X-Chromosome in Female Mammals Is Distinguished by a Lack of Histone-H4 Acetylation, a Cytogenetic Marker for Gene-Expression. *Cell, 74*(2), 281-289.

Jha, D. K., & Strahl, B. D. (2014). An RNA polymerase II-coupled function for histone H3K36 methylation in checkpoint activation and DSB repair. *Nat Commun, 5*, 3965.

Jiralerspong, S., Ge, B., Hudson, T. J., & Pandolfo, M. (2001). Manganese superoxide dismutase induction by iron is impaired in Friedreich ataxia cells. *Febs Letters, 509*(1), 101-105.

Johansson, A. M., Stenberg, P., Pettersson, F., & Larsson, J. (2007). POF and HP1 bind expressed exons, suggesting a balancing mechanism for gene regulation. *Plos Genetics, 3*(11), 2235-2246.

Johnston, J. A., Ward, C. L., & Kopito, R. R. (1998). Aggresomes: a cellular response to misfolded proteins. *Journal of Cell Biology, 143*(7), 1883-1898.

Jolly, C., Konecny, L., Grady, D. L., Kutskova, Y. A., Cotto, J. J., Morimoto, R. I., & Vourc'h, C. (2002). In vivo binding of active heat shock transcription factor 1 to human chromosome 9 heterochromatin during stress. *J Cell Biol, 156*(5), 775-781.

Jolly, C., Metz, A., Govin, J., Vigneron, M., Turner, B. M., Khochbin, S., & Vourc'h, C. (2004a/b). Stress-induced transcription of satellite III repeats. *J Cell Biol, 164*(1), 25-33.

Jolly, C., Morimoto, R., Robert-Nicoud, M., & Vourc'h, C. (1997). HSF1 transcription factor concentrates in nuclear foci during heat shock: relationship with transcription sites. *J Cell Sci, 110 (Pt 23)*, 2935-2941.

Jolma, A., Yan, J., Whitington, T., Toivonen, J., Nitta, K. R., Rastas, P., . . . Taipale, J. (2013). DNA-binding specificities of human transcription factors. *Cell, 152*(1-2), 327-339.

Jones, K. W., Prosser, J., Corneo, G., & Ginelli, E. (1973). The chromosomal location of human satellite DNA 3. *Chromosoma, 42*(4), 445-451.

Jones, P. L., Veenstra, G. J., Wade, P. A., Vermaak, D., Kass, S. U., Landsberger, N., . . . Wolffe, A. P. (1998a/b). Methylated DNA and MeCP2 recruit histone deacetylase to repress transcription. *Nat Genet, 19*(2), 187-191.

Jorgensen, S., Elvers, I., Trelle, M. B., Menzel, T., Eskildsen, M., Jensen, O. N., . . . Sorensen, C. S. (2007). The histone methyltransferase SET8 is required for S-phase progression. *Journal of Cell Biology, 179*(7), 1337-1345.

Jorgensen, S., Schotta, G., & Sorensen, C. S. (2013). Histone H4 Lysine 20 methylation: key player in epigenetic regulation of genomic integrity. *Nucleic Acids Research, 41*(5), 2797-2806.

Joshi, A. A., & Struhl, K. (2005). Eaf3 chromodomain interaction with methylated H3-K36 links histone deacetylation to Pol II elongation. *Molecular Cell, 20*(6), 971-978.

Josling, G. A., Selvarajah, S. A, Petter, M & Duffy, M. F. (2012). The Role of Bromodomain Proteins in Regulating Gene Expression. *Genes*, 3, 320-343

Jung, J., Kim, E. J., Chung, H. K., Park, H. J., Jeong, S. Y., & Choi, E. K. (2012). c-Myc down-regulation is involved in proteasome inhibitor-mediated enhancement of radiotherapeutic efficacy in non-small cell lung cancer. *International Journal of Oncology, 40*(2), 385-390.

Jung, T., & Grune, T. (2013). The proteasome and the degradation of oxidized proteins: Part I-structure of proteasomes. *Redox Biology, 1*(1), 178-182.

Jurka, J. (1997). Sequence patterns indicate an enzymatic involvement in integration of mammalian retroposons. *Proc Natl Acad Sci U S A, 94*(5), 1872-1877.

Kallio, M., Chang, Y. H., Manuel, M., Alastalo, T. P., Rallu, M., Gitton, Y., . . . Mezger, V. (2002). Brain abnormalities, defective meiotic chromosome synapsis and female subfertility in HSF2 null mice. *Embo Journal, 21*(11), 2591-2601.

Kang, Z. G., Pirskanen, A., Janne, O. A., & Palvimo, J. J. (2002). Involvement of proteasome in the dynamic assembly of the androgen receptor transcription complex. *Journal of Biological Chemistry, 277*(50), 48366-48371.

Kanno, T., Kanno, Y., Siegel, R.M., Jang, M.K., Lenardo, M.J., & Ozato, K. (2004). Selective recognition of acetylated histones by bromodomain proteins visualized in living cells. *Mol. Cell*, 13 (1), 33-43.

Kanno, T., Kanno, Y., LeRoy, G., Campos, E., Sun, H.W., Brooks, S. R., Vahedi, G., Heightman, T.D., Garcia, B. A., Reinberg,D., Siebenlist, U., O'Shea J.J., & Ozato K. BRD4 assists elongation

of both coding and enhancer RNAs by interacting with acetylated histones. *Nat. Structural and Molecular Biology*, 21, 1047-1057.

Kapoor, M., & Lozano, G. (1998). Functional activation of p53 via phosphorylation following DNA damage by UV but not gamma radiation. *Proceedings of the National Academy of Sciences of the United States of America, 95*(6), 2834-2837.

Karakasili, E., Burkert-Kautzsch, C., Kieser, A., & Strasser, K. (2014). Degradation of DNA damage-independently stalled RNA polymerase II is independent of the E3 ligase Elc1. *Nucleic Acids Research, 42*(16), 10503-10515.

Kato, H., Goto, D. B., Martienssen, R. A., Urano, T., Furukawa, K., & Murakami, Y. (2005). RNA polymerase II is required for RNAi-dependent heterochromatin assembly. *Science, 309*(5733), 467-469.

Kawazoe, Y., Nakai, A., Tanabe, M., & Nagata, K. (1998). Proteasome inhibition leads to the activation of all members of the heat-shock-factor family. *European Journal of Biochemistry, 255*(2), 356-362.

Kellum, R., & Alberts, B. M. (1995). Heterochromatin Protein-1 Is Required for Correct Chromosome Segregation in Drosophila Embryos. *Journal of Cell Science, 108*, 1419-1431.
Keogh, M. C., Kurdistani, S. K., Morris, S. A., Ahn, S. H., Podolny, V., Collins, S. R., . . . Krogan, N. J. (2005). Cotranscriptional set2 methylation of histone H3 lysine 36 recruits a repressive Rpd3 complex. *Cell, 123*(4), 593-605.

Kerppola, T. K., & Kane, C. M. (1988). Intrinsic sites of transcription termination and pausing in the c-myc gene. *Molecular and Cellular Biology, 8*(10), 4389-4394.

Khaleque, M., Bharti, A., Gong, J., Gray, P. J., Sachdev, V., Ciocca, D. R., . . . Calderwood, S. K. (2008). Heat shock factor 1 represses estrogen-dependent transcription through association with MTA1. *Oncogene, 27*(13), 1886-1893.

Kichine, E., Roze, V., Di Cristofaro, J., Taulier, D., Navarro, A., Streichemberger, E., . . . Mitchell, M. J. (2012). HSFY genes and the P4 palindrome in the AZFb interval of the human Y chromosome are not required for spermatocyte maturation. *Hum Reprod, 27*(2), 615-624.

Kikuchi, J., Wada, T., Shimizu, R., Izumi, T., Akutsu, M., Mitsunaga, K., . . . Furukawa, Y. (2010). Histone deacetylases are critical targets of bortezomib-induced cytotoxicity in multiple myeloma. *Blood, 116*(3), 406-417.

Kim, E., Napierala, M., & Dent, S. Y. (2011). Hyperexpansion of GAA repeats affects post-initiation steps of FXN transcription in Friedreich's ataxia. *Nucleic Acids Res, 39*(19), 8366-8377.

Kim, H. N., Han, L., Iyer, S., de Cabo, R., Zhao, H., O'Brien, C. A., . . . Almeida, M. (2015). Sirtuin1 Suppresses Osteoclastogenesis by Deacetylating FoxOs. *Mol Endocrinol, 29*(10), 1498-1509.

Kim, J. H., Ebersole, T., Kouprina, N., Noskov, V. N., Ohzeki, J. I., Masumoto, H., . . . Larionov, V. (2009). Human gamma-satellite DNA maintains open chromatin structure and protects a transgene from epigenetic silencing. *Genome Research, 19*(4), 533-544.

Kim, S. J., Tsukiyama, T., Lewis, M. S., & Wu, C. (1994). Interaction of the DNA-Binding Domain of Drosophila Heat-Shock Factor with Its Cognate DNA Site - a Thermodynamic Analysis Using Analytical Ultracentrifugation. *Protein Science, 3*(7), 1040-1051.

Kim, S. M., Dubey, D. D., & Huberman, J. A. (2003). Early-replicating heterochromatin. *Genes Dev, 17*(3), 330-335.

Kim, T., & Buratowski, S. (2009). Dimethylation of H3K4 by Set1 recruits the Set3 histone deacetylase complex to 5' transcribed regions. *Cell, 137*(2), 259-272.

Kim, T., Xu, Z., Clauder-Munster, S., Steinmetz, L. M., & Buratowski, S. (2012). Set3 HDAC mediates effects of overlapping noncoding transcription on gene induction kinetics. *Cell, 150*(6), 1158-1169.

Kim, Y. J., Lee, J., & Han, K. (2012). Transposable Elements: No More 'Junk DNA'. *Genomics Inform, 10*(4), 226-233.

Kinoshita, K., Shinka, T., Sato, Y., Kurahashi, H., Kowa, H., Chen, G., . . . Nakahori, Y. (2006). Expression analysis of a mouse orthologue of HSFY, a candidate for the azoospermic factor on the human Y chromosome. *J Med Invest, 53*(1-2), 117-122.

Kinyamu, H. K., & Archer, T. K. (2007). Proteasome activity modulates chromatin modifications and RNA polymerase II phosphorylation to enhance glucocorticoid receptor-mediated transcription. *Mol Cell Biol, 27*(13), 4891-4904.

Kireeva, M. L., Hancock, B., Cremona, G. H., Walter, W., Studitsky, V. M., & Kashlev, M. (2005). Nature of the nucleosomal barrier to RNA polymerase II. *Molecular Cell, 18*(1), 97-108.

Kisselev, A. F., & Goldberg, A. L. (2001). Proteasome inhibitors: from research tools to drug candidates. *Chem Biol, 8*(8), 739-758.

Kitagawa, T., Ishii, K., Takeda, K., & Matsumoto, T. (2014a/b). The 19S proteasome subunit Rpt3 regulates distribution of CENP-A by associating with centromeric chromatin. *Nat Commun, 5*, 3597.

Kline, M. P., & Morimoto, R. I. (1997). Repression of the heat shock factor 1 transcriptional activation domain is modulated by constitutive phosphorylation. *Molecular and Cellular Biology, 17*(4), 2107-2115.

Kloc, A., Zaratiegui, M., Nora, E., & Martienssen, R. (2008). RNA interference guides histone modification during the S phase of chromosomal replication. *Curr Biol, 18*(7), 490-495.

Knauf, U., Newton, E. M., Kyriakis, J., & Kingston, R. E. (1996). Repression of human heat shock factor 1 activity at control temperature by phosphorylation. *Genes & Development, 10*(21), 2782-2793.

Knight, J. C. (2009). Human Genetic Diversity . Functional Consequences for Health and Disease. *Oxford University Press*.

Knip, M., Douek, I. F., Moore, W. P. T., Gillmor, H. A., McLean, A. E. M., Bingley, P. J., . . . Grp, E. (2000). Safety of high dose nicotinamide: a review. *Diabetologia, 43*(11), 1337-1345.

Knoll, B., Kretz, O., Fiedler, C., Alberti, S., Schutz, G., Frotscher, M., & Nordheim, A. (2006). Serum response factor controls neuronal circuit assembly in the hippocampus. *Nature Neuroscience, 9*(2), 195-204.

Knutsen, J. H., Rein, I. D., Rothe, C., Stokke, T., Grallert, B., & Boye, E. (2011). Cell-cycle analysis of fission yeast cells by flow cytometry. *PLoS One, 6*(2), e17175.

Kodadek, T. (2010). No Splicing, No Dicing: Non-proteolytic Roles of the Ubiquitin-Proteasome System in Transcription. *Journal of Biological Chemistry, 285*(4), 2221-2226.

Koeppen, A. H. (2011). Friedreich's ataxia: pathology, pathogenesis, and molecular genetics. *J Neurol Sci, 303*(1-2), 1-12.

Koeppen, A. H. (2013). Nikolaus Friedreich and degenerative atrophy of the dorsal columns of the spinal cord. *J Neurochem, 126 Suppl 1*, 4-10.

Kolasinska-Zwierz, P., Down, T., Latorre, I., Liu, T., Liu, X. S., & Ahringer, J. (2009). Differential chromatin marking of introns and expressed exons by H3K36me3. *Nat Genet, 41*(3), 376-381.

Komissarov, A. S., Gavrilova, E. V., Demin, S. J., Ishov, A. M., & Podgornaya, O. I. (2011). Tandemly repeated DNA families in the mouse genome. *BMC Genomics, 12*, 531.

Kong, X. G., Lin, Z., Liang, D. M., Fath, D., Sang, N. L., & Caro, J. (2006). Histone deacetylase inhibitors induce VHL and ubiquitin-independent proteasomal degradation of hypoxia-inducible factor 1 alpha. *Molecular and Cellular Biology, 26*(6), 2019-2028.

Konkel, M. K., & Batzer, M. A. (2010). A mobile threat to genome stability: The impact of non-LTR retrotransposons upon the human genome. *Seminars in Cancer Biology, 20*(4), 211-221.

Kornberg, R. D. (1974). Chromatin structure: a repeating unit of histones and DNA. *Science, 184*(4139), 868-871.

Kourmouli, N., Jeppesen, P., Mahadevhaiah, S., Burgoyne, P., Wu, R., Gilbert, D. M., . . . Singh, P. B. (2004). Heterochromatin and tri-methylated lysine 20 of histone H4 in animals. *Journal of Cell Science, 117*(12), 2491-2501.

Koutnikova, H., Campuzano, V., Foury, F., Dolle, P., Cazzalini, O., & Koenig, M. (1997). Studies of human, mouse and yeast homologues indicate a mitochondrial function for frataxin. *Nature Genetics, 16*(4), 345-351.

Koutnikova, H., Campuzano, V., & Koenig, M. (1998). Maturation of wild-type and mutated frataxin by the mitochondrial processing peptidase. *Hum Mol Genet, 7*(9), 1485-1489.

Kouzarides, T. (2007). Chromatin modifications and their function. *Cell, 128*(4), 693-705.

Kramerov, D. A., & Vassetzky, N. S. (2005). Short retroposons in eukaryotic genomes. *Int Rev Cytol, 247*, 165-221.

Krishnamurthy, S., He, X., Reyes-Reyes, M., Moore, C., & Hampsey, M. (2004). Ssu72 Is an RNA polymerase II CTD phosphatase. *Molecular Cell, 14*(3), 387-394.

Kroeger, P. E., Sarge, K. D., & Morimoto, R. I. (1993). Mouse heat shock transcription factors 1 and 2 prefer a trimeric binding site but interact differently with the HSP70 heat shock element. *Mol Cell Biol, 13*(6), 3370-3383.

Krogan, N. J., Kim, M., Tong, A., Golshani, A., Cagney, G., Canadien, V., . . . Greenblatt, J. (2003). Methylation of histone H3 by Set2 in Saccharomyces cerevisiae is linked to transcriptional elongation by RNA polymerase II. *Molecular and Cellular Biology, 23*(12), 4207-4218.

Krogan, N. J., Lam, M. H., Fillingham, J., Keogh, M. C., Gebbia, M., Li, J., . . . Greenblatt, J. F. (2004a/b). Proteasome involvement in the repair of DNA double-strand breaks. *Mol Cell, 16*(6), 1027-1034.

Krumm, A., Meulia, T., Brunvand, M., & Groudine, M. (1992). The Block to Transcriptional Elongation within the Human C-Myc Gene Is Determined in the Promoter - Proximal Region. *Genes & Development, 6*(11), 2201-2213.

Kultz, D. (2003). Evolution of the cellular stress proteome: from monophyletic origin to ubiquitous function. *J Exp Biol, 206*(Pt 18), 3119-3124.

Kultz, D. (2005). Molecular and evolutionary basis of the cellular stress response. *Annu Rev Physiol, 67*, 225-257.

Kumari, D., Biacsi, R. E., & Usdin, K. (2011). Repeat Expansion Affects Both Transcription Initiation and Elongation in Friedreich Ataxia Cells. *Journal of Biological Chemistry, 286*(6), 4209-4215.

Kung, A. L., Zetterberg, A., Sherwood, S. W., & Schimke, R. T. (1990). Cytotoxic effects of cell cycle phase specific agents: result of cell cycle perturbation. *Cancer Research, 50*(22), 7307-7317.

Kunjappu, M. J., & Hochstrasser, M. (2014). Assembly of the 20S proteasome. *Biochim Biophys Acta, 1843*(1), 2-12.

Kuramochi-Miyagawa, S., Watanabe, T., Gotoh, K., Totoki, Y., Toyoda, A., Ikawa, M., . . . Nakano, T. (2008). DNA methylation of retrotransposon genes is regulated by Piwi family members MILI and MIWI2 in murine fetal testes. *Genes & Development, 22*(7), 908-917.

Kwon, S. H., Florens, L., Swanson, S. K., Washburn, M. P., Abmayr, S. M., & Workman, J. L. (2010). Heterochromatin protein 1 (HP1) connects the FACT histone chaperone complex to the phosphorylated CTD of RNA polymerase II. *Genes & Development, 24*(19), 2133-2145.

Lachner, M., O'Carroll, N., Rea, S., Mechtler, K., & Jenuwein, T. (2001). Methylation of histone H3 lysine 9 creates a binding site for HP1 proteins. *Nature, 410*(6824), 116-120.

Lander, E. S., Consortium, I. H. G. S., Linton, L. M., Birren, B., Nusbaum, C., Zody, M. C., . . . Conso, I. H. G. S. (2001). Initial sequencing and analysis of the human genome. *Nature, 409*(6822), 860-921.

Lander, G. C., Estrin, E., Matyskiela, M. E., Bashore, C., Nogales, E., & Martin, A. (2012). Complete subunit architecture of the proteasome regulatory particle. *Nature, 482*(7384), 186-U175.

Lange, U. C., Siebert, S., Wossidlo, M., Weiss, T., Ziegler-Birling, C., Walter, J., . . . Schneider, R. (2013). Dissecting the role of H3K64me3 in mouse pericentromeric heterochromatin. *Nat Commun, 4*, 2233.

Lanikova, L., Kucerova, J., Indrak, K., Divoka, M., Issa, J. P., Papayannopoulou, T., . . . Divoky, V. (2013). beta-Thalassemia due to intronic LINE-1 insertion in the beta-globin gene (HBB): molecular mechanisms underlying reduced transcript levels of the beta-globin(L1) allele. *Hum Mutat, 34*(10), 1361-1365.

Lasker, K., Forster, F., Bohn, S., Walzthoeni, T., Villa, E., Unverdorben, P., . . . Baumeister, W. (2012). Molecular architecture of the 26S proteasome holocomplex determined by an integrative approach. *Proceedings of the National Academy of Sciences of the United States of America, 109*(5), 1380-1387.

Lassot, I., Latreille, D., Rousset, E., Sourisseau, M., Linares, L. K., Chable-Bessia, C., . . . Kiernan, R. E. (2007). The proteasome regulates HIV-1 transcription by both proteolytic and nonproteolytic mechanisms. *Molecular Cell, 25*(3), 369-383.

Latonen, L., Taya, Y., & Laiho, M. (2001). UV-radiation induces dose-dependent regulation of p53 response and modulates p53-HDM2 interaction in human fibroblasts (vol 20, pg 6784, 2001). *Oncogene, 20*(56), 8165-8165.

Lauberth, S. M., Nakayama, T., Wu, X. L., Ferris, A. L., Tang, Z. Y., Hughes, S. H., & Roeder, R. G. (2013). H3K4me3 Interactions with TAF3 Regulate Preinitiation Complex Assembly and Selective Gene Activation. *Cell, 152*(5), 1021-1036.

Law, J. A., & Jacobsen, S. E. (2010). Establishing, maintaining and modifying DNA methylation patterns in plants and animals. *Nat Rev Genet, 11*(3), 204-220.

Lee, C. M., Kumar, V., Riley, R. I., & Morgan, E. T. (2010). Metabolism and action of proteasome inhibitors in primary human hepatocytes. *Drug Metab Dispos, 38*(12), 2166-2172.

Lee, D. Y., Ezhkova, E., Li, B., Pattenden, S. G., Tansey, W. P., & Workman, J. L. (2005). The proteasome regulatory particle alters the SAGA coactivator to enhance its interactions with transcriptional activators. *Cell, 123*(3), 423-436.

Lee, D. Y., Teyssier, C., Strahl, B. D., & Stallcup, M. R. (2005). Role of protein methylation in regulation of transcription. *Endocrine Reviews, 26*(2), 147-170.

Lee, H. R., Neumann, P., Macas, J., & Jiang, J. M. (2006). Transcription and evolutionary dynamics of the centromeric satellite repeat CentO in rice. *Molecular Biology and Evolution, 23*(12), 2505-2520.

Lee, J. H., & Skalnik, D. G. (2008). Wdr82 is a C-terminal domain-binding protein that recruits the Setd1A histone H3-Lys4 methyltransferase complex to transcription start sites of transcribed human genes. *Molecular and Cellular Biology, 28*(2), 609-618.

Lee, J. H., Tate, C. M., You, J. S., & Skalnik, D. G. (2007). Identification and characterization of the human Set1B histone H3-Lys(4) methyltransferase complex. *Journal of Biological Chemistry, 282*(18), 13419-13428.

Lee, K. B., & Sharp, P. A. (2004). Transcription-dependent polyubiquitination of RNA polymerase II requires lysine 63 of ubiquitin. *Biochemistry, 43*(48), 15223-15229.

Lee, K. B., Wang, D., Lippard, S. J., & Sharp, P. A. (2002). Transcription-coupled and DNA damage-dependent ubiquitination of RNA polymerase II in vitro. *Proc Natl Acad Sci U S A, 99*(7), 4239-4244.

Lee, T. I., & Young, R. A. (2013). Transcriptional regulation and its misregulation in disease. *Cell, 152*(6), 1237-1251.

Lehnertz, B., Ueda, Y., Derijck, A. A. H. A., Braunschweig, U., Perez-Burgos, L., Kubicek, S., . . . Peters, A. H. F. M. (2003). Suv39h-mediated histone H3 lysine 9 methylation directs DNA methylation to major satellite repeats at pericentric heterochromatin. *Current Biology, 13*(14), 1192-1200.

Lele, S. (1993). Euclidean Distance Matrix Analysis (Edma) - Estimation of Mean Form and Mean Form Difference. *Mathematical Geology, 25*(5), 573-602.

Levin, H. L., & Moran, J. V. (2011). Dynamic interactions between transposable elements and their hosts. *Nature Reviews Genetics, 12*(9), 615-627.

Levsky, J. M., Shenoy, S. M., Pezo, R. C., & Singer, R. H. (2002). Single-cell gene expression profiling. *Science, 297*(5582), 836-840.

Levy, J., Teuerstein, I., Marbach, M., Radian, S., & Sharoni, Y. (1984). Tyrosine protein kinase activity in the DMBA-induced rat mammary tumor: inhibition by quercetin. *Biochem Biophys Res Commun, 123*(3), 1227-1233.

Li, B., Howe, L., Anderson, S., Yates, J. R., & Workman, J. L. (2003). The Set2 histone methyltransferase functions through the phosphorylated carboxyl-terminal domain of RNA polymerase II. *Journal of Biological Chemistry, 278*(11), 8897-8903.

Li, F., Chong, Z. Z., & Maiese, K. (2006). Cell Life versus cell longevity: the mysteries surrounding the NAD+ precursor nicotinamide. *Curr Med Chem, 13*(8), 883-895.

Li, J., Moazed, D., & Gygi, S. P. (2002). Association of the histone methyltransferase Set2 with RNA polymerase II plays a role in transcription elongation. *J Biol Chem, 277*(51), 49383-49388.

Li, K. Y., Besse, E. K., Ha, D., Kovtunovych, G., & Rouault, T. A. (2008). Iron-dependent regulation of frataxin expression: implications for treatment of Friedreich ataxia. *Human Molecular Genetics, 17*(15), 2265-2273.

Li, K. Y., Singh, A., Crooks, D. R., Dai, X. M., Cong, Z. Z., Pan, L. A., . . . Rouault, T. A. (2010). Expression of Human Frataxin Is Regulated by Transcription Factors SRF and TFAP2. *PLoS One, 5*(8).

Li, T. H., Spearow, J., Rubin, C. M., & Schmid, C. W. (1999). Physiological stresses increase mouse short interspersed element (SINE) RNA expression in vivo. *Gene, 239*(2), 367-372.

Li, W., Bengtson, M. H., Ulbrich, A., Matsuda, A., Reddy, V. A., Orth, A., . . . Joazeiro, C. A. P. (2008). Genome-Wide and Functional Annotation of Human E3 Ubiquitin Ligases Identifies MULAN, a Mitochondrial E3 that Regulates the Organelle's Dynamics and Signaling. *PLoS One, 3*(1).

Li, Y., Lu, Y., Polak, U., Lin, K., Shen, J., Farmer, J., . . . Napierala, M. (2015). Expanded GAA repeats impede transcription elongation through the FXN gene and induce transcriptional silencing that is restricted to the FXN locus. *Hum Mol Genet*.

Li, Y. X., & Kirby, M. L. (2003). Coordinated and conserved expression of alphoid repeat and alphoid repeat-tagged coding sequences. *Developmental Dynamics, 228*(1), 72-81.

Liang, P., & MacRae, T. H. (1997). Molecular chaperones and the cytoskeleton. *Journal of Cell Science, 110*, 1431-1440.

Libri, V., Yandim, C., Athanasopoulos, S., Loyse, N., Natisvili, T., Law, P. P., . . . Festenstein, R. (2014). Epigenetic and neurological effects and safety of high-dose nicotinamide in patients

with Friedreich's ataxia: an exploratory, open-label, dose-escalation study. *Lancet, 384*(9942), 504-513.

Lim, H. W., Kang, S. G., Ryu, J. K., Schilling, B., Fei, M., Lee, I. S., . . . Verdin, E. (2015). SIRT1 deacetylates RORgammat and enhances Th17 cell generation. *J Exp Med, 212*(6), 973.

Lima-de-Faria, A., & Jaworska, H. (1968). Late DNA synthesis in heterochromatin. *Nature, 217*(5124), 138-142.

Ling, Y. H., Liebes, L., Jiang, J. D., Holland, J. F., Elliott, P. J., Adams, J., . . . Perez-Soler, R. (2003). Mechanisms of proteasome inhibitor PS-341-induced G(2)-M-phase arrest and apoptosis in human non-small cell lung cancer cell lines. *Clin Cancer Res, 9*(3), 1145-1154.

Ling, Y. H., Liebes, L., Ng, B., Buckley, M., Elliott, P. J., Adams, J., . . . Perez-Soler, R. (2002). PS-341, a novel proteasome inhibitor, induces Bcl-2 phosphorylation and cleavage in association with G2-M phase arrest and apoptosis. *Mol Cancer Ther, 1*(10), 841-849.

Lipford, J. R., Smith, G. T., Chi, Y., & Deshaies, R. J. (2005). A putative stimulatory role for activator turnover in gene expression. *Nature, 438*(7064), 113-116.

Littlefield, O., & Nelson, H. C. M. (1999). A new use for the 'wing' of the 'winged' helix-turn-helix motif in the HSF-DNA cocrystal. *Nature Structural Biology, 6*(5), 464-470.

Liu, C. L., Kaplan, T., Kim, M., Buratowski, S., Schreiber, S. L., Friedman, N., & Rando, O. J. (2005). Single-nucleosome mapping of histone modifications in S-cerevisiae. *Plos Biology, 3*(10), 1753-1769.

Liu, C. W., & Jacobson, A. D. (2013). Functions of the 19S complex in proteasomal degradation. *Trends Biochem Sci, 38*(2), 103-110.

Liu, J., Lee, P., Galbiati, F., Kitsis, R. N., & Lisanti, M. P. (2001). Caveolin-1 expression sensitizes fibroblastic and epithelial cells to apoptotic stimulation. *Am J Physiol Cell Physiol, 280*(4), C823-835.

Liu, Z., Oughtred, R., & Wing, S. S. (2005). Characterization of E3Histone, a novel testis ubiquitin protein ligase which ubiquitinates histones. *Mol Cell Biol, 25*(7), 2819-2831.

Lopez-Serra, P., & Esteller, M. (2012). DNA methylation-associated silencing of tumor-suppressor microRNAs in cancer. *Oncogene, 31*(13), 1609-1622.

Loria, F., & Diaz-Nido, J. (2015). Frataxin knockdown in human astrocytes triggers cell death and the release of factors that cause neuronal toxicity. *Neurobiology of Disease, 76*, 1-12.

Lu, H. Y., Liu, X. Z., Deng, Y. L., & Qing, H. (2013). DNA methylation, a hand behind neurodegenerative diseases. *Frontiers in Aging Neuroscience, 5*.

Lu, J., & Gilbert, D. M. (2007). Proliferation-dependent and cell cycle regulated transcription of mouse pericentric heterochromatin. *J Cell Biol, 179*(3), 411-421.

Lu, P. P. Y., & Ramanan, N. (2011). Serum Response Factor Is Required for Cortical Axon Growth But Is Dispensable for Neurogenesis and Neocortical Lamination. *Journal of Neuroscience, 31*(46), 16651-16664.

Luco, R. F., Pan, Q., Tominaga, K., Blencowe, B. J., Pereira-Smith, O. M., & Misteli, T. (2010). Regulation of alternative splicing by histone modifications. *Science, 327*(5968), 996-1000.

Luger, K., Mader, A. W., Richmond, R. K., Sargent, D. F., & Richmond, T. J. (1997). Crystal structure of the nucleosome core particle at 2.8 angstrom resolution. *Nature, 389*(6648), 251-260.

Luo, S., & Preuss, D. (2003). Strand-biased DNA methylation associated with centromeric regions in Arabidopsis. *Proceedings of the National Academy of Sciences of the United States of America, 100*(19), 11133-11138.
Ly, T., Ahmad, Y., Shlien, A., Soroka, D., Mills, A., Emanuele, M. J., . . . Lamond, A. I. (2014). A proteomic chronology of gene expression through the cell cycle in human myeloid leukemia cells. *Elife, 3*, e01630.

Ma, Y., Kanakousaki, K., & Buttitta, L. (2015). How the cell cycle impacts chromatin architecture and influences cell fate. *Front Genet, 6*, 19.

Machiels, B. M., Henfling, M. E., Gerards, W. L., Broers, J. L., Bloemendal, H., Ramaekers, F. C., & Schutte, B. (1997). Detailed analysis of cell cycle kinetics upon proteasome inhibition. *Cytometry, 28*(3), 243-252.

Mahl, P., Lutz, Y., Puvion, E., & Fuchs, J. P. (1989). Rapid effect of heat shock on two heterogeneous nuclear ribonucleoprotein-associated antigens in HeLa cells. *J Cell Biol, 109*(5), 1921-1935.

Maison, C., Bailly, D., Peters, A. H., Quivy, J. P., Roche, D., Taddei, A., . . . Almouzni, G. (2002). Higher-order structure in pericentric heterochromatin involves a distinct pattern of histone modification and an RNA component. *Nat Genet, 30*(3), 329-334.

Maison, C., Bailly, D., Roche, D., Montes de Oca, R., Probst, A. V., Vassias, I., . . . Almouzni, G. (2011). SUMOylation promotes de novo targeting of HP1alpha to pericentric heterochromatin. *Nat Genet, 43*(3), 220-227.

Malik, S., Bagla, S., Chaurasia, P., Duan, Z., & Bhaumik, S. R. (2008). Elongating RNA polymerase II is disassembled through specific degradation of its largest but not other Subunits in response to DNA damage in vivo. *Journal of Biological Chemistry, 283*(11), 6897-6905.

Malik, S., Shukla, A., Sen, P., & Bhaumik, S. R. (2009). The 19 s proteasome subcomplex establishes a specific protein interaction network at the promoter for stimulated transcriptional initiation in vivo. *J Biol Chem, 284*(51), 35714-35724.

Marchetto, M. C. N., Narvaiza, I., Denli, A. M., Benner, C., Lazzarini, T. A., Nathanson, J. L., . . . Gage, F. H. (2013). Differential L1 regulation in pluripotent stem cells of humans and apes. *Nature, 503*(7477), 525

Marek, L., Hamacher, A., Hansen, F. K., Kuna, K., Gohlke, H., Kassack, M. U., & Kurz, T. (2013). Histone deacetylase (HDAC) inhibitors with a novel connecting unit linker region reveal a selectivity profile for HDAC4 and HDAC5 with improved activity against chemoresistant cancer cells. *J Med Chem, 56*(2), 427-436.

Mariner, P. D., Walters, R. D., Espinoza, C. A., Drullinger, L. F., Wagner, S. D., Kugel, J. F., & Goodrich, J. A. (2008). Human Alu RNA is a modular transacting repressor of mRNA transcription during heat shock. *Molecular Cell, 29*(4), 499-509.

Marshall, N. F., Peng, J., Xie, Z., & Price, D. H. (1996). Control of RNA polymerase II elongation potential by a novel carboxyl-terminal domain kinase. *J Biol Chem, 271*(43), 27176-27183.

Martens, J. H. A., O'Sullivan, R. J., Braunschweig, U., Opravil, S., Radolf, M., Steinlein, P., & Jenuwein, T. (2005). The profile of repeat-associated histone lysine methylation states in the mouse epigenome. *Embo Journal, 24*(4), 800-812.

Masumoto, H., Masukata, H., Muro, Y., Nozaki, N., & Okazaki, T. (1989). A human centromere antigen (CENP-B) interacts with a short specific sequence in alphoid DNA, a human centromeric satellite. *Journal of Cell Biology, 109*(5), 1963-1973.

Mateescu, B., Bourachot, B., Rachez, C., Ogryzko, V., & Muchardt, C. (2008). Regulation of an inducible promoter by an HP1beta-HP1gamma switch. *EMBO Rep, 9*(3), 267-272.

Mateos-Langerak, J., Brink, M. C., Luijsterburg, M. S., van der Kraan, I., van Driel, R., & Verschure, P. J. (2007). Pericentromeric heterochromatin domains are maintained without accumulation of HP1. *Mol Biol Cell, 18*(4), 1464-1471.

Mathew, A., Mathur, S. K., & Morimoto, R. I. (1998). Heat shock response and protein degradation: regulation of HSF2 by the ubiquitin-proteasome pathway. *Molecular and Cellular Biology, 18*(9), 5091-5098.

Matsui, T., Leung, D., Miyashita, H., Maksakova, I. A., Miyachi, H., Kimura, H., . . . Shinkai, Y. (2010). Proviral silencing in embryonic stem cells requires the histone methyltransferase ESET. *Nature, 464*(7290), 927-931.

Matter, W. F., Brown, R. F., & Vlahos, C. J. (1992). The inhibition of phosphatidylinositol 3-kinase by quercetin and analogs. *Biochem Biophys Res Commun, 186*(2), 624-631.

Maupin-Furlow, J. (2012). Proteasomes and protein conjugation across domains of life. *Nat Rev Microbiol, 10*(2), 100-111.

Mayer, R., Brero, A., von Hase, J., Schroeder, T., Cremer, T., & Dietzel, S. (2005). Common themes and cell type specific variations of higher order chromatin arrangements in the mouse. *BMC Cell Biol, 6*, 44.

McCann, T. S., & Tansey, W. P. (2014). Functions of the proteasome on chromatin. *Biomolecules, 4*(4), 1026-1044.

McIvor, E. I., Polak, U., & Napierala, M. (2010). New insights into repeat instability Role of RNA.DNA hybrids. *Rna Biology, 7*(5), 551-558.

McMillan, D. R., Xiao, X. Z., Shao, L., Graves, K., & Benjamin, I. J. (1998). Targeted disruption of heat shock transcription factor 1 abolishes thermotolerance and protection against heat-inducible apoptosis. *Journal of Biological Chemistry, 273*(13), 7523-7528.
McMurray, C. T. (2010). Mechanisms of trinucleotide repeat instability during human development. *Nat Rev Genet, 11*(11), 786-799.

Meehan, R. R., Kao, C. F., & Pennings, S. (2003). HP1 binding to native chromatin in vitro is determined by the hinge region and not by the chromodomain. *Embo Journal, 22*(12), 3164-3174.

Meenaghan, T., O'Dwyer, M., Hayden, P., Hayat, A., Murray, M., & Dowling, M. (2010a/b). Home administration of bortezomib: making a difference to myeloma patients' lives. *Eur J Oncol Nurs, 14*(2), 134-136.

Mengual, E., Arizti, P., Rodrigo, J., GimenezAmaya, J. M., & Castano, J. G. (1996). Immunohistochemical distribution and electron microscopic subcellular localization of the proteasome in the rat CNS. *Journal of Neuroscience, 16*(20), 6331-6341.

Mercier, P. A., Winegarden, N. A., & Westwood, J. T. (1999). Human heat shock factor 1 is predominantly a nuclear protein before and after heat stress. *Journal of Cell Science, 112*(16), 2765-2774.

Metz, A., Soret, J., Vourc'h, C., Tazi, J., & Jolly, C. (2004). A key role for stress-induced satellite III transcripts in the relocalization of splicing factors into nuclear stress granules. *J Cell Sci, 117*(Pt 19), 4551-4558.

Metzler, B., Abia, R., Ahmad, M., Wernig, F., Pachinger, O., Hu, Y., & Xu, Q. (2003). Activation of heat shock transcription factor 1 in atherosclerosis. *Am J Pathol, 162*(5), 1669-1676.

Meyne, J., Ratliff, R. L., & Moyzis, R. K. (1989). Conservation of the Human Telomere Sequence (Ttaggg)N among Vertebrates. *Proceedings of the National Academy of Sciences of the United States of America, 86*(18), 7049-7053.

Michishita, E., Park, J. Y., Burneskis, J. M., Barrett, J. C., & Horikawa, I. (2005). Evolutionarily conserved and nonconserved cellular localizations and functions of human SIRT proteins. *Molecular Biology of the Cell, 16*(10), 4623-4635.

Mikhaylova, O., Ignacak, M. L., Barankiewicz, T. J., Harbaugh, S. V., Yi, Y., Maxwell, P. H., . . . Czyzyk-Krzeska, M. F. (2008). The von Hippel-Lindau tumor suppressor protein and Egl-9-Type proline hydroxylases regulate the large subunit of RNA polymerase II in response to oxidative stress. *Mol Cell Biol, 28*(8), 2701-2717.

Millanes-Romero, A., Herranz, N., Perrera, V., Iturbide, A., Loubat-Casanovas, J., Gil, J., . . . Peiro, S. (2013). Regulation of heterochromatin transcription by Snail1/LOXL2 during epithelial-to-mesenchymal transition. *Mol Cell, 52*(5), 746-757.

Min, J. N., Han, M. Y., Lee, S. S., Kim, K. J., & Park, Y. M. (2000). Regulation of rat heat shock factor 2 expression during the early organogenic phase of embryogenesis. *Biochimica Et Biophysica Acta-Gene Structure and Expression, 1494*(3), 256-262.
Min, J. N., Zhang, Y., Moskophidis, D., & Mivechi, N. F. (2004). Unique contribution of heat shock transcription factor 4 in ocular lens development and fiber cell differentiation. *Genesis, 40*(4), 205-217.

Minc, E., Allory, Y., Worman, H. J., Courvalin, J. C., & Buendia, B. (1999). Localization and phosphorylation of HP1 proteins during the cell cycle in mammalian cells. *Chromosoma, 108*(4), 220-234.

Minc, E., Courvalin, J. C., & Buendia, B. (2000). HP1gamma associates with euchromatin and heterochromatin in mammalian nuclei and chromosomes. *Cytogenet Cell Genet, 90*(3-4), 279-284.

Mincheva-Tasheva, S., Obis, E., Tamarit, J., & Ros, J. (2014). Apoptotic cell death and altered calcium homeostasis caused by frataxin depletion in dorsal root ganglia neurons can be prevented by BH4 domain of Bcl-xL protein. *Hum Mol Genet, 23*(7), 1829-1841.

Miniou, P., Jeanpierre, M., Blanquet, V., Sibella, V., Bonneau, D., Herbelin, C., . . . Viegaspequignot, E. (1994). Abnormal Methylation Pattern in Constitutive and Facultative (X-Inactive Chromosome) Heterochromatin of Icf Patients. *Human Molecular Genetics, 3*(12), 2093-2102.

Mitsiades, N., Mitsiades, C. S., Poulaki, V., Chauhan, D., Fanourakis, G., Gu, X., . . . Anderson, K. C. (2002). Molecular sequelae of proteasome inhibition in human multiple myeloma cells. *Proc Natl Acad Sci U S A, 99*(22), 14374-14379.

Mitsui, A., & Sharp, P. A. (1999). Ubiquitination of RNA polymerase II large subunit signaled by phosphorylation of carboxyl-terminal domain. *Proc Natl Acad Sci U S A, 96*(11), 6054-6059.

Montermini, L., Andermann, E., Labuda, M., Richter, A., Pandolfo, M., Cavalcanti, F., . . . Cocozza, S. (1997). The friedreich ataxia GAA triplet repeat: Premutation and normal alleles. *Human Molecular Genetics, 6*(8), 1261-1266.

Montermini, L., Richter, A., Morgan, K., Justice, C. M., Julien, D., Castellotti, B., . . . Pandolfo, M. (1997). Phenotypic variability in Friedreich ataxia: Role of the associated GAA triplet repeat expansion. *Annals of Neurology, 41*(5), 675-682.

Monticelli, A., Giacchetti, M., De Biase, I., Pianese, L., Turano, M., Pandolfo, M., & Cocozza, S. (2004). New clues on the origin of the Friedreich ataxia expanded alleles from the analysis of new polymorphisms closely linked to the mutation. *Hum Genet, 114*(5), 458-463.

Moreau, P., Richardson, P. G., Cavo, M., Orlowski, R. Z., San Miguel, J. F., Palumbo, A., & Harousseau, J. L. (2012). Proteasome inhibitors in multiple myeloma: 10 years later. *Blood, 120*(5), 947-959.

Morimoto, R. I. (1993). Cells in stress: transcriptional activation of heat shock genes. *Science, 259*(5100), 1409-1410.
Morimoto, R. I. (1998). Regulation of the heat shock transcriptional response: cross talk between a family of heat shock factors, molecular chaperones, and negative regulators. *Genes Dev, 12*(24), 3788-3796.

Morris, M. C., Kaiser, P., Rudyak, S., Baskerville, C., Watson, M. H., & Reed, S. I. (2003). Cks1-dependent proteasome recruitment and activation of CDC20 transcription in budding yeast. *Nature, 423*(6943), 1009-1013.

Mosch, K., Franz, H., Soeroes, S., Singh, P. B., & Fischle, W. (2011). HP1 recruits activity-dependent neuroprotective protein to H3K9me3 marked pericentromeric heterochromatin for silencing of major satellite repeats. *PLoS One, 6*(1), e15894.

Mottamal, M., Zheng, S. L., Huang, T. L., & Wang, G. D. (2015). Histone Deacetylase Inhibitors in Clinical Studies as Templates for New Anticancer Agents. *Molecules, 20*(3), 3898-3941.

Moyzis, R. K., Buckingham, J. M., Cram, L. S., Dani, M., Deaven, L. L., Jones, M. D., . . . Wu, J. R. (1988). A Highly Conserved Repetitive DNA-Sequence, (Ttaggg)N, Present at the Telomeres of Human-Chromosomes. *Proceedings of the National Academy of Sciences of the United States of America, 85*(18), 6622-6626.

Muchardt, C., Guilleme, M., Seeler, J. S., Trouche, D., Dejean, A., & Yaniv, M. (2002). Coordinated methyl and RNA binding is required for heterochromatin localization of mammalian HP1 alpha. *Embo Reports, 3*(10), 975-981.

Muller-Ott, K., Erdel, F., Matveeva, A., Mallm, J. P., Rademacher, A., Hahn, M., . . . Rippe, K. (2014). Specificity, propagation, and memory of pericentric heterochromatin. *Mol Syst Biol, 10*, 746.

Munoz-Lopez, M., & Garcia-Perez, J. L. (2010). DNA Transposons: Nature and Applications in Genomics. *Current Genomics, 11*(2), 115-128.

Muramatsu, D., Singh, P. B., Kimura, H., Tachibana, M., & Shinkai, Y. (2013). Pericentric heterochromatin generated by HP1 protein interaction-defective histone methyltransferase Suv39h1. *Journal of Biological Chemistry, 288*(35), 25285-25296.

Murata, S., Yashiroda, H., & Tanaka, K. (2009). Molecular mechanisms of proteasome assembly. *Nature Reviews Molecular Cell Biology, 10*(2), 104-115.

Muratani, M., Kung, C., Shokat, K. M., & Tansey, W. R. (2005). The F box protein Dsg1/Mdm30 is a transcriptional coactivator that stimulates Gal4 turnover and cotranscriptional mRNA processing. *Cell, 120*(6), 887-899.

Murnane, J. P. (2012). Telomere dysfunction and chromosome instability. *Mutat Res, 730*(1-2), 28-36.

Musova, Z., Hedvicakova, P., Mohrmann, M., Tesarova, M., Krepelova, A., Zeman, J., & Sedlacek, Z. (2006). A novel insertion of a rearranged L1 element in exon 44 of the dystrophin gene: Further evidence for possible bias in retroposon integration. *Biochemical and Biophysical Research Communications, 347*(1), 145-149.

Nachbauer, W., Bodner, T., Boesch, S., Karner, E., Eigentler, A., Neier, L., . . . Delazer, M. (2014). Friedreich Ataxia: Executive Control Is Related to Disease Onset and GAA Repeat Length. *Cerebellum, 13*(1), 9-16.

Nagai, N., Nakai, A., & Nagata, K. (1995). Quercetin suppresses heat shock response by down regulation of HSF1. *Biochem Biophys Res Commun, 208*(3), 1099-1105.

Nakai, A., Tanabe, M., Kawazoe, Y., Inazawa, J., Morimoto, R. I., & Nagata, K. (1997). HSF4, a new member of the human heat shock factor family which lacks properties of a transcriptional activator. *Molecular and Cellular Biology, 17*(1), 469-481.

Nakayama, J., Rice, J. C., Strahl, B. D., Allis, C. D., & Grewal, S. I. (2001). Role of histone H3 lysine 9 methylation in epigenetic control of heterochromatin assembly. *Science, 292*(5514), 110-113.

Nakayasu, H., & Berezney, R. (1989). Mapping replicational sites in the eucaryotic cell nucleus. *J Cell Biol, 108*(1), 1-11.

Nalley, K., Johnston, S. A., & Kodadek, T. (2006). Proteolytic turnover of the Gal4 transcription factor is not required for function in vivo. *Nature, 442*(7106), 1054-1057.

Nan, X., Ng, H. H., Johnson, C. A., Laherty, C. D., Turner, B. M., Eisenman, R. N., & Bird, A. (1998). Transcriptional repression by the methyl-CpG-binding protein MeCP2 involves a histone deacetylase complex. *Nature, 393*(6683), 386-389.

Narayan, A., Ji, W., Zhang, X. Y., Marrogi, A., Graff, J. R., Baylin, S. B., & Ehrlich, M. (1998). Hypomethylation of pericentromeric DNA in breast adenocarcinomas. *Int J Cancer, 77*(6), 833-838.

Natarajan, A. T., & Schmid, W. (1971). Differential response of constitutive and facultative heterochromatin in the manifestation of mitomycin induced chromosome aberrations in Chinese hamster cells in vitro. *Chromosoma, 33*(1), 48-62.

Navarro, J. A., Llorens, J. V., Soriano, S., Botella, J. A., Schneuwly, S., Martinez-Sebastian, M. J., & Molto, M. D. (2011). Overexpression of Human and Fly Frataxins in Drosophila Provokes Deleterious Effects at Biochemical, Physiological and Developmental Levels. *PLoS One, 6*(7).

Nelson, J. D., Denisenko, O., & Bomsztyk, K. (2006). Protocol for the fast chromatin immunoprecipitation (ChIP) method. *Nature Protocols, 1*(1), 179-185.
Ng, H. H., Robert, F., Young, R. A., & Struhl, K. (2003). Targeted recruitment of set1 histone methylase by elongating pol II provides a localized mark and memory of recent transcriptional activity. *Molecular Cell, 11*(3), 709-719.

Nguyen, V. T., Giannoni, F., Dubois, M. F., Seo, S. J., Vigneron, M., Kedinger, C., & Bensaude, O. (1996). In vivo degradation of RNA polymerase II largest subunit triggered by alpha-amanitin. *Nucleic Acids Research, 24*(15), 2924-2929.

Nickell, S., Beck, F., Scheres, S. H. W., Korinek, A., Forster, F., Lasker, K., . . . Baumeister, W. (2009). Insights into the molecular architecture of the 26S proteasome. *Proceedings of the National Academy of Sciences of the United States of America, 106*(29), 11943-11947.

Nielsen, A. L., Oulad-Abdelghani, M., Ortiz, J. A., Remboutsika, E., Chambon, P., & Losson, R. (2001). Heterochromatin formation in mammalian cells: Interaction between histones and HP1 proteins. *Molecular Cell, 7*(4), 729-739.

Nishida, N., Kudo, M., Nagasaka, T., Ikai, I., & Goel, A. (2012). Characteristic patterns of altered DNA methylation predict emergence of human hepatocellular carcinoma. *Hepatology, 56*(3), 994-1003.

Nishioka, K., Rice, J. C., Sarma, K., Erdjument-Bromage, H., Werner, J., Wang, Y. M., . . . Reinberg, D. (2002). PR-Set7 is a nucleosome-specific methyltransferase that modifies lysine 20 of histone H4 and is associated with silent chromatin. *Molecular Cell, 9*(6), 1201-1213.

Noma, K., Sugiyama, T., Cam, H., Verdel, A., Zofall, M., Jia, S., . . . Grewal, S. I. (2004). RITS acts in cis to promote RNA interference-mediated transcriptional and post-transcriptional silencing. *Nat Genet, 36*(11), 1174-1180.

Nowak, S. J., & Corces, V. G. (2000). Phosphorylation of histone H3 correlates with transcriptionally active loci. *Genes Dev, 14*(23), 3003-3013.

O'Donnell, K. A., & Burns, K. H. (2010). Mobilizing diversity: transposable element insertions in genetic variation and disease. *Mob DNA, 1*(1), 21.

O'Keefe, R. T., Henderson, S. C., & Spector, D. L. (1992). Dynamic organization of DNA replication in mammalian cell nuclei: spatially and temporally defined replication of chromosome-specific alpha-satellite DNA sequences. *J Cell Biol, 116*(5), 1095-1110.

O'Sullivan, R. J., & Karlseder, J. (2010). Telomeres: protecting chromosomes against genome instability. *Nat Rev Mol Cell Biol, 11*(3), 171-181.

Obeng, E. A., Carlson, L. M., Gutman, D. M., Harrington, W. J., Lee, K. P., & Boise, L. H. (2006). Proteasome inhibitors induce a terminal unfolded protein response in multiple myeloma cells. *Blood, 107*(12), 4907-4916.

Ohkuni, K., & Kitagawa, K. (2011). Endogenous Transcription at the Centromere Facilitates Centromere Activity in Budding Yeast. *Current Biology, 21*(20), 1695-1703.
Ohshima, K., Montermini, L., Wells, R. D., & Pandolfo, M. (1998). Inhibitory effects of expanded GAA.TTC triplet repeats from intron I of the Friedreich ataxia gene on transcription and replication in vivo. *J Biol Chem, 273*(23), 14588-14595.

Okano, M., Bell, D. W., Haber, D. A., & Li, E. (1999). DNA methyltransferases Dnmt3a and Dnmt3b are essential for de novo methylation and mammalian development. *Cell, 99*(3), 247-257.

Oliva, J., Dedes, J., Li, J., French, S. W., & Bardag-Gorce, F. (2009). Epigenetics of proteasome inhibition in the liver of rats fed ethanol chronically. *World Journal of Gastroenterology, 15*(6), 705-712.

Ong, C. T., & Corces, V. G. (2014). CTCF: an architectural protein bridging genome topology and function. *Nat Rev Genet, 15*(4), 234-246.

Osborne, C. S., Chakalova, L., Brown, K. E., Carter, D., Horton, A., Debrand, E., . . . Fraser, P. (2004). Active genes dynamically colocalize to shared sites of ongoing transcription. *Nature Genetics, 36*(10), 1065-1071.

Ostling, P., Bjork, J. K., Roos-Mattjus, P., Mezger, V., & Sistonen, L. (2007). Heat shock factor 2 (HSF2) contributes to inducible expression of hsp genes through interplay with HSF1. *Journal of Biological Chemistry, 282*(10), 7077-7086.

Ouni, I., Flick, K., & Kaiser, P. (2011). Ubiquitin and transcription: The SCF/Met4 pathway, a (protein-) complex issue. *Transcription, 2*(3), 135-139.

Oya, E., Kato, H., Chikashige, Y., Tsutsumi, C., Hiraoka, Y., & Murakami, Y. (2013). Mediator directs co-transcriptional heterochromatin assembly by RNA interference-dependent and -independent pathways. *Plos Genetics, 9*(8), e1003677.

Padeken, J., Zeller, P., & Gasser, S. M. (2015). Repeat DNA in genome organization and stability. *Curr Opin Genet Dev, 31*, 12-19.

Pajonk, F., & McBride, W. H. (2001). The proteasome in cancer biology and treatment. *Radiat Res, 156*(5 Pt 1), 447-459.

Palm, W., & de Lange, T. (2008). How Shelterin Protects Mammalian Telomeres. *Annual Review of Genetics, 42*, 301-334.

Palmer, A., Mason, G. G. F., Paramio, J. M., Knecht, E., & Rivett, A. J. (1994). Changes in Proteasome Localization during the Cell-Cycle. *European Journal of Cell Biology, 64*(1), 163-175.

Palmer, A., Rivett, A. J., Thomson, S., Hendil, K. B., Butcher, G. W., Fuertes, G., & Knecht, E. (1996). Subpopulations of proteasomes in rat liver nuclei, microsomes and cytosol. *Biochemical Journal, 316*, 401-407.

Palmer, D. K., O'Day, K., Trong, H. L., Charbonneau, H., & Margolis, R. L. (1991). Purification of the centromere-specific protein CENP-A and demonstration that it is a distinctive histone. *Proc Natl Acad Sci U S A, 88*(9), 3734-3738.

Palomo, G. M., Cerrato, T., Gargini, R., & Diaz-Nido, J. (2011). Silencing of frataxin gene expression triggers p53-dependent apoptosis in human neuron-like cells. *Hum Mol Genet, 20*(14), 2807-2822.

Pan, Y. R., Sun, M., Wohlschlegel, J., & Reed, S. I. (2013). Cks1 Enhances Transcription Efficiency at the GAL1 Locus by Linking the Paf1 Complex to the 19S Proteasome. *Eukaryotic Cell, 12*(9), 1192-1201.

Pardee, A. B., & Keyomarsi, K. (1992). Modification of cell proliferation with inhibitors. *Curr Opin Cell Biol, 4*(2), 186-191.

Park, S., Gakh, O., Mooney, S. M., & Isaya, G. (2002). The ferroxidase activity of yeast frataxin. *Journal of Biological Chemistry, 277*(41), 38589-38595.

Parkinson, M. H., Boesch, S., Nachbauer, W., Mariotti, C., & Giunti, P. (2013). Clinical features of Friedreich's ataxia: classical and atypical phenotypes. *J Neurochem, 126 Suppl 1*, 103-117.

Pathare, G. R., Nagy, I., Sledz, P., Anderson, D. J., Zhou, H. J., Pardon, E., . . . Baumeister, W. (2014). Crystal structure of the proteasomal deubiquitylation module Rpn8-Rpn11. *Proc Natl Acad Sci U S A, 111*(8), 2984-2989.

Payne, R. M., Pride, P. M., & Babbey, C. M. (2011). Cardiomyopathy of Friedreich's Ataxia: Use of Mouse Models to Understand Human Disease and Guide Therapeutic Development. *Pediatric Cardiology, 32*(3), 366-378.

Pelham, H. R. (1982). A regulatory upstream promoter element in the Drosophila hsp 70 heat-shock gene. *Cell, 30*(2), 517-528.

Peng, J. C., & Karpen, G. H. (2009). Heterochromatic genome stability requires regulators of histone H3 K9 methylation. *PLoS Genet, 5*(3), e1000435.

Perisic, O., Xiao, H., & Lis, J. T. (1989). Stable binding of Drosophila heat shock factor to head-to-head and tail-to-tail repeats of a conserved 5 bp recognition unit. *Cell, 59*(5), 797-806.

Perpelescu, M., & Fukagawa, T. (2011). The ABCs of CENPs. *Chromosoma, 120*(5), 425-446.

Peteranderl, R., & Nelson, H. C. (1992). Trimerization of the heat shock transcription factor by a triple-stranded alpha-helical coiled-coil. *Biochemistry, 31*(48), 12272-12276.

Peters, A. H., Kubicek, S., Mechtler, K., O'Sullivan, R. J., Derijck, A. A., Perez-Burgos, L., . . . Jenuwein, T. (2003). Partitioning and plasticity of repressive histone methylation states in mammalian chromatin. *Mol Cell, 12*(6), 1577-1589.

Peters, A. H., O'Carroll, D., Scherthan, H., Mechtler, K., Sauer, S., Schofer, C., . . . Jenuwein, T. (2001). Loss of the Suv39h histone methyltransferases impairs mammalian heterochromatin and genome stability. *Cell, 107*(3), 323-337.

Peters, A. H. F. M., O'Carroll, D., Scherthan, H., Mechtler, K., Sauer, S., Schofer, C., . . . Jenuwein, T. (2001). Loss of the Suv39h histone methyltransferases impairs mammalian heterochromatin and genome stability. *Cell, 107*(3), 323-337.

Peters, J. M., Franke, W. W., & Kleinschmidt, J. A. (1994). Distinct 19-S and 20-S Subcomplexes of the 26-S Proteasome and Their Distribution in the Nucleus and the Cytoplasm. *Journal of Biological Chemistry, 269*(10), 7709-7718.

Peters, J. M., Tedeschi, A., & Schmitz, J. (2008). The cohesin complex and its roles in chromosome biology. *Genes Dev, 22*(22), 3089-3114.

Petesch, S. J., & Lis, J. T. (2012). Activator-induced spread of poly(ADP-ribose) polymerase promotes nucleosome loss at Hsp70. *Mol Cell, 45*(1), 64-74.

Pezer, Z., & Ugarkovic, D. (2008). RNA Pol II Promotes Transcription of Centromeric Satellite DNA in Beetles. *PLoS One, 3*(2).

Pham, L. V., Tamayo, A. T., Yoshimura, L. C., Lo, P., & Ford, R. J. (2003). Inhibition of constitutive NF-kappa B activation in mantle cell lymphoma B cells leads to induction of cell cycle arrest and apoptosis. *J Immunol, 171*(1), 88-95.

Phatnani, H. P., & Greenleaf, A. L. (2006). Phosphorylation and functions of the RNA polymerase II CTD. *Genes Dev, 20*(21), 2922-2936.

Phillips, D. M. (1963). The presence of acetyl groups of histones. *Biochem J, 87*, 258-263.

Piacentini, L., Fanti, L., Berloco, M., Perrini, B., & Pimpinelli, S. (2003). Heterochromatin protein 1 (HP1) is associated with induced gene expression in Drosophila euchromatin. *Journal of Cell Biology, 161*(4), 707-714.

Pianese, L., Turano, M., Lo Casale, M. S., De Biase, I., Giacchetti, M., Monticelli, A., . . . Cocozza, S. (2004). Real time PCR quantification of frataxin mRNA in the peripheral blood leucocytes of Friedreich ataxia patients and carriers. *Journal of Neurology Neurosurgery and Psychiatry, 75*(7), 1061-1063.

Pickart, C. M. (1997). Targeting of substrates to the 26S proteasome. *FASEB J, 11*(13), 1055-1066.

Pickart, C. M., & Eddins, M. J. (2004). Ubiquitin: structures, functions, mechanisms. *Biochimica Et Biophysica Acta-Molecular Cell Research, 1695*(1-3), 55-72.
Pidoux, A. L., & Allshire, R. C. (2005). The role of heterochromatin in centromere function. *Philos Trans R Soc Lond B Biol Sci, 360*(1455), 569-579.

Pinheiro, I., Margueron, R., Shukeir, N., Eisold, M., Fritzsch, C., Richter, F. M., . . . Jenuwein, T. (2012). Prdm3 and Prdm16 are H3K9me1 Methyltransferases Required for Mammalian Heterochromatin Integrity. *Cell, 150*(5), 948-960.

Pirkkala, L., Nykanen, P., & Sistonen, L. (2001). Roles of the heat shock transcription factors in regulation of the heat shock response and beyond. *FASEB J, 15*(7), 1118-1131.

Plath, K., Fang, J., Mlynarczyk-Evans, S. K., Cao, R., Worringer, K. A., Wang, H. B., . . . Zhang, Y. (2003). Role of histone H3 lysine 27 methylation in X inactivation. *Science, 300*(5616), 131-135.

Pokholok, D. K., Harbison, C. T., Levine, S., Cole, M., Hannett, N. M., Lee, T. I., . . . Young, R. A. (2005). Genome-wide map of nucleosome acetylation and methylation in yeast. *Cell, 122*(4), 517-527.

Powers, G. L., Rajbhandari, P., Solodin, N. M., Bickford, B., & Alarid, E. T. (2013). The Proteasome Inhibitor Bortezomib Induces an Inhibitory Chromatin Environment at a Distal Enhancer of the Estrogen Receptor-alpha Gene. *PLoS One, 8*(12).

Powers, M. V., & Workman, P. (2007). Inhibitors of the heat shock response: biology and pharmacology. *FEBS Lett, 581*(19), 3758-3769.

Probst, A. V., & Almouzni, G. (2011). Heterochromatin establishment in the context of genome-wide epigenetic reprogramming. *Trends Genet, 27*(5), 177-185.

Probst, A. V., Okamoto, I., Casanova, M., El Marjou, F., Le Baccon, P., & Almouzni, G. (2010). A Strand-Specific Burst in Transcription of Pericentric Satellites Is Required for Chromocenter Formation and Early Mouse Development. *Developmental Cell, 19*(4), 625-638.

Punga, T., & Buhler, M. (2010). Long intronic GAA repeats causing Friedreich ataxia impede transcription elongation. *Embo Molecular Medicine, 2*(4), 120-129.

Purgato, S., Belloni, E., Piras, F. M., Zoli, M., Badiale, C., Cerutti, F., . . . Giulotto, E. (2015). Centromere sliding on a mammalian chromosome. *Chromosoma, 124*(2), 277-287.

Qian, M. X., Pang, Y., Liu, C. H., Haratake, K., Du, B. Y., Ji, D. Y., . . . Qiu, X. B. (2013). Acetylation-Mediated Proteasomal Degradation of Core Histones during DNA Repair and Spermatogenesis. *Cell, 153*(5), 1012-1024.

Qu, G. Z., Dubeau, L., Narayan, A., Yu, M. C., & Ehrlich, M. (1999). Satellite DNA hypomethylation vs. overall genomic hypomethylation in ovarian epithelial tumors of different malignant potential. *Mutation Research-Fundamental and Molecular Mechanisms of Mutagenesis, 423*(1-2), 91-101.

Rabindran, S. K., Haroun, R. I., Clos, J., Wisniewski, J., & Wu, C. (1993). Regulation of heat shock factor trimer formation: role of a conserved leucine zipper. *Science, 259*(5092), 230-234.

Rabl, J., Smith, D. M., Yu, Y., Chang, S. C., Goldberg, A. L., & Cheng, Y. (2008). Mechanism of gate opening in the 20S proteasome by the proteasomal ATPases. *Molecular Cell, 30*(3), 360-368.

Raha, D., Wang, Z., Moqtaderi, Z., Wu, L., Zhong, G., Gerstein, M., . . . Snyder, M. (2010). Close association of RNA polymerase II and many transcription factors with Pol III genes. *Proc Natl Acad Sci U S A, 107*(8), 3639-3644.

Rai, M., Soragni, E., Chou, C. J., Barnes, G., Jones, S., Rusche, J. R., . . . Pandolfo, M. (2010). Two new pimelic diphenylamide HDAC inhibitors induce sustained frataxin upregulation in cells from Friedreich's ataxia patients and in a mouse model. *PLoS One, 5*(1), e8825.

Rai, M., Soragni, E., Jenssen, K., Burnett, R., Herman, D., Coppola, G., . . . Pandolfo, M. (2008). HDAC inhibitors correct frataxin deficiency in a Friedreich ataxia mouse model. *PLoS One, 3*(4), e1958.

Rajkumar, S. V., Richardson, P. G., Hideshima, T., & Anderson, K. C. (2005). Proteasome inhibition as a novel therapeutic target in human cancer. *Journal of Clinical Oncology, 23*(3), 630-639.

Rallu, M., Loones, M., Lallemand, Y., Morimoto, R., Morange, M., & Mezger, V. (1997). Function and regulation of heat shock factor 2 during mouse embryogenesis. *Proceedings of the National Academy of Sciences of the United States of America, 94*(6), 2392-2397.

Ramanan, N., Shen, Y., Sarsfield, S., Lemberger, T., Schutz, G., Linden, D. J., & Ginty, D. D. (2005). SRF mediates activity-induced gene expression and synaptic plasticity but not neuronal viability. *Nat Neurosci, 8*(6), 759-767.

Rao, R. V., & Bredesen, D. E. (2004). Misfolded proteins, endoplasmic reticulum stress and neurodegeneration. *Curr Opin Cell Biol, 16*(6), 653-662.

Ratner, J. N., Balasubramanian, B., Corden, J., Warren, S. L., & Bregman, D. B. (1998). Ultraviolet radiation-induced ubiquitination and proteasomal degradation of the large subunit of RNA polymerase II. Implications for transcription-coupled DNA repair. *J Biol Chem, 273*(9), 5184-5189.

Rea, S., Eisenhaber, F., O'Carroll, D., Strahl, B. D., Sun, Z. W., Schmid, M., . . . Jenuwein, T. (2000). Regulation of chromatin structure by site-specific histone H3 methyltransferases. *Nature, 406*(6796), 593-599.

Reddy, K., Tam, M., Bowater, R. P., Barber, M., Tomlinson, M., Edamura, K. N., . . . Pearson, C. E. (2011). Determinants of R-loop formation at convergent bidirectionally transcribed trinucleotide repeats. *Nucleic Acids Research, 39*(5), 1749-1762.
Reinhart, B. J., & Bartel, D. P. (2002). Small RNAs correspond to centromere heterochromatic repeats. *Science, 297*(5588), 1831.

Reits, E. A. J., Benham, A. M., Plougastel, B., Neefjes, J., & Trowsdale, J. (1997). Dynamics of proteasome distribution in living cells. *Embo Journal, 16*(20), 6087-6094.

Reyes-Reyes, M., & Hampsey, M. (2007). Role for the Ssu72 C-terminal domain phosphatase in RNA polymerase II transcription elongation. *Molecular and Cellular Biology, 27*(3), 926-936.

Ricci, M. A., Manzo, C., Garcia-Parajo, M. F., Lakadamyali, M., & Cosma, M. P. (2015). Chromatin Fibers Are Formed by Heterogeneous Groups of Nucleosomes In Vivo. *Cell, 160*(6), 1145-1158.

Richard, G. F., Kerrest, A., & Dujon, B. (2008). Comparative Genomics and Molecular Dynamics of DNA Repeats in Eukaryotes. *Microbiology and Molecular Biology Reviews, 72*(4), 686

Richardson, P. G., Mitsiades, C., Hideshima, T., & Anderson, K. C. (2006). Bortezomib: Proteasome inhibition as an effective anticancer therapy. *Annual Review of Medicine, 57*, 33-47.

Richardson, P. G., Sonneveld, P., Schuster, M. W., Irwin, D., Stadtmauer, E. A., Facon, T., . . . Assessment of Proteasome Inhibition for Extending Remissions, I. (2005). Bortezomib or high-dose dexamethasone for relapsed multiple myeloma. *N Engl J Med, 352*(24), 2487-2498.

Richon, V. M., Webb, Y., Merger, R., Sheppard, T., Jursic, B., Ngo, L., . . . Marks, P. A. (1996). Second generation hybrid polar compounds are potent inducers of transformed cell differentiation. *Proc Natl Acad Sci U S A, 93*(12), 5705-5708.

Ricke, R. M., & Bielinsky, A. K. (2004). Mcm10 regulates the stability and chromatin association of DNA polymerase-alpha. *Molecular Cell, 16*(2), 173-185.

Riggs, A. D. (1975). X inactivation, differentiation, and DNA methylation. *Cytogenet Cell Genet, 14*(1), 9-25.

Rivett, A. J., Palmer, A., & Knecht, E. (1992). Electron-Microscopic Localization of the Multicatalytic Proteinase Complex in Rat-Liver and in Cultured-Cells. *Journal of Histochemistry & Cytochemistry, 40*(8), 1165-1172.

Rizzi, N., Denegri, M., Chiodi, I., Corioni, M., Valgardsdottir, R., Cobianchi, F., . . . Biamonti, G. (2004). Transcriptional activation of a constitutive heterochromatic domain of the human genome in response to heat shock. *Molecular Biology of the Cell, 15*(2), 543-551.

Robbins, A. R., Jablonski, S. A., Yen, T. J., Yoda, K., Robey, R., Bates, S. E., & Sackett, D. L. (2005). Inhibitors of histone deacetylases alter kinetochore assembly by disrupting pericentromeric heterochromatin. *Cell Cycle, 4*(5), 717-726.

Roguev, A., Schaft, D., Shevchenko, A., Pijnappel, W. W. M. P., Wilm, M., Aasland, R., & Stewart, A. F. (2001). The Saccharomyces cerevisiae Set1 complex includes an Ash2 homologue and methylates histone 3 lysine 4. *Embo Journal, 20*(24), 7137-7148.

Roh, T. Y., Cuddapah, S., & Zhao, K. (2005). Active chromatin domains are defined by acetylation islands revealed by genome-wide mapping. *Genes Dev, 19*(5), 542-552.

Rollins, R. A., Haghighi, F., Edwards, J. R., Das, R., Zhang, M. Q., Ju, J., & Bestor, T. H. (2006). Large-scale structure of genomic methylation patterns. *Genome Res, 16*(2), 157-163.

Rosenzweig, R., Bronner, V., Zhang, D. N., Fushman, D., & Glickman, M. H. (2012). Rpn1 and Rpn2 Coordinate Ubiquitin Processing Factors at Proteasome. *Journal of Biological Chemistry, 287*(18), 14659-14671.

Rosic, S., Kohler, F., & Erhardt, S. (2014). Repetitive centromeric satellite RNA is essential for kinetochore formation and cell division (vol 207, pg 335, 2014). *Journal of Cell Biology, 207*(5), 673-673.

Rudd, M. D., & Luse, D. S. (1996). Amanitin greatly reduces the rate of transcription by RNA polymerase II ternary complexes but fails to inhibit some transcript cleavage modes. *Journal of Biological Chemistry, 271*(35), 21549-21558.

Rudd, M. K., Wray, G. A., & Willard, H. F. (2006). The evolutionary dynamics of alpha-satellite. *Genome Research, 16*(1), 88-96.

Rudert, F., Bronner, S., Garnier, J. M., & Dolle, P. (1995). Transcripts from opposite strands of gamma satellite DNA are differentially expressed during mouse development. *Mamm Genome, 6*(2), 76-83.

Rufini, A., Cavallo, F., Condo, I., Fortuni, S., De Martino, G., Incani, O., . . . Testi, R. (2015). Highly specific ubiquitin-competing molecules effectively promote frataxin accumulation and partially rescue the aconitase defect in Friedreich ataxia cells. *Neurobiology of Disease, 75*, 91-99.

Rufini, A., Fortuni, S., Arcuri, G., Condo, I., Serio, D., Incani, O., . . . Testi, R. (2011). Preventing the ubiquitin-proteasome-dependent degradation of frataxin, the protein defective in Friedreich's ataxia. *Hum Mol Genet, 20*(7), 1253-1261.

Sabari, B. R., Tang, Z. Y., Huang, H., Yong-Gonzalez, V., Molina, H., Kong, H. E., . . . Allis, C. D. (2015). Intracellular Crotonyl-CoA Stimulates Transcription through p300-Catalyzed Histone Crotonylation. *Molecular Cell, 58*(2), 203-215.

Sacca, F., Marsili, A., Puorro, G., Antenora, A., Pane, C., Tessa, A., . . . Filla, A. (2013). Clinical use of frataxin measurement in a patient with a novel deletion in the FXN gene. *Journal of Neurology, 260*(4), 1116-1121.

Sadeghi, L., Siggens, L., Svensson, J. P., & Ekwall, K. (2014). Centromeric histone H2B monoubiquitination promotes noncoding transcription and chromatin integrity. *Nature Structural & Molecular Biology, 21*(3), 236-243.

Sadowski, M., & Sarcevic, B. (2010). Mechanisms of mono- and poly-ubiquitination: Ubiquitination specificity depends on compatibility between the E2 catalytic core and amino acid residues proximal to the lysine. *Cell Division, 5*.

Saint-Andre, V., Batsche, E., Rachez, C., & Muchardt, C. (2011). Histone H3 lysine 9 trimethylation and HP1 gamma favor inclusion of alternative exons. *Nature Structural & Molecular Biology, 18*(3), 337-U127.

Sakamoto, N., Chastain, P. D., Parniewski, P., Ohshima, K., Pandolfo, M., Griffith, J. D., & Wells, R. D. (1999). Sticky DNA: self-association properties of long GAA.TTC repeats in R.R.Y triplex structures from Friedreich's ataxia. *Mol Cell, 3*(4), 465-475.

Sakamoto, N., Ohshima, K., Montermini, L., Pandolfo, M., & Wells, R. D. (2001). Sticky DNA, a self-associated complex formed at long GAA center dot TTC repeats in intron 1 of the frataxin gene, inhibits transcriptions. *Journal of Biological Chemistry, 276*(29), 27171-27177.

Saksouk, N., Barth, T. K., Ziegler-Birling, C., Olova, N., Nowak, A., Rey, E., . . . Simboeck, E. (2014). Redundant mechanisms to form silent chromatin at pericentromeric regions rely on BEND3 and DNA methylation. *Mol Cell, 56*(4), 580-594.

Saksouk, N., Simboeck, E., & Dejardin, J. (2015). Constitutive heterochromatin formation and transcription in mammals. *Epigenetics Chromatin, 8*, 3.

San Miguel, J. F., Schlag, R., Khuageva, N. K., Dimopoulos, M. A., Shpilberg, O., Kropff, M., . . . Investigators, V. T. (2008). Bortezomib plus melphalan and prednisone for initial treatment of multiple myeloma. *N Engl J Med, 359*(9), 906-917.

Sanders, S. L., Portoso, M., Mata, J., Bahler, J., Allshire, R. C., & Kouzarides, T. (2004). Methylation of histone H4 lysine 20 controls recruitment of Crb2 to sites of DNA damage. *Cell, 119*(5), 603-614.

Sandi, C., Pinto, R. M., Al-Mahdawi, S., Ezzatizadeh, V., Barnes, G., Jones, S., . . . Pook, M. A. (2011). Prolonged treatment with pimelic o-aminobenzamide HDAC inhibitors ameliorates the disease phenotype of a Friedreich ataxia mouse model. *Neurobiol Dis, 42*(3), 496-505.

Sandqvist, A., Bjork, J. K., Akerfelt, M., Chitikova, Z., Grichine, A., Vourch, C., . . . Sistonen, L. (2009). Heterotrimerization of Heat-Shock Factors 1 and 2 Provides a Transcriptional Switch in Response to Distinct Stimuli. *Molecular Biology of the Cell, 20*(5), 1340-1347.

Santenard, A., Ziegler-Birling, C., Koch, M., Tora, L., Bannister, A. J., & Torres-Padilla, M. E. (2010). Heterochromatin formation in the mouse embryo requires critical residues of the histone variant H3.3. *Nat Cell Biol, 12*(9), 853-862.

Santos-Rosa, H., Schneider, R., Bannister, A. J., Sherriff, J., Bernstein, B. E., Emre, N. C. T., . . . Kouzarides, T. (2002). Active genes are tri-methylated at K4 of histone H3. *Nature, 419*(6905), 407-411.

Santos, M. M., Ohshima, K., & Pandolfo, M. (2001). Frataxin deficiency enhances apoptosis in cells differentiating into neuroectoderm. *Human Molecular Genetics, 10*(18), 1935-1944.

Sarge, K. D., Murphy, S. P., & Morimoto, R. I. (1993). Activation of heat shock gene transcription by heat shock factor 1 involves oligomerization, acquisition of DNA-binding activity, and nuclear localization and can occur in the absence of stress. *Mol Cell Biol, 13*(3), 1392-1407.

Satoh, T., Ishizuka, T., Yoshino, S., Tomaru, T., Nakajima, Y., Shibusawa, N., . . . Mori, M. (2009). Roles of proteasomal 19S regulatory particles in promoter loading of thyroid hormone receptor. *Biochem Biophys Res Commun, 386*(4), 697-702.

Sauve, A. A., Celic, I., Avalos, J., Deng, H., Boeke, J. D., & Schramm, V. L. (2001). Chemistry of gene silencing: the mechanism of NAD+-dependent deacetylation reactions. *Biochemistry, 40*(51), 15456-15463.

Sauve, A. A., Wolberger, C., Schramm, V. L., & Boeke, J. D. (2006). The biochemistry of sirtuins. *Annu Rev Biochem, 75*, 435-465.

Saveliev, A., Everett, C., Sharpe, T., Webster, Z., & Festenstein, R. (2003). DNA triplet repeats mediate heterochromatin-protein-1-sensitive variegated gene silencing. *Nature, 422*(6934), 909-913.

Schmitt, E., Gehrmann, M., Brunet, M., Multhoff, G., & Garrido, C. (2007). Intracellular and extracellular functions of heat shock proteins: repercussions in cancer therapy. *Journal of Leukocyte Biology, 81*(1), 15-27.

Schmucker, S., Argentini, M., Carelle-Calmels, N., Martelli, A., & Puccio, H. (2008). The in vivo mitochondrial two-step maturation of human frataxin. *Hum Mol Genet, 17*(22), 3521-3531.

Schneider, A. M., Duffield, A. S., Symer, D. E., & Burns, K. H. (2009). Roles of retrotransposons in benign and malignant hematologic disease. *Cellscience, 6*(2), 121-145.

Schoeftner, S., & Blasco, M. A. (2009). A 'higher order' of telomere regulation: telomere heterochromatin and telomeric RNAs. *Embo Journal, 28*(16), 2323-2336.

Schotta, G., Ebert, A., Krauss, V., Fischer, A., Hoffmann, J., Rea, S., . . . Reuter, G. (2002). Central role of Drosophila SU(VAR)3-9 in histone H3-K9 methylation and heterochromatic gene silencing. *EMBO J, 21*(5), 1121-1131.

Schotta, G., Lachner, M., Sarma, K., Ebert, A., Sengupta, R., Reuter, G., . . . Jenuwein, T. (2004). A silencing pathway to induce H3-K9 and H4-K20 trimethylation at constitutive heterochromatin. *Genes & Development, 18*(11), 1251-1262.

Schotta, G., Sengupta, R., Kubicek, S., Malin, S., Kauer, M., Callen, E., . . . Jenuwein, T. (2008). A chromatin-wide transition to H4K20 monomethylation impairs genome integrity and programmed DNA rearrangements in the mouse. *Genes & Development, 22*(15), 2048-2061.

Schulz, J. B., Dehmer, T., Schols, L., Mende, H., Hardt, C., Vorgerd, M., . . . Bogdanov, M. B. (2000). Oxidative stress in patients with Friedreich ataxia. *Neurology, 55*(11), 1719-1721.

Schulz, J. B., & Pandolfo, M. (2013). 150 years of Friedreich ataxia: from its discovery to therapy. *J Neurochem, 126 Suppl 1*, 1-3.

Schwarz, T., Sohn, C., Kaiser, B., Jensen, E. D., & Mansky, K. C. (2010). The 19S proteasomal lid subunit POH1 enhances the transcriptional activation by Mitf in osteoclasts. *J Cell Biochem, 109*(5), 967-974.

Scott, K. C. (2013). Transcription and ncRNAs: at the cent(rome)re of kinetochore assembly and maintenance. *Chromosome Research, 21*(6-7), 643-651.

Sengupta, S., Parihar, R., & Ganesh, S. (2009). Satellite III non-coding RNAs show distinct and stress-specific patterns of induction. *Biochemical and Biophysical Research Communications, 382*(1), 102-107.

Shahbazian, M. D., & Grunstein, M. (2007). Functions of site-specific histone acetylation and deacetylation. *Annu Rev Biochem, 76*, 75-100.

Shan, Y., Schoenfeld, R. A., Hayashi, G., Napoli, E., Akiyama, T., Iodi Carstens, M., . . . Cortopassi, G. A. (2013). Frataxin deficiency leads to defects in expression of antioxidants and Nrf2 expression in dorsal root ganglia of the Friedreich's ataxia YG8R mouse model. *Antioxid Redox Signal, 19*(13), 1481-1493.

Sharma, A., Meena, A. S., & Bhat, M. K. (2010). Hyperthermia-associated carboplatin resistance: differential role of p53, HSF1 and Hsp70 in hepatoma cells. *Cancer Sci, 101*(5), 1186-1193.

Sharma, R. P., Gavin, D. P., & Grayson, D. R. (2010). CpG Methylation in Neurons: Message, Memory, or Mask? *Neuropsychopharmacology, 35*(10), 2009-2020.

Sharma, S., Kelly, T. K., & Jones, P. A. (2010). Epigenetics in cancer. *Carcinogenesis, 31*(1), 27-36.

Sharma, S., & Taliyan, R. (2015). Targeting histone deacetylases: a novel approach in Parkinson's disease. *Parkinsons Dis, 2015*, 303294.

Shi, X. H., Cui, B., Wang, Z. G., Weng, L., Xu, Z. P., Ma, J. J., . . . Hu, L. D. (2009). Removal of Hsf4 leads to cataract development in mice through down-regulation of gamma S-crystallin and Bfsp expression. *Bmc Molecular Biology, 10*.

Shi, Y., & Whetstine, J. R. (2007). Dynamic regulation of histone lysine methylation by demethylases. *Molecular Cell, 25*(1), 1-14.

Shi, Y. H., Mosser, D. D., & Morimoto, R. I. (1998). Molecular chaperones as HSF1-specific transcriptional repressors. *Genes & Development, 12*(5), 654-666.

Shilatifard, A. (2006). Chromatin modifications by methylation and ubiquitination: Implications in the regulation of gene expression. *Annual Review of Biochemistry, 75*, 243-269.

Shinka, T., Sato, Y., Chen, G., Naroda, T., Kinoshita, K., Unemi, Y., . . . Nakahori, Y. (2004). Molecular characterization of heat shock-like factor encoded on the human Y chromosome, and implications for male infertility. *Biology of Reproduction, 71*(1), 297-306.

Shlyueva, D., Stampfel, G., & Stark, A. (2014). Transcriptional enhancers: from properties to genome-wide predictions. *Nat Rev Genet, 15*(4), 272-286.

Shringarpure, R., Grune, T., Mehlhase, J., & Davies, K. J. A. (2003). Ubiquitin conjugation is not required for the degradation of oxidized proteins by proteasome. *Journal of Biological Chemistry, 278*(1), 311-318.

Shumaker, D. K., Dechat, T., Kohlmaier, A., Adam, S. A., Bozovsky, M. R., Erdos, M. R., . . . Goldman, R. D. (2006). Mutant nuclear lamin A leads to progressive alterations of epigenetic control in premature aging. *Proceedings of the National Academy of Sciences of the United States of America, 103*(23), 8703-8708.

Sigismund, S., Polo, S., & Di Fiore, P. P. (2004). Signaling through monoubiquitination. *Signalling from Internalized Growth Factor Receptors, 286*, 149-185.

Sikder, D., Johnston, S. A., & Kodadek, T. (2006). Widespread, but non-identical, association of proteasomal 19 and 20 S proteins with yeast chromatin. *Journal of Biological Chemistry, 281*(37), 27346-27355.

Silva, A. M., Brown, J. M., Buckle, V. J., Wade-Martins, R., & Lufino, M. M. (2015). Expanded GAA repeats impair FXN gene expression and reposition the FXN locus to the nuclear lamina in single cells. *Hum Mol Genet, 24*(12), 3457-3471.

Simoes-Pires, C., Zwick, V., Nurisso, A., Schenker, E., Carrupt, P. A., & Cuendet, M. (2013). HDAC6 as a target for neurodegenerative diseases: what makes it different from the other HDACs? *Molecular Neurodegeneration, 8*.

Simon, J. A., & Kingston, R. E. (2013). Occupying Chromatin: Polycomb Mechanisms for Getting to Genomic Targets, Stopping Transcriptional Traffic, and Staying Put. *Molecular Cell, 49*(5), 808-824.

Singh, I. S., He, J. R., Hester, L., Fenton, M. J., & Hasday, J. D. (2004). Bacterial endotoxin modifies heat shock factor-1 activity in RAW 264.7 cells: implications for TNF-alpha regulation during exposure to febrile range temperatures. *Journal of Endotoxin Research, 10*(3), 175-184.

Singh, P. B., Miller, J. R., Pearce, J., Kothary, R., Burton, R. D., Paro, R., . . . Gaunt, S. J. (1991). A Sequence Motif Found in a Drosophila Heterochromatin Protein Is Conserved in Animals and Plants. *Nucleic Acids Research, 19*(4), 789-794.

Singh, R. K., Kabbaj, M. H., Paik, J., & Gunjan, A. (2009). Histone levels are regulated by phosphorylation and ubiquitylation-dependent proteolysis. *Nat Cell Biol, 11*(8), 925-933.

Singh, V., & Aballay, A. (2006). Heat-shock transcription factor (HSF)-1 pathway required for Caenorhabditis elegans immunity. *Proc Natl Acad Sci U S A, 103*(35), 13092-13097.

Sledz, P., Unverdorben, P., Beck, F., Pfeifer, G., Schweitzer, A., Forster, F., & Baumeister, W. (2013). Structure of the 26S proteasome with ATP-gamma S bound provides insights into the mechanism of nucleotide-dependent substrate translocation. *Proceedings of the National Academy of Sciences of the United States of America, 110*(18), 7264-7269.

Smit, A. F. (1996). The origin of interspersed repeats in the human genome. *Curr Opin Genet Dev, 6*(6), 743-748.

Smith, S. T., Petruk, S., Sedkov, Y., Cho, E., Tillib, S., Canaani, E., & Mazo, A. (2004). Modulation of heat shock gene expression by the TAC1 chromatin-modifying complex. *Nat Cell Biol, 6*(2), 162-167.

Smith, Z. D., & Meissner, A. (2013). DNA methylation: roles in mammalian development. *Nat Rev Genet, 14*(3), 204-220.

Smothers, J. F., & Henikoff, S. (2001). The hinge and chromo shadow domain impart distinct targeting of HP1-like proteins. *Mol Cell Biol, 21*(7), 2555-2569.

Soares, L. M., Radman-Livaja, M., Lin, S. G., Rando, O. J., & Buratowski, S. (2014). Feedback Control of Set1 Protein Levels Is Important for Proper H3K4 Methylation Patterns. *Cell Reports, 6*(6), 961-972.

Somesh, B. P., Reid, J., Liu, W. F., Sogaard, T. M., Erdjument-Bromage, H., Tempst, P., & Svejstrup, J. Q. (2005). Multiple mechanisms confining RNA polymerase II ubiquitylation to polymerases undergoing transcriptional arrest. *Cell, 121*(6), 913-923.

Somesh, B. P., Sigurdsson, S., Saeki, H., Erdjument-Bromage, H., Tempst, P., & Svejstrup, J. Q. (2007). Communication between distant sites in RNA polymerase II through ubiquitylation factors and the polymerase CTD. *Cell, 129*(1), 57-68.

Song, F., Chen, P., Sun, D., Wang, M., Dong, L., Liang, D., . . . Li, G. (2014). Cryo-EM study of the chromatin fiber reveals a double helix twisted by tetranucleosomal units. *Science, 344*(6182), 376-380.

Song, M., Pinsky, M. R., & Kellum, J. A. (2008). Heat shock factor 1 inhibits nuclear factor-kappaB nuclear binding activity during endotoxin tolerance and heat shock. *J Crit Care, 23*(3), 406-415.

Sonneveld, P., Schmidt-Wolf, I. G., van der Holt, B., El Jarari, L., Bertsch, U., Salwender, H., . . . Goldschmidt, H. M. (2012). Bortezomib induction and maintenance treatment in patients with newly diagnosed multiple myeloma: results of the randomized phase III HOVON-65/ GMMG-HD4 trial. *Journal of Clinical Oncology, 30*(24), 2946-2955.

Soragni, E., Miao, W., Iudicello, M., Jacoby, D., De Mercanti, S., Clerico, M., . . . Rusche, J. R. (2014). Epigenetic therapy for Friedreich ataxia. *Ann Neurol, 76*(4), 489-508.

Soragni, E., Xu, C., Cooper, A., Plasterer, H. L., Rusche, J. R., & Gottesfeld, J. M. (2011). Evaluation of histone deacetylase inhibitors as therapeutics for neurodegenerative diseases. *Methods Mol Biol, 793*, 495-508.

Sorger, P. K., & Nelson, H. C. (1989). Trimerization of a yeast transcriptional activator via a coiled-coil motif. *Cell, 59*(5), 807-813.

South, P. F., Harmeyer, K. M., Serratore, N. D., & Briggs, S. D. (2013). H3K4 methyltransferase Set1 is involved in maintenance of ergosterol homeostasis and resistance to Brefeldin A. *Proceedings of the National Academy of Sciences of the United States of America, 110*(11), E1016-E1025.

Spector, R., & Kelley, P. (1979). Niacin and niacinamide accumulation by rabbit brain slices and choroid plexus in vitro. *J Neurochem, 33*(1), 291-298.

Stadtmueller, B. M., & Hill, C. P. (2011). Proteasome Activators. *Molecular Cell, 41*(1), 8-19.

Stangl, K., Gunther, C., Frank, T., Lorenz, M., Meiners, S., Ropke, T., . . . Stangl, V. (2002). Inhibition of the ubiquitin-proteasome pathway induces differential heat-shock protein response in cardiomyocytes and renders early cardiac protection. *Biochemical and Biophysical Research Communications, 291*(3), 542-549.

Starita, L. M., Horwitz, A. A., Keogh, M. C., Ishioka, C., Parvin, J. D., & Chiba, N. (2005). BRCA1/BARD1 ubiquitinate phosphorylated RNA polymerase II. *Journal of Biological Chemistry, 280*(26), 24498-24505.

Stehling, O., Elsasser, H. P., Bruckel, B., Muhlenhoff, U., & Lill, R. (2004). Iron-sulfur protein maturation in human cells: evidence for a function of frataxin. *Hum Mol Genet, 13*(23), 3007-3015.

Stimpson, K. M., & Sullivan, B. A. (2011). Histone H3K4 methylation keeps centromeres open for business. *Embo Journal, 30*(2), 233-234.

Stock, J.K., Giadrossi, S. Casanova, M. Brookes, E. Vidal, M. Koseki, H. Brockdorff, N. Fisher, A.G. Pombo, A. (2007). Ring1-mediated ubiquitination of H2A restrains poised RNA polymerase II at bivalent genes in mouse ES cells. *Nat Cell Biol, 9*(12), 1428-U1174.

Strahl, B. D., Grant, P. A., Briggs, S. D., Sun, Z. W., Bone, J. R., Caldwell, J. A., . . . Allis, C. D. (2002). Set2 is a nucleosomal histone H3-selective methyltransferase that mediates transcriptional repression. *Molecular and Cellular Biology, 22*(5), 1298-1306.

Strahl, B. D., Ohba, R., Cook, R. G., & Allis, C. D. (1999). Methylation of histone H3 at lysine 4 is highly conserved and correlates with transcriptionally active nuclei in Tetrahymena. *Proceedings of the National Academy of Sciences of the United States of America, 96*(26), 14967-14972.

Stratford, M. R., & Dennis, M. F. (1994). Pharmacokinetics and biochemistry studies on nicotinamide in the mouse. *Cancer Chemother Pharmacol, 34*(5), 399-404.

Stratford, M. R., Dennis, M. F., Hoskin, P., Phillips, H., Hodgkiss, R. J., & Rojas, A. (1996). Nicotinamide pharmacokinetics in humans: effect of gastric acid inhibition, comparison of rectal vs oral administration and the use of saliva for drug monitoring. *Br J Cancer, 74*(1), 16-21.

Sugito, K., Yamane, M., Hattori, H., Hayashi, Y., Tohnai, I., Ueda, M., . . . Ohtsuka, K. (1995). Interaction between Hsp70 and Hsp40, Eukaryotic Homologs of Dnak and Dnaj, in Human-Cells Expressing Mutant-Type P53. *Febs Letters, 358*(2), 161-164.

Suk, F. M., Lin, S. Y., Lin, R. J., Hsine, Y. H., Liao, Y. J., Fang, S. U., & Liang, Y. C. (2015). Bortezomib inhibits Burkitt's lymphoma cell proliferation by downregulating sumoylated hnRNP K and c-Myc expression. *Oncotarget, 6*(28), 25988-26001.

Suka, N., Suka, Y., Carmen, A. A., Wu, J. S., & Grunstein, M. (2001). Highly specific antibodies determine histone acetylation site usage in yeast heterochromatin and euchromatin. *Molecular Cell, 8*(2), 473-479.

Sulahian, R., Johnston, S. A., & Kodadek, T. (2006). The proteasomal ATPase complex is required for stress-induced transcription in yeast (vol 34, pg 1351, 2006). *Nucleic Acids Research, 34*(8), 2482-2482.

Sullivan, B. A., & Karpen, G. H. (2004). Centromeric chromatin exhibits a histone modification pattern that is distinct from both euchromatin and heterochromatin. *Nature Structural & Molecular Biology, 11*(11), 1076-1083.
Sun, L., Johnston, S. A., & Kodadek, T. (2002). Physical association of the APIS complex and general transcription factors. *Biochem Biophys Res Commun, 296*(4), 991-999.

Svejstrup, J. Q. (2007). Contending with transcriptional arrest during RNAPII transcript elongation. *Trends Biochem Sci, 32*(4), 165-171.

Szutorisz, H., Georgiou, A., Tora, L., & Dillon, N. (2006). The proteasome restricts permissive transcription at tissue-specific gene loci in embryonic stem cells. *Cell, 127*(7), 1375-1388.

Taddei, A., Maison, C., Roche, D., & Almouzni, G. (2001). Reversible disruption of pericentric heterochromatin and centromere function by inhibiting deacetylases. *Nat Cell Biol, 3*(2), 114-120.

Takaki, E., Fujimoto, M., Sugahara, K., Nakahari, T., Yonemura, S., Tanaka, Y., . . . Nakai, A. (2006). Maintenance of olfactory neurogenesis requires HSF1, a major heat shock transcription factor in mice. *J Biol Chem, 281*(8), 4931-4937.

Takii, R., Fujimoto, M., Tan, K., Takaki, E., Hayashida, N., Nakato, R., . . . Nakai, A. (2015a/b). ATF1 modulates the heat shock response by regulating the stress-inducible heat shock factor 1 transcription complex. *Mol Cell Biol, 35*(1), 11-25.

Tang, H., Liu, Y., Madabusi, L., & Gilmour, D. S. (2000). Promoter-proximal pausing on the hsp70 promoter in Drosophila melanogaster depends on the upstream regulator. *Molecular and Cellular Biology, 20*(7), 2569-2580.

Tang, Z. Y., Wu, Y. L., Gao, S. L., & Shen, H. W. (2008). Effects of the proteasome inhibitor bortezomib on gene expression profiles of pancreatic cancer cells. *Journal of Surgical Research, 145*(1), 111-123.

Tardat, M., Brustel, J., Kirsh, O., Lefevbre, C., Callanan, M., Sardet, C., & Julien, E. (2010). The histone H4 Lys 20 methyltransferase PR-Set7 regulates replication origins in mammalian cells. *Nature Cell Biology, 12*(11), 1086-U1082.

Teneng, I., Montoya-Durango, D. E., Quertermous, J. L., Lacy, M. E., & Ramos, K. S. (2011). Reactivation of L1 retrotransposon by benzo(a)pyrene involves complex genetic and epigenetic regulation. *Epigenetics, 6*(3), 355-367.

Terrell, J., Shih, S., Dunn, R., & Hicke, L. (1998). A function for monoubiquitination in the internalization of a G protein-coupled receptor. *Molecular Cell, 1*(2), 193-202.

Tessari, A., Salata, E., Ferlin, A., Bartoloni, L., Slongo, M. L., & Foresta, C. (2004). Characterization of HSFY, a novel AZFb gene on the Y chromosome with a possible role in human spermatogenesis. *Molecular Human Reproduction, 10*(4), 253-258.

Thiru, A., Nietlispach, D., Mott, H. R., Okuwaki, M., Lyon, D., Nielsen, P. R., . . . Laue, E. D. (2004). Structural basis of HP1/PXVXL motif peptide interactions and HP1 localisation to heterochromatin. *EMBO J, 23*(3), 489-499.

Ting, D. T., Lipson, D., Paul, S., Brannigan, B. W., Akhavanfard, S., Coffman, E. J., . . . Haber, D. A. (2011). Aberrant overexpression of satellite repeats in pancreatic and other epithelial cancers. *Science, 331*(6017), 593-596.

Tomko, R. J., Funakoshi, M., Schneider, K., Wang, J. M., & Hochstrasser, M. (2010). Heterohexameric Ring Arrangement of the Eukaryotic Proteasomal ATPases: Implications for Proteasome Structure and Assembly. *Molecular Cell, 38*(3), 393-403.

Topp, C. N., Zhong, C. X., & Dawe, R. K. (2004). Centromere-encoded RNAs are integral components of the maize kinetochore. *Proceedings of the National Academy of Sciences of the United States of America, 101*(45), 15986-15991.

Trabzuni, D., Ramasamy, A., Imran, S., Walker, R., Smith, C., Weale, M. E., . . . North American Brain Expression, C. (2013). Widespread sex differences in gene expression and splicing in the adult human brain. *Nat Commun, 4*, 2771.

Trask, D. K., & Muller, M. T. (1988). Stabilization of type I topoisomerase-DNA covalent complexes by actinomycin D. *Proc Natl Acad Sci U S A, 85*(5), 1417-1421.

Tremethick, D. J. (2007). Higher-order structures of chromatin: the elusive 30 nm fiber. *Cell, 128*(4), 651-654.

Trinklein, N. D., Chen, W. C., Kingston, R. E., & Myers, R. M. (2004). Transcriptional regulation and binding of heat shock factor 1 and heat shock factor 2 to 32 human heat shock genes during thermal stress and differentiation. *Cell Stress Chaperones, 9*(1), 21-28.

Tsankova, N., Renthal, W., Kumar, A., & Nestler, E. J. (2007). Epigenetic regulation in psychiatric disorders. *Nat Rev Neurosci, 8*(5), 355-367.

Tse, C., Sera, T., Wolffe, A. P., & Hansen, J. C. (1998). Disruption of higher-order folding by core histone acetylation dramatically enhances transcription of nucleosomal arrays by RNA polymerase III. *Molecular and Cellular Biology, 18*(8), 4629-4638.

Tsirigos, A., & Rigoutsos, I. (2009). Alu and B1 Repeats Have Been Selectively Retained in the Upstream and Intronic Regions of Genes of Specific Functional Classes. *Plos Computational Biology, 5*(12).

Tsubuki, S., Kawasaki, H., Saito, Y., Miyashita, N., Inomata, M., & Kawashima, S. (1993). Purification and Characterization of a Z-Leu-Leu-Leu-Mca Degrading Protease Expected to Regulate Neurite Formation - a Novel Catalytic Activity in Proteasome. *Biochemical and Biophysical Research Communications, 196*(3), 1195-1201.

Turelli, P., Castro-Diaz, N., Marzetta, F., Kapopoulou, A., Raclot, C., Duc, J., . . . Trono, D. (2014). Interplay of TRIM28 and DNA methylation in controlling human endogenous retroelements. *Genome Res, 24*(8), 1260-1270.

Unno, M., Mizushima, T., Morimoto, Y., Tomisugi, Y., Tanaka, K., Yasuoka, N., & Tsukihara, T. (2002). The structure of the mammalian 20S proteasome at 2.75 angstrom resolution. *Structure, 10*(5), 609-618.

Uprety, B., Lahudkar, S., Malik, S., & Bhaumik, S. R. (2012). The 19S proteasome subcomplex promotes the targeting of NuA4 HAT to the promoters of ribosomal protein genes to facilitate the recruitment of TFIID for transcriptional initiation in vivo. *Nucleic Acids Res, 40*(5), 1969-1983.

Urbani, L., Sherwood, S. W., & Schimke, R. T. (1995). Dissociation of nuclear and cytoplasmic cell cycle progression by drugs employed in cell synchronization. *Exp Cell Res, 219*(1), 159-168.

Vakoc, C. R., Mandat, S. A., Olenschock, B. A., & Blobel, G. A. (2005). Histone H3 lysine 9 methylation and HP1 gamma are associated with transcription elongation through mammalian chromatin. *Blood, 106*(11), 493a-493a.

Valgardsdottir, R., Chiodi, I., Giordano, M., Cobianchi, F., Riva, S., & Biamonti, G. (2005). Structural and functional characterization of noncoding repetitive RNAs transcribed in stressed human cells. *Mol Biol Cell, 16*(6), 2597-2604.

Valgardsdottir, R., Chiodi, I., Giordano, M., Rossi, A., Bazzini, S., Ghigna, C., . . . Biamonti, G. (2008). Transcription of Satellite III non-coding RNAs is a general stress response in human cells. *Nucleic Acids Research, 36*(2), 423-434.

Van de Vosse, D. W., Wan, Y., Wozniak, R. W., & Aitchison, J. D. (2011). Role of the nuclear envelope in genome organization and gene expression. *Wiley Interdiscip Rev Syst Biol Med, 3*(2), 147-166.

Vankan, P. (2013). Prevalence gradients of Friedreich's ataxia and R1b haplotype in Europe co-localize, suggesting a common Palaeolithic origin in the Franco-Cantabrian ice age refuge. *J Neurochem, 126 Suppl 1*, 11-20.

Vaquero, A., Scher, M., Erdjument-Bromage, H., Tempst, P., Serrano, L., & Reinberg, D. (2007). SIRT1 regulates the histone methyl-transferase SUV39H1 during heterochromatin formation. *Nature, 450*(7168), 440-444.

Vaquero, A., Scher, M., Lee, D. H., Erdjument-Bromage, H., Tempst, P., & Reinberg, D. (2004). Human SirT1 interacts with histone H1 and promotes formation of facultative heterochromatin. *Molecular Cell, 16*(1), 93-105.

Vassen, L., Fiolka, K., & Moroy, T. (2006). Gfi1b alters histone methylation at target gene promoters and sites of gamma-satellite containing heterochromatin. *Embo Journal, 25*(11), 2409-2419.

Vaziri, H., Dessain, S. K., Eagon, E. N., Imai, S. I., Frye, R. A., Pandita, T. K., . . . Weinberg, R. A. (2001). hSIR2(SIRT1) functions as an NAD-dependent p53 deacetylase. *Cell, 107*(2), 149-159.
Velichko, A. K., Kantidze, O. L., & Razin, S. V. (2011). HP1alpha is not necessary for the structural maintenance of centromeric heterochromatin. *Epigenetics, 6*(3), 380-387.

Venkatesh, S., Smolle, M., Li, H., Gogol, M. M., Saint, M., Kumar, S., . . . Workman, J. L. (2012). Set2 methylation of histone H3 lysine 36 suppresses histone exchange on transcribed genes. *Nature, 489*(7416), 452-455.

Ventii, K. H., & Wilkinson, K. D. (2008). Protein partners of deubiquitinating enzymes. *Biochemical Journal, 414*, 161-175.

Verdel, A., Jia, S., Gerber, S., Sugiyama, T., Gygi, S., Grewal, S. I., & Moazed, D. (2004). RNAi-mediated targeting of heterochromatin by the RITS complex. *Science, 303*(5658), 672-676.

Verma, R., Aravind, L., Oania, R., McDonald, W. H., Yates, J. R., Koonin, E. V., & Deshaies, R. J. (2002). Role of Rpn11 metalloprotease in deubiquitination and degradation by the 26S proteasome. *Science, 298*(5593), 611-615.

Verma, R., Oania, R., Fang, R., Smith, G. T., & Deshaies, R. J. (2011). Cdc48/p97 mediates UV-dependent turnover of RNA Pol II. *Molecular Cell, 41*(1), 82-92.

Vermeulen, M., Mulder, K. W., Denissov, S., Pijnappel, W. W. M. P., van Schaik, F. M. A., Varier, R. A., . . . Timmers, H. T. M. (2007). Selective anchoring of TFIID to nucleosomes by trimethylation of histone H3 lysine 4. *Cell, 131*(1), 58-69.

Vetcher, A. A., Napierala, M., Iyer, R. R., Chastain, P. D., Griffith, J. D., & Wells, R. D. (2002). Sticky DNA, a long GAA center dot GAA center dot TTC triplex that is formed intramolecularly, in the sequence of intron 1 of the frataxin gene. *Journal of Biological Chemistry, 277*(42), 39217-39227.

Vihervaara, A., & Sistonen, L. (2014). HSF1 at a glance. *Journal of Cell Science, 127*(2), 261-266.

Vinas-Castells, R., Beltran, M., Valls, G., Gomez, I., Garcia, J. M., Montserrat-Sentis, B., . . . Diaz, V. M. (2010). The hypoxia-controlled FBXL14 ubiquitin ligase targets SNAIL1 for proteasome degradation. *J Biol Chem, 285*(6), 3794-3805.

Vissel, B., Nagy, A., & Choo, K. H. (1992). A satellite III sequence shared by human chromosomes 13, 14, and 21 that is contiguous with alpha satellite DNA. *Cytogenet Cell Genet, 61*(2), 81-86.

Vjestica, A., Zhang, D., Liu, J., & Oliferenko, S. (2013). Hsp70-Hsp40 chaperone complex functions in controlling polarized growth by repressing Hsf1-driven heat stress-associated transcription. *PLoS Genet, 9*(10), e1003886.

Volpe, T., & Martienssen, R. A. (2011). RNA interference and heterochromatin assembly. *Cold Spring Harb Perspect Biol, 3*(9), a003731.
Volpe, T. A., Kidner, C., Hall, I. M., Teng, G., Grewal, S. I., & Martienssen, R. A. (2002). Regulation of heterochromatic silencing and histone H3 lysine-9 methylation by RNAi. *Science, 297*(5588), 1833-1837.

Vos, L. J., Famulski, J. K., & Chan, G. K. T. (2006). How to build a centromere: from centromeric and pericentromeric chromatin to kinetochore assembly. *Biochemistry and Cell Biology-Biochimie Et Biologie Cellulaire, 84*(4), 619-639.

Voss, T. C., & Hager, G. L. (2014). Dynamic regulation of transcriptional states by chromatin and transcription factors. *Nat Rev Genet, 15*(2), 69-81.

Vuister, G. W., Kim, S. J., Orosz, A., Marquardt, J., Wu, C., & Bax, A. (1994). Solution structure of the DNA-binding domain of Drosophila heat shock transcription factor. *Nat Struct Biol, 1*(9), 605-614.

Vujanac, M., Fenaroli, A., & Zimarino, V. (2005). Constitutive nuclear import and stress-regulated nucleocytoplasmic shuttling of mammalian heat-shock factor 1. *Traffic, 6*(3), 214-229.

Wagner, E. J., & Carpenter, P. B. (2012). Understanding the language of Lys36 methylation at histone H3. *Nature Reviews Molecular Cell Biology, 13*(2), 115-126.

Walkinshaw, D. R., & Yang, X. J. (2008). Histone deacetylase inhibitors as novel anticancer therapeutics. *Current Oncology, 15*(5), 237-243.

Walsh, C. P., Chaillet, J. R., & Bestor, T. H. (1998). Transcription of IAP endogenous retroviruses is constrained by cytosine methylation. *Nature Genetics, 20*(2), 116-117.

Wang, F., Koyama, N., Nishida, H., Haraguchi, T., Reith, W., & Tsukamoto, T. (2006). The assembly and maintenance of heterochromatin initiated by transgene repeats are independent of the RNA interference pathway in mammalian cells. *Molecular and Cellular Biology, 26*(11), 4028-4040.

Wang, G. H., Ying, Z. K., Jin, X. J., Tu, N. X., Zhang, Y., Phillips, M., . . . Mivechi, N. F. (2004). Essential requirement for both hsf1 and hsf2 transcriptional activity in spermatogenesis and male fertility. *Genesis, 38*(2), 66-80.

Wang, G. H., Zhang, J., Moskophidis, D., & Mivechi, N. F. (2003). Targeted disruption of the heat shock transcription factor (hsf)-2 gene results in increased embryonic lethality, neuronal defects, and reduced spermatogenesis. *Genesis, 36*(1), 48-61.

Wang, R. H., Lahusen, T. J., Chen, Q., Xu, X. L., Jenkins, L. M. M., Leo, E., . . . Deng, C. X. (2014). SIRT1 Deacetylates TopBP1 and Modulates Intra-S-Phase Checkpoint and DNA Replication Origin Firing. *International Journal of Biological Sciences, 10*(10), 1193-1202.

Wang, S. P., Wang, W. L., Chang, Y. L., Wu, C. T., Chao, Y. C., Kao, S. H., . . . Yang, P. C. (2009). p53 controls cancer cell invasion by inducing the MDM2-mediated degradation of Slug. *Nat Cell Biol, 11*(6), 694-704.

Warburton, P. E., Cooke, C. A., Bourassa, S., Vafa, O., Sullivan, B. A., Stetten, G., . . . Earnshaw, W. C. (1997). Immunolocalization of CENP-A suggests a distinct nucleosome structure at the inner kinetochore plate of active centromeres. *Current Biology, 7*(11), 901-904.

Wassenegger, M. (2005). The role of the RNAi machinery in heterochromatin formation. *Cell, 122*(1), 13-16.

Waters, E. R., Lee, G. J., & Vierling, E. (1996). Evolution, structure and function of the small heat shock proteins in plants. *Journal of Experimental Botany, 47*(296), 325-338.

Waterston, R. H., Lindblad-Toh, K., Birney, E., Rogers, J., Abril, J. F., Agarwal, P., . . . Consor, M. G. S. (2002). Initial sequencing and comparative analysis of the mouse genome. *Nature, 420*(6915), 520-562.

Welch, W. J. (1992). Mammalian stress response: cell physiology, structure/function of stress proteins, and implications for medicine and disease. *Physiol Rev, 72*(4), 1063-1081.

Welle, S., Tawil, R., & Thornton, C. A. (2008). Sex-Related Differences in Gene Expression in Human Skeletal Muscle. *PLoS One, 3*(1).

Westerheide, S. D., Anckar, J., Stevens, S. M., Sistonen, L., & Morimoto, R. I. (2009). Stress-Inducible Regulation of Heat Shock Factor 1 by the Deacetylase SIRT1. *Science, 323*(5917), 1063-1066.

Westhorpe, F. G., & Straight, A. F. (2013). Functions of the centromere and kinetochore in chromosome segregation. *Curr Opin Cell Biol, 25*(3), 334-340.

Wicker, T., Sabot, F., Hua-Van, A., Bennetzen, J. L., Capy, P., Chalhoub, B., . . . Schulman, A. H. (2007). A unified classification system for eukaryotic transposable elements. *Nat Rev Genet, 8*(12), 973-982.

Wicky, C., Villeneuve, A. M., Lauper, N., Codourey, L., Tobler, H., & Muller, F. (1996). Telomeric repeats (TTAGGC)n are sufficient for chromosome capping function in Caenorhabditis elegans. *Proc Natl Acad Sci U S A, 93*(17), 8983-8988.

Widom, J. (1992). A Relationship between the Helical Twist of DNA and the Ordered Positioning of Nucleosomes in All Eukaryotic Cells. *Proceedings of the National Academy of Sciences of the United States of America, 89*(3), 1095-1099.

Williams, W. P., Tamburic, L., & Astell, C. R. (2004). Increased levels of B1 and B2 SINE transcripts in mouse fibroblast cells due to minute virus of mice infection. *Virology, 327*(2), 233-241.
Wilson, M. D., Harreman, M., & Svejstrup, J. Q. (2013). Ubiquitylation and degradation of elongating RNA polymerase II: the last resort. *Biochim Biophys Acta, 1829*(1), 151-157. 2

Wojcik, C. (2002). Regulation of apoptosis by the ubiquitin and proteasome pathway. *J Cell Mol Med, 6*(1), 25-48.

Wojcik, C., & DeMartino, G. N. (2003). Intracellular localization of proteasomes. *Int J Biochem Cell Biol, 35*(5), 579-589.

Wojcik, C., Paweletz, N., & Schroeter, D. (1995). Localization of Proteasomal Antigens during Different Phases of the Cell-Cycle in Hela-Cells. *European Journal of Cell Biology, 68*(2), 191-198.

Wong, A., Yang, J., Cavadini, P., Gellera, C., Lonnerdal, B., Taroni, F., & Cortepassi, G. (1999). The Friedreich's ataxia mutation confers cellular sensitivity to oxidant stress which is rescued by chelators of iron and calcium and inhibitors of apoptosis. *Human Molecular Genetics, 8*(3), 425-430.

Wong, L. H., Brettingham-Moore, K. H., Chan, L., Quach, J. M., Anderson, M. A., Northrop, E. L., . . . Choo, K. H. A. (2007). Centromere RNA is a key component for the assembly of nucleoproteins at the nucleolus and centromere. *Genome Research, 17*(8), 1146-1160.

Wood, A. H., & Dubrey, S. W. (2013). Cardiomyopathy and the electrocardiogram in Friedreich's ataxia. *Br J Hosp Med (Lond), 74*(4), 232-233.

Wood, H. (2013). Neurodegenerative disease: altered DNA methylation and RNA splicing could be key mechanisms in Huntington disease. *Nat Rev Neurol, 9*(3), 119.

Woodcock, C. L., & Dimitrov, S. (2001). Higher-order structure of chromatin and chromosomes. *Curr Opin Genet Dev, 11*(2), 130-135.

Woodcock, C. L., Skoultchi, A. I., & Fan, Y. H. (2006). Role of linker histone in chromatin structure and function: H1 stoichiometry and nucleosome repeat length. *Chromosome Research, 14*(1), 17-25.

Wreggett, K. A., Hill, F., James, P. S., Hutchings, A., Butcher, G. W., & Singh, P. B. (1994). A Mammalian Homolog of Drosophila Heterochromatin Protein-1 (Hp1) Is a Component of Constitutive Heterochromatin. *Cytogenetics and Cell Genetics, 66*(2), 99-103.

Wu, H., & Zhang, Y. (2014). Reversing DNA methylation: mechanisms, genomics, and biological functions. *Cell, 156*(1-2), 45-68.

Wu, L. P., Wang, X., Li, L., Zhao, Y., Lu, S. L., Yu, Y., . . . Zhu, W. G. (2008). Histone deacetylase inhibitor depsipeptide activates silenced genes through decreasing both CpG and H3K9 methylation on the promoter. *Molecular and Cellular Biology, 28*(10), 3219-3235.

Wu, R., Singh, P. B., & Gilbert, D. M. (2006). Uncoupling global and fine-tuning replication timing determinants for mouse pericentric heterochromatin. *J Cell Biol, 174*(2), 185-194.

Wu, S. M., Wang, W. P., Kong, X. D., Congdon, L. M., Yokomori, K., Kirschner, M. W., & Rice, J. C. (2010). Dynamic regulation of the PR-Set7 histone methyltransferase is required for normal cell cycle progression. *Genes & Development, 24*(22), 2531-2542.

Wu, S.Y., & Chiang, C.M., (2007). The double bromodomain-containing chromatin adaptor Brd4 and transcriptional regulation. *J Biol Chem 282 (18),* 13141-5

Wysocka, J., Swigut, T., Xiao, H., Milne, T. A., Kwon, S. Y., Landry, J., . . . Allis, C. D. (2006). A PHD finger of NURF couples histone H3 lysine 4 trimethylation with chromatin remodelling. *Nature, 442*(7098), 86-90.

Xiao, H., & Lis, J. T. (1988). Germline Transformation Used to Define Key Features of Heat-Shock Response Elements. *Science, 239*(4844), 1139-1142.

Xiao, T., Hall, H., Kizer, K. O., Shibata, Y., Hall, M. C., Borchers, C. H., & Strahl, B. D. (2003). Phosphorylation of RNA polymerase II CTD regulates H3 methylation in yeast. *Genes Dev, 17*(5), 654-663.

Xie, S. Q., Martin, S., Guillot, P. V., Bentley, D. L., & Pombo, A. (2006). Splicing speckles are not reservoirs of RNA polymerase II, but contain an inactive form, phosphorylated on serine(2) residues of the C-terminal domain. *Mol Biol Cell, 17*(4), 1723-1733.

Xie, Y., Chen, C. M., Stevenson, M. A., Auron, P. E., & Calderwood, S. K. (2002). Heat shock factor 1 represses transcription of IL-1 beta gene through physical interaction with the nuclear factor of interleukin 6. *Journal of Biological Chemistry, 277*(14), 11802-11810.

Xu, D. M., Zalmas, L. P., & La Thangue, N. B. (2008). A transcription cofactor required for the heat-shock response. *Embo Reports, 9*(7), 662-669.

Xu, K., Dai, X. L., Huang, H. C., & Jiang, Z. F. (2011). Targeting HDACs: A Promising Therapy for Alzheimer's Disease. *Oxidative Medicine and Cellular Longevity*.

Xu, Y. M., Huang, D. Y., Chiu, J. F., & Lau, A. T. Y. (2012). Post-Translational Modification of Human Heat Shock Factors and Their Functions: A Recent Update by Proteomic Approach. *Journal of Proteome Research, 11*(5), 2625-2634.

Yamada, T., Fischle, W., Sugiyama, T., Allis, C. D., & Grewal, S. I. (2005). The nucleation and maintenance of heterochromatin by a histone deacetylase in fission yeast. *Mol Cell, 20*(2), 173-185.

Yamamoto, K., & Sonoda, M. (2003). Self-interaction of heterochromatin protein 1 is required for direct binding to histone methyltransferase, SUV39H1. *Biochemical and Biophysical Research Communications, 301*(2), 287-292.

Yamashita, K., Sato, A., Asashima, M., Wang, P. C., & Nishinakamura, R. (2007). Mouse homolog of SALL1, a causative gene for Townes-Brocks syndrome, binds to A/T-rich sequences in pericentric heterochromatin via its C-terminal zinc finger domains. *Genes Cells, 12*(2), 171-182.

Yan, H., Ito, H., Nobuta, K., Ouyang, S., Jin, W., Tian, S., . . . Jiang, J. (2006). Genomic and genetic characterization of rice Cen3 reveals extensive transcription and evolutionary implications of a complex centromere. *Plant Cell, 18*(9), 2123-2133.

Yandim, C. (2012). Heterochromatin effects in Friedreich's ataxia and sexual dimorphism. *Ph.D. thesis*. Imperial College London

Yandim, C., Natisvili, T., & Festenstein, R. (2013). Gene regulation and epigenetics in Friedreich's ataxia. *Journal of Neurochemistry, 126*, 21-42.

Yang, Z. *et al*. (2005). Recruitment of P-TEFb for stimulation of transcriptional elongation by the bromodomain protein Brd4. *Mol. Cell* 19, 535–545

Yang, L. Y., Jiang, H., & Rangel, K. M. (2003). RNA polymerase II stalled on a DNA template during transcription elongation is ubiquitinated and the ubiquitination facilitates displacement of the elongation complex. *International Journal of Oncology, 22*(3), 683-689.

Yang, N., & Kazazian, H. H. (2006). L1 retrotransposition is suppressed by endogenously encoded small interfering RNAs in human cultured cells. *Nature Structural & Molecular Biology, 13*(9), 763-771.

Yang, X., Schadt, E. E., Wang, S., Wang, H., Arnold, A. P., Ingram-Drake, L., . . . Lusis, A. J. (2006). Tissue-specific expression and regulation of sexually dimorphic genes in mice. *Genome Res, 16*(8), 995-1004.

Yang, X. J., & Seto, E. (2007). HATs and HDACs: from structure, function and regulation to novel strategies for therapy and prevention. *Oncogene, 26*(37), 5310-5318.

Yeung, F., Hoberg, J. E., Ramsey, C. S., Keller, M. D., Jones, D. R., Frye, R. A., & Mayo, M. W. (2004). Modulation of NF-kappa B-dependent transcription and cell survival by the SIRT1 deacetylase. *Embo Journal, 23*(12), 2369-2380.

Yokoyama, A., Wang, Z., Wysocka, J., Sanyal, M., Aufiero, D. J., Kitabayashi, I., . . . Cleary, M. L. (2004). Leukemia proto-oncoprotein MLL forms a SET1-like histone methyltransferase complex with menin to regulate Hox gene expression. *Molecular and Cellular Biology, 24*(13), 5639-5649.

Yoon, T., & Cowan, J. A. (2004). Frataxin-mediated iron delivery to ferrochelatase in the final step of heme biosynthesis. *Journal of Biological Chemistry, 279*(25), 25943-25946.

Yoshida, K., Nakamura, A., Yazaki, M., Ikeda, S., & Takeda, S. (1998). Insertional mutation by transposable element, L1, in the DMD gene results in X-linked dilated cardiomyopathy. *Human Molecular Genetics, 7*(7), 1129-1132.

Yoshida, M., Kijima, M., Akita, M., & Beppu, T. (1990). Potent and specific inhibition of mammalian histone deacetylase both in vivo and in vitro by trichostatin A. *J Biol Chem, 265*(28), 17174-17179.
Yu, R., Jih, G., Iglesias, N., & Moazed, D. (2014). Determinants of heterochromatic siRNA biogenesis and function. *Mol Cell, 53*(2), 262-276.

Yuan, C. M., Douglas-Nikitin, V. K., Ahrens, K. P., Luchetta, G. R., Braylan, R. C., & Yang, L. (2004). DRAQ5-based DNA content analysis of hematolymphoid cell subpopulations discriminated by surface antigens and light scatter properties. *Cytometry Part B-Clinical Cytometry, 58B*(1), 47-52.

Zaarur, N., Gabai, V. L., Porco, J. A., Calderwood, S., & Sherman, N. Y. (2006). Targeting heat shock response to sensitize cancer cells to proteasome and Hsp90 inhibitors. *Cancer Research, 66*(3), 1783-1791.

Zakian, V. A. (2012). Telomeres: the beginnings and ends of eukaryotic chromosomes. *Exp Cell Res, 318*(12), 1456-1460.

Zamudio, N., & Bourc'his, D. (2010). Transposable elements in the mammalian germline: a comfortable niche or a deadly trap? *Heredity (Edinb), 105*(1), 92-104.

Zanini, C., Giribaldi, G., Mandili, G., Carta, F., Crescenzio, N., Bisaro, B., . . . Turrini, F. (2007). Inhibition of heat shock proteins (HSP) expression by quercetin and differential doxorubicin sensitization in neuroblastoma and Ewing's sarcoma cell lines. *J Neurochem, 103*(4), 1344-1354.

Zaratiegui, M., Castel, S. E., Irvine, D. V., Kloc, A., Ren, J., Li, F., . . . Martienssen, R. A. (2011). RNAi promotes heterochromatic silencing through replication-coupled release of RNA Pol II. *Nature, 479*(7371), 135-138. doi:10.1038/nature10501

Zenke-Kawasaki, Y., Dohi, Y., Katoh, Y., Ikura, T., Ikura, M., Asahara, T., . . . Igarashi, K. (2007). Heme induces ubiquitination and degradation of the transcription factor Bach1. *Mol Cell Biol, 27*(19), 6962-6971.

Zentner, G. E., & Henikoff, S. (2013). Regulation of nucleosome dynamics by histone modifications. *Nature Structural & Molecular Biology, 20*(3), 259-266.

Zhang, C. L., McKinsey, T. A., & Olson, E. N. (2002). Association of class II histone deacetylases with heterochromatin protein 1: potential role for histone methylation in control of muscle differentiation. *Mol Cell Biol, 22*(20), 7302-7312.

Zhang, D. W., Mosley, A. L., Ramisetty, S. R., Rodriguez-Molina, J. B., Washburn, M. P., & Ansari, A. Z. (2012). Ssu72 Phosphatase-dependent Erasure of Phospho-Ser7 Marks on the RNA Polymerase II C-terminal Domain Is Essential for Viability and Transcription Termination. *Journal of Biological Chemistry, 287*(11), 8541-8551.

Zhao, T., Heyduk, T., Allis, C. D., & Eissenberg, J. C. (2000). Heterochromatin protein 1 binds to nucleosomes and DNA in Vitro. *Journal of Biological Chemistry, 275*(36), 28332-28338.
Zhao, X. D., Han, X., Chew, J. L., Liu, J., Chiu, K. P., Choo, A., . . . Wei, C. L. (2007). Whole-genome mapping of histone H3 Lys4 and 27 trimethylations reveals distinct genomic compartments in human embryonic stem cells. *Cell Stem Cell, 1*(3), 286-298.

Zhu, Q., Pao, G. M., Huynh, A. M., Suh, H., Tonnu, N., Nederlof, P. M., . . . Verma, I. M. (2011). BRCA1 tumour suppression occurs via heterochromatin-mediated silencing. *Nature, 477*(7363), 179-U176.

Zimmermann, J., Erdmann, D., Lalande, I., Grossenbacher, R., Noorani, M., & Furst, P. (2000). Proteasome inhibitor induced gene expression profiles reveal overexpression of transcriptional regulators ATF3, GADD153 and MAD1. *Oncogene, 19*(25), 2913-2920.

Zobeck, K. L., Buckley, M. S., Zipfel, W. R., & Lis, J. T. (2010). Recruitment Timing and Dynamics of Transcription Factors at the Hsp70 Loci in Living Cells. *Molecular Cell, 40*(6), 965-975.

Zofall, M., & Grewal, S. I. (2006). RNAi-mediated heterochromatin assembly in fission yeast. *Cold Spring Harb Symp Quant Biol, 71*, 487-496.

Zou, J. Y., Guo, Y. L., Guettouche, T., Smith, D. F., & Voellmy, R. (1998). Repression of heat shock transcription factor HSF1 activation by HSP90 (HSP90 complex) that forms a stress-sensitive complex with HSF1. *Cell, 94*(4), 471-480.

Zuhlke, C. H., Dalski, A., Habeck, M., Straube, K., Hedrich, K., Hoeltzenbein, M., . . . Schwinger, E. (2004). Extension of the mutation spectrum in Friedreich's ataxia: detection of an exon deletion and novel missense mutations. *European Journal of Human Genetics, 12*(11), 979-982.